

INTER-MODEL, ANALYTICAL, AND
EXPERIMENTAL VALIDATION OF
A HEAT BALANCE BASED
RESIDENTIAL COOLING
LOAD CALCULATION
PROCEDURE

By

DONGYI XIAO

Bachelor of Science in Thermal Engineering
Shenyang Architectural and Civil Engineering Institute
Shenyang, China
1995

Master of Science in Thermal Engineering
Tongji University
Shanghai, China
1998

Submitted to the Faculty of the
Graduate College of the
Oklahoma State University
in partial fulfillment of
the requirements for
the Degree of
DOCTOR OF PHILOSOPHY
December, 2006

INTER-MODEL, ANALYTICAL, AND
EXPERIMENTAL VALIDATION OF
A HEAT BALANCE BASED
RESIDENTIAL COOLING
LOAD CALCULATION
PROCEDURE

Dissertation Approved:

Dr. Jeffrey D. Spitler

Dissertation Adviser

Dr. Daniel E. Fisher

Dr. Ronald D. Delahoussaye

Dr. Khaled Mansy

Dr. A. Gordon Emslie

Dean of the Graduate College

ACKNOWLEDGEMENTS

I am so thankful to my dear husband, Xiaobing Liu, who accompanies me day and night, encourages me to continue during difficult times, and supports me all through the way. I cannot imagine how this work would have been finished without his love. I am so grateful that God gave us Rena, our daughter, who is two years old now. Bringing her up along the way was exhausting, but the joy and happiness she brings I will cherish for a lifetime. My thankfulness also goes to all my family in China, for their endless love and constant support.

I would sincerely appreciate my advisor, Dr. Jeffrey D. Spitzer. With the assistantship he offered, I was able to start this research work back in August 1999. Ever since then, I have learned a lot from him, not only in research but also in life. I thank him for his continuous support, constructive guidance, excellent leadership, and ceaseless understanding and patience during the seven years of my graduate study.

My sincere appreciation also extends to the members of my doctoral committee: Drs. Daniel E. Fisher, Ronald D. Delahoussaye, and Khaled Mansy for their ideas and suggestions that helped me improve this dissertation.

Mr. Charles S. Barnaby, currently Vice President of Research of the Wrightsoft Corporation, is one of the key personnel that developed RHB -- the subject of this

research work. He helped develop the automatic parametric run tool used for the inter-model comparison of RHB. He also assisted in the process of analytical testing and experimental validation of RHB. Dr. Simon J. Rees, currently senior research fellow in the Institute of Energy and Sustainable Development at De Montfort University, U.K., helped guide the development of the test suite used for the analytical verification of RHB. Mr. Bruce A. Wilcox, the manager and experimental designer of the Cardinal Fort Wayne Project, generously aided in providing measured data and corresponding information from the Fort Wayne house, which was used in the experimental validation of RHB. Dr. Jon W. Hand, currently senior research fellow in the Energy Systems Research Unit at the University of Strathclyde, U.K., gave useful advice on using ESP-r, the reference model used for the inter-model comparison of RHB. To them I extend my sincere gratitude and appreciation.

I would also like to thank my colleagues in the Building and Environment Thermal Systems Research Group at Oklahoma State University for their ideas, help, and friendship. Here, I only list a few: Andrew D. Chiasson, Mahadevan Ramamoorthy, David Eldridge, Hui Jin, Chanvit Chantrasrisalai, Calvin Iu, Weixiu Kong, Zheng Deng, Xia Xiao and Xiaowei Xu.

Finally, support from ASHRAE under research projects RP-1052 and RP-1199, and in the form of a Grant-in-Aid scholarship during 2005-2006 is gratefully acknowledged. Approval from Cardinal Glass Industries for using the experimental data is also gratefully acknowledged.

TABLE OF CONTENTS

Chapter	Page
1. INTRODUCTION	1
1.1 Non-residential Cooling Load Calculation Procedures	2
1.2 Residential Cooling Load Calculation Procedures	5
1.2.1 Characteristics of Residential Load Calculation	5
1.2.2 Prior Residential Cooling Load Calculation Procedures	8
1.2.3 Heat Balance Based Residential Cooling Load Calculation Procedure.....	12
1.3 Objective	14
2. LITERATURE REVIEW	16
2.1 Heat Balance Based Residential Cooling Load Calculation Procedure	16
2.1.1 Heat Balance Method for Cooling Load Calculation.....	17
2.1.2 Heat Balance for Residential Applications	28
2.1.3 Calculation Algorithms	29
2.1.4 Component Models	34
2.1.5 Modeling Assumptions	40
2.2 Validation Methods of Cooling Load Calculation Programs	43
2.2.1 Analytical Verification.....	45
2.2.2 Comparative Testing.....	46
2.2.3 Empirical Validation.....	47
2.2.4 Application of the Validation Methods.....	48
2.2.5 Summary of Prior Validation Work.....	49
3. OBJECTIVES	52
4. INTER-MODEL VALIDATION OF THE HEAT BALANCE BASED RESIDENTIAL COOLING LOAD CALCULATION PROCEDURE	54
4.1 Selecting the Comparison Tool.....	55
4.1.1 Basic Requirements of the Comparison Tool	55
4.1.2 Review of Candidate Programs	59
4.1.3 Selection of Comparison Tool	71

Chapter	Page
4.2 Methodology.....	77
4.2.1 Types of Comparison.....	77
4.2.2 Parametric Code.....	78
4.2.3 Combined Testing Process.....	79
4.2.4 RHBGen Parametric Generator.....	80
4.2.5 ESP-r System.....	80
4.2.6 Design Evaluation Figure of Merit.....	85
4.2.7 Model Assumptions Used in the Comparison.....	87
4.3 Results.....	89
4.3.1 Description of Test Sets.....	89
4.3.2 Ideal Load Comparison.....	94
4.3.3 System Design Evaluations.....	125
4.4 Conclusions.....	147
5. ANALYTICAL VERIFICATION OF THE HEAT BALANCE BASED RESIDENTIAL COOLING LOAD CALCULATION PROCEDURE.....	151
5.1 Development of the Analytical Verification Test Suite.....	152
5.1.1 The Test Suite.....	153
5.1.2 The Test Suite Software.....	160
5.1.3 The Test Documentation.....	161
5.1.4 Evaluation of the Test Suite.....	163
5.2 Analytical Test of the Heat Balance Based Residential Cooling Load Calculation Procedure.....	164
5.2.1 Testing ResHB.....	164
5.2.2 The Analytical Tests and Testing Results.....	168
5.3 Conclusions.....	193
6. EXPERIMENTAL VALIDATION OF THE HEAT BALANCE BASED RESIDENTIAL COOLING LOAD CALCULATION PROCEDURE.....	195
6.1 Experimental House.....	197
6.2 Instrumentation and Data Acquisition.....	201
6.3 Data Analysis.....	204
6.4 Simulation Approach.....	214
6.4.1 Simulation Inputs.....	214
6.4.2 Simulation Component Models.....	225
6.4.3 Comparisons Made.....	227
6.5 Results.....	228
6.5.1 Inter-zone Airflow.....	228
6.5.2 Master-slave Control.....	231
6.5.3 Ideal Control.....	239
6.5.4 ResHB and ESP-r Result Comparison.....	248

Chapter	Page
6.5.5 Uncertainty Analysis.....	251
6.6 Conclusions.....	256
7. CONCLUSIONS.....	259
REFERENCES	267
APPENDIX A. ANALYTICAL VERIFICATION OF ESP-R.....	279
A.1 Single Zone Tests.....	281
A.2 Multi-zone Tests	287
APPENDIX B. PARAMETRIC CODE USED FOR THE INTER-MODEL COMPARISON	290
APPENDIX C. SAMPLE PERL AND SHELL SCRIPTS USED FOR THE INTER- MODEL COMPARISON	294
C.1 Sample Perl Scripts	294
C.2 Sample Shell Scripts	300
Shell script 1: Climate.....	300
Shell script 2: Rotate.....	301
Shell script 3: Simulate.....	302
Shell script 4: Analyse	303

LIST OF TABLES

Table	Page
2-1 The “sys off” and “sys on” values for default model of inside surface convection coefficients (W/m ² K) in ResHB.....	34
2-2 Fractional components of internal heat sources incorporated in ResHB.....	42
2-3 Advantages and Disadvantages of the three validation methods as from Judkoff (1988).....	44
4-1 Classification of basic requirements for candidate comparison tools	59
4-2 Summary of the features of the alternative programs.....	70
4-3 Main advantages and disadvantages of the candidate programs	71
4-4 Part 1 More detailed summaries of the candidate programs	73
4-4 Part 2 More detailed summaries of the candidate programs	74
4-5 Part 1 Model assumptions used in ESP-r and RHB for the comparison	88
4-5 Part 2 Model assumptions used in ESP-r and RHB for the comparison	89
4-6 Test parameters for the 576 test cases	93
4-7 Algorithm for attributing the PPD Cause	127
5-1 Organization of the Test Suite	155
5-2 Tests Selected for Testing ResHB	165
5-3 Convection Coefficients Used in Testing ResHB	167
5-4 Differences in zone load between the ResHB program and analytically calculated loads for the convection and conduction cases.....	171
5-5 Test parameters used for the steady state convection and conduction tests	171
5-6 Constructions used for the transient conduction tests	172
5-7 Differences in zone load between ResHB and analytical result for the solar related cases	180
5-8 Parameters used for the ExtSolRad test.....	180
5-9 Parameters used for the SolRadGlazing and SolRadShade tests.....	181
5-10 Parameters used for the WinReveal and IntSolarDist tests	181
5-11 Differences in zone load between ResHB and analytical result for the interior longwave radiation tests.....	191
6-1 Construction materials of the Fort Wayne house	200
6-2 Windows of the Fort Wayne house	200
6-3 Constants <i>c</i> , <i>n</i> and ELA values derived from blower door measurements.....	209
6-4 Construction thermal properties input in ResHB/ESP-r simulation.....	217
6-5 Surface absorptances and emissivities input in ResHB/ESP-r simulation	217

Table	Page
6-6 Solar Heat Gain Coefficient (SHGC), Solar Transmittance (T) and Layer Absorptances (A) for ResHB fenestration class FCA-17c	218
6-7 Component models used in ResHB and ESP-r for experimental validation	226
6-8 Uncertainties resulting from representative simulation inputs and experimental measurements.....	252
A-1 Analytical Verification Tests of ESP-r.....	280
B-1 Parametric Code.....	291
B-2 Roof constructions	292
B-3 Ceiling constructions	292
B-4 Wall constructions	292
B-5 Fenestration.....	292
B-6 Partition wall constructions.....	293
B-7 Partition floor/ceiling constructions.....	293
B-8 Interior mass constructions	293
B-9 Exterior floor constructions	293

LIST OF FIGURES

Figure	Page
1-1. Schematic floor plan for a single family detached house with master-slave control ..	7
4-1. Overall inter-model testing process	79
4-2. Predicted Percentage of Dissatisfied (PPD) as a function of Predicted Mean Vote (PMV)	86
4-3. Schematic floor plan of the Shoebox prototype (figure drawn with front side facing north; front, left, back, right as defined in RHBGen)	90
4-4. Schematic floor plan of the 4-bedroom house prototype (figure drawn with front side facing north; front, left, back, right as defined in RHBGen).....	92
4-5. Peak cooling load comparison (Shoebox - Master).....	95
4-6. Cooling load error percentage based on peak average Shoebox load (Master).....	95
4-7. Peak cooling load comparison (4-bedroom house – Family room).....	97
4-8. Peak cooling load comparison (4-bedroom house – Laundry).....	98
4-9. Peak cooling load comparison (4-bedroom house – Foyer 1)	98
4-10. Peak cooling load comparison (4-bedroom house – Bedroom 1)	99
4-11. Peak cooling load comparison (4-bedroom house – Total).....	99
4-12. Cooling load error percentage based on peak average 4-bedroom house load (Family room)	100
4-13. Cooling load error percentage based on peak average 4-bedroom house load (Total)	100
4-14. Outside ground surface temperatures from RHB and ESP-r for Alamosa, CO	103
4-15. Comparison of the ambient dry bulb temperature and the outside surface temperatures calculated from ESP-r (Shoebox - Master)	104
4-16. Comparison of cooling load calculated by RHB and ESP-r (Shoebox - Master): (a) with external long wave radiation (b) without external long wave radiation	104
4-17. Comparison of cooling load error percentage between RHB and ESP-r (4-bedroom house – Family room): (a) with external long wave radiation (b) without external long wave radiation.....	106
4-18. Comparison of cooling load calculated by RHB and ESP-r (Shoebox – Master): (a) with internal thermal mass (b) without internal thermal mass.....	108
4-19. Comparison of cooling load error percentage between RHB and ESP-r (ESP-r with simple solar distribution, Shoebox – Master): (a) with internal thermal mass (b) without internal thermal mass.....	109
4-20. Comparison of cooling load error percentage between RHB and ESP-r (Shoebox – Master): (a) ESP-r with detailed solar distribution, with internal thermal mass (b) ESP-r with simple solar distribution, without internal thermal mass	110

Figure	Page
4-21. ESP-r simple solar distribution vs. detailed solar distribution (Shoebox – Master): (a) comparison of cooling load (b) comparison of cooling load error percentage..	111
4-22. Comparison of cooling load calculated by RHB and ESP-r (4-bedroom house – Family room): (a) ESP-r with inter-zone conduction (b) ESP-r without inter-zone conduction.....	115
4-23. Comparison of cooling load calculated by RHB and ESP-r (4-bedroom house – Laundry): (a) ESP-r with inter-zone conduction (b) ESP-r without inter-zone conduction.....	115
4-24. Comparison of cooling load calculated by RHB and ESP-r (4-bedroom house – Foyer 1): (a) ESP-r with inter-zone conduction (b) ESP-r without inter-zone conduction.....	116
4-25. Comparison of ESP-r calculated cooling loads (without inter-zone conduction vs. with inter-zone conduction): (a) 4-bedroom house – Family room (b) 4-bedroom house – Foyer 1	116
4-26. Comparison of cooling load calculated by RHB and ESP-r (Shoebox – Master): (a) with internal longwave radiation (b) without internal longwave radiation.....	118
4-27. Comparison of cooling load calculated by RHB and ESP-r (Shoebox – Master): without external long wave radiation, internal thermal mass, inter-zone conduction, internal long wave radiation and windows	120
4-28. (a) Ambient air temperatures used for Alamosa, CO in RHB and ESP-r (b) Outside surface absorbed solar radiation in RHB and ESP-r (Shoebox - Master, Alamosa, CO).....	121
4-29. Comparison of cooling load calculated by RHB and ESP-r (Shoebox – Master, without external and internal longwave radiation, without thermal mass, inter-zone conduction, and windows)	122
4-30. Analytically calculated zone loads and those predicted by RHB and ESP-r.....	124
4-31. Processed PPD showing night time ambient cooling, system designed with zero temperature swing (Shoebox)	129
4-32. Processed PPD showing system under-sizing and inadequate distribution, system designed with zero temperature swing (Shoebox)	130
4-33. Hourly PPD vs. temperature, system designed with zero temperature swing (Shoebox - case 17).....	131
4-34. Hourly PPD vs. temperature, system designed with zero temperature swing (Shoebox - case 20).....	131
4-35. Processed PPD showing night time ambient cooling, system designed with zero temperature swing (4-bedroom house)	133
4-36. Processed PPD showing system under-sizing and inadequate distribution, system designed with zero temperature swing (4-bedroom house)	135
4-37. Hourly PPD vs. temperature, system designed with zero temperature swing (4- bedroom house: case 121).....	135
4-38. Processed PPD showing night time ambient cooling, system designed with medium temperature swing (Shoebox)	137
4-39. Processed PPD showing system under-sizing and inadequate distribution, system designed with medium temperature swing (Shoebox).....	137

Figure	Page
4-40. Hourly PPD vs. temperature, system designed with medium temperature swing (Shoebox - case 355).....	138
4-41. Processed PPD showing night time ambient cooling, system designed with medium temperature swing (4-bedroom house)	139
4-42. Processed PPD showing system under-sizing and inadequate distribution, system designed with medium temperature swing (4-bedroom house).....	139
4-43. Hourly PPD vs. temperature, system designed with medium temperature swing (4-bedroom house: case 144).....	141
4-44. Hourly PPD vs. temperature, system designed with medium temperature swing (4-bedroom house: case 451).....	141
4-45. Average degree hours for systems designed with zero or medium temperature swing (4-bedroom house): (a) Family room (b) whole house	143
4-46. Average processed PPD values for systems designed with zero or medium temperature swing (4-bedroom house): (a) night time ambient cooling (b) inadequate distribution	145
4-47. Average processed PPD values for systems designed with zero or medium temperature swing (4-bedroom house): (a) system under-sizing (b) inadequate distribution and system under-sizing	146
5-1. Example parameter input screen (Test SSCond).....	161
5-2. Sinusoidal driving external dry bulb temperature profile used in the transient conduction test TC3	169
5-3. Analytically calculated zone loads and those predicted by the ResHB program for the transient conduction test with sinusoidal driving temperature: Case 1.....	174
5-4. Analytically calculated zone loads and those predicted by the ResHB program for the transient conduction test with sinusoidal driving temperature: case 2.	174
5-5. Analytically calculated zone loads and those predicted by the ResHB program for the transient conduction test with sinusoidal driving temperature: case 3.	175
5-6: Zone geometry of the internal solar distribution test (a) plan view showing two vertical fins (b) vertical view showing horizontal fin at the top of the window. The dimensions W, Rv and Rh are 0.5m (1.64ft), and the dimensions H and B are 1.0m (3.28ft).	178
5-7. Analytically calculated zone loads and those predicted by different versions of ResHB for the solar shading test: horizontal and right side vertical fin on a south-facing window.....	182
5-8. Analytically calculated zone loads and those predicted by different versions of ResHB for the solar shading test: horizontal and left side vertical fin on a south-facing window.....	183
5-9. Analytically calculated zone loads and those predicted by ResHB for the window reveal test: before reveal depth was added to the depths of vertical fins.....	184
5-10. Analytically calculated zone loads and those predicted by ResHB for the window reveal test: after reveal depth was added to the depths of vertical fins.....	184
5-11. Analytically calculated zone loads and those predicted by ResHB for the internal solar distribution test: Case 1, the floor in RHB test zone is heavy weight.....	185

5-12. Analytically calculated zone loads and those predicted by ResHB for the internal solar distribution test: Case 2, the floor in RHB test zone is mass-less.....	186
5-13: Zone load variation with zone aspect ratio and different surface emissivities. The emissivities are: Case 1, external surface 0.9, opposite surface 0.1, other surfaces 0.3; Case 2, external surface 0.9, all other surfaces 0.1; Case 3, all surfaces 0.9...	190
5-14. Analytical and ResHB-predicted zone load variation with zone aspect ratio and different surface emissivities. The emissivities are: Case 1, external surface 0.9, all other surfaces 0.1; Case 2, all surfaces 0.9; Case 3, external surface 0.9, opposite surface 0.1, other surfaces 0.3.....	191
6-1(a). Front view of the house in Ft. Wayne, Indiana (Wilcox 2004).....	198
6-1(b). Back view of the house in Ft. Wayne, Indiana (Wilcox 2004).....	198
6-2. Floor plans of the house in Ft. Wayne, Indiana (Wilcox 2004)	199
6-3. Campbell Scientific CR10X data logger: measurement and control module (left), wiring panel CR10XWP (right). (Picture from http://www.campbellsci.com)	202
6-4. Aspirated temperature thermocouple (Wilcox 2004)	202
6-5. Conceptual flow chart of the experimental validation.....	205
6-6. Hourly averaged outside dry-bulb and wet-bulb temperature for 09/21/2005	207
6-7. Hourly averaged beam and diffuse solar radiation for 09/21/2005	207
6-8. Hourly averaged internal heat gain for 09/21/2005.....	208
6-9. Hourly return air temperature and hourly flow-weighted run-time supply air temperature for 09/21/2005, values shown only for hours when the system was on	211
6-10. Hourly air conditioning “on” fraction for 09/21/2005.....	212
6-11. Hourly basement duct gain (including run-time part and average ΔT part) for 09/21/2005, values shown only for hours when the system was on	213
6-12. House total sensible cooling load for 09/21/2005	214
6-13. Minutely measured room air temperature during the system-off hours for 09/21/2005: (a) kitchen and living room (b) master bedroom and master bathroom	219
6-14. Minutely measured room air temperature for 09/21/2005: dining room.....	222
6-15. Schematic representation of the ESP-r airflow network for the first and second floor	224
6-16. Simulated and experimental total house cooling load comparison: ESP-r with/without inter-zone airflow, ResHB with/without internal heat gain and ventilation distribution.....	229
6-17. Simulated and experimental total house cooling load comparison: ResHB with dining room specified as master room, fixed set point of 23.89 oC with 0.0, 0.2, 0.4, 0.6, 0.8 oC temperature swing, with internal heat gain and ventilation distribution	232
6-18. Simulated and experimental room temperature comparison, ResHB with dining room specified as master room, fixed set point of 23.89 oC with 0.0, 0.2, 0.4, 0.6, 0.8 oC temperature swing, with internal heat gain and ventilation distribution: (a) Dining room (b) Living room	233

6-19. Simulated and experimental total house cooling load comparison: ResHB with master room specified as dining room, living room, Foyer 1 and bedroom 2, master room uses experimental hourly average room air temperature as set point without temperature swing, with internal heat gain and ventilation distribution.....	235
6-20. Simulated and experimental room temperature comparison, ResHB with master room specified as dining room, living room, Foyer 1 and bedroom 2, master room uses experimental hourly average room air temperature as set point without temperature swing, with internal heat gain and ventilation distribution: (a) Dining room (b) Living room	237
6-21. Simulated and experimental total house cooling load comparison: ResHB uses ideal control, every room uses fixed set point of 23.89 oC with 0.8 oC or 0.0 oC temperature swing, with internal heat gain and ventilation distribution.....	241
6-22. Simulated and experimental room temperature comparison, ResHB uses ideal control, every room uses fixed set point of 23.89 oC with 0.8 oC temperature swing, with internal heat gain and ventilation distribution: (a) Dining room (b) Kitchen (c) Bedroom 3.....	244
6-23. Simulated and experimental total house cooling load comparison: ResHB uses ideal control, every room uses fixed set point of 23.89 oC with 0.8 oC or 0.0 oC temperature swing or every room uses experimental hourly average room air temperature as set point without temperature swing, with internal heat gain and ventilation distribution.....	245
6-24. Simulated and experimental room temperature comparison, ResHB uses ideal control, every room uses fixed set point of 23.89 oC with 0.8 oC temperature swing or every room uses experimental hourly average room air temperature as set point without temperature swing, with internal heat gain and ventilation distribution: (a) Dining room (b) Kitchen (c) Bedroom 3	247
6-25. Simulated and experimental total house cooling load comparison: ResHB uses ideal control, every room uses fixed set point of 23.89 oC with 0.8 oC temperature swing, with internal heat gain and ventilation distribution; ESP-r models system control with airflow network under master-slave on-off control	249
6-26. Minutely ESP-r simulated and experimental dining room (master) temperature comparison: ESP-r models system control with airflow network under master-slave on-off control	250
6-27. Simulated and experimental room temperature comparison: ResHB uses ideal control, every room uses fixed set point of 23.89 oC with 0.8 oC temperature swing, with internal heat gain and ventilation distribution; ESP-r models system control with airflow network under master-slave on-off control: (a) Dining room (b) Kitchen (c) Attic	251
6-28. Simulated and experimental total house cooling load comparison: ResHB uses ideal control, every room uses experimental hourly average room air temperature as set point without temperature swing, with internal heat gain and ventilation distribution, cases with infiltration rate of 0.2, 0.4, 0.6 and 0.8ACH	254

Figure	Page
6-29. Simulated and experimental room temperature comparison: ResHB uses ideal control, every room uses experimental hourly average room air temperature as set point without temperature swing, with internal heat gain and ventilation distribution, cases with infiltration rate of 0.2, 0.4, 0.6 and 0.8ACH: (a) Dining room (b) Master bedroom	255
A-1a Analytically calculated zone loads and those calculated by ESP-r for Solar Radiation – Glazed Surfaces test: East, west and south facing window.....	282
A-1b Analytically calculated zone loads and those calculated by ESP-r for Solar Radiation – Glazed Surfaces test: East, west and south facing window (with hourly instantaneous weather data)	283
A-1c Comparison of solar beam irradiance used by ESP-r and Analytical solution	283
A-2 Analytically calculated zone loads and those calculated by ESP-r for Solar Radiation – Window Shading test: south facing window with left side vertical fin	284
A-3 Analytically calculated zone loads and those calculated by ESP-r for the Internal Long Wave Radiation test: emissivity of the external surface = 0.9, emissivity of other surfaces = 0.1	285
A-4 Analytically calculated zone loads and those calculated by ESP-r for the Internal Long Wave Radiation test: emissivity of all surfaces = 0.9	286
A-5 The convective heat input profiles of the test zones used in the VAV and On-Off control tests with ESP-r program	288
A-6 Zone air temperatures predicted by ESP-r program and analytical solution for the VAV control test.....	288
A-7 Zone air temperatures predicted by ESP-r program and analytical solution for the On-Off control test.....	289

NOMENCLATURE

Symbols

c_p	specific heat, Btu/(lb-°F) or J/(kg-°C)
c, n	empirical constants from regression analysis
h	convection coefficient, Btu/h.ft ² or W/m ² K
k	thermal conductivity, Btu/(h-ft-°F) or W/(m-K)
N	the number of cases used in calculating mean bias error
O	observed value, equals the ESP-r predicted loads in our case, Btu/h or W
P	predicted value, equals the RHB predicted loads in our case, Btu/h or W
Q	volume air flow rate, CFM or m ³ /s
T_{master}	master room temperature, °F or °C
$T_{setpoint}$	room temperature set point, °F or °C
T_{slave}	slave room temperature, °F or °C
U	conductance, W/m ² K or Btu/h.ft ²
ρ	density, lb _m /ft ³ or kg/m ³
Δp	pressure difference across the house envelope, Pa
ΔT	difference between the system supply and return air temperature, °C
δT	temperature tolerance used in calculating integrated PPD values, °F or °C

Abbreviations

CLF	Cooling Load Factor
CLTD	Cooling Load Temperature Difference
CTF	Conduction Transfer Functions
DH	Degree Hours
ELA	Effective Leakage Area
ETD	Equivalent Temperature Difference
GLF	Glass Load Factors
HVAC	Heating, Ventilating and Air Conditioning
MBE	Mean Bias Error
PMV	Predicted Mean Vote
PPD	Predicted Percentage of Dissatisfied
RHB	Residential Heat Balance load calculation procedure
SCL	Solar Cooling Load
SHGC	Solar Heat Gain Coefficient
TA	Time Averaging
TETD	Total Equivalent Temperature Difference
TFM	Transfer Function Method

1. INTRODUCTION

Properly designed residential heating, ventilating and air conditioning (HVAC) systems should provide good comfort and high efficiency at minimum cost. Oversized HVAC systems compromise indoor comfort, reduce system efficiency, and increase the initial investment and energy cost. (Khattar et al. 1987; Reddy and Claridge 1993; Neal and O'Neal 1994; Proctor et al. 1995; James et al. 1997). Since load calculation is the main factor affecting the selection of HVAC system capacities, it is essential to use a reliable heating and cooling load calculation procedure to obtain high efficiency and good quality both for the design and energy utilization of a residential HVAC system.

It is important at the outset to define three inter-related but often-confused concepts: heat gain, cooling load, and heat extraction rate. Heat gain is the rate at which energy enters into or is generated within a space. Heat gains can occur in various forms such as solar radiation, heat conduction, internal heat gain, ventilation and infiltration air, etc.

Cooling load is the rate at which energy must be removed from a space to maintain the temperature and humidity at the design values. The space heat gain usually does not equal the space cooling load. This is because the radiant heat gains must first be absorbed by the surfaces enclosing the space and the objects in the space. Only when the surfaces and objects receiving the radiant heat become warmer than the surrounding air,

will some of this energy be transferred to the air by convection and become a part of the cooling load.

The heat extraction rate is the rate at which energy is removed from the space by the cooling and dehumidifying equipment. It equals the space cooling load only if the space conditions are kept constant by the operating equipment. Although the heat extraction rate is usually not calculated for commercial building equipment selection, permissible temperature swings in residential buildings require that this be considered in the development of a residential load calculation procedure.

Since the subject of this validation work is a newly developed residential load calculation procedure based on the heat balance method, it is of interest to consider the background of this procedure. Accompanying the historical development of air conditioning, building heating and cooling load calculations have gone through a continuous development. Romine (1992) gave a short summary of the development of load calculations in ASHRAE (American Society of Heating, Refrigerating and Air-Conditioning Engineers) until 1992. The load calculation development history both in ASHRAE and CIBSE (Chartered Institution of Building Services Engineers) is also reviewed by Rees, et al. (2000).

1.1 Non-residential Cooling Load Calculation Procedures

For nonresidential (commercial and industrial) applications, three methods were presented for calculating cooling loads in the 1997 *ASHRAE Handbook of Fundamentals*. These are the transfer function method (TFM), the cooling load temperature

difference/solar cooling load/ cooling load factor (CLTD/SCL/CLF) method, and the total equivalent temperature difference/time averaging (TETD/TA) method.

The three methods are directly or indirectly an approximation of the heat balance method (to be discussed in more detail later). This is because calculating cooling load for a space inevitably involves the calculation of a conductive, convective, and radiative heat balance for each room surface and a convective heat balance for the room air. Exact solutions of space cooling load by heat balance procedures requires a rigorous and laborious calculation of the heat balance equations and is impractical for widespread or routine use without the speed of modern digital computers (ASHRAE 1997). Due to the limited computer capability available in earlier days, various simplified forms of the heat balance procedure were developed for routine cooling load calculation purposes.

As an ongoing effort in developing cooling load calculation methods, ASHRAE funded a research project entitled “Advanced Methods for Calculating Peak Cooling Loads (RP-875)” in 1996. As the goal of this project, two new methods -- the Heat Balance (HB) method (Pedersen, et al. 1997) and the Radiant Time Series (RTS) method (Spitler, et al. 1997) -- have been developed. As mentioned before, the heat balance concept is the foundation of the three simplified methods recommended by the 1997 *ASHRAE Handbook of Fundamentals*. It has been applied in many energy calculation programs in one form or another for many years. It was first implemented in NBSLD (Kusuda 1967), and has also been applied to BLAST and TARP by Walton (1981, 1983).

The heat balance method is introduced for load calculation purposes because it has the potential to be the most accurate method for calculating space heating and cooling

loads and may be the most understandable method to practicing engineers. It accounts for all energy flows in their most basic, fundamental form and does not impose any simplifications on the solution technique (Strand et al., 1999). It calculates space heating or cooling load by solving the heat balance equations for each of the outside and inside zone surfaces and for the zone air. Transient conduction heat transfer through building fabric is estimated by applying conduction transfer functions. Radiant and convective heat exchanges at both external and internal surfaces are treated separately, with internal radiant exchange calculated by the method of mean radiant temperature with balance (Walton 1980). The heat balance method is also the first ASHRAE load calculation method that completely relies on computer implementation (Rees, et al. 2000).

Derived from the heat balance method, the radiant time series method is the new ASHRAE simplified cooling load calculation method for non-residential buildings, effectively replacing the TFM, TETD/TA and CLTD/SCL/CLF methods (Spitler, et al. 1997). Sharing many heat transfer sub-models with the heat balance method, the radiant time series method is most similar to the transfer function method and can be shown equivalent in some aspects (Spitler and Fisher 1999).

Experimental validation of both the heat balance method and the radiant time series method has been done in test cells at Oklahoma State University (Chantrasrisalai, et al. 2003; Iu, et al. 2003). As a result of the development and validation work, the heat balance method and the radiant time series method are presented in the 2001 *ASHRAE Handbook of Fundamentals*, superseding the TFM, TETD/TA and CLTD/SCL/CLF methods.

1.2 Residential Cooling Load Calculation Procedures

1.2.1 Characteristics of Residential Load Calculation

In comparison to the nonresidential applications, the situation with the residential cooling load calculation is somewhat different because of some unique features inherent in residential buildings.

Load patterns of residences differ significantly from those of commercial structures because of different building scale, construction, occupancy, and controls. Compared to commercial or industrial buildings, residential buildings are usually smaller, and their constructions usually have less thermal mass (product of mass and specific heat). Loads from the residential envelope usually compose a much greater fraction of the total building load. The internal heat gains of residences, especially those from occupants and lights, are relatively small. Current ASHRAE design procedure (ASHRAE 1997) assumes that residences usually will be occupied and conditioned for 24 hours a day, every day during the heating and cooling seasons.

Residential load calculation usually must be done with a quick and simple method. This limits the usage of whole building energy analysis programs (such as DOE-2, BLAST and EnergyPlus) in the residential realm. Large, sophisticated programs usually allow the possibility of comprehensively describing the buildings. For example, an energy analysis program may allow the user to specify fairly detailed information on the cracks and openings of a building in order to compute the infiltration load. This level

of input can be overwhelming for the typical residential HVAC system designer. Instead, a method that allows simple input is usually preferred.

In general, most single-family detached houses use constant air volume systems with one return and a single central thermostat to control the temperatures of all rooms (Figure 1-1). This type of temperature control necessarily allows temperatures to fluctuate through out the house. It usually results in temperature swings of several degrees Fahrenheit between different rooms of a house, which is generally considered acceptable from the standpoint of the occupants' comfort. These temperature swings also result in inter-zone heat transfer and heat storage in building elements, which have the effect of moderating peak loads. Inter-zone airflow driven by the air distribution system or thermal buoyancy also produces load-moderating effects in residences. These thermal interactions, including inter-zone heat transfer and inter-zone air flow, contribute to the result that the peak or peak total load of the building is significantly less than the sum of peak room loads. For individual units in multifamily buildings that do not have exposures facing all directions, the load-moderating effect is not as significant as in the single-family detached houses, and the loads are usually closer to the sum of the room peak loads. With the inter-zone thermal communication as an important feature of residential buildings, the capability to simultaneously model all zones to reflect this feature becomes one of the primary requirements of the detailed reference tool used to evaluate a residential load calculation procedure (See Chapter 4).

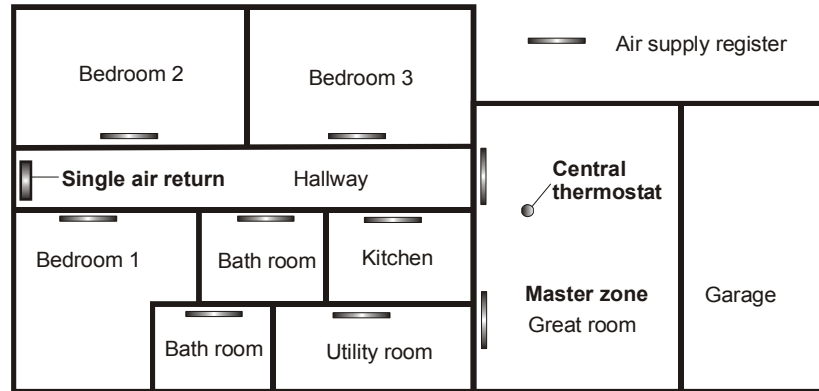


Figure 1-1 Schematic floor plan for a single family detached house with master-slave control

In addition to thermal communication, the control strategy becomes another important issue in this case. If the zone containing the central thermostat is called the “master” zone (Figure 1-1), and other zones are called “slave” zones accordingly, this problem can then be briefly described as the master-slave zone control problem. Because of the single thermostat control, the temperatures generally cannot be simultaneously controlled at the design set point in all rooms. The master zone temperature can be well controlled by the thermostat. The slave zone air temperatures will float depending on the relation between the zone load and the output of the air conditioning system. The slave zones may maintain reasonable temperatures if they have load profiles similar to that of the master zone. Poor zone configurations can result if the slave zones have load profiles significantly different than the master zone. This “master-slave” zone control problem is another unique feature of the residential load calculation.

All the features discussed above make the residential load calculation a unique problem. The load calculation techniques developed for commercial buildings therefore cannot be applied directly to residential load calculation.

1.2.2 Prior Residential Cooling Load Calculation Procedures

Prior to the development of the Residential Heat Balance (RHB) load calculation procedure, there were three common procedures in use for residential cooling load calculations. One is the procedure recommended by ASHRAE. Fully described in Chapter 28 of the *ASHRAE 2001 Handbook of Fundamentals*, this procedure is primarily based on research project RP-342 of ASHRAE (McQuiston et al. 1984). The second is the procedure presented in Manual J, published by the Air Conditioning Contractors of America (ACCA), including the widely used Manual J Seventh Edition (Rutkowski 1986) and Manual J Eighth Edition (Rutkowski 2002). Sharing an ASHRAE heritage, Manual J is based on pre-RP-342 data, and in some cases, techniques that date from the 1950s. The third is the procedure stated in Standard CAN/CSA-F280-M90 (CSA 1990). Maintained by the Heating, Refrigerating, and Air-Conditioning Institute of Canada (HRAI), it is actually an adaptation of the ASHRAE procedure to Canadian use.

Though differing in many details, this family of methods uses the same general approach to residential load calculation. For cooling load calculations, cooling load temperature differences (CLTD, or equivalent temperature differences (ETD)) and glass load factors (GLF) are used since peak cooling conditions occur intermittently for different rooms during several hours of the day, and buildings do not reach steady state. Here, the CLTD is a purposely defined and pre-calculated effective temperature difference so that the steady state formulation can be used for cooling load from opaque surfaces. The GLF is the effective cooling load produced by a unit area of glazing. It is defined and generated for the same purpose as the CLTD. The values of CLTD and GLF vary with building construction, orientation, environmental climate, and residence type.

With CLTD and GLF pre-calculated, the cooling load for each opaque element is computed as the CLTD multiplied by its U-factor and area. Cooling load from fenestration gain is computed as the GLF multiplied by the glazing area. The cooling load of the building fabric is then obtained by summing up cooling loads for opaque elements and glazing surfaces.

The CLTD/GLF form of the cooling load calculation is actually an application of the CLTD/SCL/CLF method in residential buildings. It is not only conceptually clear but also simple to implement, in that each building element creates a load per unit area and only an accumulation of component loads is required. However, this “sum up the component loads” approach is an approximation considering the fact that the real load in the conditioned space is a combined effect of component gains. Although this approximation is generally accurate and conservative, consideration of radiant heat transfer, heat storage effects in the space and the possibility that some heat gains are reflected or conducted back out again (as explained by Rees, et al. 1998) may cause this approximation to be inordinately conservative.

Except Manual J 8th edition (which requires an evaluation of the design-day fenestration gain profiles), all prior methods use single design condition in the cooling load calculation. The single design-condition cooling load calculation has long been problematic. To avoid over-predicting zone loads with the “sum up the component loads” approach and account for heat gain diversity (heat gains generally occur at different times over the day), semi-empirical adjustments such as multi-hour averaging were used to derive the cooling load factors in prior methods. However, for multi-family units with

limited exposure (apartments), it is more appropriate to use the “sum up the component loads” approach, as the dominant fenestration gains peak simultaneously in this case. To deal with such configurations, prior methods have used alternative factors and/or adjustments. User judgment is required to select the appropriate application.

There is also concern about the accuracy in terms of the derivation of the CLTD/GLF values. The CLTD/GLF values are derived based on the cooling loads calculated by the transfer function method, which is already an approximation to the heat balance method. (The Heat Transfer Multipliers (HTM) in *ACCA Manual J* are derived from the ETD or CLTD values (which are based on the TFM method) recommended by the *ASHRAE Handbook of Fundamentals* (1985 for the 7th Edition, 1989 and 1997 for the 8th Edition), supplemented by information from other sources that the manual does not list.) The approximate nature of the transfer function method and its associated errors are therefore unavoidably brought into the results derived from this method. With the development of the computer based heat balance load calculation procedure, there is no apparent reason why this most fundamental method should not be used directly to derive the CLTD/GLF values (if it is still needed) instead of the transfer function method.

It is also problematic to estimate other important component loads such as infiltration load. The documentation on air-change method of infiltration is nearly nonexistent (ASHRAE RP-342, 1984). The widely used crack length methods require an unreasonably large amount of input for a simplified method (Spitler 2000). Its accuracy depends on the accuracy of the air leakage data for individual buildings and the designer’s experience. The ASHRAE method uses the simple mathematical linear model

(Bahnfleth et al. 1957; Coblenz and Achenbach 1963) to estimate the infiltration rate, which relates the air changes per hour as a linear function of the wind velocity and the indoor-outdoor design temperature difference (Details can be found in ASHRAE RP-342, 1984).

Another concern regards the validation of the prior procedures. Although the evaluation of a load calculation procedure can be very comprehensive, time-consuming and expensive (if empirical test is performed), the validity of a load calculation procedure is very important. Unfortunately, none of the prior procedures has been thoroughly evaluated and validated since their development. Systematic testing of the prior procedures is not documented in the literature.

In summary, the formulation of the prior residential cooling load calculation procedures is satisfactory for most residential buildings. However, problems and questions exist concerning the accuracy of the resulting loads, the method of deriving the CLTD and GLF values, the method of estimating some important component loads, and the validity of the prior methods. A new heat balance based residential cooling load calculation procedure is highly desirable. In the development of the new procedure, attention must be paid to consider and model the inter-zone thermal interactions and master-slave zone controls. It is also desirable that the new procedure be well tested and the system design resulted from the new procedure be carefully evaluated.

1.2.3 Heat Balance Based Residential Cooling Load Calculation Procedure

In response to the problems of the prior procedures, ASHRAE sponsored a research project (1199-RP) “Updating the ASHRAE/ACCA Residential Heating and Cooling Load Calculation Procedures and Data” (Barnaby et. al. 2004). In this project, a new residential loads calculation procedure - Residential Heat Balance (RHB) – was developed. RHB is a detailed heat balance based procedure. It requires computer execution, as the room-by-room hourly design-day simulation used in this procedure is computationally extensive. The hourly design-day simulation eliminates issues of gain diversity that are problematic in prior procedures, which use single design condition. The average/peak distinction used in prior procedures is no longer necessary, as the design load is simply the peak hourly load.

For calculation of sensible cooling load, RHB applies the general approach of the ASHRAE Heat Balance (HB) method. As the heat transfer equations are solved in their most basic, fundamental form in the heat balance method, prior concerns about the “sum up the component loads” approximation are eliminated. The concern regarding the approximate accuracy of the transfer function method, which is used in the derivation of the CLTD/GLF factors of the prior methods, is also eliminated. Considering the unique features of residential load calculation, RHB includes algorithms for calculating sensible cooling loads with temperature swing and addresses the master-slave zone control problem.

As part of 1199-RP, the ResHB computer program was developed as the reference implementation of the RHB procedure. The ResHB source code is derived from the ASHRAE Loads Toolkit (Pedersen et. al. 2001). An additional utility program, RHBGen, was also developed to automatically generate and run parametrically varied ResHB cases for testing and research purposes.

The RHB development also involved review, refinement, and extension of the ASHRAE Loads Toolkit models. Component models and assumptions used for RHB are considered appropriate for residential application. For example, the AIM-2 infiltration model was selected for RHB (Walker and Wilson 1990, 1998, and “enhanced model” in Chapter 26, ASHRAE 2001). An algorithm was developed to derive a homogeneous layer that corresponds to a framed construction layer, which is common in residential buildings. Details of the component models and assumptions of RHB are documented in the project final report (Barnaby et. al. 2004) and are summarized in the literature review section (see Chapter 2).

One concern left and deserving detailed investigation is the validity of RHB. As a newly developed cooling load calculation procedure, no validation has been conducted prior to the work described in this dissertation. Independent and objective assessment of RHB is clearly necessary in view of the important effect it will have on the residential HVAC system design.

Theoretically, RHB includes the most fundamental heat balance method, which potentially is the most accurate method. However, individual heat transfer mechanisms implemented in ResHB need to be tested. The algorithms included in RHB to handle

temperature swing and master-slave zone control need to be checked. Cooling loads calculated by ResHB and hence the system capacity and design need to be evaluated. Integrated performance of the component models in ResHB also needs to be validated. In a word, a thorough validation of RHB is highly desirable and has not been done yet.

1.3 Objective

Therefore, the objective of this research is to conduct a systematic validation and evaluation of the new heat balance based residential cooling load calculation procedure - RHB. Three types of testing methods will be applied to validate RHB: inter-model comparison, analytical verification and experimental validation. For inter-model comparison, a detailed heat balance based computer program will be selected as a reference tool to evaluate RHB. A parametric analysis tool will be developed for systematic and automatic implementation of large amounts of inter-model comparisons. Cooling loads calculated by ResHB will be compared to that calculated by the reference tool. System designs resulting from ResHB will also be evaluated by detailed simulations with the reference tool. Inter-model validation of RHB is discussed in detail in Chapter 4.

For analytical verification, RHB will be tested against an analytical verification test suite that the author has previously developed together with other colleagues in Oklahoma State University: the Analytical Verification Test Suite for Whole Building Energy Simulation Programs -- Building Fabric (ASHRAE 1052-RP, Spitler, et al. 2001). The test suite consists of sixteen individual tests, each with the objective to test the ability of a building energy simulation program to model a particular heat transfer phenomena, including convection, conduction, solar radiation, long wave radiation and infiltration.

Tests appropriate for application to RHB will be done and analysis and diagnosis will be made based on the test results. Analytical verification of RHB is presented in Chapter 5.

Finally, appropriate residential experimental data will be used to validate RHB. Experimental data will be obtained from a well-instrumented house located in Fort Wayne, IN. ResHB input files will be created for the house and ResHB-calculated cooling loads and room temperatures will be compared to measured data. Experimental validation of RHB is discussed in Chapter 6.

2. LITERATURE REVIEW

The literature review in this chapter includes two parts. First, a review is given for the subject of this research work – the heat balance based residential cooling load calculation procedure. The purpose is to gain a full knowledge and familiarity of RHB, with regards to its basic structure and algorithm, theoretical principles and assumptions, and component models. Second, a review is given for the general validation methods of building thermal simulation programs. The purpose is to identify possible methodologies and available tools for validating cooling load calculation programs.

2.1 Heat Balance Based Residential Cooling Load Calculation

Procedure

The recent ASHRAE research project (1199-RP) “Updating the ASHRAE/ACCA Residential Heating and Cooling Load Calculation Procedures and Data” (Barnaby et al. 2004) developed a new detailed heat balance based residential loads calculation procedure: Residential Heat Balance (RHB). For calculation of sensible cooling load, RHB applies the general approach of the ASHRAE Heat Balance (HB) method, based on room-by-room 24-hour design-day simulation. RHB includes algorithms for calculating sensible cooling loads with temperature swing and addresses the master / slave zone control problem that is unique for residential load calculation.

As part of 1199-RP, the ResHB computer program was developed as the reference implementation of the RHB procedure. The ResHB source code is derived from the ASHRAE Loads Toolkit (Pedersen et al. 2001). An additional utility program, RHBGen, was also developed to automatically generate and run parametrically varied ResHB cases for testing and research purposes. As will be described later in Chapter 4, RHBGen helps running all the inter-model comparison cases on the ResHB side. Documentation of ResHB and RHBGen is included in the 1199-RP final report (Barnaby et al. 2004).

In this section, theoretical principles of RHB - the heat balance method – are summarized first. Calculation algorithms, modeling assumptions and component models of RHB and their implementation in ResHB are described second.

2.1.1 Heat Balance Method for Cooling Load Calculation

As mentioned in the introduction section, heat balance method has been applied in many energy calculation programs in one form or another for many years. It was first implemented in NBSLD (Kusuda 1967), and has also been applied to BLAST and TARP by Walton (1981, 1983). In ASHRAE Research Project 875, the heat balance method was first described in a form applicable to cooling load calculations. Details of the method are described in Pedersen et al. (1997, 1998, 2001), and Chapter 29 of *ASHRAE Handbook of Fundamentals* (2001). It is summarized here for completeness.

2.1.1.1 Heat Balance Model Elements

The heat balance method is first of all based on some model assumptions, which assume that:

- The zone air is well mixed and has a uniform temperature
- The surfaces of the zone have uniform surface temperatures, uniform long-wave (LW) and short-wave (SW) irradiation, diffuse radiating surfaces and one-dimensional heat conduction within.

Based on these assumptions, the heat balance model involves four distinct elements: Outside heat balance, wall conduction process (for transparent surfaces, the conduction process is accompanied by solar absorption and transmission), inside heat balance and air heat balance. Each of these elements is briefly discussed below. Note that each element has several heat transfer processes, to which particular models can be applied. These models are not to be enumerated here. Details of available models can be found in the ASHRAE Loads Toolkit (Pedersen, et al. 2001), from which the residential heat balance cooling load calculation procedure is derived.

Outside Heat Balance

The outside heat balance for opaque surfaces has four heat exchange processes, of which the summation of the heat fluxes should be zero:

$$q_{\text{sol}}'' + q_{\text{LWR}}'' + q_{\text{conv}}'' - q_{\text{ko}}'' = 0 \quad (2.1)$$

where:

$q''_{\alpha sol}$ = absorbed direct and diffuse solar radiation heat flux, W/m²

q''_{LWR} = net long-wave radiation flux exchange with the air and surroundings, W/m²

q''_{conv} = convective flux exchange with outside air, W/m²

q''_{ko} = conductive heat flux into the wall, W/m²

All terms are positive for net flux to the surface except the conduction term, which is traditionally taken to be positive in the direction from outside to inside of the wall. For transparent surfaces, the absorbed solar component would appear in the conduction process (to be discussed next) instead of at the outside surface. It would also split into an inward- and an outward- flowing fraction and participate in the inside and outside surface heat balance.

Wall Conduction Process

For building load calculation purpose, it is usually appropriate to assume the wall conduction process as a one-dimensional transient process through multi-layer construction, with each layer material considered homogeneous and having constant thermal properties. The governing equation for transient one-dimensional heat conduction, assuming constant thermal properties, is expressed as:

$$\frac{\partial^2 T(x,t)}{\partial x^2} = \frac{1}{\alpha} \frac{\partial T(x,t)}{\partial t} \quad (2.2)$$

where

T = the wall temperature as a function of position (x) and time (t), K

$\alpha = \frac{k}{\rho C_p}$ is the thermal diffusivity of the layer material, m²/s

k = thermal conductivity of the layer material, W/(m-K)

ρ = density of the layer material, Kg/m³

C_p = specific heat of the layer material, J/(kg-K)

This equation is typically coupled with Fourier's law of conduction that relates the heat flux at any position and time to temperature as follows:

$$q''(x,t) = -k \frac{\partial T(x,t)}{\partial x} \quad (2.3)$$

Analytical solutions to equation (2.2) and (2.3) exist for a single homogeneous layer. For a multi-layer slab, the solution becomes extremely tedious. Possible ways to model this process are:

- Numerical finite difference
- Numerical finite element
- Transform methods
- Time series methods

While each of these methods has advantages over the others in various applications, traditionally, building thermal simulations have used either time series based or finite difference based methods. In the ASHRAE Loads Toolkit (Pedersen, et al. 2001), from which the residential heat balance cooling load calculation procedure is

derived, a time series method using conduction transfer functions is used because of the computational time advantage.

Inside Heat Balance

The inside heat balance involves four coupled heat transfer components: 1) wall conduction, 2) convection to the inside air, 3) short-wave radiation absorption and reflectance and 4) long-wave radiant interchange. The short-wave radiation includes transmitted solar radiation from windows and emittance from internal sources such as lights. The long-wave radiation interchange includes those from all other zone surfaces and those from internal sources such as equipment and people. The inside heat balance for each surface is written as (all terms are positive for net flux to the surface):

$$q''_{LWX} + q''_{SW} + q''_{LWS} + q''_{ki} + q''_{sol} + q''_{conv} = 0 \quad (2.4)$$

where:

$$q''_{LWX} = \text{net long wave radiant exchange flux between zone surfaces, W/m}^2$$

$$q''_{SW} = \text{net short wave radiation flux to surface from lights, W/m}^2$$

$$q''_{LWS} = \text{long wave radiation flux from equipment in zone, W/m}^2$$

$$q''_{ki} = \text{conduction flux through the wall, W/m}^2$$

$$q''_{sol} = \text{transmitted solar radiation flux absorbed at surface, W/m}^2$$

$$q''_{conv} = \text{convective heat flux to inside air, W/m}^2$$

Air Heat Balance

In the air heat balance formulated for cooling load calculation purposes, it is usually assumed that the capacitance of the zone air can be ignored and the zone air is at quasi-steady state at each simulation time step such as an hour. Therefore, the air heat balance reduces to a form similar to that of the surface heat balances—a summation of four heat transfer terms equal to zero (all terms are positive for net heat flow to the air):

$$q_{conv} + q_{CE} + q_{IV} + q_{sys} = 0 \quad (2.5)$$

where:

q_{conv} = convection heat transfer from the inside zone surfaces, W

q_{CE} = convection from internal sources, i.e. people, lights, equipment, etc., W

q_{IV} = sensible load due to infiltration and ventilation, W

q_{sys} = heat transfer to/from the HVAC system, W

2.1.1.2 Mathematical Description of Heat Balance Procedure

The above section describes the physical process of the heat balance model conceptually. This section introduces the basic equations used in the heat balance procedure mathematically. All information is based on the ASHRAE Loads Toolkit (Pedersen, et al. 2001), from which the residential heat balance cooling load calculation procedure is derived.

Conduction Process

As mentioned above, the ASHRAE Loads Toolkit formulates the wall conduction process using Conduction Transfer Functions (CTFs), which relate conductive heat fluxes to the current and past surface temperatures and the past heat fluxes. The basic form for the inside heat flux is as follows:

$$q_{ki}''(t) = -Z_0 T_{si,t} - \sum_{j=1}^{nz} Z_j T_{si,t-j\delta} + Y_0 T_{so,t} + \sum_{j=1}^{nz} Y_j T_{so,t-j\delta} + \sum_{j=1}^{nq} \Phi_j q_{ki,t-j\delta}'' \quad (2.6)$$

For the outside heat flux, the form is:

$$q_{ko}''(t) = -Y_0 T_{si,t} - \sum_{j=1}^{nz} Y_j T_{si,t-j\delta} + X_0 T_{so,t} + \sum_{j=1}^{nz} X_j T_{so,t-j\delta} + \sum_{j=1}^{nq} \Phi_j q_{ko,t-j\delta}'' \quad (2.7)$$

where:

X_j = Outside CTF coefficient, $j= 0,1,\dots,nz$, W/m^2K

Y_j = Cross CTF coefficient, $j= 0,1,\dots,nz$, W/m^2K

Z_j = Inside CTF coefficient, $j= 0,1,\dots,nz$, W/m^2K

Φ_j = Flux CTF coefficient, $j = 1,2,\dots,nq$

t = time, s

δ = time step, s

T_{si} = Inside face temperature, °C

T_{so} = Outside face temperature, °C

q_{ki}'' = conduction heat flux on outside face, W/m^2

q_{ko}'' = conduction heat flux on inside face, W/m^2

The subscript following the comma indicates the time period for the quantity in terms of the time step δ . Note that the first terms in the series (those with subscript 0) have been separated from the rest in order to facilitate solving for the current temperature in the solution scheme.

There are two main methods for calculating conduction transfer functions: the Laplace Transform method and the State Space method. Detailed documentation and Fortran Modules are available for both methods in the ASHRAE Loads Toolkit.

Heat Balance Equations

The heat balance processes for the thermal zone are formulated for a 24-hour steady periodic condition. The primary variables in the heat balance equations are the inside face temperatures, the outside face temperatures, and the sensible cooling load at each of the 24 hours. Assigning i as the surface index and j as the hour index, then, the primary variables are:

$T_{so,i,j}$ = outside face temperature, ($i=1, 2, \dots$ number of surfaces; $j=1, 2, \dots 24$), °C

$T_{si,i,j}$ = inside face temperature, ($i=1, 2, \dots$ number of surfaces; $j=1, 2, \dots 24$), °C

$q_{sys,j}$ = sensible cooling load, ($j=1,2, \dots 24$), W

Equation (2.1) is combined with equation (2.7) to solve for T_{so} to produce equations applicable at each time step for each surface:

$$T_{so_{i,j}} = \frac{-\sum_{k=1}^{nz} T_{si_{j-k}} Y_{i,k} + \sum_{k=1}^{nz} T_{so_{i,j-k}} X_{i,k} - \sum_{k=1}^{nq} \Phi_{i,k} q''_{ko_{i,j-k}} + q''_{\alpha so_{i,j}} + q''_{LWR_{i,j}} - T_{si_{i,j}} Y_{i,0} + T_{o_j} h_{co_{i,j}}}{-X_{i,0} + h_{co_{i,j}}} \quad (2.8)$$

where:

T_o = outside air temperature, °C

h_{co} = outside convection coefficient, obtained from $q''_{conv} = h_{co} (T_o - T_{so})$, W/(m²-K)

Equation (2.4) is combined with equation (2.6) to solve for T_{si} to produce equations applicable at each time step for each surface:

$$T_{si_{i,j}} = \frac{T_{so_{i,j}} Y_{i,0} + \sum_{k=1}^{nz} T_{so_{i,j-k}} Y_{i,k} - \sum_{k=1}^{nz} T_{si_{i,j-k}} Z_{i,k} + \sum_{k=1}^{nq} \Phi_{i,k} q''_{ki_{i,j-k}} + T_{a_j} h_{ci_{i,j}} + q''_{LWS} + q''_{LWX} + q''_{SW} + q''_{sol}}{Z_{i,0} + h_{ci_{i,j}}} \quad (2.9)$$

where:

T_a = zone air temperature, °C

h_{ci} = inside convection coefficient, obtained from $q''_{conv} = h_{ci} (T_a - T_{si})$, W/(m²-K)

Note that in Equations (2.8) and (2.9), the opposite surface temperature at the current time appears on the right hand side. The two equations can be solved simultaneously to eliminate that variable. Depending on the order of updating the other terms in the equations, this can have a beneficial effect on the solution stability.

The remaining equation comes from the air heat balance, Equation (2.5). It determines the cooling load q_{sys} at each hour:

$$q_{sys_j} = \sum_{i=1}^{12} A_i h_{c,i} (T_{si,j} - T_{a_j}) + q_{CE} + q_{IV} \quad (2.10)$$

where:

A = surface area, m²

The convective heat transfer term in equation (2.10) is expanded to show the relationship between the surface temperatures and the cooling load. Note that equation (2.10) is formulated this way in the cooling load calculation procedure implemented in the ASHRAE Loads Toolkit. But, it may also be formulated other ways. For example, it may be formulated to give zone air temperature with or without system input, as in the case when temperature swing is considered in RHB.

2.1.1.3 Solution Method of Heat Balance Procedure

The solution method of the heat balance procedure implemented in the ASHRAE Loads Toolkit is a basic iterative, or successive substitution method, which is inherited in the residential heat balance cooling load calculation procedure with some modifications and extensions. The Toolkit implementation consists of a series of initial calculations that proceed sequentially, followed by a double iteration loop. The initial calculations include the following:

- Initialize the areas, thermal properties, and surface temperatures for all surfaces for 24 hours.
- Calculate incident and transmitted solar flux for all surfaces for 24 hours.
- Distribute transmitted solar energy to all inside surfaces for 24 hours in a prescribed manner.

- Calculate internal load quantities for 24 hours.
- Distribute long-wave, short-wave, and convective energy from internal loads to all surfaces for 24 hours in a prescribed manner.
- Calculate infiltration and ventilation loads for 24 hours.

After the above initial calculations, the iterative solution scheme is as follows:

Repeat Day

For Hour = 1 to 24

For Iteration = 1 to Maximum Iterations per Hour

For Surface = 1 to Number of Surfaces

Evaluate Equation (2.8)

Evaluate Equation (2.9)

Next Surface

Evaluate Equation (2.10)

Next Iteration (or until Hour results converge)

Next Hour

Until day converged

There are two iteration loops in this solution scheme. The outer loop, or the day iteration, is necessary to arrive at the steady periodic response and thus eliminate any initial condition influence on the solution. This is a result of the fact that conduction is transient and inherently slower than other thermal processes. The inner loop, or the hour

iteration, is necessary to allow the radiation balance between surfaces. This is a result of the fact that not all surfaces are solved simultaneously but successively.

It should be noted that the heat balance procedure requires a fair amount of input information for the thermal zone, such as the design conditions, details about the walls and windows, roof and floor information, thermal mass, internal heat gains, etc. A more detailed list can be found in Pedersen et al. (1997) and in Chapter 29 of *ASHRAE Handbook of Fundamentals* (2001) and will not be repeated here.

2.1.2 Heat Balance for Residential Applications

The Residential Heat Balance method is a specialized application of the ASHRAE Heat Balance method. Compared to the ASHRAE Heat Balance method, RHB has the following changes:

- *Multi-room, multi-zone, and multi-system.* Independent heat balances are performed for each room. Because of the simplified geometric input (where surface areas and orientations are known but their positions are not), room adjacencies required by a detailed inter-room heat transfer calculation are not available. However, as shown in the calculation sequence below, inter-room references are available for the current hour during a simulation, allowing room temperatures in one room being used as the boundary condition for another room. Zones and systems are accounting structures to which loads are accumulated to provide overall results.

- *Specialized algorithms.* Specialized algorithm was implemented to handle temperature swing and master / slave control.
- *Residential models and assumptions.* Component models and assumptions used for RHB are considered appropriate for residential application.
- *Simple latent cooling procedures.* Latent load can be estimated from moisture gain from infiltration, ventilation, duct leakage, and occupants.

The remaining parts of this section briefly describe the above aspects of RHB. More details can be found in Barnaby et al. (2004).

2.1.3 Calculation Algorithms

As discussed in the introduction section, residential air conditioning applications use constant volume systems controlled by a single thermostat (master/slave control). Typically a thermostat located in one room (master room) controls system output for multiple rooms (slave rooms).

As a result, the temperature of the master room can be well controlled. The temperatures of the slave rooms will float depending on the relation between their particular load profiles and the output of the air conditioning system. Usually their temperatures will not be held at the set point even when the system is operating. This hour-to-hour temperature variation, or temperature swing, has a significant moderating effect on peak loads, due to heat storage in building components.

The level of the load moderating effect caused by the master/slave control and temperature swing varies in different residence categories. It is more significant in single-

family detached houses that have exposed walls in four directions than in multi-family houses that have exposures in only one or two directions.

The master/slave control and the resulting temperature swing have long been recognized as a major consideration in residential cooling load calculations. In prior methods, load factors were derived using semi-empirical adjustments such as multi-hour averaging to account for the peak load moderating effects. In RHB, specialized algorithms were developed to model master/slave control and temperature swing.

As an application of the heat balance method, RHB basically is a design day procedure that requires iteration to find the steady-periodic solution at which all heat flows correctly balance. In order to handle temperature swing and master/slave control, RHB has the additional requirement of finding loads under floating temperature conditions, as described below.

2.1.3.1 Calculation Sequence and Convergence Criteria

The basic RHB load calculation sequence is:

repeat swing

repeat day

for hour = 1 to 24

for all rooms

repeat

for all surfaces

perform surface heat balance

end for surfaces
perform air heat balance
until room convergence for current hour
end for rooms
end for hours
until day convergence
determine room supply air flow rates for next swing iteration
until swing convergence

Note that the goal of the RHB procedure is to find the room-by-room capacity required to meet the combination of design condition with permitted temperature swing. (The cooling load used for sizing the capacity of the central air conditioning system is the sum of all peak room loads. The room-by-room capacities are also used to design the air distribution system.) Temperature swing occurs when the cooling capacity for a particular room is less than that required to hold that room at the set point. (The cooling capacity could be less than that required in two cases: 1. When the system is operating but does not have enough capacity. 2. When the system is turned off by the thermostat located in the master room, but the slave rooms still need cooling.)

In the calculation sequence shown above, the outer loop handles temperature swing (discussed below). The swing search algorithm adjusts the supply air flow rate to each room and repeats the entire calculation until the permitted temperature swing is reached. Note that the hour loop is outside the room loop, so that current hour conditions are available for all rooms for inter-room references.

The following criteria were used in ResHB to determine whether the solution has converged:

- Hour. The convergence criterion of the hour calculation is: For each room, the sum of the absolute change in surface and air temperatures is less than 0.0005 °K (0.0009 °F).
- Day. The convergence criteria of the day calculation are: For all rooms, a) the fractional difference between inside and outside surface flux summed over the day is less than 0.005 and b) the area-weighted total absolute temperature change for all surfaces plus air is less than 0.0002 °K (0.00036 °F). Note that the all-room requirement means that some rooms will be iterated beyond this point.
- Swing. The convergence criterion of the swing search is: For all rooms, swings are within 0.01 °K (0.018 °F) of specified. (RHB allows a different swing specified for each room.) Again, the all-room requirement means extra iteration for some rooms.

2.1.3.2 Temperature Swing

When temperature swing is permitted, ResHB uses a secant method search algorithm to search for the load. The calculations are based on varying system air volume flow rate with an assumed supply air temperature. The calculation sequence for the swing search is:

- The required cooling air flow rate is found first for the 0 swing situation (that is, maximum available air supply volume is unlimited and room temperature held at the set-point or floating below it with no supply air flow).
- This maximum supply air flow rate is then reduced by 20% per °K (11% per °F) of target swing and the room is calculated again.
- The supply air flow rate is iteratively adjusted in proportion to the error in temperature swing, as indicated by the secant method.

This algorithm is reported to be extremely efficient. Convergence to within 0.01 °K (0.018 °F) of the target swing usually occurs in less than 10 cycles. However, it is also reported that specific room characteristics can cause the search to fail.

2.1.3.3 Master/slave Control

RHB models master/slave control with the temperature swing algorithm. The problem is to find the peak slave room supply air volume flow rate so that the maximum room temperature is the set point plus permitted temperature swing (the swing could be zero). At each swing iteration, the peak flow rate is adjusted using the temperature swing search described above (the search is used even if the specified swing is zero). Then the flow rates for all hours are set by applying the master room profile. (By definition, a slave room has the same supply air flow rate profile as the master room). The next day iteration proceeds without any further adjustment of air flow rate. It is reported that when the master and slave rooms have significantly different load profiles, sub-cooling can occur in the slave rooms.

2.1.4 Component Models

This section describes the main component models that were refined or extended during the RHB development. Other component models are inherited from the ASHRAE Loads Toolkit and can be found in its documentation (Pedersen et al. 2001).

2.1.4.1 Inside Surface Convection Coefficients

The choice of inside surface convection coefficients is very important as it directly affects the cooling load. (The cooling load is the total convective heat transfer from all internal surfaces plus convective gain from other sources). The default model for inside surface convection coefficients in ResHB is a variant of the TARP simple model (Walton 1983). For each hour, the coefficient used is the system-run-fraction-weighted combination of the “sys off” and “sys on” values. The “sys off” values are those from the TARP simple model. To improve convergence stability, the transition between heat flow up and down values is made linearly over 2°C (3.6°F), rather than abruptly. The “sys on” value was chosen to be 5 W/m²K (0.88 Btu/h-ft²-F) for all surfaces, based on analysis of experimental data from ASHRAE research projects 529-RP and 664-RP for air change rates of approximately 8 ACH (typical for residential systems). Table 2-1 shows the “sys off” and “sys on” values for the default model.

Table 2-1. The “sys off” and “sys on” values for default model of inside surface convection coefficients (W/m²K) in ResHB

	Ceiling		Wall	Floor	
	Heat flow up	Heat flow down		Heat flow up	Heat flow down
Sys on	5.000	5.000	5.000	5.000	5.000
Sys off	4.043	0.920	3.078	4.043	0.920

In addition to the default model, ResHB also has optional models of fixed convection coefficients (1.250 ceiling, 4.679 wall, 4.370 floor (all W/m²K)), TARP detailed model and Fisher model (documented in Pedersen et al. 2001).

2.1.4.2 Elevation Effects on Convective Heat Transfer

During the development of RHB, efforts have been made to study the effect of elevation on convection coefficients. The investigation showed that applying an elevation correction to convection coefficients has a significant effect on predicted loads for high elevation locations (about 13% for Denver). A simple linear approximation was developed and used in RHB:

$$h = h_0 \cdot \left(0.24 + 0.76 \frac{P}{P_0} \right) \quad (2.11)$$

where

h = convective coefficient at pressure P (units consistent with h_0)

h_0 = convective coefficient at sea level pressure

P = atmosphere pressure at site elevation (units consistent with P_0)

P_0 = sea level atmospheric pressure

2.1.4.3 Buffer Spaces

Taking advantage of the heat balance approach, buffer space temperatures are predicted by modeling an unconditioned room in ResHB. These temperatures are then used as outside boundary conditions for surfaces of adjacent conditioned spaces. Although this treatment maintains the single zone methodology, it deviates from the real heat balance approach. The inter-room reference in ResHB is different from those

available in a detailed inter-room heat transfer analysis. In ResHB, the unconditioned rooms do not take the actual variations in the adjacent conditioned room temperatures into account, while in a detailed inter-room heat transfer analysis, it does.

2.1.4.4 Infiltration

The default infiltration model for RHB is the AIM-2 model (Walker and Wilson 1990, Walker and Wilson 1998, and “enhanced model” in Chapter 26, ASHRAE 2001). AIM-2 is a single zone model in which infiltration is determined for the whole building. In RHB, the overall infiltration rate is allocated to rooms in proportion to volume – that is, the same air change rate is assumed for all rooms. RHB provides typical default values for several required inputs of the AIM-2 model that are difficult to determine, including effective leakage area, leakage area distribution, and wind shelter parameters. Leakage area can be specified based on pressurization test or defaulted based on leakage classes defined by ANSI/ASHRAE Standard 119 (ASHRAE 1994).

Modeling of the interaction between mechanical ventilation and infiltration in RHB follows Palmiter and Bond (1991) and Sherman (1992). First, overall supply and exhaust flow rates must be determined and then divided into “balanced” and “unbalanced” components.

$$Q_{bal} = MIN(Q_{sup}, Q_{exh}) \quad (2.12)$$

$$Q_{unbal} = MAX(Q_{sup}, Q_{exh}) - Q_{bal} \quad (2.13)$$

where

Q_{bal} = balanced air flow rate, L/s or cfm

Q_{sup} = total ventilation supply air flow rate, L/s or cfm

Q_{exh} = total ventilation exhaust air flow rate (including any combustion air requirements), L/s or cfm

Q_{unbal} = unbalanced air flow rate, L/s or cfm

The air flow components are combined with infiltration leakage as follows:

$$Q_{vi} = Q_{bal} + MAX(Q_{unbal}, Q_{inf} + 0.5 \cdot Q_{unbal}) \quad (2.14)$$

where

Q_{vi} = combined infiltration/ventilation flow rate (not including balanced component), L/s or cfm

Q_{inf} = infiltration leakage rate determined assuming no mechanical pressurization, L/s or cfm

2.1.4.5 Distribution Losses

ResHB duct losses are calculated using models specified in ANSI/ASHRAE 152-2004, *Method of Test for Determining the Design and Seasonal Efficiencies of Residential Thermal Distribution Systems* and Palmiter and Francisco 1997. The method estimates the overall steady-state thermal efficiency of residential forced-air distribution systems by accounting for the conduction loss through the duct walls to the buffer zones and air leakage out of the supply ducts or into the return ducts. The conduction efficiency is calculated as:

$$\beta = \exp\left(-\frac{UPL}{mc_p}\right) \quad (2.15)$$

where

β = the conduction efficiency of the pipe

U = the overall duct wall conductance, W/m²K

P = the inside perimeter of the pipe, m

L = the length of the pipe, m

m = the mass flow rate of the air in the pipe, Kg/s

C_p = the specific heat of the air, KJ/kgK

The air leakage efficiency α of the pipe is defined as:

$$\alpha = 1 - \text{Leak Fraction} \quad (2.16)$$

The overall duct efficiency with combined conduction and air leakage is (the subscripts s and r refer to the supply and return ducts respectively):

$$\eta_0 = \alpha_s \beta_s - \alpha_s \beta_s (1 - \alpha_r \beta_r) \frac{\Delta T_r}{\Delta T_e} - \alpha_s (1 - \beta_s) \frac{\Delta T_s}{\Delta T_e} \quad (2.17)$$

where

η_0 = the overall duct system efficiency

ΔT_r = the difference between the temperature of the air in the pipe at the return register and the temperature of the air around the return duct, K

ΔT_s = the difference between the temperature of the air in the pipe at the return register and the temperature of the air around the supply duct, K

ΔT_e = the temperature rise across the equipment, it equals the difference between the temperature of the air in the pipe at the supply plenum and the temperature of the air in the pipe at return plenum, K

Impacts of duct interaction with natural infiltration on efficiency are considered by subtracting the efficiency loss η_{in} due to the interaction from the overall efficiency.

η_{in} is calculated as:

$$\eta_{in} = \frac{1}{2}(\alpha_r - \alpha_s) \frac{\Delta T}{\Delta T_e} \quad (2.18)$$

where

ΔT = the difference between the temperature of the air in the pipe at the return register and the temperature of infiltration air, K

2.1.4.6 Framed Constructions

Framed constructions are common in residential buildings. As from the ASHRAE Loads Toolkit, the CTF-based conduction model in ResHB assumes one-dimensional conduction heat flow and requires layer-by-layer construction input. ResHB includes an algorithm that derives fictitious material properties for a homogeneous layer that corresponds to a framed layer. The resistance of the layer is chosen to preserve the overall U-factor of the construction. Density and specific heat of the layer are the volumetric averages of the framed layer components.

2.1.4.7 Fenestration and Solar Gain Distribution

ResHB implements fenestration class and includes built-in fenestration class definitions for common residential glazing types. The fenestration class embodies the ratio of transmission to absorption and the angular characteristics of the fenestration system. An actual fenestration is specified by its U-factor, SHGC, and its fenestration class. The required angular characteristics of a specified fenestration are taken from the

specified fenestration class and are scaled by the ratio of specified SHGC to nominal (fenestration class) SHGC.

Interior and exterior shading treatments in ResHB are represented by the ASHRAE Interior Attenuation Coefficient (IAC) and Exterior Attenuation Coefficient (EAC) models (Chapter 30, *2001 ASHRAE Handbook of Fundamentals*). Overhang and fin shading is modeled with ASHRAE Loads Toolkit methods. Hourly scheduled shading is also allowed in ResHB.

For internal solar distribution, a modified version of the Loads Toolkit BLAST model is used. It distributes radiative gains in proportion to surface area-absorptance product. Beam solar gain is assumed to hit floor surfaces. One refinement to this model in RHB is that internal mass surfaces are assumed to be “half floor” with respect to beam radiation, as furnishings typically intercept some of the incoming beam.

2.1.4.8 Ground Heat Transfer

RHB models slabs as 300 mm (1 ft) of earth with adiabatic boundary conditions. This construction captures some of the diurnal heat storage effects of slab construction, but not net conduction to the ground.

2.1.5 Modeling Assumptions

The following sections describe the modeling assumptions of RHB.

2.1.5.1 Outdoor Design Conditions

RHB requires hourly design day outdoor conditions. In addition to the ability of accepting 24-hour profiles from user input, ResHB can also automatically generate 24-hour profiles from design dry-bulb temperature and its daily range, coincident wet-bulb temperature, site coordinates, and site elevation, as follows:

- *Dry-bulb temperature.* The design dry bulb and daily range are expanded to 24 hours using the generic profile from Table 17, Chapter 29 of the *2001 ASHRAE Handbook of Fundamentals*. The generic profile is shifted 1 hour later when daylight savings time is specified.
- *Wet-bulb temperature and other moisture-related values.* The design dry bulb and coincident wet bulb are used to determine the design dew point temperature. The hourly dew point is the minimum of the design dew point and the hourly dry bulb (that is, constant absolute humidity is assumed, limited by saturation). Other hourly psychrometric values (wet bulb temperature, humidity ratio, and enthalpy) are derived from the hourly dry bulb and dew point temperatures.
- *Solar radiation.* Hourly incident solar is derived using the ASHRAE clear sky model (Chapters 29 and 30, *2001 ASHRAE Handbook of Fundamentals*) with updated coefficients from Machler and Iqbal (1985).
- *Sky temperature.* Sky temperature is required for calculation of exterior surface long wave radiant exchange. The model of Berdahl and Martin (1984) is used to calculate hourly sky temperature from hourly dry-bulb and dew point temperatures (cloud cover assumed to be 0).

All psychrometric calculations are done with ASHRAE Loads Toolkit procedures (originally from Brandemuehl et al. 1993) assuming a constant barometric pressure determined from site elevation according to a standard atmosphere relationship (Eqn (3), Chapter 6, *2001 ASHRAE Handbook of Fundamentals*).

2.1.5.2 Internal Gain

Internal gain assumptions in RHB are based on *Building America (2003)*, which provides gain intensities and schedules for significant residential end uses as a function of building floor area and number of occupants. Also, RHB requires the radiant/convective/latent split for each gain source, which *Building America (2003)* does not fully define. Estimates were developed from *2001 ASHRAE Handbook of Fundamentals* and other sources as needed, as shown in Table 2-2.

Table 2-2. Fractional components of internal heat sources incorporated in ResHB

Source	Internal gain (to space)			Exhausted
	Radiant	Convective	Latent	
Refrigerator	0	1	0	0
Range	.24	.16	.30	.30
Dishwasher	.51	.34	.15	0
Clothes washer	.40	.60	0	0
Clothes dryer	.09	.06	.05	.80
Lighting	.79	.21	0	0
Other appliances and plug loads	.54	.36	.1	0
People (living)	.33	.22	.45	0
People (sleeping)	.30	.30	.40	0

2.1.5.3 Internal Mass

In RHB, the recommended assumption regarding internal mass is: each room should be modeled including internal mass having surface area equal to room floor area and consisting of 12 mm (0.5 in) wood exposed on one side (adiabatic outside surface

conditions). This surface should be radiantly coupled to all room internal surfaces. ResHB implements a special surface type “IM” for internal thermal mass.

2.1.5.4 Other Assumptions

Surface absorptance. Surface absorptance values in ResHB can either be the defaults (documented in Barnaby et al. 2004) or specified by the user.

Material properties. ResHB includes default material properties as documented in Barnaby et al. (2004). Again the user can also specify material properties.

2.2 Validation Methods of Cooling Load Calculation Programs

The word *validation* has been widely used with a variety of meanings. Strachan (1993) gave the following definition of validation:

“The rigorous testing of a program – comprising its theoretical basis, software implementation and user interface – under a range of conditions which typify its expected use.”

In practice, it is impossible and also unnecessary to conduct an absolute validation of a simulation program. The aim instead is to apply a developed validation method so that the simulation program is good enough to predict building performance for most situations with specific purposes. In this section, three validation methods are introduced along with a discussion of the advantages and disadvantages of each method. Some general ideas about the application of the validation methods are described. Finally, a brief summary is given for prior validation work.

In view of the increased use of building energy simulation programs, it has been long recognized that some form of validation is needed for the purpose of objective quality control. A number of attempts have been made over the last two decades to identify suitable validation procedures for building energy simulation programs. However, no standard validation procedures have been universally accepted.

Judkoff et al. (1983) first attempted to document the three most commonly used validation methods of building energy simulation programs. These are analytical verification, comparative testing and empirical validation. In each method, results from one program are compared with results from other sources, as will be discussed in the following sections. Judkoff (1988) also summarized the advantages and disadvantages of the three validation methods, as shown in Table 2-3.

Table 2-3. Advantages and Disadvantages of the three validation methods as from Judkoff (1988)

Technique	Advantages	Disadvantages
<i>Comparative</i> Relative test of model and solution process	No input uncertainty Any level of complexity Inexpensive Quick, many comparisons possible	No truth standard
<i>Analytical</i> Test of numerical solution	No input uncertainty Exact truth standard given the simplicity of the model Inexpensive	No test of model Limited to cases for which analytical solutions can be derived
<i>Empirical</i> Test of model and solution process	Approximate truth standard within experimental accuracy Any level of complexity	Measurement involves some degree of input uncertainty Detailed measurements of high quality are expensive and time-consuming A limited number of data sites are economically practical

2.2.1 Analytical Verification

In analytical verification, the output from a program, subroutine, or algorithm is compared to the result from a known analytical solution for isolated heat transfer mechanisms, under very simple boundary conditions. (Here, the term “analytical” means a mathematical model of reality that has an analytically determinable solution for a given set of parameters and boundary conditions.)

Where test specifications have to be interpreted in some way by a user in the form of input data for a particular test program, differences may arise from different interpretations of the specifications. This has been shown in the past on several projects (Allen et al. 1985). Fortunately, these problems can be minimized in the case of analytical tests due to the simplified nature of the building zone specifications and the possibility of using idealized zone constructions.

Analytical tests are (partly by necessity) simplified in nature and should usually be designed to allow only one particular feature to be tested at a time. This should allow not only the ability of the program to model particular features to be verified, but also the identification of particular model components or algorithms as the source of any problems. As noted above, in testing a building energy analysis program it is both the underlying algorithms of the code and their implementation that are tested. Inadequacies in both the algorithms or in their implementation (code bugs) can be the source of discrepancies. It is not possible to test the algorithms without implicitly testing their coding. Therefore developers can use analytical tests as a diagnostic tool to find bugs in the implementation as well as verify the operation of the various component models.

Being most abstracted from the full complexities of real building simulation problems, analytical testing has the advantage of offering the most certain form of reference or ‘truth’ model with which comparisons can be made. The nature of analytical testing also makes it only applicable to limited cases for which analytical solutions can be derived. Errors arising from the integrated performance of all the sub-models and algorithms in a program are beyond the scope of an analytical test.

2.2.2 Comparative Testing

In comparative testing, a program is compared to itself or to other programs that may be considered better validated or more detailed and, presumably, more physically correct. The comparative approach includes “sensitivity testing” and “inter-model comparisons”.

Comparative testing cannot directly address the issue of a truth standard, but can be a very powerful way of identifying errors by doing many comparisons quickly and inexpensively. One comparative testing approach is parametric sensitivity analysis. It provides information on the influence of the uncertainties in the program’s input parameters.

The other comparative testing approach is inter-model comparison. It involves checking the agreement of several different programs with different thermal solution and modeling approaches in a variety of representative cases. Cases for which the program predictions diverge indicate areas for further investigation. (Judkoff and Neymark 1995) Inter-model comparisons are useful in two aspects. Firstly, they provide a “useful”

evaluation in the case where one of the programs has already been the subject of rigorous validation. Secondly, they often highlight serious shortcomings in one or more of the programs. An important consideration in an inter-model comparison is the requirement for input equivalence. (Strachan 1993)

2.2.3 Empirical Validation

In empirical validation, calculated results from a program, subroutine, or algorithm are compared to monitored data from a real structure, test cell, or laboratory experiment.

Empirical validation is the most widely used technique for testing a simulation program, as it can be considered to be a conclusive test of whether model predictions reflect reality. In particular, whole model empirical validation ensures that the overall performance of the simulation program is tested. In this case, it is not only an individual process, but also the interaction of those processes that are tested. (Strachan 1993)

Empirical validation offers an approximate truth standard within the accuracy of the data acquisition system and many parameter values that are on measurement. Also, empirical validation can be applied with any level of complexity. However, detailed, high quality measurements are usually expensive, difficult and time-consuming, even for one or a few cases. Even if high-quality experimental data sets are available for performing empirical validation and a program has performed satisfactorily, it is still difficult to generalize results from one particular combination of building type, climate and operating conditions to others. In addition, measurements of both building performance parameters

and program input parameters have a finite accuracy. The uncertainty in program input parameters (air change rates, material properties, occupant behavior etc.) leads to uncertainty in the program predictions that may be quite apart from the adequacy of the algorithms employed by the program. (Bloomfield 1989, 1999)

2.2.4 Application of the Validation Methods

In any type of validation, three things are implicitly tested, each of which may contribute to the overall ‘error’ in the results (Rees, et al. 2002):

- The interpretation of the input data
- The model(s) or algorithm(s)
- The computer implementation of the algorithm(s)

A general principle applies to any type of validation method: the more realistic the test case, the more difficult it is to establish cause and effect, and to diagnose problems. The simpler and more controlled the test case, the easier it is to pinpoint the sources of error or inaccuracy. (Judkoff and Neymark 1995) In fact, the three validation methods may be used together in a number of ways. For example, analytical verification can be conducted at first to check the mathematical solution of major heat transfer models of a program. If discrepancy occurs, the source of the difference must be corrected before any further validation is done. Then, inter-model comparisons may be done in advance of an empirical validation to better define the experiment and to help estimate experimental uncertainty by propagating all known sources of uncertainty through one or several whole-building energy simulation programs.

2.2.5 Summary of Prior Validation Work

Independent work on model validation started in the late seventies and early eighties, after the growth of popularity of energy simulation because of the 1973 energy crisis. Examples of the early work include Judkoff et al. (1980, 1981), IEA (1981), and Hoellwarth (1980), which showed significant disagreements between codes for very simple test cases. Over the last two decades, a number of organizations have attempted to identify suitable validation procedures for building energy simulation programs, e.g. NREL (Judkoff, et al. 1983; Judkoff and Neymark 1995), BRE (BRE 1988) and the IEA (Bloomfield et al. 1988). A good summary overview is found in Judkoff (1988) and Judkoff and Neymark (1995). Further updated validation/testing literature review is included in Ahmad (1997), Bloomfield (1999), and Judkoff and Neymark (2002).

Much less emphasis has been placed on design load calculation procedures, perhaps since design load calculation methods have historically relied less heavily on computer implementation than annual energy calculation (Rees and Spitler 1999). A brief overview of published inter-model comparisons of cooling load calculation procedures is found in Spitler and Rees (1998).

The Comité Européen De Normalisation (CEN) (1997) has developed a standard approach to load calculations. It consists of a set of heat balance equations and a set of qualification tests against which particular computer codes can be evaluated. The purpose of the tests is qualification to a certain standard of accuracy and not diagnosis of particular faults. The tests are based on a single test zone that is exposed to a combination of loads. The tests are varied by changing shading, internal loads, wall construction,

system controls, etc. In each case a number of sub-models of the load calculation method are tested together.

One notable attempt of inter-model comparison for design cooling load calculation methods has been completed as part of ASHRAE 942-RP (Rees et al. 1998; Spitler and Rees 1998), which consists of a large number of test cases (of the order one thousand) where certain parameters are systematically varied. The comparison was primarily organized as a parametric study for three cooling load calculation procedures: the ASHRAE heat balance procedure, the ASHRAE radiant time series procedure, and the CIBSE admittance procedure. 18 different parameters describing different constructions, internal heat gains, zone dimensions and weather data were systematically varied for the comparison.

Rees and Spitler (1999) also proposed a diagnostic test procedure for building loads, named BUILDTEST, in which the ASHRAE heat balance method is used as a reference model. A series of 25 simplified tests were devised to be used in inter-model comparisons with the reference model. The purpose of the tests is diagnosing deficiencies in the load calculation method and/or its implementation. This was done by subjecting the test zone to a particular type of heat gain or use a particular heat transfer path in turn, rather than using different combinations of loads. Thus the results are functions of either individual (or at most only a few) sub-models alone and not the whole zone heat transfer model.

As will be discussed in detail later in Chapter 5, Spitler et al. (2001) have developed an analytical verification test suite for building fabric models in whole

building energy simulation programs — ASHRAE 1052-RP. The tests are intended to be used in support of ASHRAE Standard 140 ‘Standard Method of Test for Building Energy Analysis Software’ (ASHRAE 1998). The test suite consists of sixteen individual tests, each with the objective to test the ability of a building energy simulation program to model a particular heat transfer phenomena. The test is applied by comparing the output of the energy simulation program to be tested with the analytical solution for a special test zone. The data to be compared may be a single zone load, heat flux, temperature, or hourly loads over one or more days of output.

More recently, experimental validation of both the ASHRAE heat balance method and radiant time series method has been done in test cells at Oklahoma State University (Chantrasrisalai, et al. 2003; Iu, et al. 2003).

For the RHB method, no validation work has been done prior to this dissertation as it has just been developed in 2004. Analytical, inter-model, and experimental validation of RHB is highly desirable and therefore is the objective of this research.

3. OBJECTIVES

The objectives of this research have been briefly outlined in the Introduction. In more detail, the task of validating a heat balance based residential cooling load calculation procedure is discussed below.

Firstly, a literature review will be done for the RHB cooling load calculation procedure and validation methods of cooling load calculation program. For RHB, the subject of the validation work, the goal is to obtain an in-depth comprehension of its basic structure and algorithm, theoretical principles and assumptions, and component models. This is very important as the testing, analyzing and diagnosing process involved in the validation work requires a full knowledge and familiarity of RHB. For validation methods, the goal is to identify possible methods and available tools for validating cooling load calculation programs. The literature review section has attempted to do this by introducing the RHB procedure and general validation methods. Another part of the literature review is a systematic review of candidate programs that could be used as inter-model comparison tool. This is covered under the section of selecting comparison tool in Chapter 4.

Secondly, inter-model validation of ResHB, the reference computer implementation of the RHB procedure, will be performed. Inter-model validation requires the selection of a comparison tool. Therefore, a systematic review and comparison of

candidate building simulation programs, with regard to their capabilities of modeling residential buildings, will be made. Based on the review results, one program will be selected as the comparison tool. Modifications will be made to the selected comparison tool if necessary. A parametric analysis tool will be developed for systematic and automatic implementation of large amounts of inter-model comparisons for typical residences. The parametric analysis tool should be able to create input files, run simulations and process outputs of interest for the comparison tool automatically. Cooling loads calculated by ResHB will be compared to that calculated by the comparison tool. System design resulted from ResHB will also be evaluated by the detailed simulation with the comparison tool.

Thirdly, analytical verification of ResHB will be conducted. The ResHB program will be tested with the Analytical Verification Test Suite for Whole Building Energy Simulation Programs -- Building Fabric (ASHRAE 1052-RP, Spitler, et al. 2001). Applicable analytical tests from the test suite will be applied and modifications of the input structure of ResHB will be made as needed. All the analytical tests completed will be used as a set of reference tests that can be run after each revision of ResHB, assisting diagnosis of any new problems that could possibly be introduced.

Finally, experimental validation of the ResHB program will be done. Experimental data will be obtained from a well-instrumented house located in Fort Wayne, IN. ResHB input files will be created for the house and ResHB-calculated cooling loads and room temperatures will be compared to measured data.

4. INTER-MODEL VALIDATION OF THE HEAT BALANCE BASED RESIDENTIAL COOLING LOAD CALCULATION PROCEDURE

As mentioned in the literature review, of the three types of validation methods, inter-model comparison cannot directly address the issue of a truth standard, but can be a very powerful way of identifying errors by doing many comparisons quickly and inexpensively. The inter-model validation desired and conducted for the Residential Heat Balance (RHB) cooling load calculation procedure is similar to the study performed by (Rees et al. 1998; Spitler and Rees 1998). It consists of a large number of test cases (of the order one thousand) where certain parameters are systematically varied. It is desirable that this type of inter-model comparison be made in a highly-automated fashion, so that the RHB procedure can be tested and evaluated throughout the development cycle. How has this been implemented for the RHB procedure is discussed in the following sections, which include the selection of the comparison tool, the methodology employed and the comparison results obtained.

4.1 Selecting the Comparison Tool

4.1.1 Basic Requirements of the Comparison Tool

In choosing the comparison tool, the following basic requirements regarding the code robustness, required features and/or feasibility of extension are considered.

1. Heat balance method

The heat balance method is generally considered as the most scientifically rigorous method. It accounts for every energy flow in the most basic, fundamental way and does not impose any simplification on the solution technique (Strand et al. 1999), while other methods make many simplifying assumptions along the way from the initial model to the final procedure that the basic processes are essentially lost (Pedersen et al. 1997). Therefore, to supply inter-model validation of the new heat balance based residential cooling load calculation procedure, a heat balance based comparison tool is the best choice. A comparison tool with an approximate method will not be accurate and fundamental enough to serve as a reference in the inter-model validation.

2. Include well-developed models for most aspects of building load calculation

Although modification and extension is expected if necessary, it would be best to choose a tool that requires a minimum amount of modification. Therefore, well-developed models for most aspects of building load calculation are desired in the selected tool. These aspects include:

- Transient heat conduction: Obviously, the detailed heat balance method needs a transient heat conduction model to account for the dynamic effects of the thermal mass on the zone loads. This is necessary for both exterior and interior/inter-zone walls. This requirement exists because the typical central located thermostat in residences cannot simultaneously control the temperatures in all rooms and the resultant temperature swings lead to inter-zone conduction.
- Detailed convection model: Although there is sensitivity analysis showing that the effect of the outside convection coefficient on the cooling load is very low (McClellan and Pedersen 1997), the inside convection coefficient can be important (Beausoleil-Morrison 2000). The comparison tool should be able to deal with a detailed convection model and permit variable convection coefficients.
- Solar radiation/window shading: Solar gain is an important part of the cooling load, both that absorbed by opaque surfaces and that transmitted through fenestration. It may become even more important for residential buildings because the loads in residences are primarily from the building envelope and are greatly affected by outside conditions. Therefore, accurate models for solar radiation, fenestration and window shading are required in the comparison tool.
- Detailed inside/outside long wave radiation: The simplified approaches that use a combined coefficient to predict the total convective and radiative gain on a surface mask their respective effects on zone loads and depart from the

heat balance principle. These models therefore should not be used in the comparison tool. Instead, a detailed inside/outside long wave radiation model is recommended. Long wave radiation from internal sources may have to be dealt with in the traditional way by defining a radiant/convective split. Although the surface temperature of the internal sources could be calculated based on the heat balance principle, it is difficult to predict their locations since occupants of the space may move them from time to time.

- Infiltration and inter-zone airflow and mixing: In comparison to those in commercial or industrial buildings, zone load from infiltration is important for residential buildings because the internal heat gains in residences are relatively low. Inter-zone airflow and mixing is also an important feature required to model inter-zone thermal interaction.

3. Short time step

Usually, one-hour time steps are used in energy simulation programs. But short time steps may be necessary in the comparison tool if system on/off behavior is modeled. Shorter time steps are already available in several simulation tools.

4. Flexible HVAC system simulation/control tool

The comparison tool should permit the “master-slave” zone control feature of residences. From the HVAC system simulation concept, it would be good to realize an integrated simultaneous simulation, so that feedback from system response can be seen by the zone load procedure. But for the validation of a load calculation method that aims to be the basis of system design and equipment sizing, this may not be necessary. Instead,

an idealized representation of the system may be sufficient. E.g., a system control profile based on zone temperature and system capacity may be satisfactory for this application.

5. Convenient to be modified or extended

If necessary, extension or modification of the selected comparison tool is expected. Therefore, a well-documented and well-organized source code of the selected program is desired. As to the program language, Fortran 90 is preferred, with Fortran 77 being a second choice.

6. Source code availability

The status of the source code availability, or the cost to obtain the source code is another condition that limits the choice of the programs. Since the research project funding is limited, it is preferred to keep the cost of the source code reasonably low.

7. Status of the program validation

The comparison tool needs to be validated as it is used as a reference. With everything else being equal, the program that has been best validated should be chosen. Even with other advantages, fatal errors that cannot be fixed will eliminate the program from consideration.

8. Support

It's important that technical support of the selected comparison tool is available since help from the original developer usually saves time.

Among the basic requirements discussed above, some features are necessary, some features may be necessary, while other features are desirable. Table 4-1 summarizes the classification of these features. Consideration should be given to distinguish these features in choosing the comparison tool.

Table 4-1 Classification of basic requirements for candidate comparison tools

Basic requirements		Necessary	May be necessary	Desirable
Heat balance method		X		
Include well-developed model for most aspects of building load calculation	Transient, inside-outside/inter-zone heat conduction	X		
	Detailed convection model		X	
	Solar radiation/window shading	X		
	Detailed inside/outside long wave radiation	X		
	Infiltration and inter-zone airflow/mixing	X		
Short time step			X	
Flexible HVAC system simulation/control tool			X	
Convenient to be modified or extended			X	
Source code availability		X		
Program validation				X
Support		X		

4.1.2 Review of Candidate Programs

With the basic requirements for the comparison tool discussed above, a systematic review of candidate computer programs is needed. Although we are looking for a detailed load calculation program, the unique features of residential load calculation and hence the specific requirements of the comparison tool make it necessary to look into a range of whole building simulation tools in terms of their system simulation and control possibilities.

Generally speaking, two types of building simulation tools are in use today: general-purpose tools and special purpose tools. General-purpose tools, such as IDA and SPARK, treat mathematical models as input data and allow the simulation of a wide variety of systems. Their main advantage is flexibility, but their potential drawbacks may be difficulty of use, low execution speed and risk of non-convergent solution. Special purpose tools, such as DOE-2, BLAST, ESP-r, and EnergyPlus, aim to solve a specific class of building simulation problems. Their main advantage is high execution speed and low risk of non-convergent solution if reasonable input data are provided. Their drawback is the limitations on their application scale and difficulty of modification.

Coming specifically to load calculation, three methods used in whole building simulation for calculating instantaneous space load are presented in chapter 30 of the ASHRAE Handbook of Fundamentals (1997). These three methods are: heat balance method, weighting factor method, and thermal network method. As discussed earlier, the heat balance method uses the law of conservation of energy in calculating space heating or cooling loads. Sample simulation tools using heat balance method include BLAST, HVACSIM+, and EnergyPlus.

Like the transfer function method, the weighting factor method uses weighting factors (also called room response factors) to convert heat gain components to corresponding space load components. A well-known weighting factor method-based program is DOE-2.

Thermal network methods discretize the building into a network of nodes and apply heat balance to each of the nodes in the simulation. Thermal network methods

provide much more flexibility in building simulation since usually the solution solvers are separated from the simulation models in their implementation. While not widely used because of the additional computation time required and additional effort needed to take advantage of its flexibility, thermal network methods may be considered a refinement of the heat balance method in many aspects regarding multiple nodes and the inter-connection of the nodes. Example tools using the thermal network method are HTB2 and ESP-r.

Based on this background of building simulation tools to be chosen from, two general-purpose tools currently in use are included for review. These are the IDA ICE (IDA Indoor Climate and Energy) and SPARK (Simulation Problem Analysis and Research Kernel). Going to special purpose tools, four heat balance method-based tools and three thermal network method based tools are included. The heat balance based tools include the HVACSIM+ (HVAC SIMulation Plus other systems), BLAST (Building Loads Analysis and System Thermodynamics), and the more recently developed EnergyPlus. The thermal network based tools are HTB2 (A Model for the Thermal Environment of Buildings in Operation), ESP-r (The ESP-r System for Building Energy Simulation), and the program presented in NISTIR 5322 (Computer Programs for Simulation of Lighting/HVAC Interactions).

A brief review and description for each of these candidate programs follow.

1. SPARK

The Simulation Problem Analysis and Research Kernel (SPARK) is an equation-based, object oriented, general differential/algebraic equation solver. It was first

implemented to solve algebraic problems at the Lawrence Berkeley Laboratory (Anderson 1986), and then extended to allow differential equations solution (Sowell and Buhl 1988). Prior to its initial public release, it was completely rewritten with new developments made such as MACSYMA and Maple interfaces (Nataf and Winkelmann 1992). The program is written in C and C++. It comes with user-selectable time step, which allows modeling short time-step dynamics. Being developed for use in building service systems, an HVAC Toolkit library was built based on the ASHRAE Secondary Systems Toolkit (Brandemuehl 1993) and supplemented with primary equipment models from DOE-2 (LBL 1984). But models related to building loads calculation are not found in SPARK at this time. In order to use SPARK as the comparison tool, a building loads library would need to be developed from the beginning, rather than modifying or extending an existing library. This will significantly increase the work to be done and is the main drawback of selecting SPARK.

2. IDA Indoor Climate and Energy

IDA Indoor Climate and Energy (ICE) is a tool for simulation of thermal comfort, indoor air quality and energy consumption in buildings. It is implemented in a general-purpose simulation environment, IDA (Björnell, et al. 1999). In IDA, the mathematical models are described in terms of differential and algebraic equations in a formal language, Neutral Model Format (NMF), and solved with a variable time step solver, IDA solver. The model library of IDA ICE is that developed in the project of International Energy Agency SHC (Solar Heating and Cooling program) Task 22 Subtask B, in which many ASHRAE models have been used (Bring, et al. 1999). This library has the capability of solving multi-zone thermal and airflow models simultaneously. Solar

radiation and full 3D window shading are accounted for. The external convection coefficient is calculated as a function of the local wind velocity using the correlation suggested by Clarke (1985). Internal convection coefficient is estimated as a function of temperature difference between the air and the surface and the slope of the surface as that suggested by Brown and Isfält (1974). Both external and internal long wave radiation are included. For detailed secondary system simulations, the ASHRAE secondary toolkit models have been translated into NMF and are compatible with other models in the library. Control models include proportional controllers with piece-wise linear control curve or smooth control curve, proportion and integration controller (PI controller) and liquid flow controller.

The programming language of IDA ICE is Common Lisp and Fortran. Compared to the similar equation based simulation tool SPARK, it is much more completely developed and the library models are in a shape ready to be used. However, the cost of IDA ICE is prohibitively high even for single software license. (It may be necessary, during the course of the project, to run simulations on multiple computers simultaneously. This would be impossible at the per-machine cost for the software.)

3. HLITE/VLITE (Walton 1993)

HLITE and VLITE are two parts of the program presented in the technical report (National Institute of Standards and Technology, NISTIR 5322) named “Computer Programs for Simulation of Lighting/HVAC Interactions”. VLITE is used to calculate the view factors describing the radiation interchange between surfaces. HLITE solves the thermal network model for transient temperatures and cooling loads, with view factors

computed by VLITE. HLITE is based on simple finite volume model for heat transfer combined with sufficiently short time steps to permit explicit time integration in most of the simulation. The convection model provided in this program can vary from simple to very complex and non-linear formulae based on experimental research (Spitler 1990). Radiant interchange is modeled with accurately computed view factors. Dead band control of air temperature using a special node and proportional-integral controls are also provided.

The program is written in C language, which is not our preferred language. The main disadvantage of this program is, as stated in the report, it does not include many of the features necessary for a general building energy analysis program such as solar gains, latent loads, ground heat transfer and detailed HVAC equipment models. In order to include solar gains in the program, it would need to be computed and added to internal heat gains of the nodes (nodes are defined as the primary components of the thermal network and correspond to some volume of material which can be characterized by a single temperature). In addition, inter-zone airflow and mixing, which is another important feature in our requirement list, is dealt with only by user specified airflows. If this program is going to be selected, an airflow network model would also need to be added.

4. HTB2

The HTB2 (A Model for the Thermal Environment of Buildings in Operation) program (Alexander 1997) developed at University of Wales, Cardiff, U.K., is a general-purpose dynamic simulation tool of the energy and environmental performance of

buildings. The simulation of HTB2 is based on finite difference method and thermal network model. Regarding its flexibility to simulate the thermal interactions in residential load calculation: inter-zone transient heat transfer is provided as a feature of the thermal network model; in HTB2 release 1 (Alexander and Lewis 1986), inter-zone air flow and mixing was done by specifying the space to space air flows as in NISTIR 5322, but a multi-cell network ventilation model has since been implemented (Alexander 2001). Detailed solar gains and shading are provided. External convection coefficients are determined from the wind speed and the surface orientation relative to the wind direction. The formulation was claimed to be a good approximation to published data (Fig. 3.9 of Kimura, 1977). The internal convection coefficient is chosen from three predefined values using the orientation of the surface and the direction of the temperature gradient between the surface and the adjacent space air as input. External long wave radiation is calculated by the simplified form of the equations reported by Austin and Cole (1974). Internal long wave radiation is estimated by determining an equivalent star network, in which the net radiant gain of each surface is calculated relative to a star temperature determined from the area-long-wave emissivity weighted radiosities of the internal surfaces.

The system simulation in HTB2 provides three options for specifying the heating system (Alexander 1997): an “ideal”, fast response room-based system which will maintain a space air temperature regardless of heating load; a typical wet central heating system, with associated time delays and warm-up times, and with local TRV (Thermostatic Radiator Valve) type control, and a central time clock and thermostat; an electric off-peak storage heating system. Cooling load can be estimated as an option to

the “ideal” heating system. While the subject of this research work focuses on the cooling load, this may be a drawback of HTB2 since much work and time will be required if detailed cooling system simulation is going to be used.

HTB2 is written in standard Fortran 77. Short time steps are permitted. Support for HTB2 may be not as convenient as those tools having in-house expertise. The research license cost for HTB2 is also high.

5. ESP-r

The ESP-r System for Building Energy Simulation has been in evolution and renewal for more than two decades since its first development in 1970s (Clarke 1977). It is a finite volume and thermal network method based transient energy simulation system. To this end, ESP-r considers multi-zone heat transfer, inter-zone airflow, intra-zone airflow, water flow (in hydronic plant system), electric power flow, moisture transfer and illumination. ESP-r employs a partitioned solution approach, which applies customized solvers to each model domain (thermal, inter-zone air flow, electric power flow, etc.). Interdependencies are handled by passing information between solution domains on a time-step basis (Beausoleil-Morrison 2000). This manner enables the optimal treatment of each model domain and the global solution to evolve in a coupled manner.

In the thermal model domain of ESP-r, transient inter-zone heat transfer is realized through thermal network method, solar radiation and window shading is fully considered, and detailed long wave radiation treatment is implemented. Convection coefficients can either be specified by the user or computed at simulation time based on the convection correlations selected by the user. The inter-zone airflow network model is

available also. Time steps are allowed to be as short as one minute. ESP-r is written in C++ and Fortran 77. All these make ESP-r competitive to EnergyPlus (to be described later) in terms of capability completeness. ESP-r also has an advantage over EnergyPlus on its availability of interface. While its support may be not as convenient as EnergyPlus and the author has no prior experience on working with ESP-r.

6. *HVACSIM+*

The HVACSIM+ program developed at the National Bureau of Standards (NBS) consists of a main simulation program, a library of HVAC system components models, a building shell model, and interactive front and data generation programs. The main program employs a hierarchical, modular approach and advanced equation-solving techniques to perform dynamic simulations of building/HVAC/control systems. The building load portion of HVACSIM+ includes a building shell model and a building zone model. The building shell model uses a fixed but user selectable time step in simulation, while the zone model uses variable time intervals. The program language is Fortran 77.

The building thermal loads determination in HVACSIM+ is primarily based on NBSLD (Kusuda 1967) and TARP (Walton 1983). Inter-zone heat transfer is considered in the transient heat conduction calculation, but no signs from the document (Park et al. 1986) show that inter-zone airflow and mixing is solved. A combined radiant and convective coefficient is used for the outside surfaces, while long wave radiation and convection are dealt with separately for inside surfaces. Inside convection model is the same as the detailed inside algorithm for natural convection used in TARP and BLAST. Internal long wave radiation is modeled with the mean radiant temperature network

(MRTN) method introduced by Carroll (1981). In addition to the features that need to be either added (inter-zone air flow) or modified (outside convection and long wave radiation), HVACSIM+ has another severe disadvantage: the program is not well supported.

7. BLAST

The Building Loads Analysis and System Thermodynamics (BLAST) program is a comprehensive program for predicting hourly energy consumption and hourly system performance in buildings. It calculates thermal loads using the heat balance method. Most of the thermal interactions including exterior solar radiation between the zones and the environment are considered in solving the heat balance equations. Inter-zone transient heat conduction is modeled in BLAST. Inter-zone airflow and mixing is done in the way that the user specifies the airflows rather than solving the detailed flow equations. Various levels of outside and inside convection models can be specified. Long wave radiation is calculated with the “balanced mean radiant temperature” method (Walton 1980).

In BLAST, systems are controlled by a “piece wise” linear control profile that approximates the system response as a function of the zone air temperature. The building load calculation, the HVAC system and the plant performance are simulated in a sequential way. The difference between the amount of the conditioning required by the zones and the amount supplied by the system is reported as the unmet load. This is usually considered as one of the disadvantages of BLAST since there is no feedback between zones, systems and plants. Also, it may not be convenient to model the master-

slave zone control problem with this type of system control. Another disadvantage of BLAST is that its simulation can only be done on hourly basis. Short time steps are not allowed in BLAST but may be very important in terms of system response. Modifying BLAST to permit short time steps would be very difficult.

8. EnergyPlus

The U.S. Department of Energy (DOE)'s EnergyPlus program is a new building performance simulation program that combines the best capabilities and features from BLAST and DOE-2 along with new capabilities. The basic heat balance engine of BLAST forms the foundation for the EnergyPlus load calculation with advanced simulation ideas from the IBLAST (a research version of BLAST) and DOE-2 programs. The integrated simulation of zone loads and system and plants in EnergyPlus permits the space temperature be adjusted according to the system feedback. In EnergyPlus, inter-zone air flow is modeled by the COMIS module, which is a network-based multi-zone air flow model permitting the modeling of air flows within a building as well as through the building fabric from the outside. It is able to model inter-zone heat transfer. The program is written in Fortran 90 with a modular structure. User specified time steps in the simulation are permitted.

The features of all the candidates discussed above are summarized in Table 4-2.

Table 4-2 Summary of the features of the alternative programs

(Note: ? means insufficient experience to reach a judgment.)

Feature		SPARK	IDA ICE	HLITE/ VLITE	HTB2	ESP-r	HVACSIM+	BLAST	EnergyPlus
Zone analysis method		No load calculation yet	Equation based heat balance method	Thermal network method	Thermal network method	Thermal network method	Heat balance method	Heat balance method	Heat balance method
Include well-developed model for most aspects of building load calculation	Inter-zone transient heat conduction	-	Yes	Yes	Yes	Yes	Yes	Yes	Yes
	Detailed convection model	-	Yes	Yes	Yes	Yes	Yes	Yes	Yes
	Solar radiation, window shading	-	Yes	No	Yes	Yes	Yes	Yes	Yes
	Detailed inside, outside long wave radiation	-	Yes	Yes (Inside)	Yes	Yes	Yes-inside No-outside	Yes	Yes
	Infiltration and inter-zone airflow and mixing	-	Yes	User specify air flow rates	Yes	Yes	No	User specify air flow rates	Modeled by COMIS
Program language		C/C++	Common lisp, Fortran	C	Fortran 77	C++, Fortran 77	Fortran 77	Fortran 77	Fortran 90
Sub-hourly short time step		Yes	Yes	Yes	Yes	Yes	Yes	No	Yes
Flexible HVAC system simulation/control tool		?	Yes	?	?	Yes	?	?	Yes
Convenient to be modified or extended		?	?	?	?	No	No	No	No
Support		?	?	?	?	?	No	Yes	Yes
Interface availability		Yes	Yes	No	Yes	Yes	No	Yes	No
Status of source code availability		Software license fee of US\$250, waived for U.S. Government agencies	Models and user interfaces can be added with IDA simulation environment and IDA ICE	Government program (free?)	A research license with core source code: £2000 (about US\$3810)	Open source: free	Free	Already available	Already available
Status of executable file availability		Same as source code status	Software single user license: 5,000 SEK (about US\$709)	Same as source code status	An evaluation version limited in number of zones and elements already available	Free	Free	Already available	Already available

4.1.3 Selection of Comparison Tool

Initial review of the candidate programs shows that each program has its advantages and disadvantages. The main advantages and disadvantages for each candidate are briefly listed in Table 4-3:

Table 4-3 Main advantages and disadvantages of the candidate programs

Candidates	Main advantage	Main disadvantage
SPARK	New equation based general solver	No load calculation library
HLITE/VLITE	No obvious advantage	Needs solar gains and detailed network airflow model
HVACSIM+	No obvious advantage	Support is almost unavailable
BLAST	In-house expertise	No short time step permitted
IDA ICE	Contains most of the features required	Cost is prohibitively high
HTB2	Contains most of the features required	Cost is prohibitively high
ESP-r	Contains most of the features required; much validation work has been done	No in-house expertise
EnergyPlus	Contains most of the features required; in-house expertise	Relatively large and complex

Based on the facts listed above, four candidates are eliminated because of their lack of one or more features that are hard to be added or need much effort to be modified. These are SPARK, HLITE/VLITE, HVACSIM+, and BLAST. For SPARK, the load calculation library needs to be developed from the start. For HLITE/VLITE, the main problem is the solar gains and detailed network airflow model need to be developed. HVACSIM+, having no obvious advantage, has a severe disadvantage of no technical support. BLAST doesn't permit short time steps and it would be difficult to add this feature into BLAST.

The remaining four candidates (IDA ICE, HTB2, ESP-r and EnergyPlus) were examined in more detail. They contain most of the required features and already have the capability to deal with the two main features of inter-zone thermal communications (inter-zone heat transfer and inter-zone airflow) and realistic system controls. EnergyPlus also has the advantage of having some in-house expertise.

A more detailed summary of the retained four candidates is given in Table 4-4. In Table 4-4, details on the component models of load calculation are listed in as much detail as possible at the time of review. The possibility to implement the “master-slave” zone control is added as one feature of the candidates. Another feature that added to Table 4-4 is the status of validation. Note that all information listed is based on literature review and experiences from the research work team at Oklahoma State University.

Table 4-4 Part 1 More detailed summaries of the candidate programs

Feature		IDA ICE	HTB2	ESP-r	EnergyPlus
Zone analysis method		Equation based heat balance method	Finite difference thermal network method	Finite volume thermal network method	Heat balance method with conduction transfer functions
Component models of load calculation	Inter-zone transient heat conduction	Implemented	Implemented	Implemented	Implemented
	Detailed convection model	External coefficient: calculated as a function of the local wind velocity using the correlation suggested by Clarke; Internal coefficient: estimated as a function of temperature difference between the air and the surface and the slope of the surface as suggested by Brown and Isfält	External coefficients: determined from the wind speed and the surface orientation relative to the wind direction; Internal coefficient: chosen from three predefined values using input information	Convection coefficient can either be specified by the user or computed at simulation time on the basis of natural convection considerations (the Alamdari and Hammond method, the Khalifa method, the Awbi and Hatton method, the Fisher method) and of a method for mixed flow regime builds on the strength of the Alamdari-Hammond method and the Fisher method.	External: several methods available; Internal: include two natural convection models and one mixed and forced convection model
	Solar radiation, window shading	Implemented	Implemented	Implemented	Implemented
	Detailed inside, outside long wave radiation	Outside: calculated from surface absorptivity, surface temperature, ground and sky temperature, ground and sky view factors; Inside: calculated in net radiation method, which include both long wave and short wave (from sun and lighting) radiation for internal surface	Outside: calculated by simplified form of the equations reported by Austin and Cole; Inside: estimated by determining an equivalent star network	Implemented	Outside: calculated from surface absorptivity, surface temperature, ground and sky temperature, ground and sky view factors; Inside: treated in detailed manner
	Inter-zone airflow and mixing	A fully integrated airflow network model implemented	A multi-cell network ventilation model has been implemented	Inter-zone airflow network model implemented	A link to COMIS has been created
	Program language	Common lisp, Fortran	Fortran 77	C++ and Fortran 77	Fortran 90
Sub-hourly short time step		Time step down to minutes	Time step down to minutes	Time step down to minutes	Time step down to minutes

Table 4-4 Part 2 More detailed summaries of the candidate programs

Feature	IDA ICE	HTB2	ESP-r	EnergyPlus
Master-slave zone control availability	Different control models together with zone sensors can be used to implement various control strategy for different zones	Can specify a heating/cooling system with a thermostat sensor and control criteria associated with it, the thermostat can be connected to only one space	Different control regime can be specified in terms of sensors, actuators and control laws through the <i>configuration control</i> file	Control schedules can be built for different nodes through input file, and the feedback from the system simulation on loads not met can be reflected in adjusted space temperature in the next time step
Modification feasibility	No experience obtained, Models and user interfaces can be added with IDA simulation environment and IDA ICE	No experience obtained	No experience obtained	May be difficult because of its complexity
Support	Technical manual, telephone/email support	Technical manual, and 8 man-hour telephone/email support only	Technical manual, telephone/email support, training course available	In house support available
Interface availability	Models and user interfaces can be added with IDA simulation environment and IDA ICE	Available	Available	Not available
Source code availability	Available	Available with £2000 (about US\$3810)	Available	Already available
Executable file availability	Software single user license: 5,000 SEK (about US\$709)	An evaluation version limited in number of zones and elements already available	Available	Already available
Model validation	<p>1. Inter-model comparisons have been made against BRIS program, which in turn has been validated against measurements and is well trusted by Swedish professionals. (Brown 1990)</p> <p>2. An empirical validation based on test cell measurements has been carried out within IEA SH&C Task12. Problems arise due to thermal bridges in the exercise and internal film coefficient not as high as that of the test cell. It was said IDA ICE predictions were very accurate if thermal bridges were compensated for. (Guyon et al. 1999)</p>	<p>1. Included as one of the models in the empirical validation against the test room data in IEA Task 12 (Lomas et al. 1994, 1991).</p> <p>2. Included in the validation project of SERC and BRE (BRE/SERC 1988; Lomas 1992)</p> <p>3. The external solar shading modeling has been validated against measurements. Agreement obtained with correct ground reflectance and use of detailed geometric model of shading devices (Alexander et al. 1997).</p> <p>4. Simulation results were said in agreement with filed measurements in two low cost houses in Malaysia (Jones et al. 1993).</p>	<p>Has extensive validation records from many validation projects, including: IEA Annex 1, 4, 10, 21 and task 8; Scottish test houses; Australian test houses; SERC; EC; EC PASSYS; BRE/EDF (EMC test cells, BRE Office, BRE House, Lisses House); ASHRAE Project 852-RP; Germany Daylight study; Comparison with DOE2.1C etc. Validations also found as part of several PhD thesis. Validations involve analytical test, inter-model comparison and empirical validation. (Strachan, P. 2000)</p>	<p>Testing using the IEA Loads BESTest test suite has been implemented</p>

Based on the information in Table 4-4, consideration were given to the following aspects while choosing the candidate program:

- Modifications needed

In terms of the modifications needed, no explicit features need to be added to either one of the four candidates. The work needed to make them capable of dealing with master-slave zone control will vary depending on their current control features, but most of them supply the possibility to associate different control strategy with separate zones.

- Program complexity

Program complexity is another aspect that should be considered. Recognizing that the goal is to find an advanced heat balance based load calculation program, not a large whole building energy simulation program, it would be wise to keep the choice as small and simple as possible. Complexity and inconvenience that could possibly be resulted from inter-connection between load calculation and system simulation are probably unnecessary.

- Multi-zone interactions and controls

A contradiction exists when coming to this point. In order to model the inter-zone heat transfer and airflow accurately, and to simulate the master-slave zone control appropriately, it seems necessary to go to detailed system simulation. While this makes the system simulation inevitable, a load calculation procedure is for the purpose of sizing system and equipment capacity during the design stage. At this stage, it would be difficult

to know and specify the exact system for use in the system simulation. Therefore, some idealized representation of the system may be sufficient for this application.

However, considering that multi-zone interactions and controls are the main features that are required of the comparison tool, priority should be given to candidate programs capable of modeling multi-zone interactions and controls.

- Status of source code availability and support

Considering the source code availability and support status, priority should be given to EnergyPlus because some in-house expertise and its source code are already available. The cost of the software license is prohibitively high for both IDA ICE and HTB2, nor is in-house expertise available. ESP-r is freely available as it is open source, but no in-house support is available.

- Status of validation

The validation status of EnergyPlus is not as good as that of the other three (IDA ICE, HTB2 and ESP-r) since it is relatively new and little validation had been done at the time of review. In addition to the validation work reported in the literature, analytical tests based on ASHRAE 1052-RP (Spitler, et al. 2001) and tests developed for testing inter-zone heat transfer, inter-zone air flow, and master-slave zone control (Xiao, et al. 2002), were performed with the most promising candidate: ESP-r. Details of the analytical tests are summarized in Appendix A.

- Automated parametric run feasibility

An automatic parametric run generator will be developed to systematically run simulations for large sets of prototypical residences in the inter-model comparison. Therefore, the feasibility of doing this has to be considered in choosing the comparison tool.

Considering all these aspects and weighing the advantages and disadvantages of each candidate, ESP-r was selected as the comparison tool. IDA ICE was rejected because the price of the software license is prohibitively high. HTB2 was not chosen because its price for a research license is also high. Although newly developed EnergyPlus has most of the required modeling capabilities, ESP-r has been much more extensively validated with over 20 years of development and use. Compared to ESP-r, EnergyPlus also lacks an interface, which makes it much more difficult to create input files for automatic parametric runs.

4.2 Methodology

4.2.1 Types of Comparison

Two types of inter-model comparison between the residential heat balance load calculation procedure (RHB) and ESP-r are performed:

- *Load Comparisons.* In these comparisons, loads predicted by RHB are compared to those calculated by ESP-r. These comparisons serve to verify RHB calculations and to reconcile RHB and ESP-r input used for system design evaluation.

- *System Design Evaluation.* In these comparisons, the RHB procedure is used to generate design system capacities. In ESP-r, the buildings are simulated with a residential cooling system, with system capacity and room airflows taken from the RHB procedure. Room temperatures and comfort levels are then evaluated. These comparisons provide guidance for refinement of the RHB procedure.

4.2.2 Parametric Code

Both types of inter-model comparisons depend on a parametric code that identifies the specific case to be run by both programs. A typical code is:

```
R2HsLCASDO000Q00m00AmmmmCwmhtmWwmmG1000mmmmPwwMwmFwm0m
```

Each sub-field of the code controls one aspect of input file generation. In this example, “Hs” indicates that building “s” (shoebox) should be used, “LCASD” means that the location is San Diego, CA, and O000 specifies building orientation of 0 (building front facing north). “Q00m00” means zero internal gain, zero infiltration, medium cooling set point, zero room temperature swing, and zero set point setoff in the controls. “Ammmm” means all interior surfaces have medium short wave and long wave absorptivities. Other fields determine surface construction and configuration, fenestration type and amount, shadings, internal mass, etc. (e.g. “Cwmhtm” means the exterior ceiling is of wood frame construction with medium insulation, and the roof above the hip attic has tile construction with medium short wave absorptivity.) A complete description of the parametric code is found in the RHBGen documentation (Barnaby, et al. 2004) and is included in Appendix B for readers’ convenience.

There are literally a huge number of combinations (billions) that can be generated using this scheme. In the results presented below, cases have been chosen to capture typical residential building features and cover a variety of applications.

4.2.3 Combined Testing Process

Figure 4-1 illustrates the combined test process, which includes both types of comparisons. It starts with the parametric run generator RHBGen (described below), which takes as input the basic parametric case list, a description of the parameter variations and building prototypes. It then generates an expanded case list and RHB input files, and runs RHB. Then, the ESP-r input generator (described below) takes in the expanded case list and the system capacities and design airflow rates determined by RHB, and creates the ESP-r input files. Perl scripts (described below) will then run the ESP-r simulations, both with an ideal system (to determine the loads for a load comparison) and with a residential cooling system with RHB-determined system capacities and design airflow rates (for the system design evaluation.) ESP-r results are then processed by the ESP-r output processor and post processor (described below).

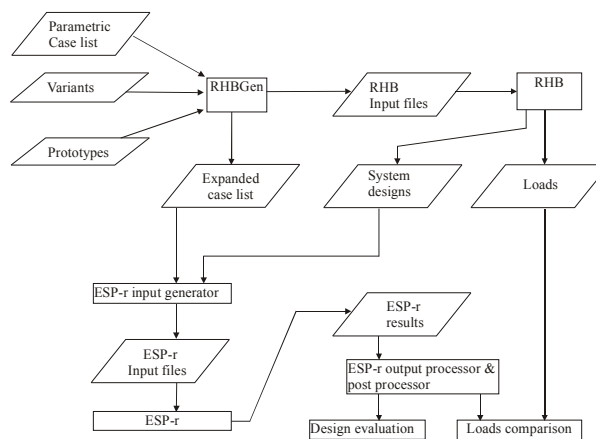


Figure 4-1. Overall inter-model testing process

4.2.4 RHBGen Parametric Generator

RHBGen is a FORTRAN application built with the same general framework as RHB. Starting with a parametric case list, a description of the parameter variations and building prototypes, it generates and runs large numbers of RHB cases. In the inter-model comparison, RHBGen is not only used to generate and run RHB cases, but also to generate a list of codes of the cases to be compared, loads for comparison to ESP-r and system capacities and airflow rates as inputs to ESP-r.

An important RHBGen feature is its ability to apply variants to a given parametric code. For example, the variant “O=000|090|180|270” causes each base case to be expanded into 4 cases – one for each orientation. Variants are applied in a nested fashion, so “L=CASD|TNME|FLKW, O=000|090|180|270” generates 12 runs. (In this case, it would generate all combinations of locations San Diego, Memphis and Key West, and orientations of north, east, south, and west.) This makes it straightforward to generate large case sets in an automated fashion.

4.2.5 ESP-r System

4.2.5.1 ESP-r Input Generator

The ESP-r input generator starts with a set of base case input files for each house prototype that is going to be tested. In the base case input files, there are no windows, shading, internal mass, internal gains or infiltrations defined. Given the parametric code for the specific case, the ESP-r input generator will modify the corresponding input parameters.

The ESP-r input generator is created taking advantage of the text mode interface of ESP-r. It exists in the form of shell scripts managed by a set of Perl scripts, rather than a FORTRAN program as in RHBGen. There are two types of shell scripts: one type modifies the prototype dependent input parameters; the other type modifies the prototype independent input parameters. There is a set of the first type of shell scripts for each house prototype and a set of the second type of shell scripts for all prototypes.

Each shell script serves to modify a group of input parameters and is manipulated by the Perl scripts, which manage the entire ESP-r test procedure. (Some sample shell scripts and Perl scripts are included in Appendix C.) The parameters are grouped to be modified by individual shell scripts as follows:

- Location: The location information (weather file name and latitude, longitude difference) is modified by the shell script *Climate*. (The ESP-r weather file for each location is created beforehand by a separate weather file generator.)
- Orientation: The orientation of the building is modified by the shell script *Rotate*, which rotates the building to the required orientation. When external shading obstructions are present, they are rotated together.
- Fenestration: The fenestration area, type, and internal shading information are modified by the shell script *WinAreaTyIsh*. External shading, if present, is added by the shell script *ExtSh*. All fenestration types are predefined in the ESP-r optics database and are selected by the database index.
- Internal gain and infiltration: The internal gains and infiltration are modified by the shell scripts *IntGain* and *Infiltration*.

- Construction and surface properties: The construction and surface properties of the external walls, external ceilings and roofs, external floors, internal partitions and internal floors/ceilings are modified by the shell script *Modcon*. The surface properties (short wave absorptivity and long wave emissivity) are stored in the material property database in ESP-r and then incorporated into the construction type. So for each combination of construction and surface property, a construction type needs to be defined in the ESP-r construction database. The construction index in the database is assigned to a specific fabric component using the “construction anchor” of ESP-r, which can be used to attribute a property to a group of components.
- Internal thermal mass: if present, the internal thermal mass and its construction type are added by the shell script *ThermalMass*.
- Floor configuration: the external floor boundary condition is modified by the shell script *FloorConfig*.
- Set point: in the system design evaluation mode, the internal air set point in the master zone is modified by the shell script *Setpoint*. In an ideal load comparison mode, the set points for all zones are modified by the shell script *Setpoint_Ideal*.
- After the above parameters are modified, the view factors for internal long wave radiation, the solar shading and insolation files, the convection coefficient files (if fixed convection coefficients is being used) will be updated by the shell scripts *ViewFactor*, *Shade* and *ShInsolation* (or *Insolation*), and *HcConv*.

The input generator modifies the parameters in an order that will not cause any conflicts between various input files (since the ESP-r input is a multi-file system) and

ensures that all information is updated. The order that has been found to work well is as follows:

- House Model (select base case)
- Location (Climate)
- Floor boundary condition configuration
- Constructions except for windows and internal thermal mass
- Thermal mass (construction, surface/floor area ratio)
- Window area, type, internal shading
- Window external shading (overhangs, fins)
- Internal gain level
- Infiltration level
- Orientation (rotate building)
- Update internal surface view factors
- Update shading/insolation files
- Update convection coefficient files if necessary
- Set point modification

4.2.5.2 ESP-r Test Procedure

As shown in the overall flow diagram, the ESP-r test procedure reads in the parametric codes and creates corresponding input files; takes the system capacities designed by RHB; runs the simulations; and processes the results. PERL scripts are written to manage the whole procedure. Specifically, the PERL scripts:

- Read in the parametric code for each case. (The case code list is generated by RHBGen.)
- Make a copy of the base case input files.
- Call the input generator (shell scripts) to modify input parameters.
- Read in the system inputs from the RHB result file (generated by RHBGen).
- Call shell scripts to modify the system airflow rates if in the design evaluation mode.
- Call shell scripts to run the simulation.
- Call shell scripts to analyze the result.

4.2.5.3 ESP-r Output Processor and Post Processor

The ESP-r output processor extracts and summarizes the results from each test case and writes the results of interest to files for further analysis and plotting. The ESP-r output processor is also written in Perl. All output files are in comma-separated format for convenience of post processing in a spreadsheet.

For load comparisons, both the peak loads and hourly loads of ESP-r and RHB are extracted and output into four separate files. (ESP-r peak, ESP-r hourly, RHB peak, and RHB hourly.)

For system design evaluations, the output processor writes a file containing the maximum, minimum, and mean values of room temperature and Predicted Percentage Dissatisfied (PPD). Times of occurrence for the minimum and maximum values are also

output. In addition, hourly room temperature and PPD values are output in two separate files.

Some output from ESP-r (such as PPD values) needs to be further processed in order to present the evaluation results clearly. This is dealt with by the ESP-r post processor (in the form of PERL scripts). Having a separate post-processor allows experimentation with the post-processing algorithm without having to rerun the time-consuming ESP-r simulations.

4.2.6 Design Evaluation Figure of Merit

For purposes of the design evaluation testing procedure, it is desirable to have a figure of merit for each system design (designed for a specific building case with a given version of the load calculation procedure). The figure of merit should have the following characteristics:

- Feasible to calculate with ESP-r, or to calculate with results given by ESP-r.
- Somehow capture the overall suitability of the design, as experienced by the occupants.
- Useful in identifying bad systems – ones that have too much temperature swing or too much temperature variation between rooms.
- Simple – preferably one number.

Some thermal comfort related parameter would seem to be ideal, as it should be useful in representing the suitability of the design as experienced by the occupants. ESP-

r can give the predicted mean vote (PMV) or the predicted percentage of dissatisfied (PPD) at each time step in the simulation or averaged over each hour. (Time steps in ESP-r may be as short as a minute.) While PMV has the advantage of giving information as to whether the space is too cold or too hot, if a simple figure of merit is to be reached, it is preferable to further simplify the thermal comfort information by using the PPD. As shown in Figure 4-2 below, there is a direct relationship between PPD and PMV.

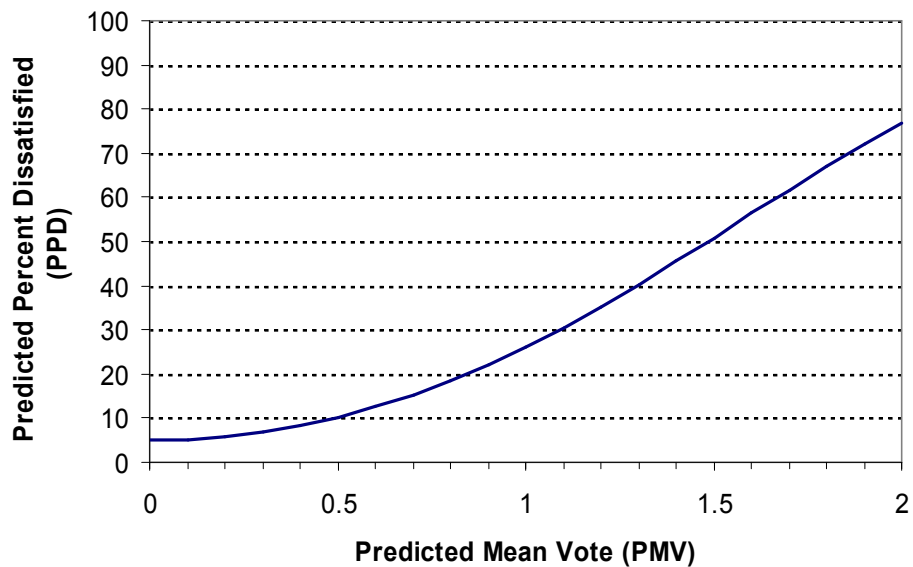


Figure 4-2. Predicted Percentage of Dissatisfied (PPD) as a function of Predicted Mean Vote (PMV)

This relationship is given by Equation 64 in Chapter 8 of the *2001 ASHRAE Handbook of Fundamentals*:

$$PPD = 100 - 95 \exp\left[-\left(0.03353PMV^4 + 0.2179PMV^2\right)\right] \quad (4.1)$$

Being able to determine PPD for any given room at any given time step is useful, but does not yet allow us to develop a single figure of merit. Unfortunately, no single figure of merit was identified that distinguished between a “good” system and a “bad” system. As described in Section 4.3.3, a procedure has been developed which gives integrated PPD values that distinguish between undersizing, inadequate distribution / control problems, and nighttime ambient overcooling. Another figure of merit called Degree Hours (DH) has also been developed to evaluate whether or not the system design is over-sized.

4.2.7 Model Assumptions Used in the Comparison

When comparing the results and determining the source of possible discrepancies between ESP-r and ResHB, it is necessary to look into the building sub-models used in each program. Both ESP-r and ResHB may have one or several options for each sub - model. In the load comparison mode, the ResHB calculations were verified and ResHB and ESP-r input used for design evaluation was reconciled. In order to reconcile the differences, it was necessary to use the same sub-models in both programs whenever possible.

In the design evaluation mode, the system design produced by ResHB was evaluated through the relatively detailed simulation of ESP-r so that guidance could be provided for the refinement of ResHB. Therefore, in ESP-r, the “best available” sub-models were chosen. Table 4-5 shows the sub-models used for the comparison results presented below. (Models that have not caused significant discrepancies in the detailed studies were ignored in the table.)

Table 4-5 Part 1 Model assumptions used in ESP-r and RHB for the comparison

Models		ESP-r	RHB	
Solar irradiance	Clear sky solar	ASHRAE clear sky model with Machler/Iqbal revised A, B, and C coefficients (1985)	ASHRAE clear sky model with Machler/Iqbal revised A, B, and C coefficients (1985)	
	Sloped surface incident diffuse solar (i.e. short wave sky model)	Perez (1990, 1987)	Perez (1990, 1987)	
Internal solar distribution	Load comparison mode	Beam on the floor, diffuse distributed on a area/absorptance weighting basis	Beam on the floor with internal mass surfaces treated as “half floor” ³ , diffuse distributed in proportion to surface area-absorptance product	
	Design evaluation mode	Beam distribution calculated with detailed ESP-r model (by Module <i>ish</i>), diffuse distributed on a area/absorptance weighting basis	Beam on the floor with internal mass surfaces treated as “half floor” ³ , diffuse distributed in proportion to surface area-absorptance product	
External long wave radiation	Clear sky temperature model	Martin and Berdahl (1984)	Martin and Berdahl (1984)	
	Outside ground surface temperature	ESP-r algorithm ¹	Equals outside air temperature	
	Surrounding buildings’ surface temperature	ESP-r algorithm ²	Equals outside air temperature	
	View factor for vertical surfaces	To the sky	0.45	0.35
		To the ground	0.45	0.5
To surrounding buildings		0.1	0.15	

¹ Ground temperature at 1.2m depth calculated from the procedure of Kusuda and Achenbach (1965) was input to ESP-r. ESP-r calculates the ground surface temperature with a 6-node finite volume scheme, assuming the 1.2m depth ground temperature as a constant.

² The average temperature of the surrounding external buildings for a surface is estimated by using the temperature of the zone surface, which has an azimuth difference of 180 Deg. This method is assumed to be applicable for surfaces with elevations > -30 and < 30 deg. For all other surfaces (i.e. elevations < -30 and > 30 deg.) use a mean weighted average of all external surfaces in all zones under simulation. (*From ESP-r code*)

³ half of the internal thermal mass surface receives beam solar irradiation (the total floor surface receives beam solar irradiation, hence the phrase “half floor”).

Table 4-5 Part 2 Model assumptions used in ESP-r and RHB for the comparison

Models			ESP-r	RHB
Convection coefficients	Load comparison mode	Inside	Fixed- Ceiling: 1.25 W/m ² -K (0.22 Btu/hr-ft ² -F) Walls: 4.7 W/m ² -K (0.82 Btu/hr-ft ² -F) Floor: 4.4 W/m ² -K (0.77 Btu/hr-ft ² -F)	Fixed- Ceiling: 1.25 W/m ² -K (0.22 Btu/hr-ft ² -F) Walls: 4.7 W/m ² -K (0.82 Btu/hr-ft ² -F) Floor: 4.4 W/m ² -K (0.77 Btu/hr-ft ² -F)
		Outside	Fixed-12.5 W/m ² -K (2.2 Btu/hr-ft ² -F)	Fixed-12.5 W/m ² -K (2.2 Btu/hr-ft ² -F)
	Design evaluation mode	Inside	System on: correlation based on data from ASHRAE 559-RP and 664-RP System off: ESP-r default natural convection (Alamdari and Hammond, 1983)	Runtime weighted. System on: 5 W/m ² -K (0.88 Btu/hr-ft ² -F) on all surfaces System off: ASHRAE still air values with flow-direction enhancement; linear transition of value from $\Delta T = -1^{\circ}\text{C} - +1^{\circ}\text{C}$ (-1.8°F - +1.8°F)
		Outside	MoWiTT (Yazdanian and Klems, 1994)	MoWiTT (Yazdanian and Klems, 1994)
	Elevation adjustment		No	No
Conduction	Conduction methods		Finite volume method	Conduction Transfer Function method (CTF method)
	Inter-zone conduction		Modeled in detail, Inter-zone partitions are modeled in full-thickness and exposed to the air temperatures of the rooms they are connecting	Not modeled, inter-zone partition modeled in half thickness with adiabatic outside condition

4.3 Results

4.3.1 Description of Test Sets

The results presented below are for two prototypes: one is a two-zone “Shoebox” prototype, the other is a 4-bedroom house. As shown in Figure 4-3, the Shoebox prototype has two adjacent rectangular-shaped zones of dimension 8 m x 6 m x 2.4 m

(26.2 ft x 19.7 ft x 7.9 ft). With orientation equal to zero, the east-side zone is called the “slave room”, the west-side zone is the “master room.” (The two zones are connected on the 8 m x 2.4m (26.2 ft x 7.9 ft)) facade. All other facades are exposed to the outside.) If present, the windows will be at the front and left facades of the slave room, and at the back and right facades of the master room. The thermostat is located in the master room. The two rooms are connected by a doorway and the return grille is in the master room, so that all return air from the slave room passes through the doorway into the master room.

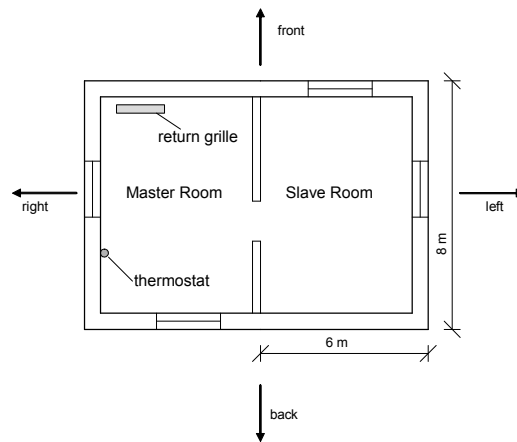


Figure 4-3. Schematic floor plan of the Shoebox prototype (figure drawn with front side facing north; front, left, back, right as defined in RHBGen)

The 4-bedroom house prototype is a slightly simplified version of the real house used for the RHB experimental validation (discussed in Chapter 6). It has two floors (Figure 4-4 shows the schematic floor plans) and an attic. The first floor includes Foyer 1, Dining room, Family room, Kitchen and Laundry. The second floor includes Foyer 2, four bedrooms (Bedrooms 1 through 4) and two bathrooms (East and West). With orientation equal to zero, the Dining room and Foyer 1 of the first floor and Bedroom 1, Bedroom 2, and Foyer 2 of the second floor are facing north. If present, the windows will

be at the front facades of the Dining room, Bedroom 1, Bedroom 2 and Foyer 2, the back facades of the Family room, Kitchen, Bedroom 3 and Bedroom 4, and at the right facades of the Laundry and West bathroom. The thermostat is located in the Family room (the master zone). The rooms are connected by doorways or stairway (between Foyer 1 and 2), and there are return grilles in the Dining room, Family room, and each of the bedrooms.

As to the attic, the detailed geometry of the real house attic was used in creating ESP-r input files, while the default approximate attic model was used in the ResHB automatic runs (when using RHBGen for ResHB automatic runs, the default attic model is the only option to use. It generates an attic hip roof with a rectangular plan. The area of the rectangular plan is based on the width and length specified by the user. The attic ridge height is assumed to be 1.5m. Details of the ResHB default attic model can be found in the ResHB documentation (Barnaby, et al. 2004)). In the real house, there is a garage adjacent to the Laundry and Foyer 1, under Bedroom 1. The garage is not included in the 4-bedroom house prototype, as the garage is not conditioned space and no garage model can be included in ResHB automatic runs. Surfaces adjacent to the garage were set to be adiabatic (treated as internal partitions in ResHB). There is a basement in the real house, controlled at 20°C for experimental purposes. The basement is also not included in the prototype. Instead of exposed to a constant basement air temperature, the floor surfaces were set to be either adiabatic or exposed to ambient air temperature.

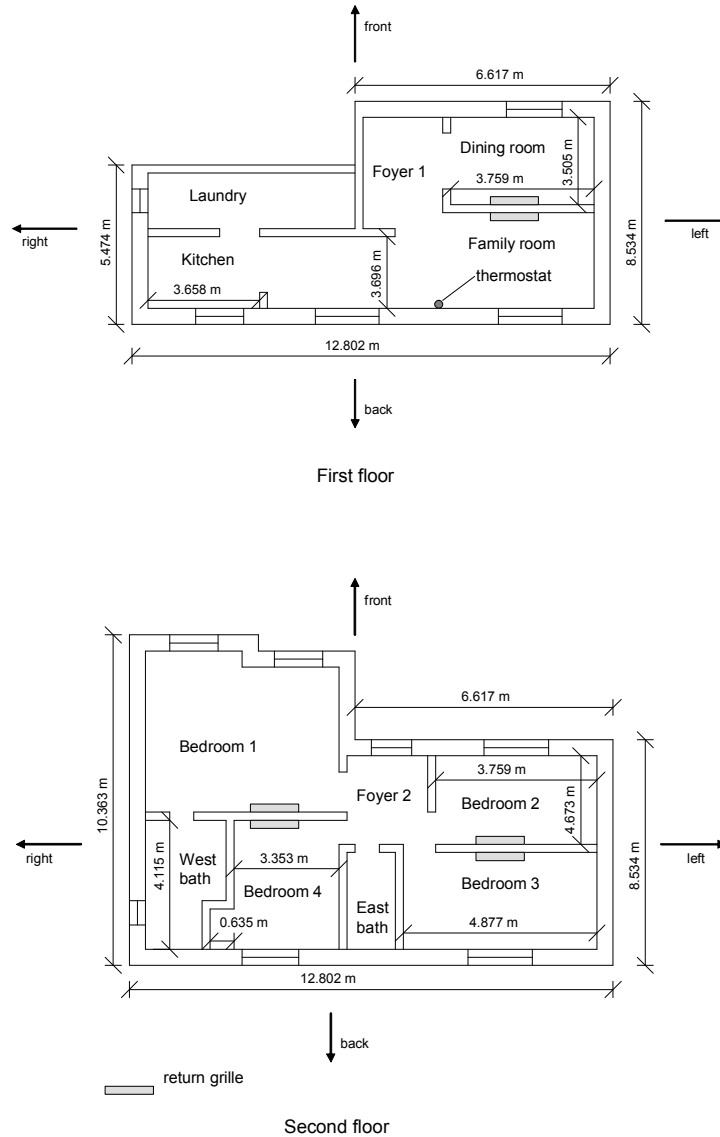


Figure 4-4. Schematic floor plan of the 4-bedroom house prototype (figure drawn with front side facing north; front, left, back, right as defined in RHBGen)

The test parameters, summarized in Table 4-6, include 9 locations, 4 orientations, 2 fenestration types, 2 fenestration areas, 2 constructions (light weight and heavy weight) for the roof, external wall and floor, and 2 floor configurations.

Table 4-6 Test parameters for the 576 test cases

	Parameters	Number of Variants	Variants
Changing parameters	Location	9	CASD, TNME, GAAT, AZPH, CASA, COAL, FLKW, MNMI, TXDA (San Diego; Memphis; Atlanta; Phoenix; Sacramento; Alamosa, Colorado; Key West; Minneapolis; Dallas)
	Orientation	4	0, 90, 180, 270
	Fenestration type	2	l: single glazing clear; x: double glazing low-E
	Fenestration area multiplier	2	l: 0.5; m: 1.0
	Roof, wall, floor construction	2	w: wood frame; c: solid concrete
	Floor configuration	2	0: adiabatic; a: exterior
	House model	2	Shoebox, 4-bedroom house
	Other parameters	Roof, wall, floor insulation	1
Interior mass floor area ratio		1	m: 100%
Internal gains, Infiltrations		1	0
Set point		1	m: 24°C (75.2°F)
Temperature swing		1	0: 0°C (0°F) or m: 1.67°C °C (3.0°F), depending on the test mode
Temperature setpoint offset		1	0: none
Exterior SW absorptivity		1	m: 0.6
Interior SW absorptivity		1	m: 0.6
Interior LW absorptivity		1	m: 0.9 (fenestration: 0.84)
Fenestration interior shading		1	0
Fenestration exterior shading		1	0
Interior partition construction		1	w: wood frame
Interior mass construction		1	w: wood frame

For both buildings, combination of the above parameter values gives 576 cases. Three variations on the analysis were done for both buildings, yielding a total of 3,456 cases. One variation was used for load comparisons -- this variation used a fixed setpoint and fixed convection coefficients. The other two variations, for system design evaluation, used the convection correlations summarized in Table 4-5. Two variations were created by varying the allowable temperature setpoint swing – in one variation, the RHB procedure sized the system and airflows using a fixed setpoint; in the other variation the

system capacity and airflows were determined which allowed a maximum temperature swing of 1.67° C (3.0°F).

4.3.2 Ideal Load Comparison

The results presented in this section for ideal load comparison and in the next section for ResHB system evaluation are for both prototypes (Shoebox and 4-bedroom house). In order to save the reader from endless similar plots, not all the results are enumerated for each prototype. If similar results are obtained for both prototypes, results are presented for only one prototype. Also, if similar results are obtained for several rooms in a prototype, only typical results for representative rooms are presented.

Generally, ResHB gives good predictions of peak cooling loads, ranging within $\pm 15\%$ ESP-r. A comparison of the ideal peak loads for the 576 test cases is shown in Figure 4-5 for the Shoebox master room. In the plot, the RHB-calculated peak load is plotted against the ESP-r calculated peak load. With the exception of a few cases, all load differences are between $-15\% \sim 10\%$. Figure 4-6 gives a clearer look of the load difference distribution for the same room. In this plot, the percentage cooling load difference based on the peak average Shoebox load is plotted against the ESP-r normalized loads (room cooling loads divided by room area). Most of the percentage load differences fall within a $\pm 5\%$ band. Out of 576 test cases, only 6 cases fall below -10% and all these 6 cases are for low load situations, with normalized loads less than 20 W/m^2 . A comparison of load predictions for the Shoebox slave room is very similar to that of the master room and is not shown here.

Peak cooling load comparison (Shoebox - Master)

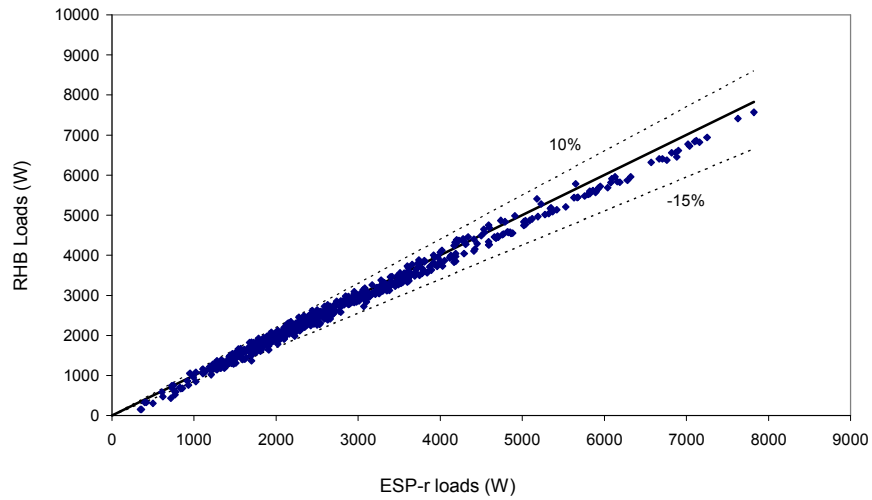


Figure 4-5. Peak cooling load comparison (Shoebox - Master)

Error percentage based on peak average Shoebox load (Master)

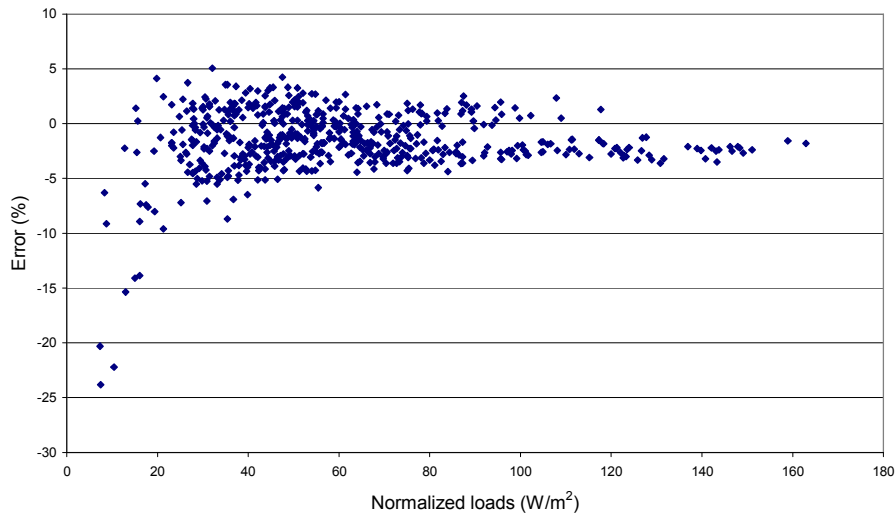


Figure 4-6. Cooling load error percentage based on peak average Shoebox load (Master)

Correspondingly, comparisons of the ideal peak loads for the 576 test cases for a few representative rooms in the 4-bedroom house prototype are shown in Figures 4-7 through 4-10. For each room, there are some cases where either ResHB or ESP-r predicts

some cooling loads (about 100~200W) while the other does not. Figure 4-7 shows the load comparison for the family room. With the exception of a few cases, all load differences are within $\pm 15\%$. For cases with relatively higher loads, ResHB tends to over-predict the peak cooling load. Load comparison for the Dining room is very similar to that of the Family room and is not presented here.

The load comparisons for both the Laundry and Foyer 1 (shown in Figure 4-8 and 4-9 respectively) are not as favorable as those of the Family room. For the Laundry room, there are some cases with load differences above 15% and many cases below -15%. For Foyer 1, most load differences are below -15%. This is caused by the different treatment of the inter-zone conduction in ResHB and ESP-r, as discussed in detail later in section 4.3.2.3. Also, there are obvious vertical bands shown in Figure 4-8 and 4-9, which is caused by ESP-r's minimum cooling load output limit (10W). Load comparisons for the Kitchen (first floor) and the two bathrooms (second floor) are very similar to that of the Laundry and Foyer 1 and are not repeated here.

Figure 4-10 shows the load comparison for Bedroom 1, which is typical for the four bedrooms and Foyer 2 on the second floor. With the exception of a few cases, all load differences are between -15% ~ 10%. For many cases, ResHB under-predicts the peak cooling load. Figure 4-11 shows the load comparison for the total house. Again, most load differences fall within a $\pm 15\%$ band and for many cases ResHB tends to under-predict the load.

The load difference distribution for the 4-bedroom house prototype is similar to that of the Shoebox prototype. Figure 4-12 plots the percentage cooling load difference

(based on the peak average 4-bedroom house load) against the ESP-r normalized loads for the Family room. Most of the percentage load differences fall within a $\pm 5\%$ band. Out of 576 test cases, only 11 cases fall below -10% or above 10% and all these 11 cases are for low load situations, with normalized loads less than 20 W/m^2 . Figure 4-13 plots the total percentage cooling load difference against the ESP-r normalized loads. Most of the percentage load differences are between $-15\% \sim 8\%$. Out of 576 test cases, only 20 cases are below -15% and 11 cases are above 8% . Again, all these cases are for low load situations, with normalized loads less than 20 W/m^2 .

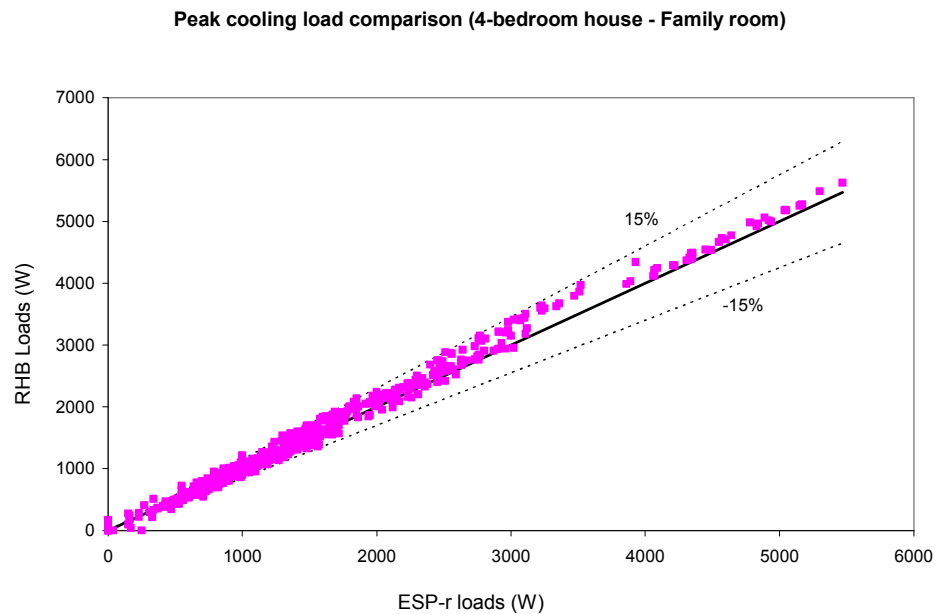


Figure 4-7. Peak cooling load comparison (4-bedroom house – Family room)

Peak cooling load comparison (4-bedroom house - Laundry)

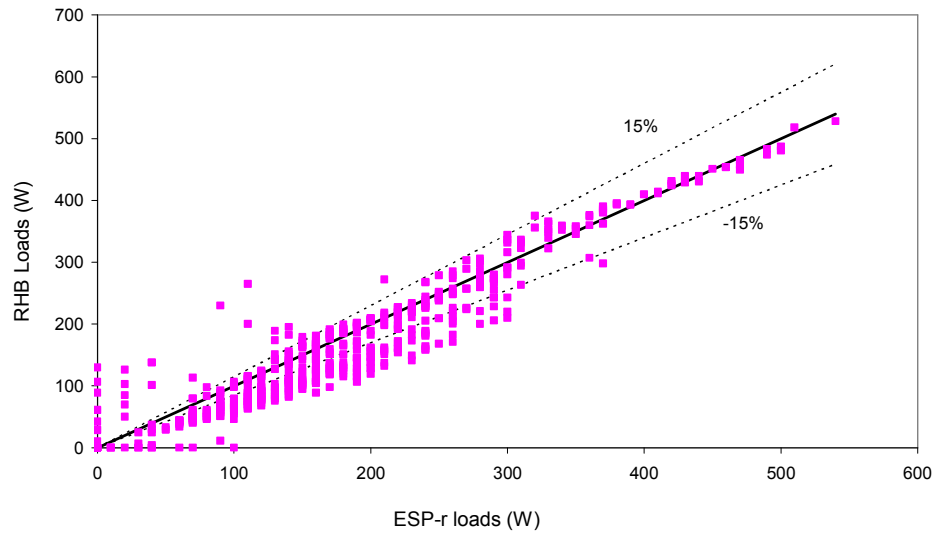


Figure 4-8. Peak cooling load comparison (4-bedroom house – Laundry)

Peak cooling load comparison (4-bedroom house - Foyer1)

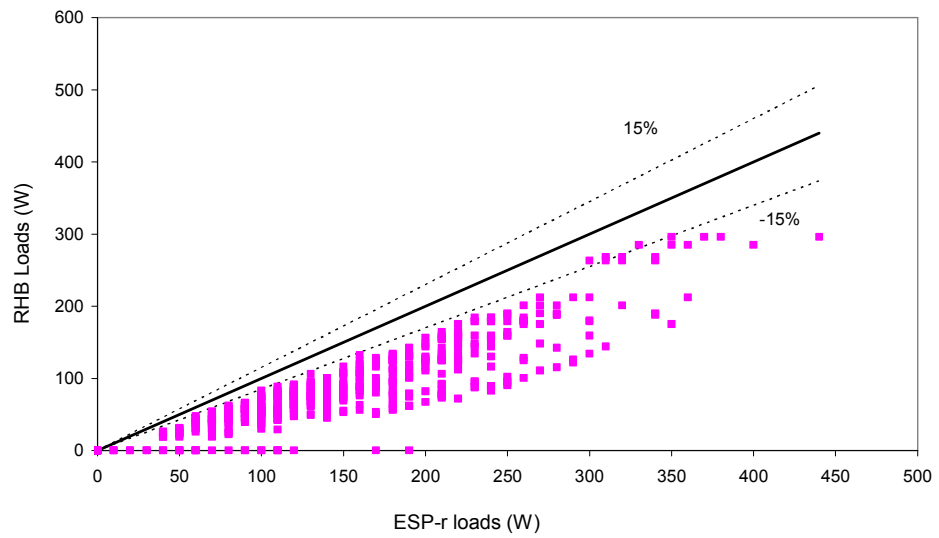


Figure 4-9. Peak cooling load comparison (4-bedroom house – Foyer 1)

Peak cooling load comparison (4-bedroom house - Bedroom 1)

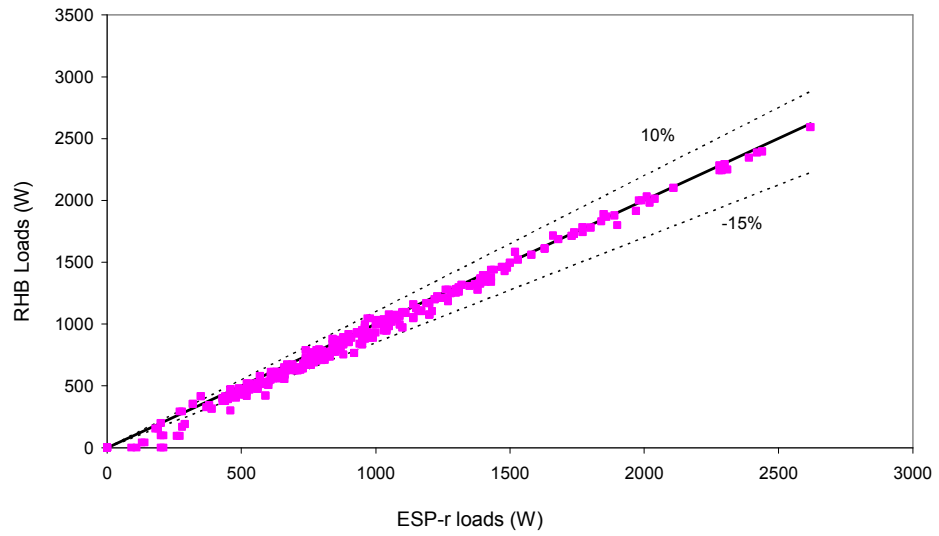


Figure 4-10. Peak cooling load comparison (4-bedroom house – Bedroom 1)

Peak cooling load comparison (4-bedroom house - Total)

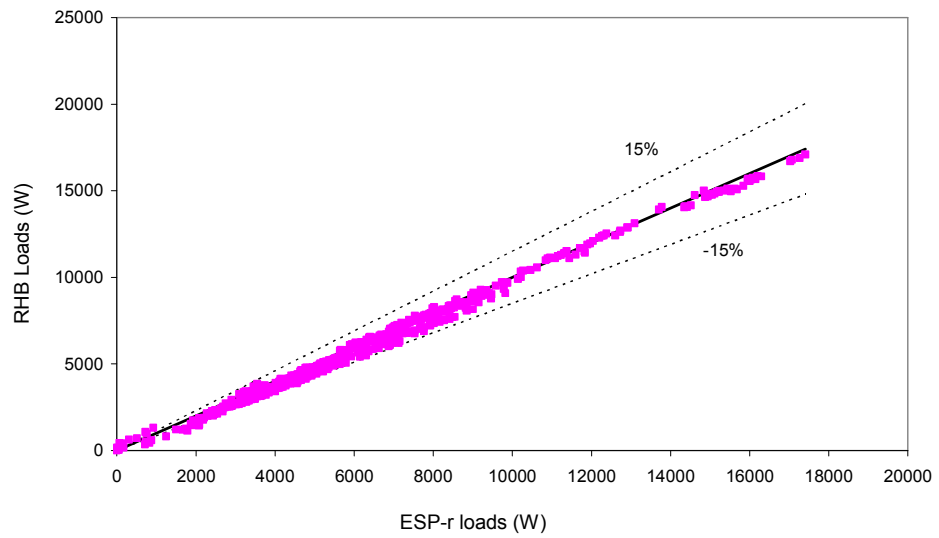


Figure 4-11. Peak cooling load comparison (4-bedroom house – Total)

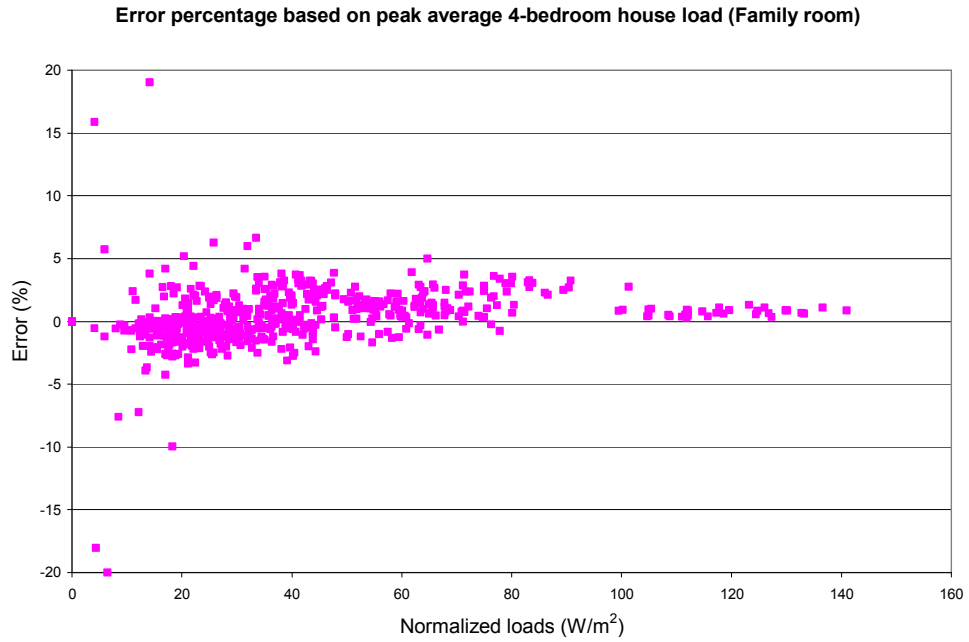


Figure 4-12. Cooling load error percentage based on peak average 4-bedroom house load (Family room)

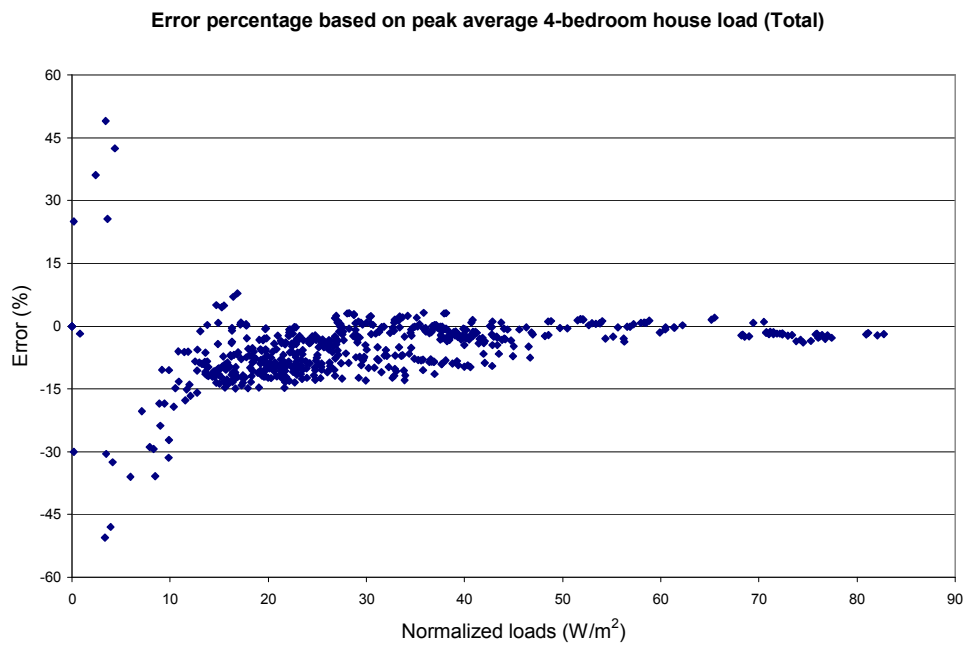


Figure 4-13. Cooling load error percentage based on peak average 4-bedroom house load (Total)

The differences between ResHB and ESP-r predicted cooling loads are caused by the differences in the heat transfer models used by each program, as discussed below.

4.3.2.1 External Long Wave Radiation Models

As summarized in Table 4-5, each building surface is assumed to exchange longwave radiation with three different source/sinks – the sky, ground, and surrounding buildings. Both the values of the source/sink temperatures and the view factors from the surface to each source/sink are important in determining the longwave radiation flux. Comparing the model assumptions in each program, the view factors are slightly different; the sky temperatures are the same; but the temperatures assumed for the surrounding buildings and ground are somewhat different.

In the RHB program, both the outside ground surface temperature and the surrounding buildings' temperature are assumed to be equal to the ambient dry bulb temperature. In ESP-r, the user may specify a ground temperature at 1.2 m (4ft) depth; then a 1-d finite volume procedure is used to calculate the ground surface temperature. I used the Kusuda and Achenbach (1965) procedure to determine the ground temperature at 1.2 m (4 ft) depth. It should be noted that the 1-d finite volume procedure only accounts for conduction in the soil and convection, solar radiation, and longwave radiation at the surface. Evapo-transpiration effects are not included – hence, this is roughly equivalent to the ground being covered with dry pavement rather than vegetation. Vegetation should lower the ground surface temperature substantially. As shown in Figure 4-14 for Alamosa, Colorado, the ESP-r ground surface temperature is quite a bit higher than the RHB ground surface temperature, which is the same as the air

temperature. This causes ESP-r to predict higher radiative heat fluxes from the surrounding ground to the building surface; hence, higher surface temperatures; hence, increased heat gains; and hence, higher cooling loads.

The surface temperature of the surrounding buildings in RHB is also assumed to be the ambient dry bulb temperature. In ESP-r, the average temperature of the surrounding buildings is estimated by using the temperature of a zone surface that has an azimuth difference of 180 degrees (for surfaces with elevations between $-30 \sim 30$ degree). For all other surfaces (with elevations less than -30 or greater than 30 degree), a mean weighted average of the temperatures of all external surfaces in all zones is used. Figure 4-15 shows the comparison of the ambient dry bulb temperature and the outside surface temperatures calculated from ESP-r for the Shoebox master room in Alamosa, Colorado. The room has light weight (wood frame) construction with medium insulation, and 25% glazing (low-E double pane) area on the south and west facades. As can be seen, during the peak load hours, the surrounding buildings' surface temperatures are higher than the ambient dry bulb temperature, which leads to higher external long wave radiation from the surrounding buildings. Again, this leads to higher cooling loads in ESP-r.

For the case with surface temperatures shown in Figure 4-15, Figure 4-16(a) shows a comparison of the hourly cooling loads. The peak cooling load from the RHB program is about 10% lower than the peak cooling load calculated by ESP-r. For comparison purposes, the load calculation was redone with both programs after setting

the longwave emissivity to 0.01. This effectively eliminates the longwave radiation. The results are shown in Figure 4-16(b). Note the peak cooling loads are now within 2%.

The conclusion is that for this case, the external longwave radiation model is the significant difference between the two calculation procedures. Astute readers may also note that the peak cooling load went up after the longwave emissivity was set to 0.01. In Alamosa, Colorado, the sky temperature varies between -11.7°C (10.9°F) and 3.0°C (37.4°F). Therefore, radiation from the roof to the sky and, to a lesser extent, from the walls to the sky, significantly reduces the cooling load. When the longwave radiation is effectively eliminated, the cooling load shows a corresponding increase.

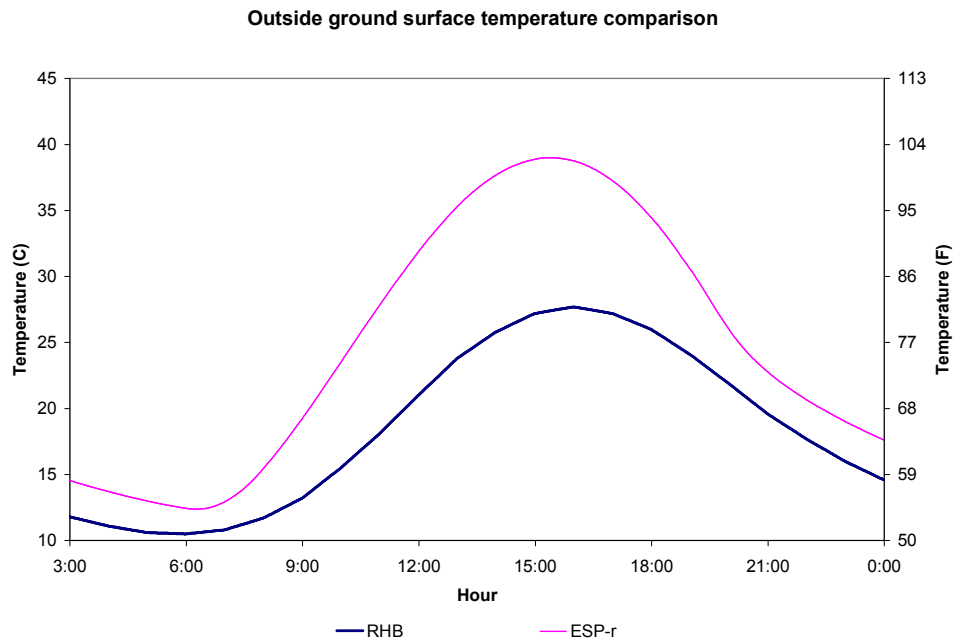


Figure 4-14. Outside ground surface temperatures from RHB and ESP-r for Alamosa, CO

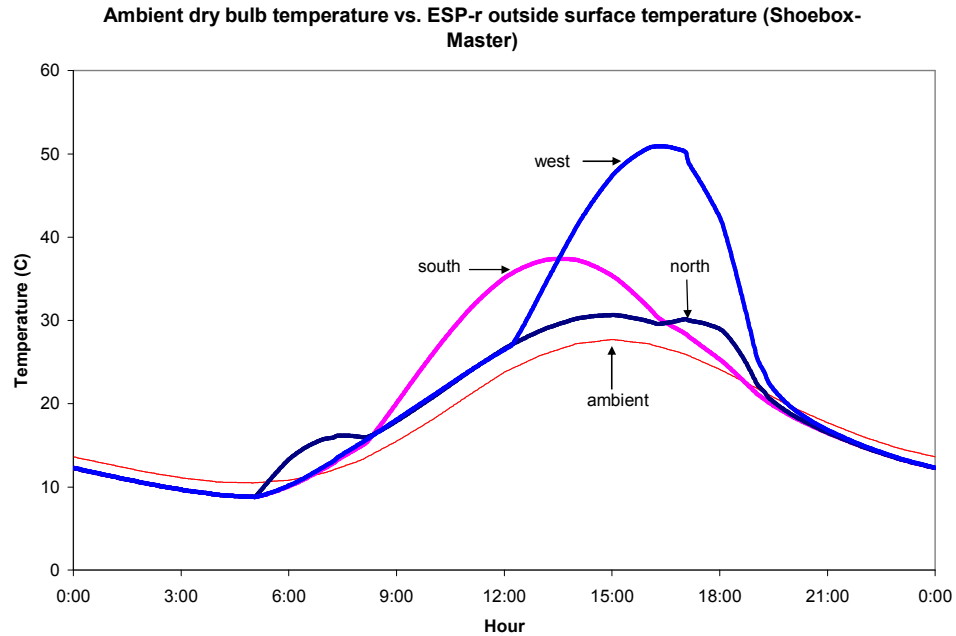


Figure 4-15. Comparison of the ambient dry bulb temperature and the outside surface temperatures calculated from ESP-r (Shoebox - Master)

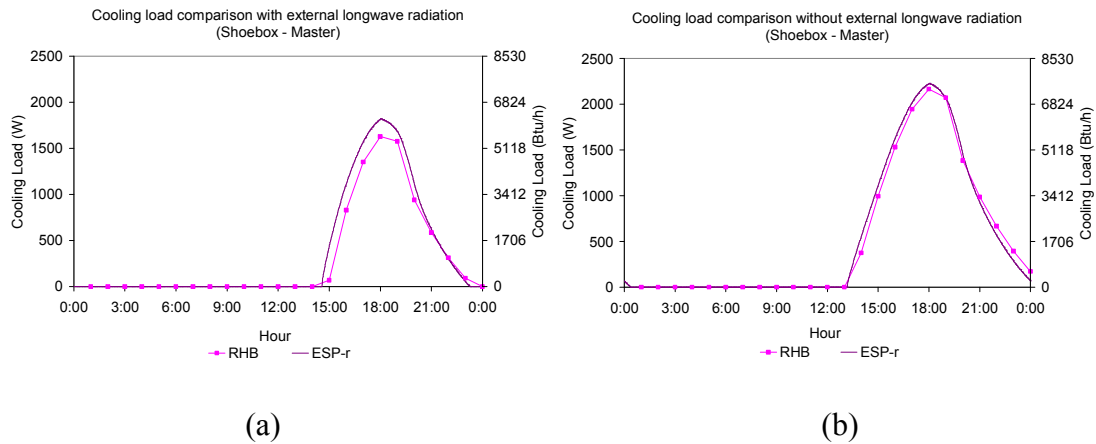


Figure 4-16. Comparison of cooling load calculated by RHB and ESP-r (Shoebox - Master): (a) with external long wave radiation (b) without external long wave radiation

To confirm the conclusion from the case study, all 576 cases were run without external long wave radiation for both the Shoebox and the 4-bedroom house prototypes. Comparisons between results with and without external long wave radiation are similar

for both prototypes. The effect caused by eliminating external longwave radiation can be seen most clearly in Figure 4-17, which plots the percentage load difference for the Family room in the 4-bedroom house against normalized ESP-r loads before (a) and after (b) the external longwave radiation was eliminated. Figure 4-17(b) shows significant improvement over Figure 4-17(a), especially in the low load area (less than 45W/m²). The points fall beyond the ±5% band in Figure 4-17(a) disappear in Figure 4-17(b). There are many points within the -5% ~ 0% band in Figure 4-17(a) move up in Figure 4-17(b) that most points in Figure 4-17(b) resides in the 0% ~ 5% band. Also, the Mean Bias Error (MBE) for the Family room is 47W with external long wave radiation and 113W without external long wave radiation. For the total 4-bedroom house, the MBE changes from -261W to -43W when the external long wave radiation was eliminated. Note that the MBE here and those in the later sections were calculated as the average of the difference between RHB and ESP-r predicted cooling loads, with ESP-r as the reference model, following the definition of MBE in Willmott (1982):

$$MBE = N^{-1} \sum_{i=1}^N (P_i - O_i) \quad (4.2)$$

where:

N = the number of cases

P = Predicted value, equals the RHB predicted loads in our case, W

O = Observed value, equals the ESP-r predicted loads in our case, W

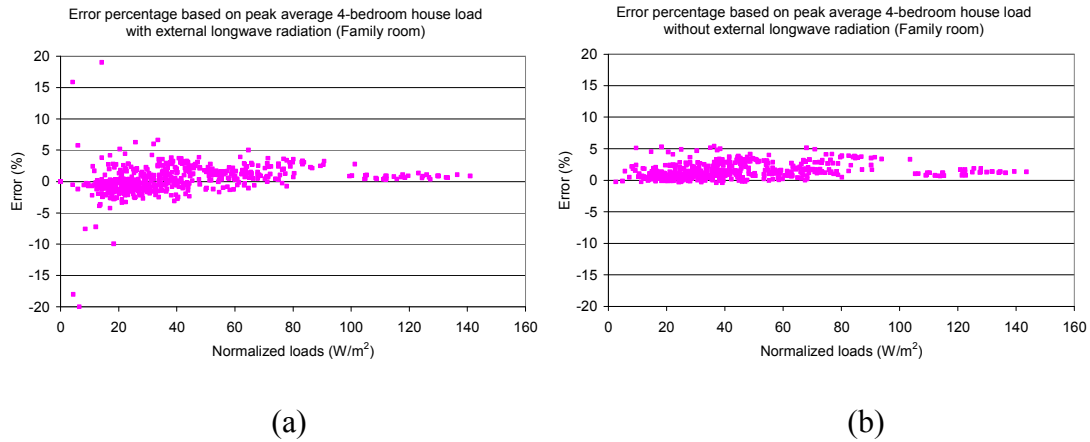


Figure 4-17. Comparison of cooling load error percentage between RHB and ESP-r (4-bedroom house – Family room): (a) with external long wave radiation (b) without external long wave radiation

In summary, ESP-r predicts higher cooling loads than RHB because of the different external longwave radiation source/sink temperature models. RHB uses very simple models, assuming that both other building temperatures and the ground surface temperature are the same as the air temperature. ESP-r has comparatively complex models, and the model for the other building temperatures seems likely to give more accurate answers. With regards to the ground surface temperature model, it should be noted that the ESP-r model is roughly equivalent to being surrounded by an empty parking lot. The ground surface temperature model does not account for evapotranspiration from the ground, nor does it account for the effects of vegetation. Presumably, the effective surface temperature for a building surrounded by lawn may be better approximated by the air temperature than a parking-lot surface temperature. While this tends to have a significant effect only on some lightly-insulated buildings, it should be a topic of further research.

4.3.2.2 Internal Solar Distribution

Internal solar distribution model is another factor that contributes to the load difference between RHB and ESP-r. As summarized in Table 4-5, the internal solar distribution model used in ResHB and ESP-r for the ideal load comparison mode differs on the treatment of internal thermal mass surfaces with respect to beam solar irradiation. In ResHB, half of the internal thermal mass surface receives beam solar irradiation. In ESP-r, a simple solar distribution option is used such that all beam solar irradiation is specified to be on the floor. This difference on internal solar distribution model leads to the effect that ResHB predicts higher cooling loads than ESP-r for cases with concrete fabric construction. The concrete cases have internal thermal mass of wood construction, but concrete floors. The light-weight wood thermal mass tends to release the incident solar radiation as cooling loads faster than the heavy-weight concrete floor, hence higher loads in ResHB. For cases with wood fabric, as both the floor and internal thermal mass are of wood construction, the effect caused by the different treatment of internal solar distribution with regard to internal thermal mass is relatively small.

To demonstrate this effect, all 576 test cases (in which external longwave radiation has already been eliminated, as stated above) for both prototypes were re-run without internal thermal mass, so that both ResHB and ESP-r have the same internal solar distribution of all beam solar irradiation on the floor. Presumably the load differences for concrete cases would significantly decrease. This was confirmed by test results for both prototypes. Figure 4-18 shows the comparison between results with and without internal thermal mass for the Shoebox Master room. We see that in Figure 4-18(a) (with internal thermal mass) there is a large group of points fall above the 1:1 correspondence line,

which means ResHB over-predicts cooling load for these cases. In Figure 4-18(b) (without internal thermal mass) the number of points fall above the 1:1 correspondence line greatly reduces. Which cases have moved downward in Figure 4-18(b) can be clearly seen in Figure 4-19, which shows the comparison of cooling load error percentage before and after the internal thermal mass was removed. The cooling load error percentage between ResHB and ESP-r (based on peak average Shoebox load) is plotted against the case number in Figure 4-19. Comparing Figure 4-19(a) (with internal thermal mass) and Figure 4-19(b) (without internal thermal mass), we see little change in the error percentage for the wood cases, but a significant drop in the error percentage for the concrete cases. The MBE for the concrete cases changes from 101W to -23W when the internal thermal mass was removed.

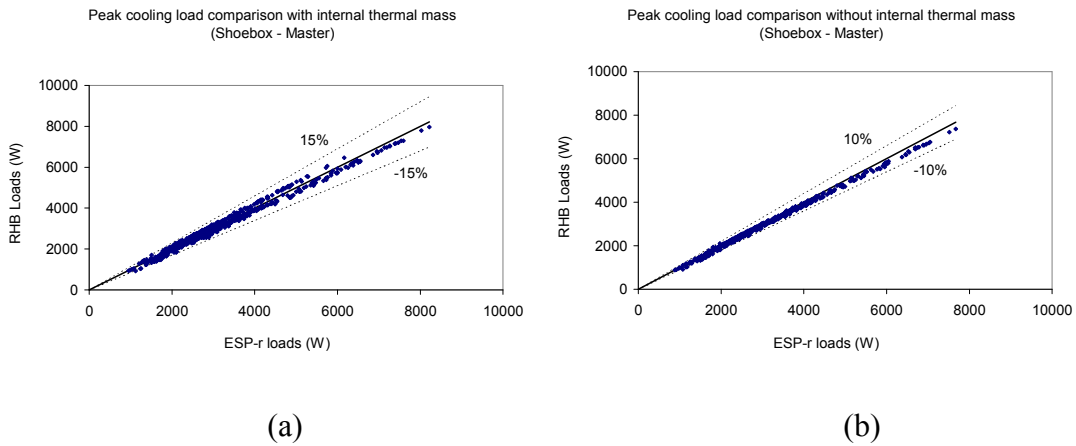


Figure 4-18. Comparison of cooling load calculated by RHB and ESP-r (Shoebox – Master): (a) with internal thermal mass (b) without internal thermal mass

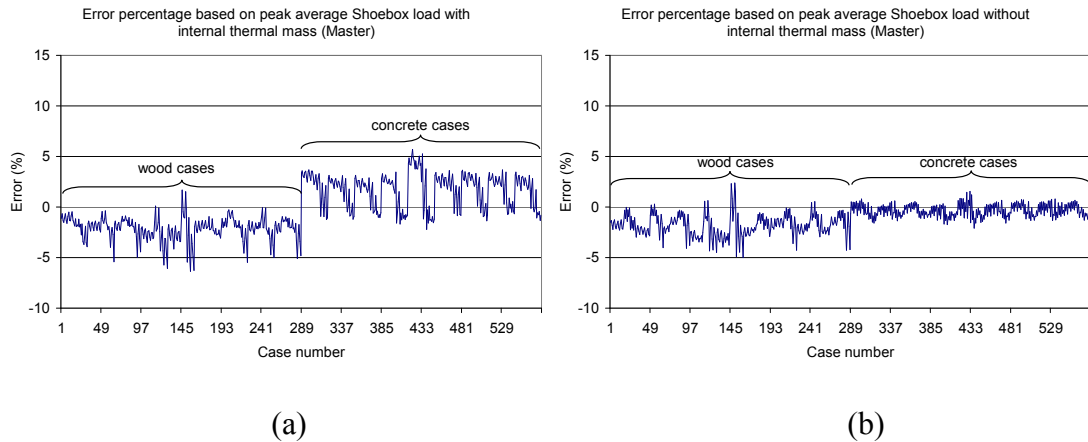


Figure 4-19. Comparison of cooling load error percentage between RHB and ESP-r (ESP-r with simple solar distribution, Shoebox – Master): (a) with internal thermal mass (b) without internal thermal mass

A detailed solar distribution option is also available in ESP-r, in which hourly solar distribution can be calculated through the module of “*ish*”. As this presumably is a more accurate treatment than the simple option, and therefore a better base case, it is interesting to look at the effects of using this option. A set of 576 test cases (with internal thermal mass, again, based on test cases without external longwave radiation) were run in ESP-r using the detailed solar distribution and an assumed position of the thermal mass surface at a height of 0.5m. The resultant cooling load error percentage between ResHB and ESP-r is plotted in Figure 4-20(a) for the same room. Instead of over-predicting, ResHB is under-predicting cooling loads for many concrete cases this time, although the under-predicting level (when the detailed ESP-r option is used) is smaller than the over-predicting level (when the simple ESP-r option is used). The MBE for the concrete cases changes from 101W to -51W when the internal solar distribution model was switched from the simple to the detailed option in ESP-r. For comparison purposes, the results for test cases in which both ESP-r and ResHB have the same simple solar distribution but without internal thermal mass (as discussed above and shown in Figure 4-19(b)) are also

plotted in Figure 4-20(b). Comparing Figure 4-20(a) and Figure 4-20(b), we see that there is a significant change in the error percentage for concrete cases, moving upward from about -4% ~ -5% to around -1%. Again, there is little change in the error percentage for the wood cases.

The comparisons in Figure 4-19 and Figure 4-20 indicate that the ResHB predicted cooling loads stand in between, higher than the ESP-r predicted loads with simple solar distribution, and lower than the ESP-r predicted loads with detailed solar distribution for the specific assumed position of the thermal mass surface.

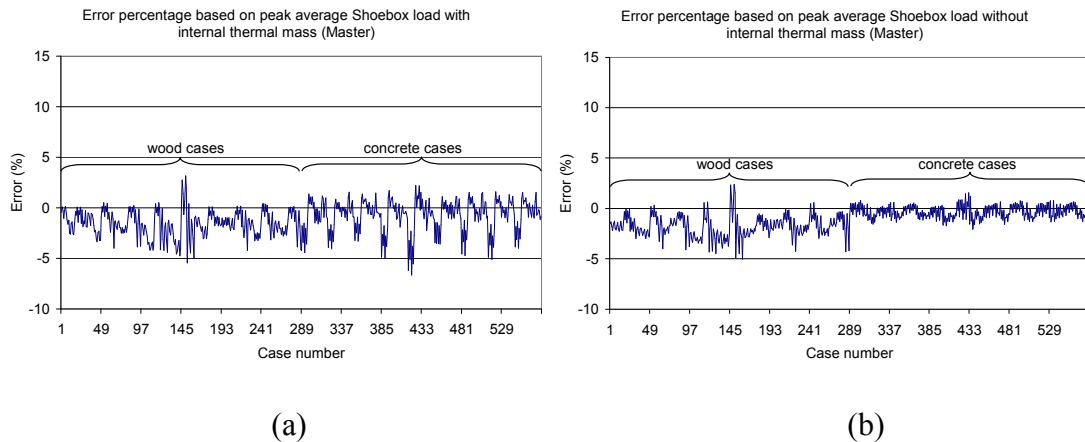


Figure 4-20. Comparison of cooling load error percentage between RHB and ESP-r (Shoebox – Master):

(a) ESP-r with detailed solar distribution, with internal thermal mass (b) ESP-r with simple solar distribution, without internal thermal mass

To give an idea of how much difference it causes by switching from simple to detailed internal solar distribution model in ESP-r, Figure 4-21 gives a direct comparison between the two options in ESP-r. In Figure 4-21(a), the ESP-r predicted cooling loads with simple solar distribution are plotted against the ESP-r predicted cooling loads with

detailed solar distribution (for the Shoebox Master room). Figure 4-21(b) gives the corresponding cooling load error percentage, using the cooling loads with detailed solar distribution as a reference. We see that for wood cases, the cooling loads with simple solar distribution are either higher or lower than the cooling loads with detailed solar distribution, with error percentage ranging $-1.5\% \sim 2.7\%$. For concrete cases, the cooling loads with simple solar distribution are mostly lower than the cooling loads with detailed solar distribution, with error percentage ranging $-11.0\% \sim 1.2\%$. Again the large difference in concrete cases can be explained by the different thermal responses to solar insolation of the concrete (fabric) and wood (internal mass and partition) constructions.

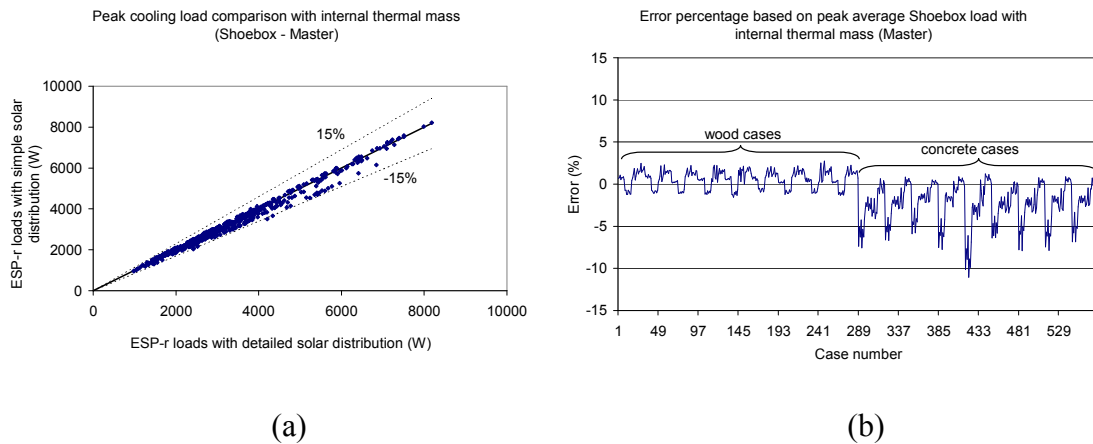


Figure 4-21. ESP-r simple solar distribution vs. detailed solar distribution (Shoebox – Master): (a) comparison of cooling load (b) comparison of cooling load error percentage

It needs to be noted that for most cooling load calculations performed for design purposes, it is actually very difficult to get a good prediction of the internal thermal mass surfaces and their positions, and correspondingly a good prediction of internal solar distribution. ResHB provides a simple model with a consideration of the fact that internal thermal mass usually captures some incident solar radiation, which is an improvement to

the model of putting all beam irradiation on the floor. This simple model is arguably an appropriate way to approach the internal solar distribution problem for design cooling load calculation procedures.

4.3.2.3 Inter-zone Conduction

As summarized in Table 4-5, inter-zone heat conduction is not modeled in RHB. Inter-zone partitions are modeled in half-thickness with adiabatic outside boundary condition. In ESP-r, detailed inter-zone heat conduction is modeled. Inter-zone partitions are modeled in full-thickness and exposed to the air temperatures of the rooms they are connecting. Inter-zone conduction can happen in two circumstances under the ideal control strategy where room air temperature is either controlled at the set point by cooling or may drop below the set point when there is no cooling load. One circumstance is when two adjacent rooms have different load profiles such that there may be periods during which these two rooms have different room air temperatures. This could occur when one room has cooling load while the other does not. The room with cooling load will have a room air temperature at the set point; the room without cooling load may have a room air temperature below the set point. Different room air temperatures could also happen during the night when both rooms do not have cooling load with the room air temperatures floating to different values below the set point. Inter-zone conduction occurred during the night time ambient cooling hours will affect the cooling storage in the room constructions and hence affect the daytime cooling loads. Another circumstance is when an internal partition connecting two rooms receives solar insolation on one side, such as the floor of a room with windows on the second story, so that the surface

temperature on that side becomes higher than the surface temperature on the other side and leads to inter-zone conduction.

Inter-zone conduction tends to moderate the cooling load difference between rooms. To demonstrate the load moderating effect caused by inter-zone conduction, all 576 test cases for both prototypes were run in ESP-r without inter-zone conduction, based on the cases without external longwave radiation and internal thermal mass. When running ESP-r without inter-zone conduction, internal partitions were changed to half thickness and set to be adiabatic outside, so that internal partitions are treated in the same way as in RHB. The load moderating effect is more obvious in the 4-bedroom house prototype, where rooms have more internal constructions and more diverse load profiles. For this prototype, Figures 4-22 through 4-24 show the comparisons of cooling load calculated by RHB and ESP-r for test results with ESP-r using or not using inter-zone conduction. In each figure, the left side part (a) shows the results with ESP-r using inter-zone conduction and the right side part (b) shows the results with ESP-r not using inter-zone conduction. Figure 4-22 shows the results for the Family room. When inter-zone conduction was used in ESP-r (Figure 4-22(a)), most RHB predicted loads are about 0% ~15% higher than ESP-r predicted loads. When inter-zone conduction was not used in ESP-r (Figure 4-22(b)), RHB predicted loads match ESP-r predicted loads much better and in many cases, RHB loads are lower than ESP-r loads, indicating that ESP-r predicts higher loads for the Family room without inter-zone conduction. (The MBE for the family room changes from 92W to -31W when the inter-zone conduction was turned off in ESP-r). The load moderating effect caused by inter-zone conduction becomes more prominent for rooms with relatively small loads. Figure 4-23 and 4-24 show the results

for the Laundry and Foyer 1 respectively. We see that with ESP-r not using inter-zone conduction, the match between RHB and ESP-r predicted loads improves dramatically for both rooms. (When the inter-zone conduction was turned off in ESP-r, the MBE changes from -18W to -3W for the Laundry, and from -58W to -0.3W for the Foyer 1). Both the Laundry and Foyer 1 have only one external surface (the Laundry has one external wall with a small window, Foyer 1 has one external wall) and relatively small loads (less than 700W). For the Laundry, ESP-r predicts higher or lower loads without inter-zone conduction; for the Foyer 1, ESP-r predicts lower loads with inter-zone conduction turned off.

A clearer comparison of ESP-r predicted loads with and without inter-zone conduction is shown in Figure 4-25 for the Family room (a) and the Foyer 1 (b). In this figure, ESP-r predicted loads without inter-zone conduction are plotted against ESP-r predicted loads with inter-zone conduction. For the Family room, the cooling loads become higher without inter-zone conduction; for foyer 1, the cooling loads become lower without inter-zone conduction. This is considered reasonable as the Family room has relatively higher load than its adjacent rooms with two external walls and two windows. When inter-zone conduction is modeled in ESP-r, the Family room tends to transfer some energy to its adjacent rooms. When inter-zone conduction is not modeled, this energy stays in the Family room; hence, higher loads occur in the Family room without inter-zone conduction. On the contrary, Foyer 1 has relatively lower load than its adjacent rooms, with only one external wall. Foyer 1 tends to receive some energy from its adjacent rooms when inter-zone conduction is modeled. When inter-zone conduction

is not modeled, there is no energy transferred to Foyer 1 from its adjacent rooms; hence, lower loads occur in Foyer 1 without inter-zone conduction.

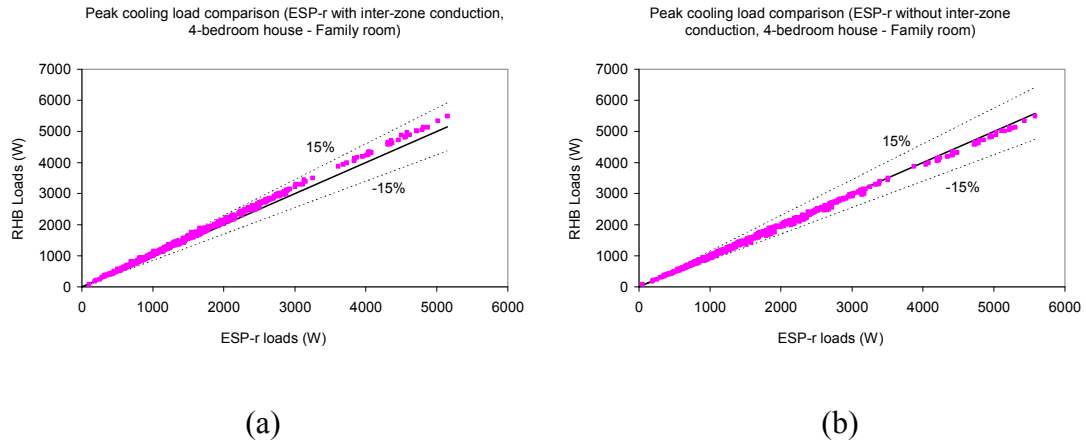


Figure 4-22. Comparison of cooling load calculated by RHB and ESP-r (4-bedroom house – Family room): (a) ESP-r with inter-zone conduction (b) ESP-r without inter-zone conduction

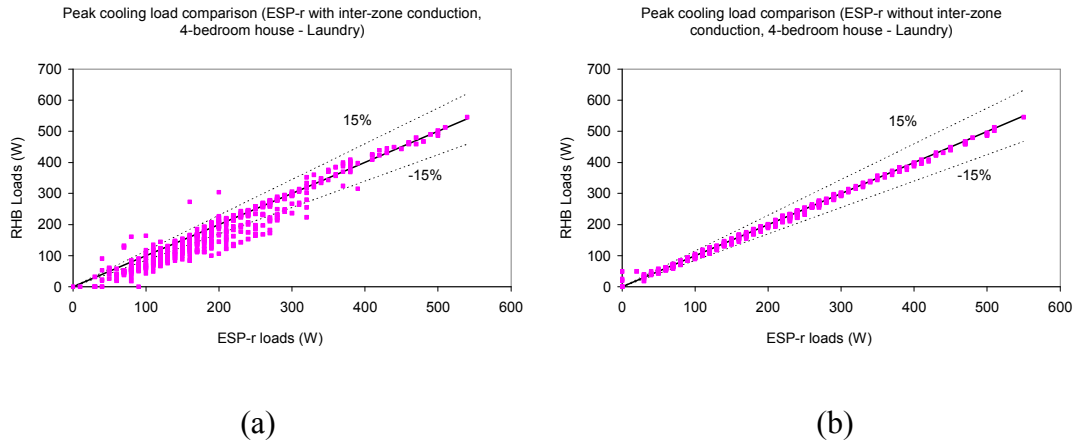


Figure 4-23. Comparison of cooling load calculated by RHB and ESP-r (4-bedroom house – Laundry): (a) ESP-r with inter-zone conduction (b) ESP-r without inter-zone conduction

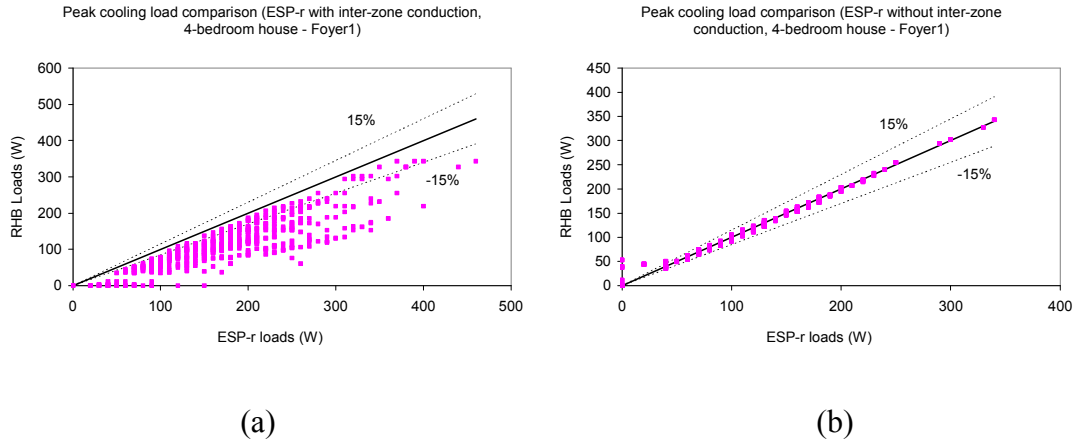


Figure 4-24. Comparison of cooling load calculated by RHB and ESP-r (4-bedroom house – Foyer 1): (a) ESP-r with inter-zone conduction (b) ESP-r without inter-zone conduction

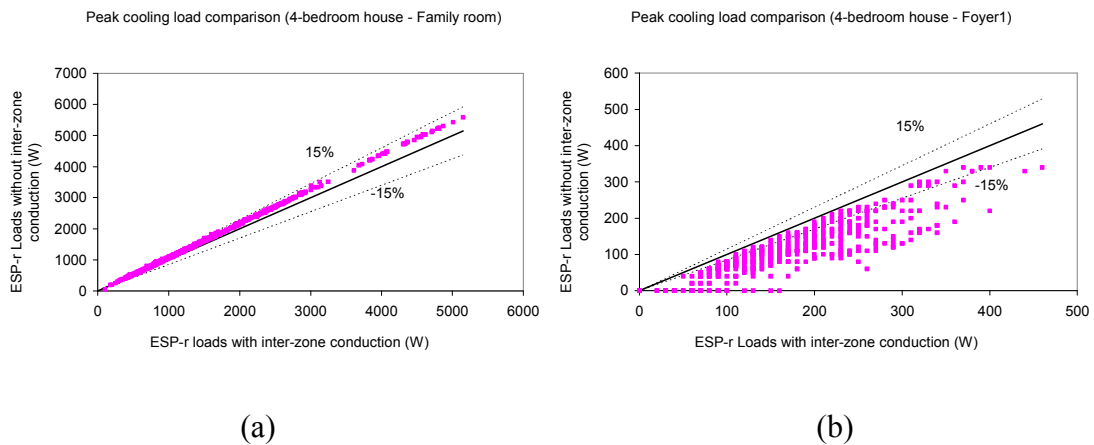


Figure 4-25. Comparison of ESP-r calculated cooling loads (without inter-zone conduction vs. with inter-zone conduction): (a) 4-bedroom house – Family room (b) 4-bedroom house – Foyer 1

It needs to be noted that although the load moderating effect caused by inter-zone conduction is most prominent in rooms with relatively small loads and seems not very important to the total house load and equipment sizing, it does explain the less favorable results in the cooling load comparisons for these rooms, as mentioned earlier. Also, if temperature swing is permitted with a master-slave control, more inter-zone conduction is expected and the corresponding effect may become more important. As temperature

swing is usually permitted in residential buildings, neglecting inter-zone conduction in residential design cooling load calculations may make a more significant difference than shown in the above simulations. Therefore, it may be of interest to add an inter-zone conduction model into RHB.

4.3.2.4 Internal Long Wave Radiation Models

For the cases discussed in the above section (4.3.2.3), the external long wave radiation was eliminated; the internal thermal mass was removed so that both ESP-r and RHB have the same internal solar distribution; inter-zone conduction was not modeled in both programs, and the same inside and outside convection coefficients were used by ESP-r and RHB. For these cases, other possible sources of load difference between ESP-r and RHB are solar radiation models, window models, conduction methods and internal longwave radiation models.

Although different internal long radiation models are used in ESP-r (detailed recursive/matrix method combined with analytical method) and RHB (MRT method), it can be shown that this has a very small effect on the load difference between ESP-r and RHB. Based on the cases described above (without external long wave radiation, internal thermal mass, and inter-zone conduction), all 576 test cases for the Shoebox prototype were run in ESP-r and RHB both with and without internal longwave radiation. The Shoebox prototype has two windows in each room and presumably is more sensitive to the internal longwave radiation model, as windows have the highest temperature difference with other surfaces in the room. The test results are very similar for both the Master and Slave rooms. For the Master room, Figure 4-26 shows the comparison of

cooling loads predicted by RHB and ESP-r for cases with (a) and without (b) internal longwave radiation. We see that after the internal longwave radiation was removed, there is some reduction both in ESP-r and RHB calculated loads, but we can hardly see the change with regards to the percentage load difference between the two programs. A calculation of the MBE shows that for the Master room it changed from -99W to -85W when the internal longwave radiation was turned off. This indicates that the difference between the internal longwave radiation models used by ESP-r and RHB has some small (but not much) contribution to the load difference between these two programs. The resultant differences will be negligible for design load calculation purposes.

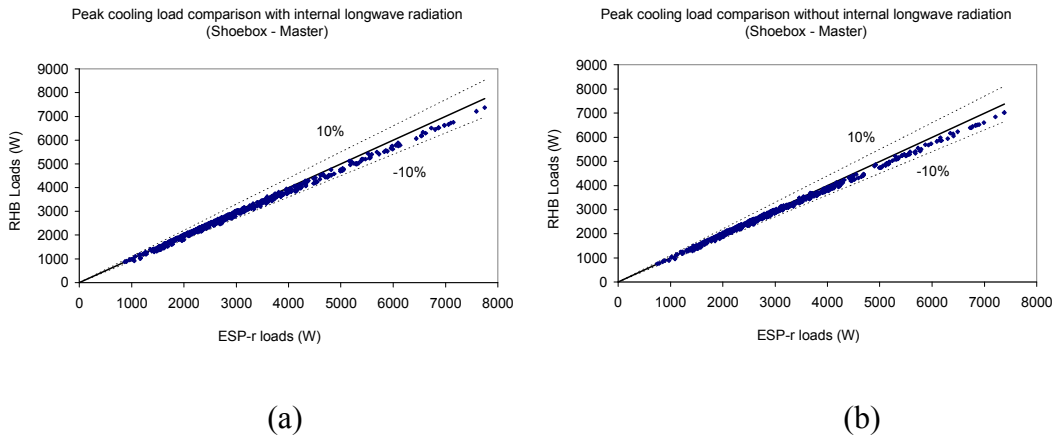


Figure 4-26. Comparison of cooling load calculated by RHB and ESP-r (Shoebox – Master): (a) with internal longwave radiation (b) without internal longwave radiation

4.3.2.5 Other Possible Sources of Load Difference

For test cases shown in Figure 4-26(b), even the negligible effect caused by the different internal long wave radiation models were eliminated. There are three possible sources of load difference left: solar radiation models, window models and conduction methods. To separate the effect of the window models from the other two sources for the

moment, a set of 144 test cases without windows were run in ESP-r and RHB, based on the cases in Figure 4-26(b) (without external long wave radiation, internal thermal mass, inter-zone conduction and internal long wave radiation). Figure 4-27 shows the comparison of the Master room peak cooling loads predicted by RHB and ESP-r in these cases. We see that after the windows were removed, there is a significant load reduction both in the ESP-r and RHB calculated loads, which is not a surprise as the solar gains through the fenestrations were removed along with the windows. Interestingly, the error percentages shown in Figure 4-27 are clearly separated into two groups: one group falls along the 1:1 correspondence line and have an MBE of -1W, indicating the RHB and ESP-r predicted loads are very close; the other group resides in the area that is closer to the -10% line and have an MBE of -70W, indicating RHB is under-predicting for these cases.

A careful examination of the percentage load differences for these cases shows that all the cases with relatively large percentage load difference have wood fabric constructions. Among the two possible sources of load difference involved in these cases, it is likely that the conduction model difference maybe the main source, as conduction can be affected by the type of fabric construction, while solar radiation will not. However, incident solar radiation absorbed on external opaque surfaces (no glazing surfaces are present for these cases) will be transferred to internal surfaces through conduction. So solar radiation and conduction are actually compounded here and it is difficult to separate their individual effects.

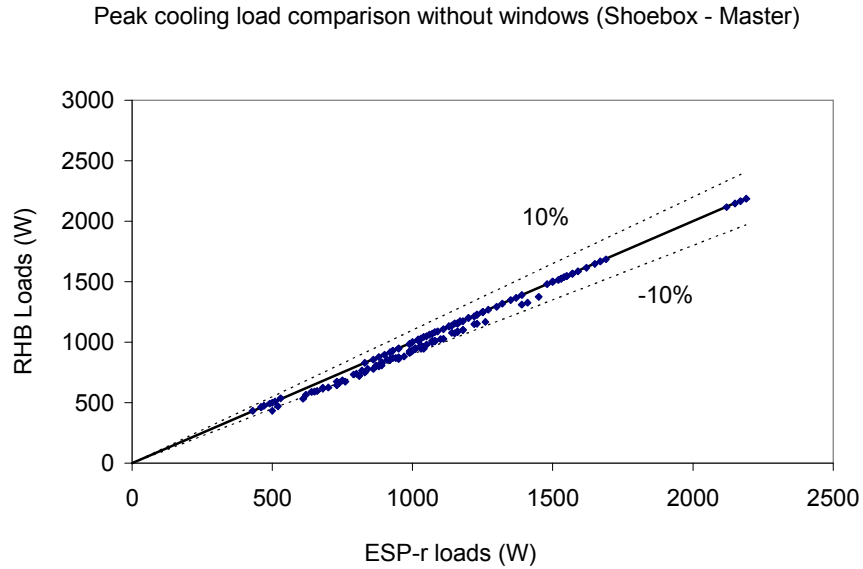


Figure 4-27. Comparison of cooling load calculated by RHB and ESP-r (Shoebox – Master): without external long wave radiation, internal thermal mass, inter-zone conduction, internal long wave radiation and windows

There are two driving forces for the conduction discussed here: one is the ambient air temperature, the other is the outside surface absorbed solar radiation. For one of the worst cases (located in Alamosa, CO) shown in Figure 4-27, Figure 4-28(a) shows the ambient air temperatures used in RHB and ESP-r. We see that the outside surfaces are exposed to the same ambient air temperature in RHB and ESP-r. So the possibility that the difference between ResHB and ESP-r predicted cooling loads is caused by the difference in the ambient air temperatures used by the two programs can be eliminated. Figure 4-28(b) shows the RHB and ESP-r predicted total outside surface absorbed solar radiation for the Master room. The values predicted by the two programs match reasonably well, with a maximum difference of 1224W occurring at hour 7:00 p.m., which is 3.34% of the peak value (36606W, occurring at hour 2:00 p.m.) predicted by

ESP-r. The difference between the RHB and ESP-r predicted peak cooling loads (63W, occurring at hour 8:00 p.m.) for the Master room is 9.55% of the ESP-r peak load. Obviously, the difference in the outside surface absorbed solar radiation contributes to the difference in the load predictions. However, it is unlikely that the difference (9.55%) between the peak cooling loads is only caused by the difference in the outside surface absorbed solar radiation. There might have been some other reasons involved in the conduction process itself. Furthermore, during the few hours when the Master room has cooling load, as shown in Figure 4-29, the maximum difference between RHB and ESP-r predicted cooling loads actually occurs at hour 6:00 p.m. (82W, which is 12.42% of the ESP-r peak load), indicating this maximum hourly load difference is not necessarily a result of the maximum difference in the outside surface absorbed solar radiation (occurring at hour 7:00 p.m.).

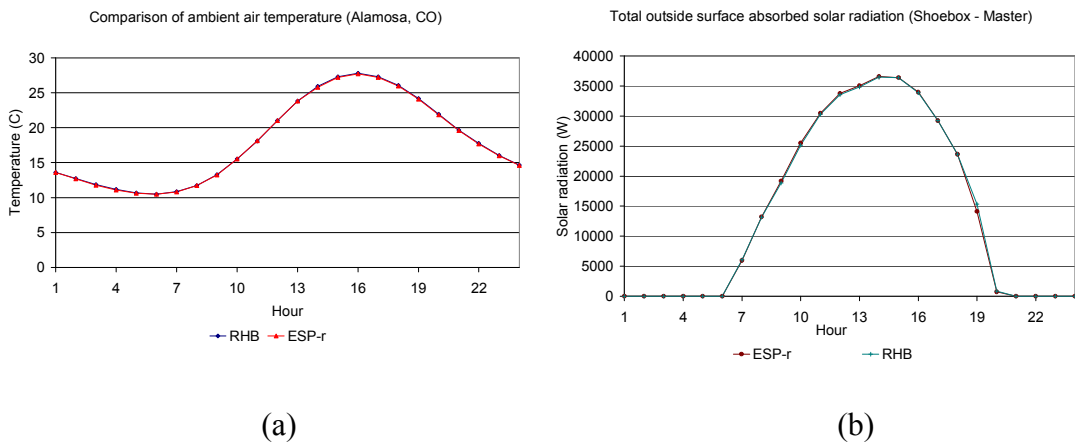


Figure 4-28. (a) Ambient air temperatures used for Alamosa, CO in RHB and ESP-r (b) Outside surface absorbed solar radiation in RHB and ESP-r (Shoebox - Master, Alamosa, CO)

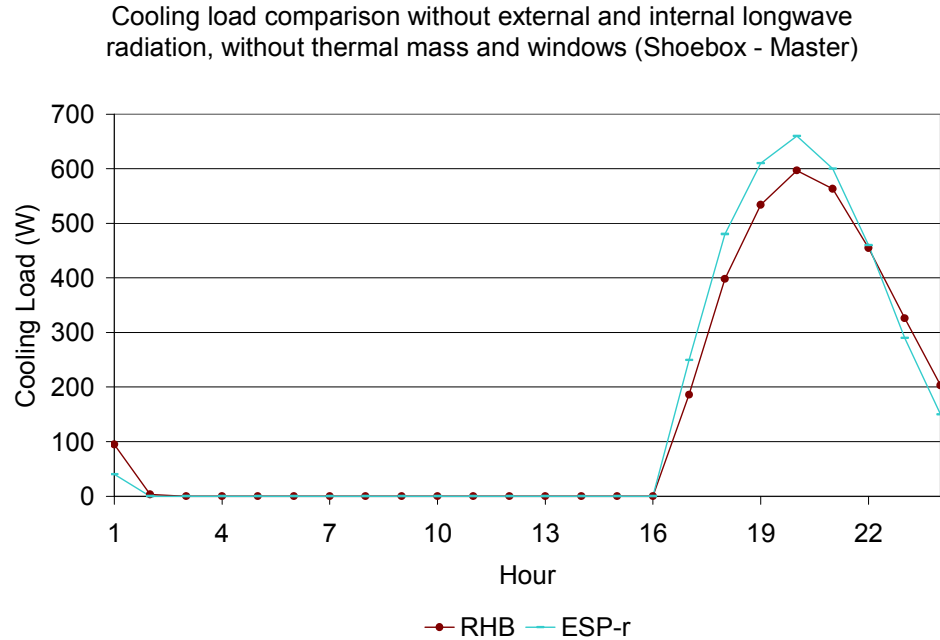


Figure 4-29. Comparison of cooling load calculated by RHB and ESP-r (Shoebox – Master, without external and internal longwave radiation, without thermal mass, inter-zone conduction, and windows)

A closer examination of the hourly load comparison for this case (Figure 4-29) reveals that RHB has a slower response to the outside driving forces than ESP-r, showing smaller loads in the first few cooling hours and higher cooling loads then after. This is in agreement with the trend shown in the comparison of outside surface absorbed solar radiation on one side, and suggests that there might be some difference caused by the different conduction methods used by the two programs on the other side. The conduction method used by RHB is the Conduction Transfer Function method (CTF method), while the conduction method used by ESP-r is the finite volume method. In order to compare the two procedures, an analytical test was conducted for both ESP-r and RHB to check the conduction process. This test is the transient conduction test with sinusoidal driving temperature as described in section 5.2.2 of Chapter 5. Three cases of this test were done

for RHB and will be presented in Chapter 5. The test case with a light-weight construction from ASHRAE 1199-RP (Case 2) is used for comparison with ESP-r. The description of this analytical test and the test parameters used are presented in Chapter 5 and not repeated here.

Figure 4-30 shows the analytically calculated zone loads and those calculated by RHB and ESP-r for this test case. Although both RHB and ESP-r results match the analytical results reasonably well, differences do exist. Compared to the analytical results, RHB calculated loads have a mean error percentage of 0.85% and a maximum error percentage of 1.58%; ESP-r calculated loads have a mean error percentage of 0.11% and a maximum error percentage of 0.18%. Also, RHB shows a slower response to the driving temperature, which is similar to the trend shown in Figure 4-29, under-predicting during the peak load hours and over-predicting during the evening load hours. Although the boundary conditions used in the analytical test are different from those in the inter-model comparison discussed above, it does reveal the different response of RHB and ESP-r to the driving force. There is only sinusoidal driving temperature present in the analytical test and the amplitude of the difference between RHB and ESP-r results seems small. With outside surface absorbed solar radiation added as the main driving force in the inter-model comparisons (the maximum outside air temperature is only 27.7 °C for the case shown in Figure 4-29, with the room air set point at 24 °C), there is possibility that the amplitude of the difference caused by the conduction process become greater than that seen in the analytical test. Or, another possibility might be that the difference in the outside surface absorbed solar radiation has been amplified during the conduction process that it simply shows up as a larger percentage cooling load difference. However,

further research is needed to clarify these possibilities and to investigate the difference between the CTF method (conduction method employed in RHB) and the finite volume method (conduction method employed in ESP-r). For example, it should be useful to develop more complicated analytical conduction tests under more comprehensive boundary conditions, such as those in this case with incident solar radiation and diurnal outside air temperature change as the driving force.

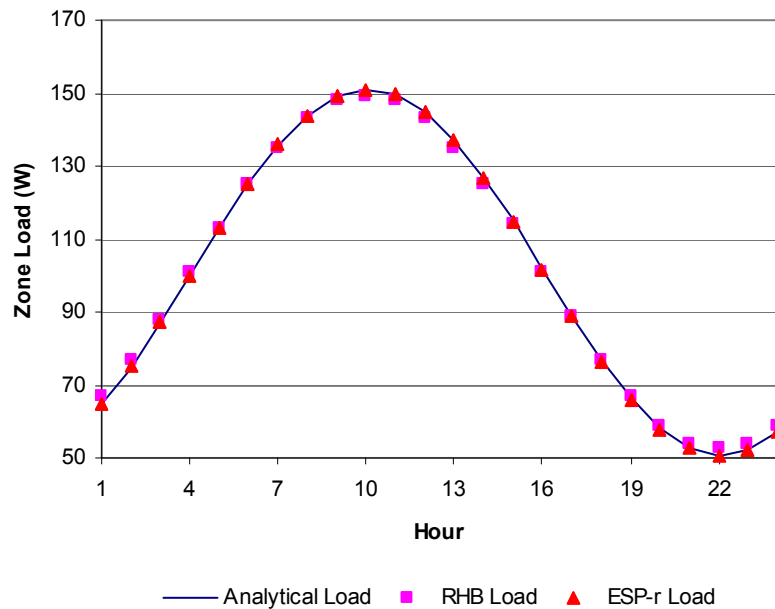


Figure 4-30. Analytically calculated zone loads and those predicted by RHB and ESP-r

Briefly, in addition to the external long wave radiation models, internal solar distribution models and inter-zone conduction models discussed in the previous sections, the difference in the conduction methods used by RHB and ESP-r is another possible source of the load difference, but the amplitude of its effect needs to be clarified by further research. The difference in outside surface absorbed solar radiation predicted by RHB and ESP-r (hence the solar radiation models) also contributes to the load difference

between these two programs, although the corresponding effect is arguably small. Note that as another possible source of load difference, window models have not been discussed in this study, due to the time limits and complexities involved in the window models. There are some ongoing ASHRAE research projects (1143-RP for example) devoted to improve the window models on the cooling load calculation. Hopefully, these will cast some light on this topic in the near future.

4.3.3 System Design Evaluations

As mentioned above, one challenge in evaluating system designs is to come up with either a single figure of merit or a small number of figures of merit. Because thermal discomfort can occur for several reasons, which vary in their cause and acceptability, it was thought desirable to develop figures of merit that differentiate between the causes:

- Night time ambient overcooling. In some locations, e.g., Alamosa, Colorado, the house will cool below the set point at night. Although this results in increased PPD, it is thought to be acceptable. In any case, it is not the “fault” of a poor air-conditioning system.
- Undersizing. In some cases, the system designed by the RHB procedure will be undersized, allowing the temperature to rise above the setpoint in the master zone (i.e. the zone with the thermostat.) While this is acceptable at some level, the PPD that results from this is tracked separately.

- Inadequate Distribution / Control Limitations. In other cases, the master zone will maintain the setpoint, but the other zones (i.e. slave zones) may drift above the setpoint or drift below the setpoint. Again, the PPD resulting from this phenomenon is tracked separately.
- Other. Finally, a small amount of PPD may result even when the system setpoint is being held within a reasonable tolerance, δT . $\delta T = \pm 0.15^\circ\text{C}$ (0.27°F) was chosen as reasonable. This was based on the ESP-r simulation of the on-off control, which will typically hold the thermostatically controlled zone within 0.15°C (0.27°F).

The algorithm may be described as follows. At each hour, the master zone temperature and slave zone temperature are checked. PPD in the master zone is attributed to one of the above causes, depending on the master zone temperature, as shown in Table 4-7. δT is taken to be 0.15°C (0.27°F). For each of the slave zones, the PPD is attributed to one of the above causes, depending on both the master zone temperature and the slave zone temperature. Further consideration of this algorithm will reveal that it is necessarily approximate – there are some conditions that are ambiguous. For example, when the temperature in the master zone exceeds the setpoint by more than δT and the temperature in the slave zone exceeds the setpoint by more than δT , the slave zone PPD is attributed to undersizing. It may also be due to inadequate distribution, but further refinement of the algorithm is probably not warranted.

At this point, the PPD has been attributed to specific causes for each zone for each hour. In order to reduce the results to just a few figures of merit, two additional steps are taken:

1. For each zone, the PPD attributed to each cause is summed for all 24 hours and the total is divided by 24. This gives a mean contribution of each cause to the discomfort.

2. These values are area-weighted to find a mean value for the building.

Table 4-7 Algorithm for attributing the PPD Cause

Master zone temperature	Master zone status	Slave zone status		
		$T_{slave} < (T_{setpoint} - \delta T)$	$(T_{setpoint} - \delta T) \leq T_{slave} \leq (T_{setpoint} + \delta T)$	$T_{slave} > (T_{setpoint} + \delta T)$
$T_{master} < (T_{setpoint} - \delta T)$	Night time Ambient Cooling	Night time Ambient Cooling	Other	Inadequate Distribution
$(T_{setpoint} - \delta T) \leq T_{master} \leq (T_{setpoint} + \delta T)$	Other	Inadequate Distribution	Other	Inadequate Distribution
$T_{master} > (T_{setpoint} + \delta T)$	Under-sizing	Inadequate Distribution	Other	Undersizing

To evaluate whether or not the RHB system design is over-sized, another figure of merit called Degree Hours (DH) has also been developed. The algorithm used to calculate DH is as follows. At each hour, for each room, the room temperature is checked to see whether it exceeds the room set point plus the permitted temperature swing. If yes, the difference between the room temperature and the sum of the room set point and the permitted temperature swing is added to the DH for that particular room. The DHs for all conditioned rooms are then averaged to get a DH for the whole house. The room DHs and whole house DHs in a set of parametric cases are further averaged to see the overall

effect of running ESP-r system evaluation under reduced system capacities designed by RHB, as will be discussed in section 4.3.3.2.

As mentioned before, there are two sets of 576 cases created for system design evaluations for both the Shoebox and the 4-bedroom house prototypes, one with zero temperature swing and the other with medium temperature swing. There are two parts of the system evaluation conducted:

1). At 100% system capacity designed by RHB, ESP-r system evaluation was done for both prototypes. The evaluation is focused on analyzing the integrated PPD values. The corresponding results are discussed in section 4.3.3.1.

2). To evaluate whether or not the RHB system design is over-sized, ESP-r system evaluation was also done for the 4-bedroom house prototype, by gradually decreasing the RHB designed system capacity used in the ESP-r simulations. The evaluation is focused on analyzing the average room DHs, average whole house DHs, and average integrated PPD values under reduced RHB designed system capacities. The corresponding results are discussed in section 4.3.3.2.

4.3.3.1 System Evaluation with 100% RHB Designed Capacity

1. System Designed with Zero Temperature Swing

Figures 4-31 through 4-34 show the result of the system design evaluations for 576 Shoebox cases where the system capacities and airflow rates were designed with the RHB program, using zero temperature swing.

Figure 4-31 shows the processed PPD values for the category of nighttime ambient cooling. For convenience in identifying specific cases, they are plotted against case number. For most cases, the processed PPD values fall in the range of 0-10%. The group of high values in this figure is for the light-weight construction cases from Alamosa, Colorado, which has the cooling design condition of 27.8°C (82.0°F) maximum dry bulb temperature and a 17.3°C (31.1°F) daily dry bulb range. As the outdoor air temperature drops to 10.5°C (50.9°F) at night, and the sky temperature drops to -11.7°C (-11.0°F) at night, it is not surprising that a lightweight house falls well below the setpoint of 24°C (75.2°F) at night.

Figure 4-32 shows the processed PPD values for the categories of system under-sizing and inadequate distribution. For most cases, the processed PPD values of the category of system under-sizing fall in the range of 0-2%; the processed PPD values for the category of inadequate distribution fall in the range of 1-6%.

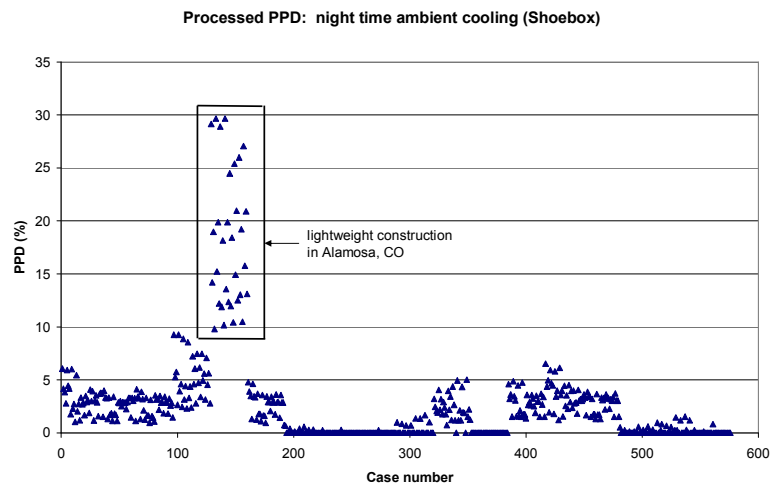


Figure 4-31. Processed PPD showing night time ambient cooling, system designed with zero temperature swing (Shoebox)

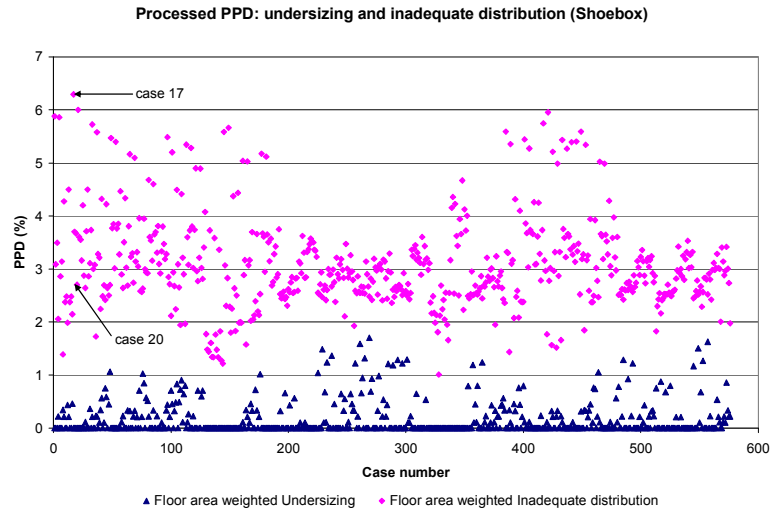


Figure 4-32. Processed PPD showing system under-sizing and inadequate distribution, system designed with zero temperature swing (Shoebox)

To understand the meaning of these values, Figures 4-33 and 4-34 plot out the hourly PPD values and hourly room air temperatures for two particular cases (case 17, case 20). In Case 17, the PPD attributed to undersizing is zero; the PPD attributed to inadequate distribution is 6.3%, the worst case of all 576. Looking at Figure 4-33, we can see that the actual hourly distribution of temperatures and PPD shows problems in the slave room. There is a lot of overcooling in the morning and significant temperature swing above the setpoint in the early evening.

On the other hand, Case 20, which has PPD attributed to undersizing equal to zero; and PPD attributed to inadequate distribution of 2.7%, a more typical value. In Figure 4-34, we see some overcooling of the slave room in the morning, and a slight drift above the setpoint in the early evening.

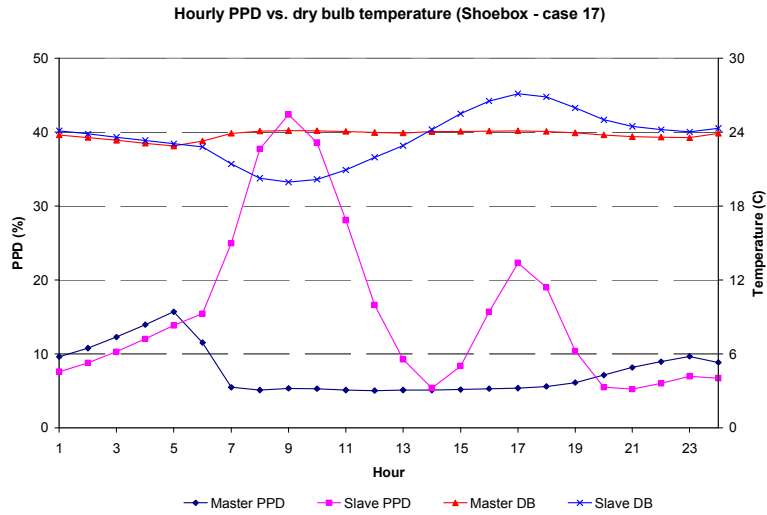


Figure 4-33. Hourly PPD vs. temperature, system designed with zero temperature swing (Shoebox - case 17)

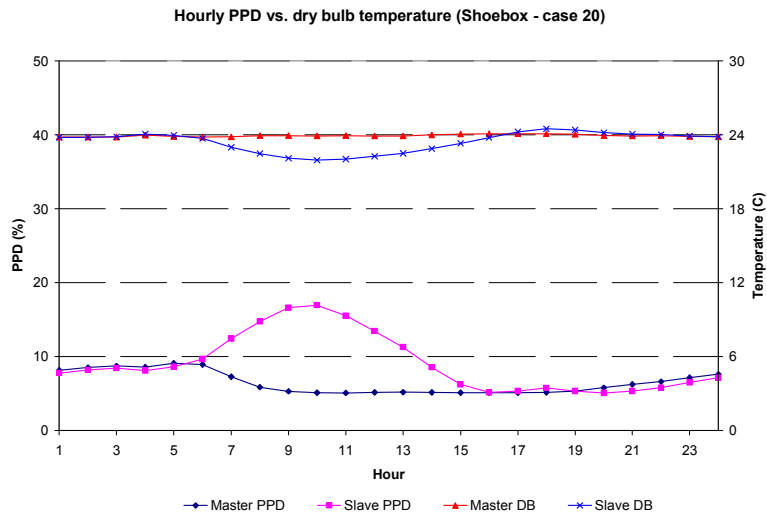


Figure 4-34. Hourly PPD vs. temperature, system designed with zero temperature swing (Shoebox - case 20)

Case 17 and 20 are both wood frame, medium insulation cases located in San Diego. For both cases, the master room has a north and an east window; the slave room has a south and a west window. However, Case 17 has single pane glazing with twice the

area of the low-e double pane glazing used in Case 20. This results in a significantly higher required system capacity – the Case 17 system capacity is over three times as high as the Case 20 system capacity. The combination of higher transient heat gains, with different profiles in the two rooms, and larger system capacity causes Case 17 to have significantly higher thermal discomfort.

Correspondingly, Figures 4-35 through 4-37 show the result of the system design evaluations for 576 4-bedroom house cases where the system capacities and airflow rates were designed with the RHB program, using zero temperature swing.

Figure 4-35 shows the processed PPD values for the category of nighttime ambient cooling. For most cases, the processed PPD values fall in the range of 0-3%, lower than those we see for the Shoebox cases. Again, the high values in this figure are for cases from Alamosa, Colorado, as explained for the Shoebox cases. One difference from the Shoebox cases is instead of one group of high values, there are two groups of high values here: one for the light-weight construction cases and the other for the heavy-weight construction cases. The reason why both the light-weight and heavy-weight 4-bedroom houses fall below the set point at night is due to the nighttime ventilation of the attic. As pointed out earlier, the default approximate attic model was used in the RHB automatic runs for the 4-bedroom house. There is a constant inside-outside ventilation rate of 4 ACH set by this default attic model. Considering the approximate geometry of the attic model in RHB, an equivalent fixed ventilation rate of $0.1\text{m}^3/\text{s}$ was used in ESP-r system design evaluations. This attic ventilation during the nighttime helps to reject more

energy from the 4-bedroom house to the outside. This is why even the heavy-weight 4-bedroom houses in Alamosa, Colorado fall below the set point at night.

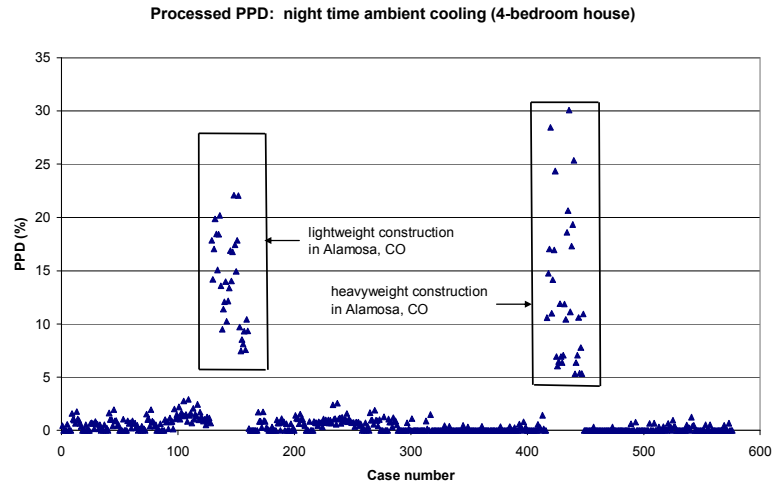


Figure 4-35. Processed PPD showing night time ambient cooling, system designed with zero temperature swing (4-bedroom house)

Figure 4-36 shows the processed PPD values for the categories of system under-sizing and inadequate distribution. For most cases, the processed PPD values of the category of system under-sizing fall in the range of 0-1%, which is a little bit lower than those in the shoebox cases; the processed PPD values for the category of inadequate distribution fall in the range of 0-8%, which is a little bit higher than those in the shoebox cases.

Again, Figure 4-37 plots out the hourly PPD values and hourly room air temperatures for three representative rooms (the master zone and two slave zones) in one particular case (case 121). Case 121 is a wood frame, medium insulation case with single pane glazing, located in Sacramento, CA. In this case, the PPD attributed to under-sizing

is 0.1%; the PPD attributed to inadequate distribution is 7.4%, the worst case of all 576. Looking at Figure 4-36, we can see that there is a small amount of system under-sizing in the master zone (the family room) and the actual hourly distribution of temperatures and PPD shows problems in the slave rooms (Bedroom 2 and 3). For Bedroom 2, there is a lot of overcooling in the morning and early afternoon, and significant temperature swing above the setpoint in the late afternoon and evening. For Bedroom 3, there is some slight overcooling in the morning and early afternoon, and less significant temperature swing above the setpoint in the late afternoon and evening.

As can be seen from the floor plan (Figure 4-4), Bedroom 2 has an orientation opposite to the Family room. For this particular case, the Family room faces east with two east windows and Bedroom 2 faces west with one west window. This difference necessarily results in great difference between the load profiles of Bedroom 2 and Family room and explains the phenomenon shown in Figure 4-37. When the family room has great solar gains in the morning, Bedroom 2 does not and is over-cooled; when Bedroom 2 has great solar gains in the afternoon but the Family room does not, the room air temperature in Bedroom 2 drifts up. On the contrary, Bedroom 3 sits right above the Family room on the second floor, with the same orientation as the Family room. Thus, the difference between the load profiles of Bedroom 3 and Family room is smaller than that between Bedroom 2 and Family room. Hence, the problems in Bedroom 3 are less significant.

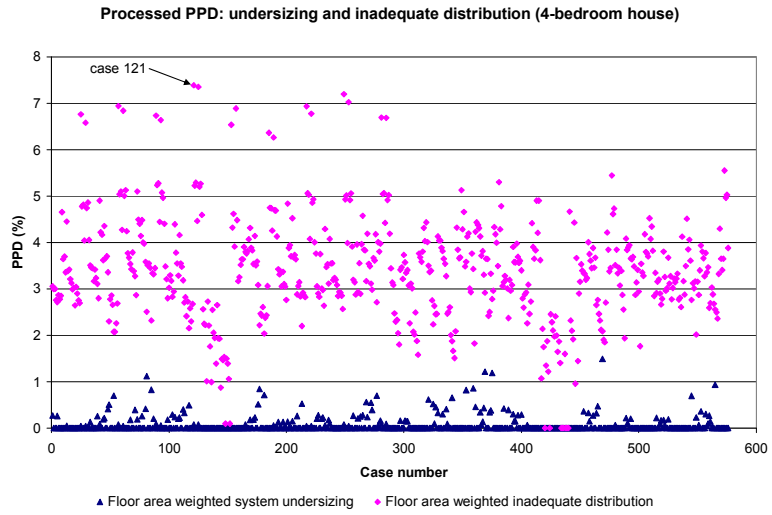


Figure 4-36. Processed PPD showing system under-sizing and inadequate distribution, system designed with zero temperature swing (4-bedroom house)

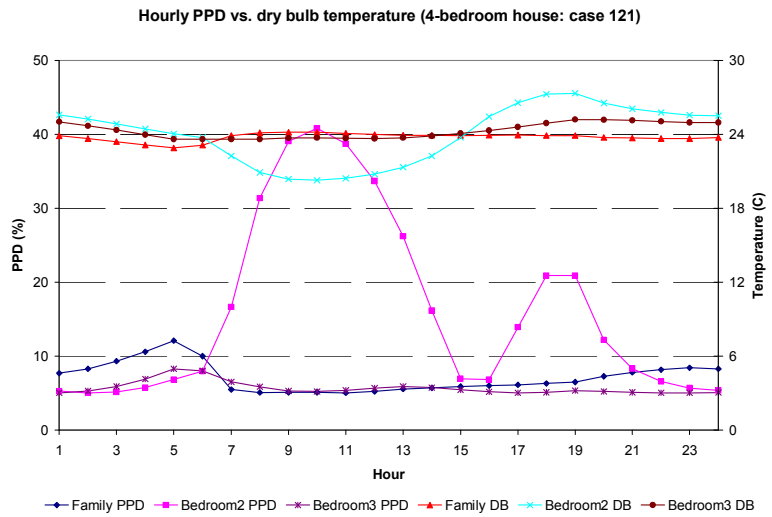


Figure 4-37. Hourly PPD vs. temperature, system designed with zero temperature swing (4-bedroom house: case 121)

2. System Designed with Medium Temperature Swing

Figures 4-38 to Figure 4-40 show the results of the Shoebox test set with RHB sizing the system capacities and room airflow rates allowing a 1.67°C (3.0°F) temperature swing.

Figure 4-38 shows the processed PPD values for the category of nighttime ambient cooling. The processed PPD values are slightly lower than those with zero design temperature swing. This is due to the fact that the smaller system capacities cause the zone temperatures to swing upward during the day. Presumably, the stored energy slightly reduces the downward temperature swing at night, resulting in slightly lower values of PPD due to nighttime ambient cooling.

Figure 4-39 shows the processed PPD values for the categories of system under-sizing and inadequate distribution. Compared to the corresponding values in the zero design temperature swing cases, the processed PPD values for the category of system under-sizing are significantly higher, because of the decrease in system design capacities resulting from permitting temperature swing in the design calculation. The processed PPD values for the category of inadequate distribution are similar or slightly lower than the zero swing cases.

Figure 4-40 plots the hourly PPD values and hourly room air temperatures for Case 355, which has a processed PPD due to undersizing of 7.2%, the worst case. The processed PPD due to inadequate distribution is 0.4%. Looking at Figure 4-40, we can see that the undersizing, while evident for a number of hours, never becomes severe. This is due to the fact that the location is Key West, FL, which has only a 4.5°C (8.1°F)

daily dry bulb range. Furthermore, this case has low fenestration area and concrete construction, both of which tend to limit the diurnal changes in cooling load.

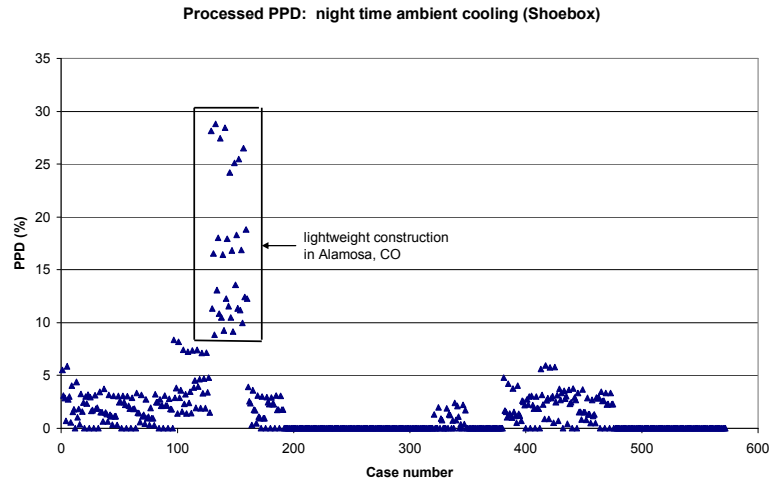


Figure 4-38. Processed PPD showing night time ambient cooling, system designed with medium temperature swing (Shoebox)

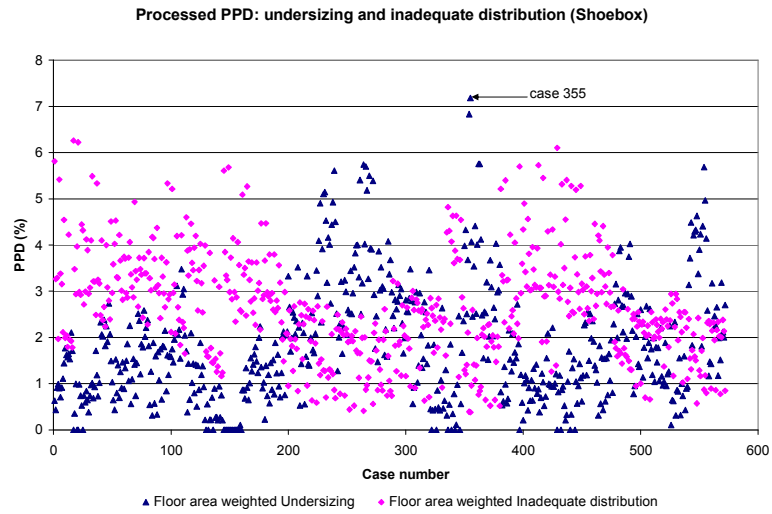


Figure 4-39. Processed PPD showing system under-sizing and inadequate distribution, system designed with medium temperature swing (Shoebox)

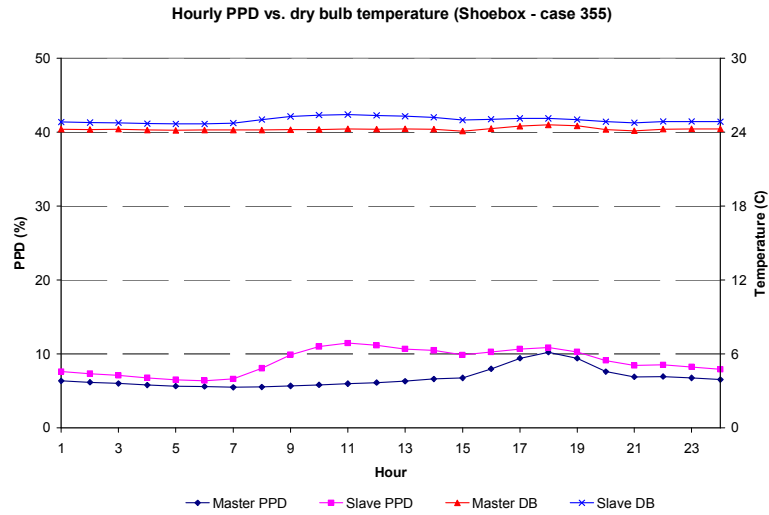


Figure 4-40. Hourly PPD vs. temperature, system designed with medium temperature swing (Shoebox - case 355)

Correspondingly, Figures 4-41 to Figure 4-44 show the results of the 4-bedroom house test set with RHB sizing the system capacities and room airflow rates allowing a 1.67°C (3.0°F) temperature swing.

Figure 4-41 shows the processed PPD values for the category of nighttime ambient cooling. Due to the same reason as stated for the Shoebox medium swing cases, the processed PPD values are slightly lower than those with zero design temperature swing.

Figure 4-42 shows the processed PPD values for the categories of system under-sizing and inadequate distribution. Again, changes from the corresponding values in the zero design temperature swing cases are similar to those changes for the Shoebox cases: the processed PPD values for the category of system under-sizing are significantly

higher; the processed PPD values for the category of inadequate distribution are similar or slightly lower than the zero swing cases.

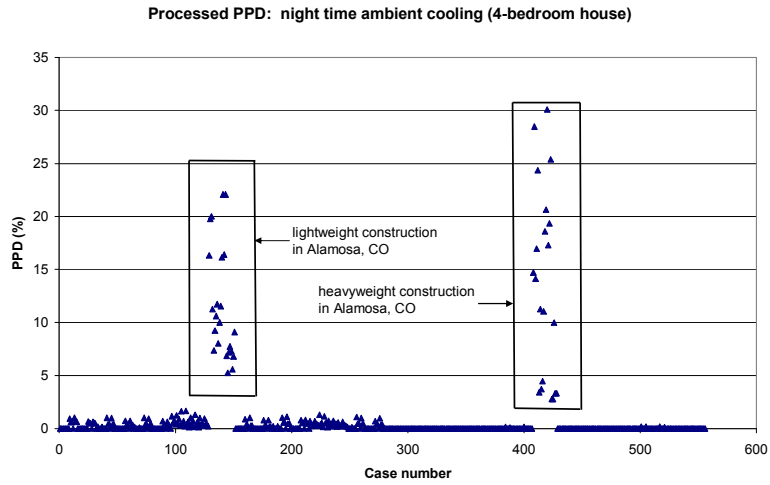


Figure 4-41. Processed PPD showing night time ambient cooling, system designed with medium temperature swing (4-bedroom house)

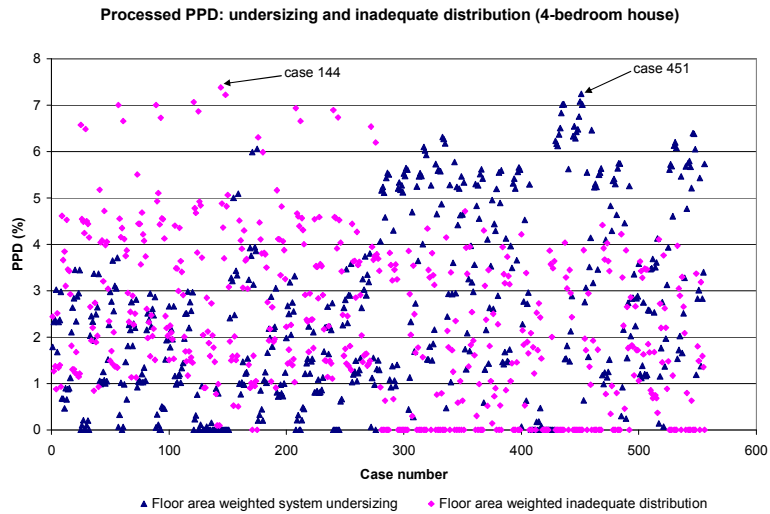


Figure 4-42. Processed PPD showing system under-sizing and inadequate distribution, system designed with medium temperature swing (4-bedroom house)

Figure 4-43 plots out the hourly PPD values and hourly room air temperatures for three representative rooms (the master zone (the family room) and two slave zones (Bedroom 2 and 3)) in the worst case (case 144), which has a processed PPD due to inadequate distribution of 7.4% and a processed PPD due to under-sizing of zero. Case 144 is a wood frame, medium insulation case with single pane glazing, located in Alamosa, CO. The Family room faces east with two east windows. Bedroom 2 faces west with one west window and Bedroom 3 faces east with one east window. Looking at Figure 4-43, we can see that there is a lot of night-time ambient cooling both in the master zone and slave zones, which is not a surprise. Similar to the worst case for the 4-bedroom house zero swing cases, the actual hourly distribution of temperatures and PPD shows problems in the slave rooms. For Bedroom 2, there is a lot of overcooling in the morning and early afternoon, and significant temperature swing above the setpoint in the late afternoon and evening. For Bedroom 3, there is some slight overcooling in the morning and early afternoon, and less significant temperature swing above the setpoint in the late afternoon and evening. The reason for the problems shown in the slave rooms is similar to that of the worst case in the 4-bedroom house zero swing cases and is not repeated here.

Figure 4-44 plots the hourly PPD values and hourly room air temperatures for three representative rooms for Case 451, which has a processed PPD due to undersizing of 7.2%, the second worst case. The processed PPD due to inadequate distribution is zero. Case 451 is a concrete frame, medium insulation case with low fenestration area of single pane glazing, located in Key West, FL (which has only a 4.5°C (8.1°F) daily dry bulb range). Due to the same reason as explained for the worst case of the Shoebox

medium swing cases, the undersizing, while evident for a number of hours, never becomes severe.

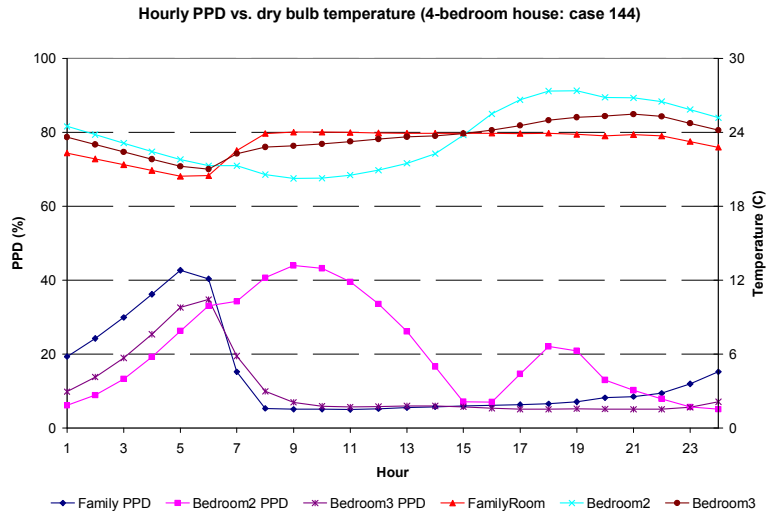


Figure 4-43. Hourly PPD vs. temperature, system designed with medium temperature swing (4-bedroom house: case 144)

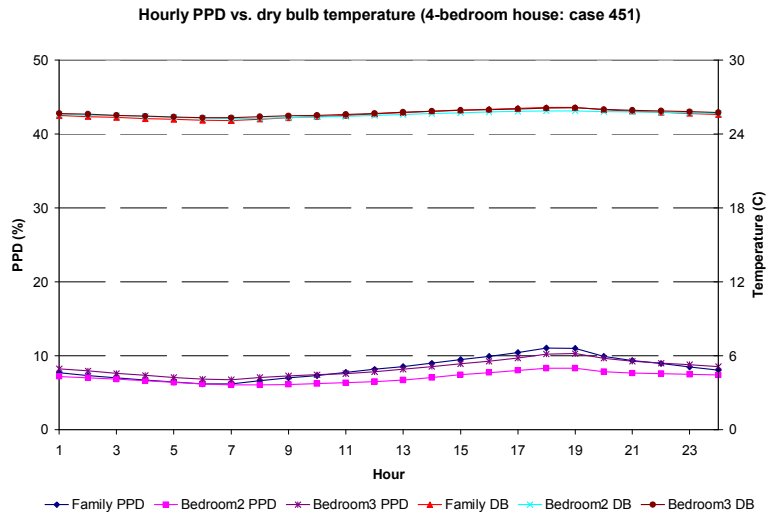


Figure 4-44. Hourly PPD vs. temperature, system designed with medium temperature swing (4-bedroom house: case 451)

4.3.3.2 System Evaluation with Reduced RHB Designed Capacity

As mentioned earlier, to investigate whether or not the RHB designed system capacity is over-sized, system evaluations were done for the 4-bedroom house under gradually reduced RHB designed system capacities. With RHB sizing the system capacities and room airflow rates allowing zero or medium (1.67°C, 3.0°F) temperature swing, the RHB designed system capacities used in the ESP-r simulations were reduced by 10% on each round of tests, from 100% to 50%. Figures 4-45 through 4-47 show the corresponding results. Note that when calculating the DHs presented below, the room set point is 24 °C and the permitted temperature swing is assumed to be 1.67°C, regardless of whether or not this permitted temperature swing is considered in the RHB system design. Also note that all the 576 cases were successfully run in ResHB when it sized the system capacities without temperature swing, but only 556 cases were successfully run in ResHB when it sized the system capacities allowing medium (1.67°C, 3.0°F) temperature swing (the other 20 cases had problem in convergence). For the 556 cases that were both successfully run in ResHB with and without temperature swing, the average decrease in RHB designed system capacity from zero swing to medium swing is about 37%.

Figure 4-45 shows the average DHs for the family room (a) and the whole house (b). We see that when zero temperature swing was used in the RHB system design, the changes in the average DHs for both the family room and the whole house are very small when the system capacities were gradually reduced from 100% to 60%: The average DHs for the family room are almost all zero (which is not a surprise, as the family room is the master room and the system on-off control in ESP-r is based on the master room temperature); the average DHs for the whole house increases from 0.16 °C to 0.24 °C.

Beginning at about 60% capacity, the changes in the average DHs become more visible if the system capacities keep being reduced. With system capacities decreasing from 60% to 50%, the average DHs for the family room increases from 0.1 °C to 1.4 °C; the average DHs for the whole house increases from 0.2 °C to 1.6 °C.

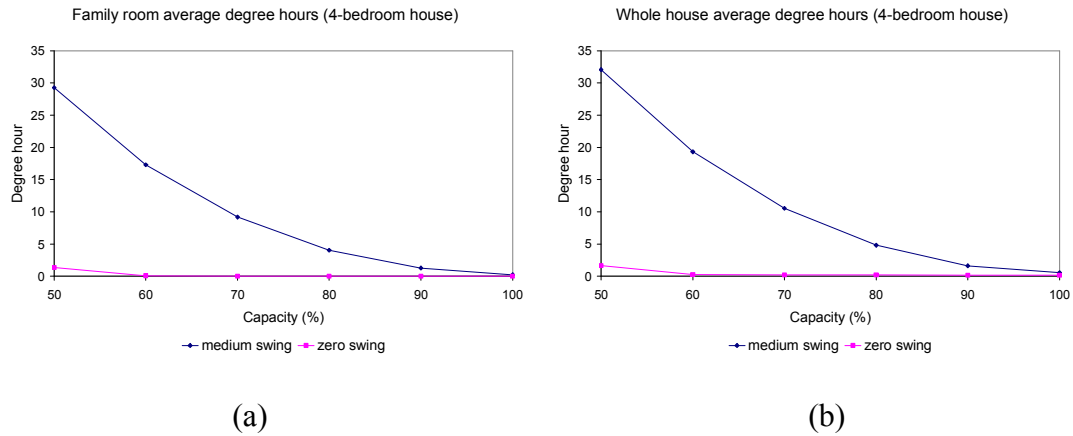


Figure 4-45. Average degree hours for systems designed with zero or medium temperature swing (4-bedroom house): (a) Family room (b) whole house

On the other hand, when medium temperature swing (equals the permitted temperature swing) was used in the RHB system design, the changes in the average DHs for both the family room and the whole house are very obvious when the system capacities were gradually reduced. With system capacities decreasing from 100% to 50%, the average DHs for the family room increases from 0.2 °C to 29.3 °C; the average DHs for the whole house increases from 0.5 °C to 32.1 °C. The lower the system capacity; the higher the rate of DH increase.

Note that the trend in the DHs resulting from the medium swing cases is actually in agreement with the trend in the DHs resulting from the zero swing cases, as the

average RHB designed system capacity with medium swing is about 63% of the average RHB designed system capacity with zero swing. So both the medium swing and zero swing results indicate that beginning at about 60% of the RHB designed system capacity with zero swing, reducing system capacities would result in noticeable increase in the average DHs.

Obviously when the permitted temperature swing is not considered in the RHB system design (the zero swing cases), there is a large chance of over-sizing; when the permitted temperature swing is considered in the RHB system design (the medium swing cases), the chance of over-sizing becomes much smaller. As a medium temperature swing is usually permitted in residential buildings, it is recommended that the permitted temperature swing be considered in the RHB system design.

Further analysis of the average processed PPD values for the same series of test cases is in agreement of the above conclusion. Figure 4-46 and 4-47 plots the corresponding average processed PPD values against different levels of RHB designed system capacities used in the ESP-r simulation.

Figure 4-46 shows the average processed PPD values for the category of nighttime ambient cooling (a) and inadequate distribution (b). The average processed PPD values for both categories decrease when the system capacities used in ESP-r are reduced. Also, for both categories, lower average processed PPD values were obtained when the permitted temperature swing was considered in the RHB system design, as the RHB designed system capacities decrease when temperature swing is allowed. For the category of nighttime ambient cooling, as explained in section 4.3.3.1, the lower average

processed PPD values under reduced system capacities is due to the fact that the smaller system capacities cause the zone temperatures to swing upward during the day and the stored energy reduces the downward temperature swing at night, resulting in lower values of PPD due to nighttime ambient cooling. For the category of inadequate distribution, the lower average processed PPD values under reduced system capacities is presumably due to the fact that the smaller system capacities tend to reduce the possible temperature drift below the set point occurred in the slave zones when the system is turned on based on the master zone temperature.

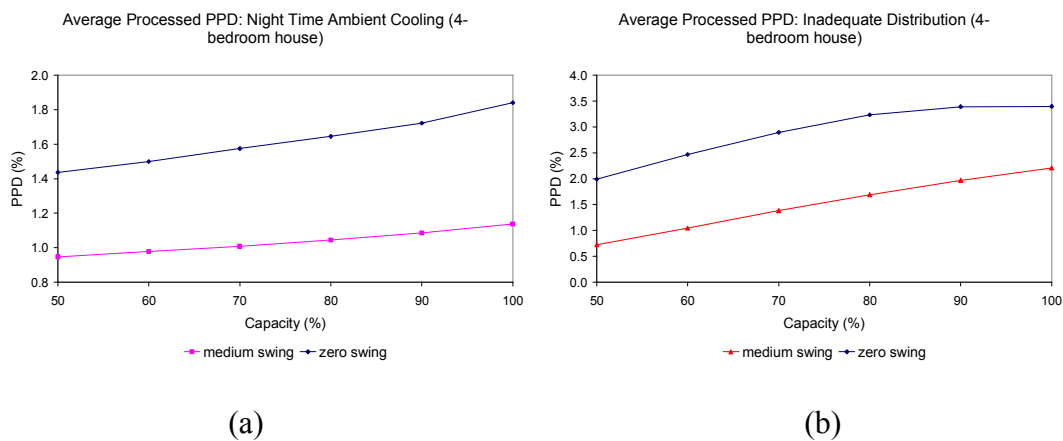


Figure 4-46. Average processed PPD values for systems designed with zero or medium temperature swing (4-bedroom house): (a) night time ambient cooling (b) inadequate distribution

Figure 4-47(a) shows the average processed PPD values for the category of system under-sizing. As expected, the average processed PPD values for this category increases when the system capacities used in ESP-r are reduced. Also, higher average processed PPD values for this category were obtained when the permitted temperature swing was considered in the RHB system design, as the RHB designed system capacities decrease when temperature swing is allowed.

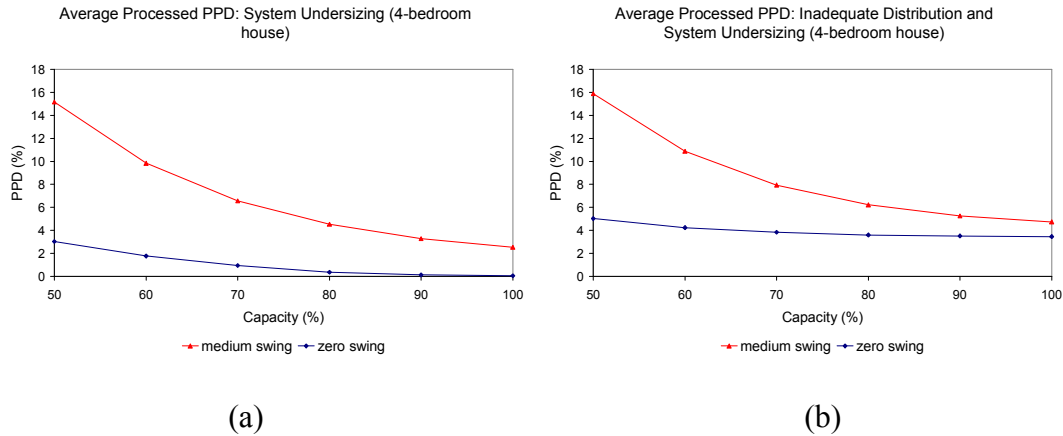


Figure 4-47. Average processed PPD values for systems designed with zero or medium temperature swing (4-bedroom house): (a) system under-sizing (b) inadequate distribution and system under-sizing

Note that the PPD trend in Figure 4-47(a) is similar to that in Figure 4-45. When zero temperature swing was used in the RHB system design, the changes in the average processed PPD values for the category of system under-sizing are very small: it increases from 0.07% to 3.04% when the system capacities were reduced from 100% to 50%. On the other hand, when medium temperature swing was used in the RHB system design, the changes in the average processed PPD values for the category of system under-sizing are much more obvious: it increases from 2.5% to 15.2% when the system capacities were reduced from 100% to 50%. Again, the lower the system capacity, the higher the rate of increase in PPD. The similarities between Figure 4-47(a) and Figure 4-45 further confirm that if permitted temperature swing is not considered in the RHB system design, there may be a large chance of over-sizing. Using the RHB temperature swing option to take into account the permitted temperature swing could greatly reduce the chance of over-sizing in the system design.

The average processed PPD values for both the categories of system under-sizing and inadequate distribution are shown in Figure 4-47(b). The PPD trend in Figure 4-47(b) basically is very similar to that in Figure 4-47(a). However, with the PPD values for the category of inadequate distribution added to the PPD values for the category of system under-sizing, the PPD curves become flatter in Figure 4-47(b), indicating a slightly lower PPD changing rate. This is considered reasonable as the PPD values for the category of system under-sizing increase when the system capacities decrease, while the PPD values for the category of inadequate distribution decrease when the system capacities decrease.

4.4 Conclusions

Inter-model validation of the ASHRAE residential heat balance load calculation method (RHB) was performed using ESP-r. The testing process was automated through parametric generation and simulation of large sets of test cases for both RHB and ESP-r.

The load comparison mode of the testing process was found effective in confirming the RHB load calculation and reconciling RHB and ESP-r input used for design evaluation. Excluding input discrepancies, load comparison results are largely dependent on the sub-models used in both programs. After review of the results, the load differences are considered reasonable, with ResHB predicted peak cooling loads ranging within $\pm 15\%$ ESP-r. Parametrically, two of the main sources of difference have been shown to be the different external long wave radiation models and internal solar distribution models used in each program. In a set of example tests, the MBE for the 4-bedroom house changes from -261W to -43W when the external long wave radiation was eliminated. In another set of example tests, the MBE for the concrete cases changes from

101W to -23W when the internal thermal mass surface was removed so that both ESP-r and RHB have the same internal solar distribution. The sensitivity of the peak load calculations to external long wave radiation and internal solar distribution suggests that this is a likely topic for further research and refinement of the methods.

Another source of error in RHB is caused by the lack of inter-zone conduction, which would cause a load moderating effect. This has been shown to be most prominent in rooms with relatively small loads. In a set of example tests for the 4-bedroom house, when the inter-zone conduction was turned off in ESP-r, the MBE changes from -17.8W to -2.5W for the Laundry, and from -57.7W to -0.3W for the Foyer 1. Note that no temperature swing has been considered in the load comparison mode of this study. As temperature swing is usually permitted in residential buildings, more inter-zone conduction is expected and the corresponding effect may become more important. Therefore, addition of an inter-zone conduction model into RHB may be an interesting topic for future research.

Different conduction methods also contribute to the load difference. For a worst case with no windows, internal heat gains, and infiltration, a 10% difference in peak cooling load was found. For real residential buildings with windows, internal heat gains, and infiltration, a 10% error in conduction heat gain would result in a much smaller error in cooling load. Never the less, it should be possible to eliminate this error. A cross-check using an analytical verification with sinusoidal boundary conditions could only show a 1.6% error in the ResHB conduction model. However, the actual boundary conditions are not sinusoidal; they include absorbed solar irradiation. It is possible that

this creates additional error that is not present in the sinusoidal test. Further research, possibly involving development of an analytical model for combined conduction and radiation absorption, may be useful in resolving this issue.

The system design evaluation mode was useful for showing the quality of designs made with the RHB procedure. There are two parts of the system evaluation conducted: one part with 100% RHB designed system capacity, the other part with gradually reduced RHB designed system capacity. In the first part of the system evaluation, two processed PPD values are used to identify system under-sizing and inadequate distribution/control limitation problems. The amount of inadequate distribution depends on the level of the load profile difference between the master and slave zones. Increased difference in the load profiles will result in more inadequate distribution. Also, increased system under-sizing is predicted if temperature swing is permitted in the RHB system design.

In the second part of the system evaluation, average room and whole house DHs and average integrated PPD values are used to evaluate whether or not the RHB system design is over-sized. It was found that when the permitted temperature swing was not considered in the RHB system design, there is a large chance of over-sizing. On the other hand, using the RHB temperature swing option to take into account the permitted temperature swing could greatly reduce the chance of over-sizing in the system design. As a medium temperature swing is usually permitted in residential buildings, it is recommended that the permitted temperature swing be considered in the RHB system design.

Based on the results of the load comparison mode and the system design evaluation mode, it is concluded that RHB is acceptable from the inter-model comparison perspective. Most of the difference found in the load comparison mode can be traced to the difference in the sub-models used by RHB and ESP-r. If desired, new sub-models could always be added into the RHB procedure. The quality of the system designs made with the RHB procedure has been shown to be reasonable and the RHB temperature swing option is recommended to reduce the chance of system over-sizing.

5. ANALYTICAL VERIFICATION OF THE HEAT BALANCE BASED RESIDENTIAL COOLING LOAD CALCULATION PROCEDURE

It is first of all helpful to define what the terms verification and validation mean in this context. The distinction between the code verification and validation is made following the definitions given by Boehm (1981) and Blotter (1990). They described verification as “solving the equations right” and validation as “solving the right equations”. As discussed in the literature review, of the three types of test methods, analytical tests are most abstracted from the full complexities of real building simulation problems but offer the most certain form of reference or ‘truth’ model with which comparisons can be made. Being slightly abstract in nature they may be of least interest to the end user of simulation codes but are arguably the most useful to the code developer in that they offer the clearest path to diagnosis of specific problems with the algorithms or their implementation. In terms of definition such tests should probably be thought of as primarily verification tests.

The analytical tests used for the verification of the residential heat balance (RHB) based cooling load calculation procedure are those from the analytical verification test suite developed for building fabric models in whole building energy simulation programs—ASHRAE 1052-RP (Spitler et al. 2001). The tests cover most of the building

fabric models, including convection, conduction, solar radiation, long wave radiation and infiltration. These tests are considered appropriate because most of the residential cooling loads come from the building envelope and the building fabric models are the most important sub-models of the procedure.

There are two sections in this chapter. The first section outlines the development of the analytical tests and the implementation of the test suite software. The second section describes the testing of the residential heat balance based cooling load calculation procedure and summarizes the testing results along with a discussion of the problems diagnosed.

5.1 Development of the Analytical Verification Test Suite

The analytical verification test suite for building fabric models in whole building energy simulation programs—ASHRAE 1052-RP (Spitler, et al. 2001)—has been developed to help verify the ability of whole building energy analysis programs to model various aspects of heat transfer through the building fabric. The tests are intended to be used in support of ASHRAE Standard 140 ‘Standard Method of Test for Building Energy Analysis Software’ (ASHRAE 1998). The test suite exists in three forms. Firstly, the tests exist as a set of documentation that defines the test zone and model parameters necessary to perform the test and includes one or two sets of test results for given sets of parameters. Secondly, software that implements the analytical tests has been developed in two forms. First, this software is available in the form of Fortran90 subroutines that were used to calculate the analytical test results as they appear in the documentation. This source code can be compiled and used by interested users and developers. Furthermore, a

user interface to the Fortran90 subroutines has been developed. The test suite software provides users a convenient way of running tests with parameter values (e.g. convection coefficients) other than those used in the documented tests.

This section summarizes the organization of the tests, the test suite design, the test suite software and documentation. As will be discussed later, not all the analytical tests in this test suite are applicable to ResHB. Therefore, a complete description of all the analytical tests developed is not included in this section. Rather, an introduction is given for each test applied to ResHB in the next section, along with the corresponding test results and problems diagnosed. Additional information for the test suite can be found in Spitler, et al. (2001) and Rees, et al. (2002).

5.1.1 The Test Suite

The test suite consists of sixteen individual tests, each with the objective to test the ability of a building energy simulation program to model a particular heat transfer phenomena. The test is applied by comparing the output of the energy simulation program to be tested with the analytical solution for a special test zone. The data to be compared may be a single zone load, heat flux, temperature, or hourly loads over one or more days of output. This section describes the organization of the tests and some general concerns relevant to the test suite design.

5.1.1.1 Organization of the Tests

The sixteen individual tests of the test suite are organized into groups relating to particular heat transfer phenomena as follows:

Group 1	-	Convection and Conduction
Group 2	-	Solar Gains and Shading
Group 3	-	Infiltration
Group 4	-	Long Wave Radiation
Group 5	-	Miscellaneous

In reality convective heat transfer occurs at all building surfaces. Although it is possible to eliminate radiant effects from both analytical solutions and the test program by selection of suitable surface properties, it is not generally possible to eliminate convective effects so conveniently. Consequently convection heat transfer is involved in nearly all the test cases. This makes it important that the steady-state convection test is carried out first, and its results analyzed prior to completion of the other test cases.

A complete list of test cases is given in Table 5-1. Each test is given an abbreviation for convenient referencing in the documentation. Group one is concerned with testing the ability of the test program to model convection and conduction heat transfer, both steady-state and transient. Three transient conduction cases with different boundary conditions and driving temperature profiles are included. Group two is concerned with solar radiation on both opaque and glazed surfaces. These tests are intended to test the program's time, solar position, glazing and shading models. Group three is concerned with infiltration and group four with internal and external long wave radiation. Tests associated with internal gains and ground coupling are in group five.

Table 5-1 Organization of the Test Suite

Test Group	Test Title	Abbreviation
Group 1	Steady-state convection	SSConv
	Steady-state conduction	SSCond
	Transient conduction – Adiabatic Wall	Tc1
	Transient conduction – Step Response	Tc2
	Transient conduction – Sinusoidal Driving Temperature and Multi-layer Wall	Tc3
Group 2	Exterior Solar Radiation – Opaque Surfaces	ExtSolRad
	Solar Radiation – Glazed Surfaces	SolRadGlazing
	Solar Radiation – Window Shading	SolRadShade
	Solar Radiation – Window Reveal Shading	WinReveal
	Solar Radiation – Internal Solar Distribution	IntSolarDist
Group 3	Infiltration – Fixed Infiltration Rate	Infiltration-1
	Infiltration – Stack Effect	Infiltration-2
Group 4	Interior Long Wave Radiation	IntRad
	External Long Wave Radiation	ExtLWRad
Group 5	Internal Heat Gains – Convective and Radiant	IntHeatGain
	Ground Coupling – Slab on Ground Floor	GrdCoup

5.1.1.2 Test Suite Design

The tests are designed so that, whenever possible, they may be useful to and used by program users, not only by developers. The following design principles were adopted:

- When possible, the tests require only simple output typically available to program users. These include annual and monthly heating and cooling loads; annual and monthly peak heating and cooling loads. However, for many tests, hourly output is also required.
- Besides the unique weather files developed for this project, the tests, for the most part, require only simple input typically available to program users. This has been done by providing the user with software implementations of the analytical solutions through which users can enter custom parameter values.

- Test as few phenomena as possible with each test to expedite identification of specific problems.
- The tests are ordered to expedite identification of specific problems.

One of the concerns in the development of the analytical tests and the development of the associated software has been the verification of their derivation and implementation. The verification has been attempted by a combination of the following methods:

- manual checking of derivation by other individuals
- checking against existing published solutions
- checking the computer implementation against published results
- cross checking one test implementation against another for similar boundary conditions and parameters
- checking against results from other computer implementations

The way in which these methods have been applied to each of the tests has depended on the availability of other sources of solutions and implementations in each case. Further details can be found in the ASHRAE 1052-RP final report (Spitler, et al. 2001).

The Test Zone

In order to make each test specific and help diagnose problems it is necessary to minimize the number of heat transfer paths (and hence number of models involved) in

each test. This requires the use of test zones that are rather different in their construction and specification than normal building zones. Considerable familiarity on the part of the tester with the operation and data requirements of the program to be tested is therefore required.

The test zone common to most of the test cases is a cube shape of 3x3x3m (9.84x9.84x9.84ft) internal size. Which surfaces are exposed or adiabatic vary from test to test. Windows may or may not be present depending on specific purpose of each test. Only in the tests dealing with internal long wave radiation, internal solar distribution and the second infiltration test (IntRad, IntSolarDist and Infiltration-2) is the aspect ratio varied. It is assumed in all the tests that the zone air has no thermal mass. This assumption is often made in whole building energy simulation programs. If the zone air is in fact modeled with thermal mass, it may be necessary for the user of the test to modify the zone geometry so that the air mass is minimized – i.e. change the depth to be very small.

Convection Coefficients

In developing analytical solutions to building heat transfer problems one would like to identify a ‘truth’ model for each heat transfer phenomena that might be applied – given certain assumptions. In the case of convection coefficients there is no one universally acceptable “right” coefficient or correlation. However, most convection correlations used for exterior and interior building heat transfer should be reducible to the form,

$$h = A + C(T_s - T_\infty)^n \quad (5-1)$$

where,

h = convection coefficient (W/m²K [Btu/h.ft²])

A = constant (W/m²K [Btu/h.ft²])

C = constant, (units vary depending on n)

n = exponent (non-dimensional)

T_s = surface temperature (°C [°F])

T_∞ = air temperature (°C [°F])

For example, in the correlation for external surfaces given by Yazdanian and Klems (1994),

$$h = \sqrt{[C_t(T_s - T_\infty)^{1/3}]^2 + [aV_o^b]^2} \quad (5-2)$$

where $C_t = 0.84$ for SI units and constants a and b depend on wind direction. In a correlation like this the wind velocity can be zero so that the correlation reduces to

$$h = 0.84(T_s - T_\infty)^{1/3} \quad (5-3)$$

In this case A , C and n of equation (5-1) can be specified as 0.0, 0.84 and 0.333 respectively. In the test suite software, users are given the opportunity to enter convection correlations by specifying coefficients A , C and n as defined in equation (5-1). This is important as convection correlations adopted by different energy simulation programs are not standardized. However, for the analytical tests involving transient

conduction it is not practical (in derivation of the solution) to use a non-linear convection correlation and a constant convection coefficient must be set.

Surface Properties

In a number of the tests it is necessary to eliminate the long-wave and/or solar radiation from the interior and/or exterior surface of the zone. This requires careful specification of the zone surface properties in the test program input data. It may be possible to achieve these goals in more than one way, depending on the exact input data requirements. A common approach would be to set solar absorptivity and long wave emissivity for the relevant surfaces to zero (for numerical reasons it may in practice be necessary to set a very small number such as 0.001).

Solar Data

Arriving at tests involving solar algorithms and data that can be considered as truly ‘analytical’ is problematic. This is because of the empirical nature of all models of diffuse solar radiation. In view of this all the solar radiation tests in this series involve only beam (direct) solar radiation. In each of the solar radiation tests it is therefore necessary that diffuse radiation and radiation reflected from surroundings are eliminated. The weather files accordingly only contain data for direct normal radiation at ground level only.

Each of the solar radiation tests involves the testing of the program models associated with calculation of solar position. Rather than generate reference data by use

of an algebraic model (of which there are several), reference data has been obtained for four sites (Atlanta, Boston, Chicago and Los Angeles) and two dates (Aug. 21st, 1999 and June 21st, 1999) from the U. S. Naval Observatory (USNO 2001).

5.1.2 The Test Suite Software

Although each of the analytical solutions can in principle be calculated ‘by hand’ (with a calculator) or with the aid of a spreadsheet the tests have been implemented in the form of a series of subroutines written in Fortran90. These, in turn, have been compiled as dynamic link libraries (‘DLL’s) that can be called from an interface. The interface allows users to easily enter custom values of the test parameters. An example parameter input screen (Test SSCond) is shown in Fig. 5-1. The software basically takes the input test parameters and runs the analytical test and produces a result file along with an accompanying weather file. The interface has a number of convenient features such as unit conversions, and allows saving of custom parameter values. Output of the test results is designed to be easily read into a spreadsheet, and weather file output can be in either TMY2, WYEC2 or IWEC formats. The procedure by which each test is intended to be carried out can be summarized as follows:

1. Choose the test parameters and enter them into the test suite software
2. Run the test suite software and save the results and weather file produced
3. Set up the input for the program to be tested to comply with the test specification
4. Convert the weather file to the necessary format for input to the test program if required

5. Run the test program for the test zone with the test weather file
6. Compare and analyze the program results and analytical test results.

If it is convenient to run the test suite software, the tests may be run with a variety of parameter values, otherwise the tests may be run using the parameter values and results given in the documentation.

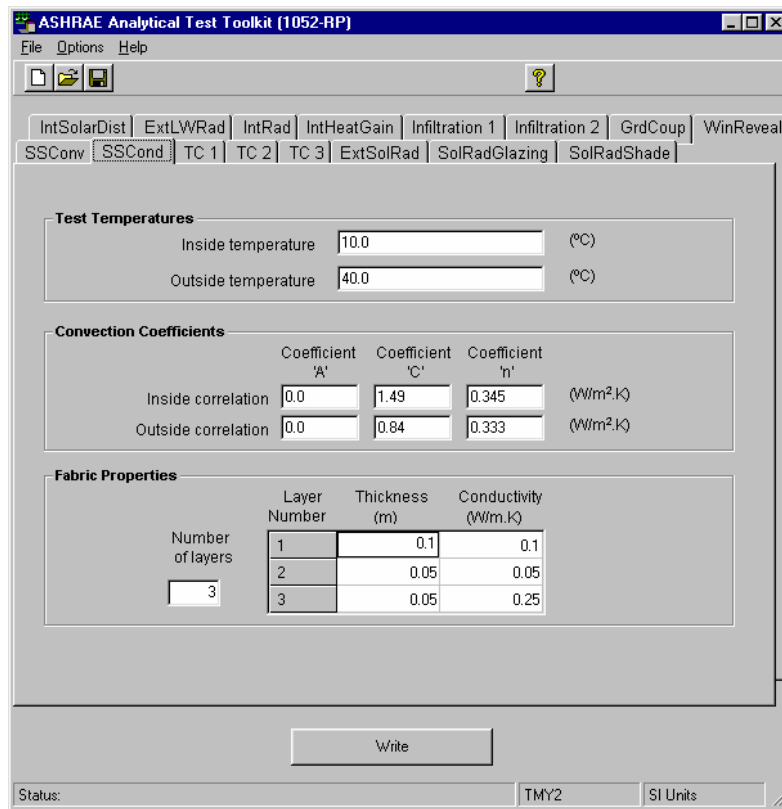


Figure 5-1. Example parameter input screen (Test SSCond)

5.1.3 The Test Documentation

The value of the test suite is heavily dependent on the quality of the documentation. It is important that the documentation is clear and unambiguous if differences in results due to different interpretations of the test conditions are to be

avoided. The documentation is designed to follow a common format for each test and so that the documentation for each test is largely self-contained. The function of each section of the documentation can be summarized as follows.

Objective: This sets out the aim of the particular test in terms of which heat transfer path or sub model of the energy simulation program is to be tested. It also summarizes the basis for the test and any assumptions made.

Analytical Model: This is provided to summarize the basis of the analytical model and its assumptions. It also shows how the analytical model is being applied to represent the behavior of the test zone.

Zone Description: This sets out the definition of the test zone to be used. Particular geometric, construction and surface properties may be specified. Any heat transfer paths to be eliminated may also be specified.

Test Parameters: The particular parameters relevant to the test are given in this section of the documentation for each test. In addition the parameter values used to get the results published in the Results section are tabulated. The input screen from the test suite software is illustrated in this section.

Test Results: Results of applying the analytical solution for one or more sets of test parameters are given in tabular and/or graphical form. These have been generated using the test suite software.

Analytical Solution: The derivation of the analytical solution that forms the basis of the test is given, along with any assumptions and limitations.

References: References are given at the end of the documentation for each test. These are the references relating to either the analytical solution or parameter values that have been cited in the documentation for that test alone.

It is hoped that the test documentation will be used in support of ASHRAE Standard 140 ‘Standard Method of Test for Building Energy Analysis Software’ (ASHRAE 1998).

5.1.4 Evaluation of the Test Suite

The development of the analytical test suite was planned to include two stages of evaluation so that any problems in the analytical tests themselves, and the documentation, could be resolved before its general release. First, evaluation was done ‘in house’ by carrying out the whole test series with one particular whole building energy simulation program, BLAST (1995). Second, the test suite was evaluated ‘blind’ by a third party using the EnergyPlus program. Feedback from both of these evaluation processes was used to improve the test documentation and software. Detailed information of the test results using the BLAST program can be found in Spitler, et al. (2001) and Rees, et al. (2002). The experience of testing EnergyPlus with the test suite can be found in Spitler, et al. (2001) and Witte, et al. (2004).

As mentioned in Chapter 4, the validity of the analytical tests has also been confirmed during the test of ESP-r while selecting the inter-model comparison tool.

Information of the test results using the ESP-r program can be found in Xiao, et al. (2002, 2005)

5.2 Analytical Test of the Heat Balance Based Residential Cooling Load Calculation Procedure

This section describes the analytical test of the ResHB computer program, which is the reference implementation of the RHB procedure. First, the tests appropriate for testing ResHB are listed, followed by a description of some general concerns and the corresponding strategies used while applying the tests. Then, an introduction is given for each test applied to ResHB, explaining the individual objective and analytical model used, along with the corresponding test results and problems diagnosed.

5.2.1 Testing ResHB

5.2.1.1 Tests Selected for Testing ResHB

As acknowledged during the test suite design, because of the limitations in the fabric models and input data structure of some programs, not all tests in the test suite can be applied to every building energy simulation program. Specifically, for ResHB, all the tests with a step change in boundary conditions are not appropriate. This is because ResHB is a design day load calculation program, which assumes steady periodic boundary conditions. This means the first two transient conduction tests with stepped driving temperature profile (TC1 and TC2) and the radiant part of the internal heat gain test (IntHeatGain) are not applicable to ResHB.

Also, the simplified geometric input structure of ResHB makes the stack effect infiltration test (Infiltration-2) impossible. The ground coupling test of slab on ground floor (GrdCoup) is beyond the scope of ResHB as well, since slabs are modeled with 300mm (1ft) of earth and adiabatic boundary conditions in ResHB. Table 5-2 lists the tests selected for Testing ResHB.

Table 5-2 Tests Selected for Testing ResHB

Test Group	Test Title	Abbreviation
Group 1	Steady-state convection	SSConv
	Steady-state conduction	SSCond
	Transient conduction – Sinusoidal Driving Temperature and Multi-layer Wall	TC3 + SSCond*
Group 2	Exterior Solar Radiation – Opaque Surfaces	ExtSolRad
	Solar Radiation – Glazed Surfaces	SolRadGlazing
	Solar Radiation – Window Shading	SolRadShade
	Solar Radiation – Window Reveal Shading	WinReveal
	Solar Radiation – Internal Solar Distribution	IntSolarDist
Group 3	Infiltration – Fixed Infiltration Rate	Infiltration-1
Group 4	Interior Long Wave Radiation	IntRad
	External Long Wave Radiation	ExtLWRad
Group 5	Internal Heat Gains – Convective	IntHeatGain

* See explanation in the result section below.

5.2.1.2 Boundary Conditions Specification

Outside and Inside Conditions

The test suite software provides the outside boundary conditions of the test zone by creating annual weather files, which are usually the preferred form for general energy calculation programs. However, being a design day load calculation application, ResHB takes the outside boundary conditions in the form of design day conditions. Therefore, the weather files created by the test suite software are not used in testing ResHB. Design day conditions are specified to satisfy the required outside conditions instead. This means

that: except for the transient conduction test with sinusoidal driving temperature, all other tests listed in Table 5-2 need a specification of fixed outside dry-bulb temperature. This is done by specifying a design day outside dry bulb temperature with zero daily range in ResHB. The sinusoidal outside temperature profile required in the transient conduction test is specified by scheduling hourly outside temperature in ResHB.

All the tests in Group 2 requires solar data input. Originally, ResHB derives hourly incident solar radiation based on the site and design date information. User input of the solar data was not available. To facilitate the solar tests, input structure was added to ResHB so that hourly solar data can be scheduled optionally by the user. For other tests requiring the elimination of outside solar radiation, solar radiation is turned off by a modeling option (-MS0) provided by ResHB.

All the tests listed in Table 5-2 requires a fixed inside dry-bulb temperature. This is done by specifying the inside air set point in ResHB.

Convection Coefficients

For all the tests, both the outside and inside convection coefficients used are those from ResHB. Basically the “fixed” values (outside 12.50 W/m².K; inside 1.25 W/m².K for ceiling, 4.68 W/m².K for wall, 4.37 W/m².K for floor) in ResHB are used. For the transient conduction case, the fixed inside values are also used for the outside of the external wall. This is because in ResHB, the outside hourly scheduled temperature boundary condition - which is used for the transient conduction case - is modeled with inside convection coefficients.

For the test of internal long wave radiation, the “runtime weighted” option with the “system on” value (5.00 W/m²K) in ResHB is used for the inside convection coefficients. This is for the purpose of keeping the same convection coefficient for all the internal surfaces, as assumed in the analytical solution. The “fixed” value option is not appropriate for this test since it has different values for different surface orientation. The convection coefficient is irrelevant for the infiltration and convective internal heat gain tests. The convection coefficients used for all the tests are summarized in Table 5-3.

Table 5-3 Convection Coefficients Used in Testing ResHB

Test Group	Test Abbreviation	Convection Coefficient (W/m ² K)	
		Inside	Outside
Group 1	SSConv	4.68	12.50
	SSCond	4.68	12.50
	TC3 + SSCond*	4.68	4.68
Group 2	ExtSolRad	4.68	12.50
	SolRadGlazing	4.68	12.50
	SolRadShade	4.68	12.50
	WinReveal	4.68	12.50
	IntSolarDist	4.68	12.50
Group 3	Infiltration-1	-	-
Group 4	IntRad	5.00	12.50
	ExtLWRad	1.25	12.50
Group 5	IntHeatGain	-	-

* See explanation in the result section below.

Surface Properties

For the tests that require the elimination of long wave radiation, long wave emissivities of the relevant surfaces are set to a very small number (0.001). For the solar tests with glazing surfaces, the solar absorptivities of the relevant surfaces are set to 1.0 to ensure total absorption of the incident solar radiation.

5.2.1.3 Batch File Automatic Tests

One purpose of doing analytical tests for ResHB is to assist in the maintenance of the program. A batch file was written to re-run all the tests automatically after each modification of the ResHB program and compare the output files to the reference outputs as set by prior runs. The batch file automatic tests make it convenient to diagnose any new problems that could be introduced in each revision of ResHB.

5.2.2 The Analytical Tests and Testing Results

The objective, analytical model and test results for the tests completed for ResHB are presented below.

Test Group 1: Convection and Conduction

The steady-state convection and conduction tests in this group are designed to find the response to a steady difference in dry bulb temperature between the inside and outside of the test zone. The heat transfer is only by convection at the inside and outside surface and by conduction through one or more surfaces. This requires suitable choice of surface properties to eliminate long-wave radiation. Steady-state results are ensured by making the zone fabric massless. As in most energy simulation programs the heat transfer is assumed to be one-dimensional. In the steady-state convection test (SSConv), the external surface consists of a single homogeneous layer. The thermal resistance of this fabric is made negligible to ensure that the heat fluxes are most sensitive to convection at the inside and outside surfaces. The steady-state conduction test (SSCond) is similar except that the fabric is to have significant thermal resistance and may be a multi-layer construction. As noted earlier, it is not usually possible to carry out any zone heat transfer

test without invoking the program's convection models (at least using the regular data input mechanisms). Consequently, the steady-state convection test – although seemingly trivial – underlies all the other tests.

Three transient conduction test cases are included in the test suite, each using different profiles of the driving external dry bulb temperature, and each with rather different analytical solutions. Only the third transient conduction test (TC3) is applicable to ResHB. This test uses a sinusoidal external dry bulb temperature profile as shown in Fig. 5-2, and allows multiple layer fabric constructions. In this test the response in terms of zone load is examined.

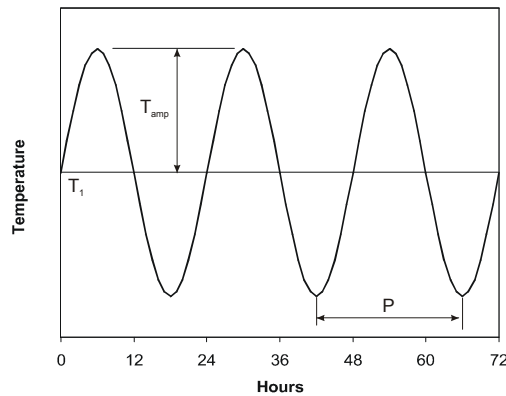


Figure 5-2. Sinusoidal driving external dry bulb temperature profile used in the transient conduction test TC3

The objective of test TC3 is to find the response to sinusoidal changes in outside dry bulb temperature when the inside dry bulb temperature is held constant at the mean external temperature. The analytical model for this test is based on the solution of the one-dimensional transient Fourier heat conduction equation for a multi-layer slab with convective boundary conditions. Solution of this analytical model by complex

representation of the temperature and use of matrix methods (Pipes 1957) allows treatment of multiple homogeneous wall layers.

The response to the driving temperature is that the inside surface temperature varies about the same mean as the outside but with reduced amplitude and a phase lag. The zone load has a similar phase lag with the driving temperature. The size of the reduction in amplitude and phase lag is dependent on the layer material properties. The inside heat flux can be described using a ‘decrement factor’ and phase lag in the same way as in the Admittance Method load calculation procedure (Holmes and Wilson, 1996) as follows,

$$q_i(t) = Uf\Delta T_o \sin(\omega(t - \phi)) \quad (5-4)$$

where, U is the overall steady-state conductance ($\text{W}/\text{m}^2\text{K}$ [$\text{Btu}/\text{h}\cdot\text{ft}^2$]), f is the decrement factor (non-dimensional), ΔT is the amplitude of the periodic outside temperature ($^{\circ}\text{C}$ [$^{\circ}\text{F}$]), ω is the period of the excitation divided by 2π , ϕ is the time lag (hours), and t is the time (hours). Details of the analytical solution to this transient conduction test are given in Spitler, et al. (2001) and Xiao, et al. (2005).

A summary of the results of the steady-state convection, steady-state conduction and transient conduction tests found with the ResHB program are given in Table 5-4. The differences in zone load are calculated from the difference at a given hour divided by the peak zone load. The steady state convection and conduction tests show agreement with the analytical solutions so close that the zone load differences are less than one watt. The ResHB program outputs the zone load to the nearest watt, so that no difference is shown

in Table 5-4. Test parameters used for the steady state convection and conduction tests are shown in Table 5-5.

Table 5-4 Differences in zone load between the ResHB program and analytically calculated loads for the convection and conduction cases

Test		Mean percentage difference in zone load	Maximum percentage difference in zone load
SSConv		0.00	0.00
SSCond		0.00	0.00
TC3 + SSCond	Case 1*	0.59	1.32
	Case 2*	0.85	1.58
	Case 3*	0.80	1.54

*Case 1: using the construction of the sample test in ASHRAE 1052-RP test suite documentation; Case 2: using a lightweight construction from ASHRAE 1199-RP; Case 3: using a heavyweight construction from ASHRAE 1199-RP.

Table 5-5 Test parameters used for the steady state convection and conduction tests

Test Parameter	Value		Units
	SSConv	SSCond	
Number of fabric layers	1	3	-
Thermal conductivity: Layer 1	1.0	0.1	W/m.K
Thickness: Layer 1	0.1	0.1	m
Thermal conductivity: Layer 2	-	0.05	W/m.K
Thickness: Layer 2	-	0.05	m
Thermal conductivity: Layer 3	-	0.25	W/m.K
Thickness: Layer 3	-	0.01	m
Inside temperature	15.0	15.0	°C
Outside Temperature	40.0	40.0	°C
Outside correlation coefficient 'A'	12.5	12.5	W/m ² .K
Outside correlation coefficient 'C'	0.0	0.0	-
Outside correlation exponent 'n'	0.8	0.8	-
Inside correlation coefficient 'A'	4.68	4.68	W/m ² .K
Inside correlation coefficient 'C'	0.0	0.0	-
Inside correlation exponent 'n'	0.8	0.8	-

There are three cases done for the transient conduction test with sinusoidal driving temperature, each with the same driving temperature profile (mean temperature equals 40 °C, temperature amplitude equals 15 °C) but different constructions. Case 1 uses the

construction as from the sample test in the test suite documentation. Case 2 and 3 use a lightweight and a heavyweight construction from ASHRAE 1199-RP (built in constructions in ResHB). Details of the construction thermal properties are listed in Table 5-6. The results for all three cases were very reasonable. Fig. 5-3 through Fig. 5-5 show the hourly comparison between the analytical and ResHB-calculated zone loads for the three cases respectively. As expected, the heavyweight case shows much lower zone loads than the lightweight case and has a longer phase lag with the driving temperature. There are step changes in the ResHB calculated loads shown in Fig. 5-5. This is again because the ResHB program outputs the zone load to the nearest watt.

Table 5-6 Constructions used for the transient conduction tests
(Note: Layer 1 is inside, layer 3 is outside)

Test Parameter	Value								Units
	Case 1			Case 2			Case 3		
	Layer 1	Layer 2	Layer 3	Layer 1	Layer 2	Layer 3	Layer 1	Layer 2	
Thermal conductivity	0.14	0.10	0.20	0.16	0.057	0.14	2.20	0.029	W/mK
Density	700	50	500	800	139	550	2240	30	Kg/m ³
Specific heat capacity	500	200	800	1090	1535	1500	900	1200	J/kgK
Thickness	0.10	0.05	0.10	0.013	0.09	0.02	0.20	0.20	m

It has to be noted that in the original TC3 test of the test suite, the inside air temperature of the test zone is assumed at the mean outside air temperature. This means heating is necessary to maintain the inside air temperature when the outside air temperature drops below the mean temperature. However, being a design cooling load calculation program, ResHB only calculates the cooling load to maintain the inside air set point. When inside air temperature drops below the set point, no heating is applied to

keep the set point and the room temperature is in a free-floating mode. To facilitate testing ResHB's performance on transient conduction with sinusoidal driving temperature, the inside air temperature has to be maintained equal to or less than the minimum outside driving air temperature, so that there will always be some cooling load. This was done in the following way.

The problem is to solve the transient conduction response with sinusoidal driving temperature while inside air temperature is maintained equal to or less than the minimum outside driving air temperature. This problem can be separated into two sub-problems: 1) the transient conduction problem as described in the original TC3 test of the test suite; 2) the steady state conduction problem with the outside air at the mean temperature of the sinusoidal driving temperature profile and the inside air at a temperature equal to or less than the minimum outside air temperature. The transient sub-problem is solved in test TC3 and the steady state sub-problem is solved in test SSCond of the test suite. Using the method of superposition, the summation of the zone loads from the two sub-problems represents the total zone load of the problem to be solved. This explains why "TC3 + SSCond" is shown in Table 5-2 and 5-3.

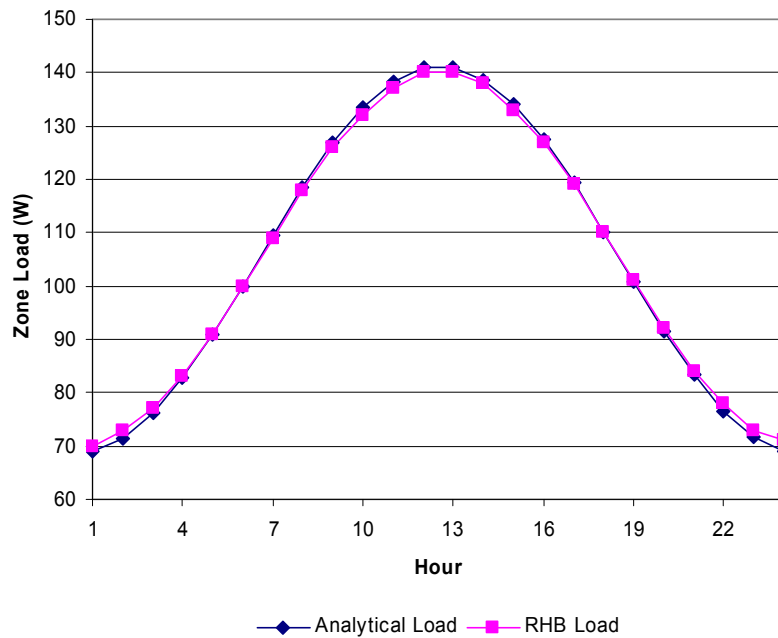


Figure 5-3. Analytically calculated zone loads and those predicted by the ResHB program for the transient conduction test with sinusoidal driving temperature: Case 1.

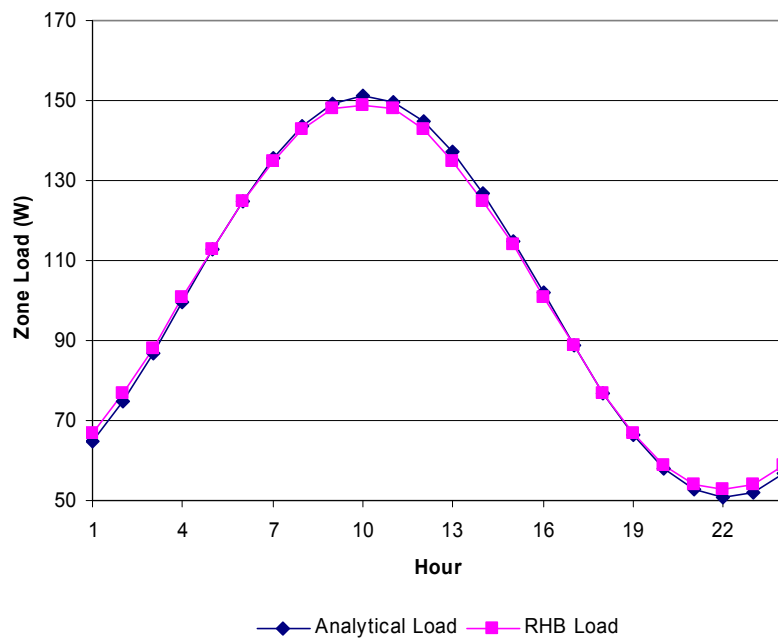


Figure 5-4. Analytically calculated zone loads and those predicted by the ResHB program for the transient conduction test with sinusoidal driving temperature: case 2.

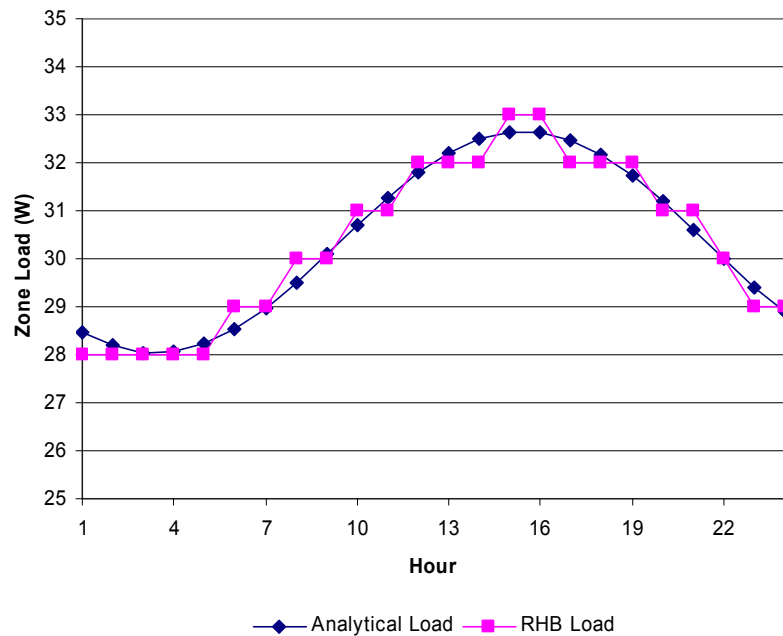


Figure 5-5. Analytically calculated zone loads and those predicted by the ResHB program for the transient conduction test with sinusoidal driving temperature: case 3.

Test Group 2: Solar Gains and Shading

A total of five test cases involving external solar irradiation are provided as part of the test suite. These range in complexity from a case of solar irradiation on an opaque surface to solar irradiation on a glazed surface with multiple shading devices. A simple internal solar distribution test is also included. The performance on each of these tests is assessed from the hourly load predictions over a single day. As only direct radiation data is present in the weather file and diffuse is set to zero, it is firstly the ability of the program to calculate the angle of incidence on the building fabric at each hour of a particular day, and consequently the incident solar flux, that is tested.

The ability of the test program to predict the normal solar fluxes is first tested with an opaque surface (test ExtSolRad). The analytical values of normal solar flux are

calculated using the same solar fluxes that are written in the weather file and using values of solar azimuth and elevation angles from US Naval Observatory data tabulated for every ten minutes of the test day. Angles of incidence in the analytical solution are calculated using an orthodox vector analysis. In this first solar test, a heat balance at each surface of the fabric and on the zone air is calculated using the same assumptions as the steady state conduction test, except that an additional term is present in the outside surface heat balance due to the solar flux. No long wave radiation at either surface is considered. The fabric is massless so that it can be assumed that the zone load is instantaneous.

The basic test for glazed surfaces (SolRadGlazing) involves a single pane of clear glass. By assuming a single pane of clear glazing, it is possible to avoid the complexities of specular coatings, inter-pane reflections and radiation and derive an analytical solution using a conventional optical analysis to find the transmission and absorption of the incident solar flux at each hour (Duffie and Beckman, 1991). The glazing is assumed to be highly conductive so that it would be at a uniform temperature. This allows a heat balance to be simply calculated on the glazing to find the thermal conduction component of the zone load. The inside of the zone is assumed to be totally absorbent of incident solar fluxes so that reflection and re-transmission of the solar energy does not have to be considered.

Two tests, Test SolRadShade and Test WinReveal, are provided to assess the ability of the test program to deal with basic shading effects. The objective of the first shading test (SolRadShade) is to test the treatment of semi-infinite external shading over

glazed surface. The shading is said to be semi-infinite in that it has a finite depth (from the face of the zone exterior surface to its front edge) but is infinite in the direction parallel to the wall surface. Three types of window shading are considered: Semi-infinite horizontal fin, semi-infinite vertical fin and a combination of both semi-infinite horizontal and vertical fins.

The analytical calculation of transmission and absorption of solar radiation in all of the shading test cases is modified from the SolRadGlazing test simply by the reduction in effective glazed area by the casting of shadows from the shading devices (there is no diffuse irradiation). Shadow geometry is calculated using published shading geometric relations (Rodriquez and Alvarez 1991). Shading devices are assumed to be completely opaque and non-reflecting. No radiation is exchanged between the glazing and shading devices. The window reveal test (WinReveal) is similar to the other shading tests except that the window can be shaded by both sides of the reveal as well as the top. This is geometrically the same as a combination of two vertical and one horizontal semi-infinite fins.

The last test in Group 2 (IntSolarDist), is intended to assess the treatment of internal solar distribution, i.e. how the test program redistributes solar energy that has entered the zone between the different internal surfaces. A small window on one surface of the zone is used with both horizontal and vertical shading applied. The dimensions of the window and shade and the depth of the zone are arranged such that no beam radiation should fall on any surface other than the wall opposite the window at any time of the day. By making the wall opposite the window lightweight, and eliminating internal long wave

radiation, the zone load corresponds to the instantaneous solar gains through the glazing. By making all other surfaces in the zone heavyweight it should be possible to determine whether the test program is redistributing the solar gains to other surfaces or not. If solar gains are redistributed to the heavyweight surfaces the peak zone load will be correspondingly reduced and the energy redistributed over the day. Accordingly, when the test program is set to explicitly model direct irradiation within the zone and no internal solar redistribution the program zone loads should match those calculated with this test solution. Transmission and absorption of solar radiation and the effect of shading is calculated in the same way as the SolRadShade test. The test zone geometry for this test case is shown in Fig. 5-6.

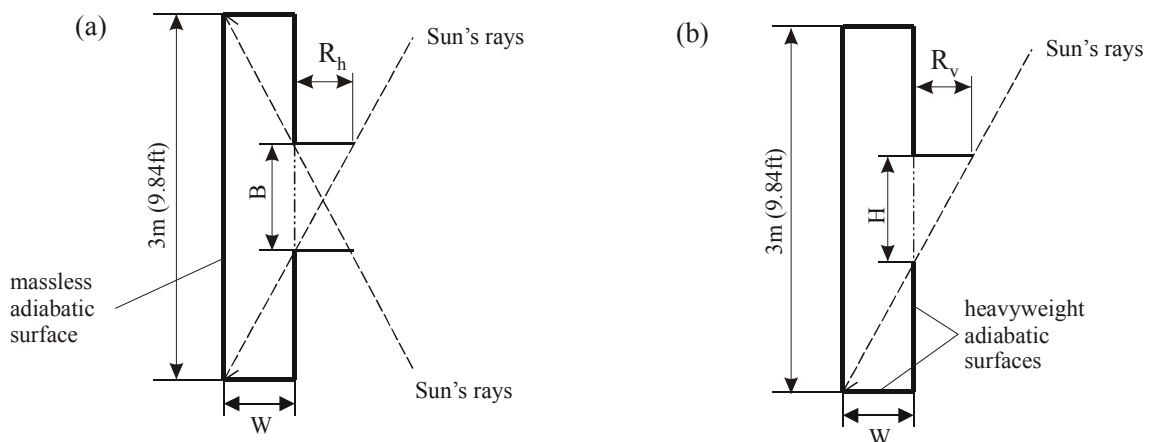


Figure 5-6: Zone geometry of the internal solar distribution test (a) plan view showing two vertical fins (b) vertical view showing horizontal fin at the top of the window. The dimensions W , R_v and R_h are 0.5m (1.64ft), and the dimensions H and B are 1.0m (3.28ft).

A summary of the test results in the solar radiation group is given in Table 5-7. Test parameters used in the ExtSolRad test are listed in Table 5-8. Test parameters used in the SolRadGlazing and SolRadShade tests are listed in Table 5-9. Test parameters used in the WinReveal and IntSolarDist tests are listed in Table 5-10. Again, the differences in

zone load are calculated from the difference at a given hour divided by the peak analytical zone load. There are two cases tested in the SolRadGlazing test, one for a south-facing window, and the other for a west-facing window. Five cases with all possible horizontal and vertical fin configurations on a south-facing window are tested in the SolRadShade test. There are two cases tested in the IntSolarDist test. In Case 1, the floor of the RHB test zone was made heavy-weight. In Case 2, the floor of the RHB test zone was made mass-less.

It needs to be pointed out that for the SolRadGlazing, SolRadShade, WinReveal and IntSolarDist tests, analytically calculated solar absorptances and transmittances for the glazing surfaces were input as a glass class in ResHB, so that the same glass properties were used in ResHB and the analytical solution. In addition to the absorptances and transmittances, ResHB also requires the input of SHGC (Solar Heat Gain Coefficient) values while defining a glass class. The SHGC values for the selected glass were calculated with the simplified method in *ASHRAE Handbook of Fundamentals* (2001, Chapter 30), so that the absorptances, transmittances and SHGC values are in agreement with each other for the defined glass class.

For the ExtSolRad, SolRadGlazing and SolRadShade tests shown in Table 5-7, the loads calculated by ResHB showed the same trends as predicted by the analytical solutions and the level of error appears acceptably small, with maximum errors on the order of 1-2% of the peak analytical zone load.

Table 5-7 Differences in zone load between ResHB and analytical result for the solar related cases

Test		Mean percentage difference in zone load	Maximum percentage difference in zone load
ExtSolRad		0.06	0.31
SolRadGlazing	South case	0.34	2.26
	West case	0.06	0.53
SolRadShade	Horizontal	0.26	2.00
	Vertical right	0.26	2.26
	Vertical left	0.29	1.65
	Horizontal + Vertical right	0.22	2.01
	Horizontal + Vertical left	0.22	1.28
	WinReveal	3.24	13.17
IntSolarDist	Case 1	9.44	49.69
	Case 2	0.02	0.26

Table 5-8 Parameters used for the ExtSolRad test
(Note: Layer 1 is outside, layer 3 is inside)

Test parameters	Value	Units
Location	Atlanta	-
Test date	08/21/1999	-
Surface tilt angle	90	Degree
Surface azimuth	180	Degree
Solar absorption of the surface	0.9	-
Number of layers	3	-
Thermal conductivity: layer 1	0.15	W/mK
Thickness: layer 1	0.1	m
Thermal conductivity: layer 2	0.05	W/mK
Thickness: layer 2	0.1	m
Thermal conductivity: layer 3	0.15	W/mK
Thickness: layer 3	0.1	m
External air temperature	20	C
Internal air temperature	20	C
Outside correlation coefficient 'A'	12.5	W/m ² K
Outside correlation coefficient 'C'	0.0	-
Outside correlation exponent 'n'	0.8	-
Inside correlation coefficient 'A'	4.68	W/m ² K
Inside correlation coefficient 'C'	0.0	-
Inside correlation exponent 'n'	0.8	-

Table 5-9 Parameters used for the SolRadGlazing and SolRadShade tests

Test parameters	Value		Units
	SolRadGlazing	SolRadShade	
Location	Atlanta	Atlanta	-
Test date	08/21/1999	08/21/1999	-
Surface tilt angle	90	90	Degree
Surface azimuth	180, 270	180	Degree
Thickness of the surface	0.0023	0.0023	m
Extinction coefficient of the surface	10.0	10.0	m ⁻¹
Refractive index of the surface	1.526	1.526	-
Depth of the horizontal fin*	-	0.6	m
Depth of the vertical fin*	-	0.6	m
Vertical fin is on which side of the window*	-	Right/Left	-
External air temperature	20	20	C
Internal air temperature	20	20	C
Outside correlation coefficient 'A'	12.5	12.5	W/m ² K
Outside correlation coefficient 'C'	0.0	0.0	-
Outside correlation exponent 'n'	0.8	0.8	-
Inside correlation coefficient 'A'	4.68	4.68	W/m ² K
Inside correlation coefficient 'C'	0.0	0.0	-
Inside correlation exponent 'n'	0.8	0.8	-

* Combinations of these parameter values were used as noted in the results

Table 5-10 Parameters used for the WinReveal and IntSolarDist tests

Test parameters	Value		Units
	WinReveal	IntSolarDist	
Location	Atlanta	Atlanta	-
Test date	08/21/1999	08/21/1999	-
Surface tilt angle	90	90	Degree
Surface azimuth	180	90	Degree
Thickness of the surface	0.0023	0.0023	m
Extinction coefficient of the surface	10.0	10.0	m ⁻¹
Refractive index of the surface	1.526	1.526	-
Depth of the horizontal fin	-	0.5	m
Depth of the vertical fin	-	0.5	m
Vertical fin is on which side of the window	-	Left and Right	-
Depth of the window reveal	0.3	-	m
Length of the window	3.0	1.0	m
Height of the window	3.0	1.0	m
Solar absorption of the internal surfaces	1.0	1.0	-
External air temperature	20	20	C
Internal air temperature	20	20	C
Outside correlation coefficient 'A'	12.5	12.5	W/m ² K
Outside correlation coefficient 'C'	0.0	0.0	-
Outside correlation exponent 'n'	0.8	0.8	-
Inside correlation coefficient 'A'	4.68	4.68	W/m ² K
Inside correlation coefficient 'C'	0.0	0.0	-
Inside correlation exponent 'n'	0.8	0.8	-

Comparisons of the ResHB results with the analytical solution for two configuration cases in the solar shading test (SolRadShade) initially showed poor results. The problematic cases have a horizontal fin and a vertical fin on either side of the glazing surface (left or right). It was found that in the earlier versions of ResHB code (Version 1.0.1 and prior versions), there was a mistakenly placed “End If” statement in the module calculating the sunlit fractions for windows under external shading. Figure 5-7 and 5-8 show the load comparisons for the two problematic cases. After the bug was fixed in ResHB Version 1.0.2, the maximum differences between the analytical and ResHB-calculated zone loads drop from 15.51% to 2.01% (for the horizontal and right-side vertical fin configuration) and from 15.59% to 1.28% (for the horizontal and left-side vertical fin configuration) respectively.

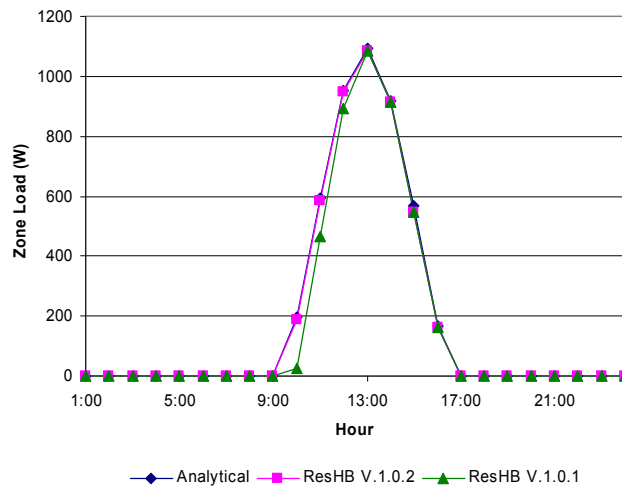


Figure 5-7. Analytically calculated zone loads and those predicted by different versions of ResHB for the solar shading test: horizontal and right side vertical fin on a south-facing window.

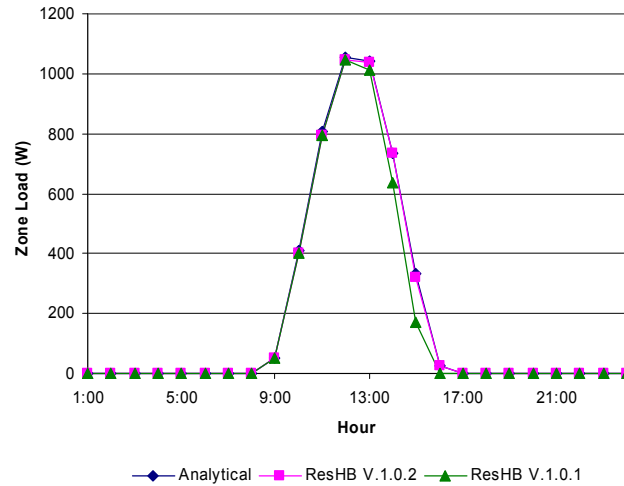


Figure 5-8. Analytically calculated zone loads and those predicted by different versions of ResHB for the solar shading test: horizontal and left side vertical fin on a south-facing window.

The difference between the RHB and analytically calculated loads shown in Table 5-7 for the WinReveal test is relatively large. This is caused by a bug in the ResHB program. Figure 5-9 plots the hourly loads for this test. It shows that RHB predicted loads are higher than analytically predicted loads, underlining there is less shading effect caused by the window reveal in RHB. As mentioned earlier, the shading considered in the WinReveal test is geometrically the same as a combination of two vertical and one horizontal semi-infinite fin. The reveal model in RHB is supposed to be a simple model in that the reveal depth is added to the depths of the over-hang and vertical fins. While this simple model may not be appropriate for some circumstances, it should predict the same shading effect as predicted analytically under the conditions designed for this test. However, it was found that this simple reveal model was not correctly implemented in ResHB. The reveal depth was only added to the depth of the over-hang, but not to the depths of the vertical fins. Figure 5-10 shows the load comparison after adding the reveal depth to the depths of vertical fins and re-building ResHB. The maximum difference

between the analytical and ResHB-calculated zone loads drops from 13.17% to 1.76% and the mean difference drops from 3.24% to 0.25%.

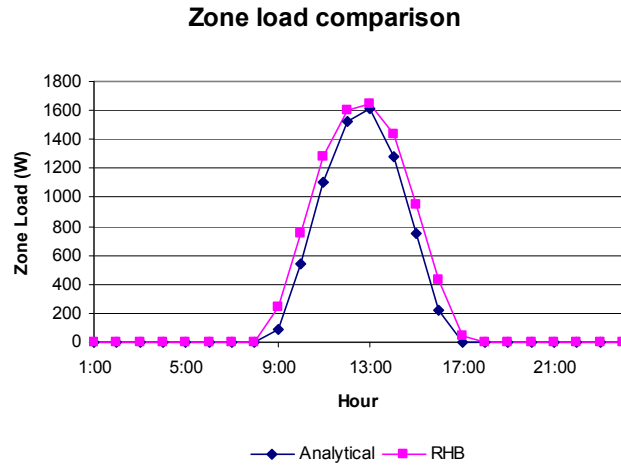


Figure 5-9. Analytically calculated zone loads and those predicted by ResHB for the window reveal test: before reveal depth was added to the depths of vertical fins

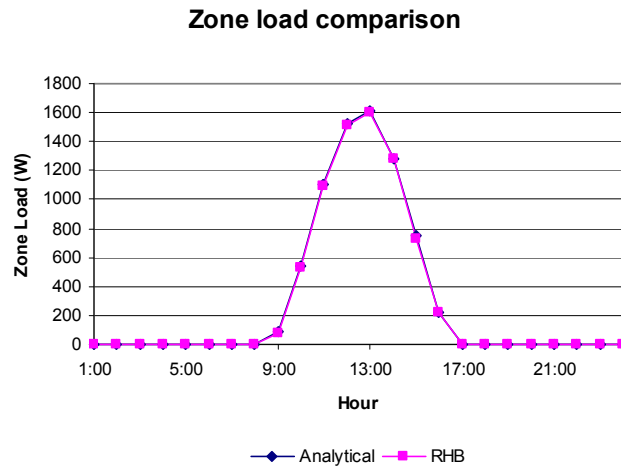


Figure 5-10. Analytically calculated zone loads and those predicted by ResHB for the window reveal test: after reveal depth was added to the depths of vertical fins

The differences between the RHB and analytically calculated loads shown in Table 5-7 for the two IntSolarDist tests are quite large for Case 1 (mean value about 10%,

maximum value about 50%) but very small for Case 2. This is as expected. The floor construction of the RHB test zone in each case was purposely made different to reflect the redistribution of the energy over the day. Basically RHB distributes the beam solar irradiation onto the floor, except that half of the internal mass surface also receives beam solar irradiation (but no internal mass is involved in this analytical test). By making the floor of the RHB test zone heavy-weight in Case 1, a redistribution of the energy over the day is expected. This is what can be seen in the hourly load comparison for Case 1, shown in Figure 5-11. In Case 2, the floor of the RHB test zone was made mass-less, so that the zone loads reflects the instantaneous solar gains through the glazing and distributed on the floor. In this case, the mass-less floor of the RHB test zone functions equivalently as the mass-less wall opposite to the window in the analytical test zone. Thus, a close match between RHB predicted loads and analytically predicted loads is expected for Case 2. This is actually what can be seen in Figure 5-12, which plots the hourly load comparison for Case 2.

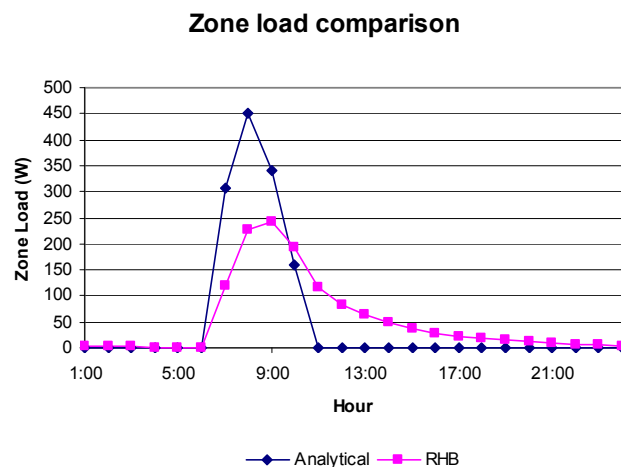


Figure 5-11. Analytically calculated zone loads and those predicted by ResHB for the internal solar distribution test: Case 1, the floor in RHB test zone is heavy weight.

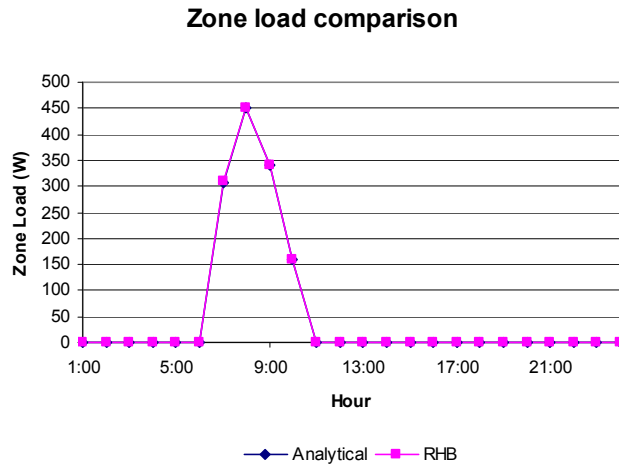


Figure 5-12. Analytically calculated zone loads and those predicted by ResHB for the internal solar distribution test: Case 2, the floor in RHB test zone is mass-less.

Test Group 3: Infiltration

Two tests are included in the test suite in which the only zone load is due to infiltration of outside air. Zone loads due to infiltration can be calculated analytically simply from the product of the mass flow rate and the difference in enthalpies of the incoming air and the air at the room condition. What has to be calculated in the analytical solution (and implicitly in the test program) are the mass flow rate and enthalpies at different psychrometric conditions. It is primarily the test programs ability to carry out the necessary psychrometric calculations that is being tested.

The difference between the two infiltration tests in group 3 (Infiltration-1 and Infiltration-2) lies in the way that the mass flow rate is specified. As mentioned earlier, only the first infiltration test is applicable to ResHB. In this test the mass flow rate is simply specified as a fixed volumetric flow rate at the outside conditions. The results therefore depend only on the programs ability to find the correct air density (to get the mass flow rate) and the enthalpies at inside and outside conditions.

A difference of 4.65% was found between the steady state load calculated by ResHB and that of the analytical solution in the first infiltration test (Infiltration-1). It appears this deviation comes from the different methods ResHB and analytical solution uses to calculate infiltration load. As described above, infiltration load is calculated analytically from the product of the infiltration mass flow rate and the difference between the entering and leaving air enthalpies. Both the enthalpies of the inside and outside air are calculated with the psychrometrics calculation routines taken from (Brandemuehl 1993, ASHRAE 1997: Chapter 6). The volume, density and specific heat of the infiltration air are in terms of outside air.

In ResHB, infiltration load is calculated as two parts: the sensible and the latent load. The following code comes from function *GetLocation* in *RHBInputMod.f90*:

```
CALL SETPATM_ELEV( Elevation)      ! PsychoMetricsMod
BarometricPressure = GETPATM()
ElevationF = BarometricPressure / 101325.    ! elevation factor
AVFSenF = 1.2 * ElevationF                ! AVF sensible factor (W/(L/s)-K)
AVFLatF = 3010. * ElevationF              ! AVF latent factor (W/(L/s)-(g/g))
```

AVFSenF and *AVFLatF* are used to calculate sensible and latent infiltration loads from air flow rates and the difference between inside and outside air temperature. The volume, density and specific heat of the infiltration air are in terms of inside air. (As described in Page 29.18-19 of the 2001 *ASHRAE Handbook of Fundamentals*, 1.2 is the air density corresponds to about 16 °C at saturation and 21 °C dry air at 101325 Pa; 3010 is the product of 1.204 and 2500, where 2500 is the approximate heat content of 50% relative humidity vapor at 24 °C less the heat content of water at 10 °C. 50% relative humidity at 24 °C is a common inside design condition and 10 °C is normal condensate

temperature from cooling and dehumidifying coils.) Also, note that there is an elevation adjustment used in ResHB.

The main difference between the two methods is the infiltration air taken as outside vs. inside. The analytical test assumes standard barometric pressure (101325 Pa), so the altitude adjustment made in ResHB is not being tested. (The elevation factor is 1.0 (at sea level) for this test.) The analytical test also assumes the inside and outside humidity ratios are equal (it was 0.0092 for the case discussed here), so there is no latent load. Using the method of ResHB, hand calculation of the infiltration load (outside air temperature 40 °C, inside air temperature 24 °C, infiltration rate 0.0375 m³/s) confirms the result reported by ResHB, which is 720 W. The analytical solution is 688 W.

Although it seems like it is just a convention to take infiltration air as inside or outside, infiltration comes from outside by definition. So it may be better to take infiltration air as outside. Also, the load difference found in this test may not be negligible. Therefore, it is arguably inappropriate to take the infiltration in terms of inside air for ResHB.

Test Group 4: Longwave Radiation

Two separate tests have been developed for the testing of treatment of internal and external longwave radiation. In each case, it is assumed that the surfaces are gray and isothermal. Radiation is treated in a single waveband using exact view factor based methods. In each case the air is assumed not to participate in the radiant exchange.

The ability of the test program to deal with longwave radiation at external surfaces is examined using a test zone with a single horizontal surface that is assumed to exchange radiation only with the sky (test ExtLWRad). It is also intended that this fabric is a massless surface so that zone loads can be assumed to be instantaneous. A single sky temperature is specified and the net steady-state heat balance on the inside and outside surfaces of the roof is calculated, assuming one-dimensional conduction through the roof, to find the surface temperatures and resultant zone load. Using this test the sensitivity of the zone load predicted by the test program to the external longwave emissivity can be evaluated.

The internal longwave radiant exchange model of the test program can be evaluated by examining the zone loads and surface temperatures predicted with zone geometries of different aspect ratio and different surface emissivities. This is done in the second test in group four (IntLWRad). In this case, energy enters the zone through one external surface by convection from the outside air, conduction through a massless wall, and enters the zone by convection to the room air and radiant exchange with all the room surfaces. Conduction through the lightweight wall is treated by a one-dimensional steady-state analysis. The radiant exchange calculation method adopted for this test is that given by Stefanizzi et al. (1988).

The aspect ratio of the test zone is changed by keeping the external wall a fixed 3x3m (9.84x9.84ft) and extending the length of the adjacent walls of the zone. As the aspect ratio increases, so does the internal surface area of the zone. The net radiation from the inside surface of the external wall increases with aspect ratio as the external wall

radiates to a larger area (effectively less radiation returns to this surface). The analytical prediction of response to different aspect ratios and surface emissivities is shown in Fig.5-13. Previous work has shown that internal long wave radiation models differ in how they are able to respond to changes in zone aspect ratio, and that this type of test is a robust test of such models (Stefanizzi et al. 1988).

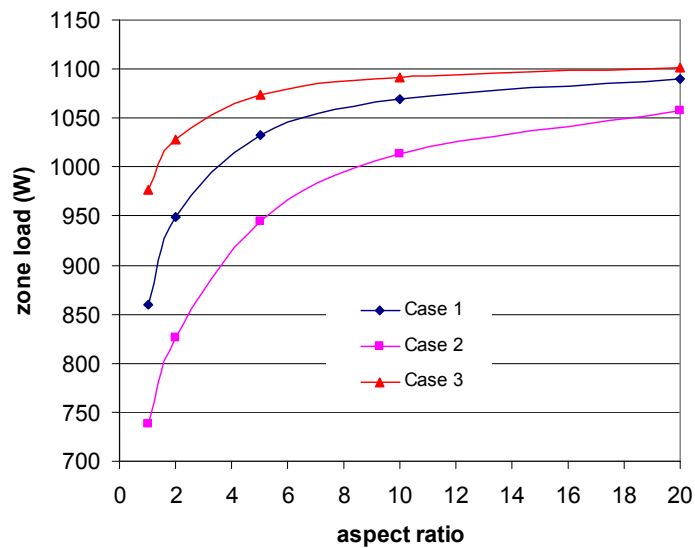


Figure 5-13: Zone load variation with zone aspect ratio and different surface emissivities. The emissivities are: Case 1, external surface 0.9, opposite surface 0.1, other surfaces 0.3; Case 2, external surface 0.9, all other surfaces 0.1; Case 3, all surfaces 0.9.

Three internal long wave radiation cases with various internal surface emissivity combinations are applied to ResHB, each with five different aspect ratios of the test zone. The outside and inside air temperatures used are 40 °C and 20 °C respectively. The differences between the analytical and ResHB-calculated zone loads are summarized in Table 5-11. The load comparisons for each case are also shown in Figure 5-14. For all the cases, ResHB results match analytical results reasonably well. Generally, better match was obtained with larger aspect ratios of the test zone. ResHB shows the same sensitivity

to aspect ratio and surface emissivity as predicted by the analytical solution. Also, it was found that in case 2, where the surface emissivities are all the same (0.9), ResHB results match analytical solution better (with maximum error percentage of -0.62%) than in the other two cases (the maximum error percentage is -1.12% for case 1 and -1.24% for case 3), where various surface emissivities were set.

Table 5-11 Differences in zone load between ResHB and analytical result for the interior longwave radiation tests

Aspect ratio	Zone load difference (%)		
	Case 1*	Case 2*	Case 3*
1	-1.12	-0.62	-1.24
2	-1.05	-0.40	-0.96
5	-0.86	-0.40	-0.61
10	-0.72	-0.39	-0.60
20	-0.60	-0.49	-0.59

*The emissivities are: Case 1, external surface 0.9, all other surfaces 0.1; Case 2, all surfaces 0.9; Case 3, external surface 0.9, opposite surface 0.1, other surfaces 0.3.

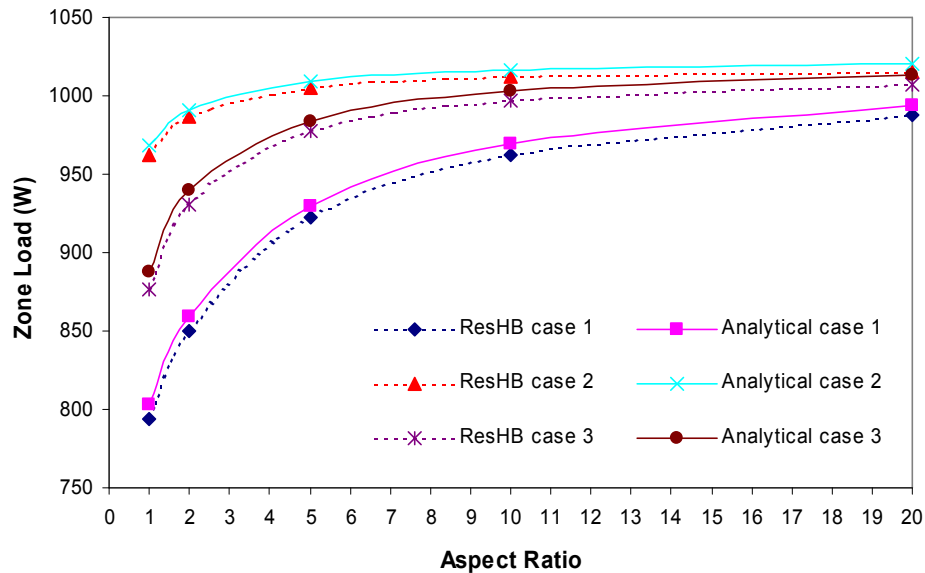


Figure 5-14. Analytical and ResHB-predicted zone load variation with zone aspect ratio and different surface emissivities. The emissivities are: Case 1, external surface 0.9, all other surfaces 0.1; Case 2, all surfaces 0.9; Case 3, external surface 0.9, opposite surface 0.1, other surfaces 0.3.

Five external long wave radiation cases with different external surface emissivities (0.1, 0.3, 0.5, 0.7, 0.9) were tested for ResHB. The outside and inside air temperatures used are 40 °C and 20 °C respectively. The external surface used in the test has a thermal conductivity of 1.0 W/mK and a thickness of 0.1 m. Satisfactory results were obtained for all cases, with a maximum difference in the steady-state load of 0.41%. The sky temperature, a test parameter required to get the analytical solution for this test, was that output by the ResHB program (34 °C for the cases tested). ResHB has two sky temperature model options. The default model of Berdahl and Martin (1984) was used in the tests.

Test Group 5: Miscellaneous

Two further tests included in the test suite deal with response to internal gains and heat transfer through slab-on-grade floors (denoted as IntHeatGain and GrdCoup). As mentioned before, the GrdCoup test is beyond the scope of ResHB. In the IntHeatGain test, internal gains are considered as a combination of radiant and convective heat fluxes. Only the convective heat gain part of the test is applicable to ResHB. The convective portion of the gains are relatively easy to deal with – both in simulation programs and in the analytical solution – in that such gains can be added instantaneously to the heat balance on the room air. The test of the convective heat gain in ResHB is thus straight forward. In one test, the test zone was set to have a constant 3000W convective heat gain. Both ResHB and analytical solution reported an instantaneous zone load of 3000W.

5.3 Conclusions

An analytical verification test suite for building fabric models of whole building energy simulation programs has been developed. The test suite consists of a series of sixteen tests covering convection, conduction, solar irradiation, longwave radiation and infiltration phenomena, as well as ground-coupled floors. The test suite consists of standardized documentation for each test case that includes results for one or more sets of test parameters along with the derivation of the analytical solution. In addition, source code used to implement the analytical solutions, and a user interface that drives this code, have been developed as part of the ASHRAE 1052-RP project.

Using the test suite, a total of twelve analytical tests have been done with the ResHB program. The analytical verification has been shown to be useful in the development and maintenance of the ResHB program. The analytical tests show the validity of ResHB in modeling several basic heat transfer phenomena, including steady state convection and conduction, transient conduction, solar radiation and internal solar distribution, and internal and external long wave radiation.

One problem was diagnosed with earlier versions of ResHB in the solar shading test. The problem has been fixed in later versions of ResHB after the diagnosis was reported. Another problem was diagnosed in the window reveal shading test. The problem has been reported to and confirmed by the ResHB developer.

Although the infiltration test with fixed infiltration rate seems relatively simple, differences between analytical and ResHB results found in this test are not ignorable.

Investigation of the ResHB source code revealed that the method used by ResHB to calculate infiltration load is different from that of the analytical solution, with the main difference being the infiltration air taken as outside vs. inside. The difference in the calculation method explained the load differences reported in this test.

It is concluded that RHB is acceptable from the analytical test perspective. Based on what was covered by the analytical tests in this study, no big problem has been found regarding its underlining mechanisms for modeling the basic heat transfer phenomena in building fabric.

6. EXPERIMENTAL VALIDATION OF THE HEAT BALANCE BASED RESIDENTIAL COOLING LOAD CALCULATION PROCEDURE

As mentioned in the literature review, experimental validation is the most widely used technique for testing a simulation program, as it can be considered to be a conclusive test of whether model predictions reflect reality. In particular, whole model empirical validation ensures that the overall performance of the simulation program is tested. It offers an approximate truth standard within the accuracy of the data acquisition system and many program input parameters.

An experimental validation has been conducted to confirm whether the Residential Heat Balance (RHB) cooling load calculation procedure provides a reasonable approximation to real-world performance, and is, overall, acceptable as a design tool on a typical North American house. The experimental data used were collected from a well-instrumented house in Ft. Wayne, Indiana. It is one of the four houses used by Cardinal Glass Industries to conduct thermal performance tests in distinct U.S. regions, known as the Cardinal Project.

There are two types of information needed for the RHB validation. The first type is information needed to create an input file for ResHB simulation. This includes the house geometry and constructions (for walls, roof, floors, partitions, windows, etc.), weather data, infiltration and ventilation, internal heat gain and room temperature set points. The other type of information is needed to compare ResHB simulation results with experimental measurements. This includes the room temperatures and house cooling loads.

As the Fort Wayne house was also used as the real house prototype for the inter-model comparison of ResHB with ESP-r (Chapter 4), it may be beneficial to also compare the ESP-r simulation results with the experimental data. This will help confirm ESP-r's validity as a "truth" model, relatively speaking. ESP-r may also be used as a diagnostic tool for the experimental validation of ResHB, since additional models contained in ESP-r, e.g. detailed inter-zone heat transfer and inter-zone airflow, may be relatively easily turned on and off. This can help troubleshoot differences between ResHB simulation results and the experimental data. Therefore, comparisons have also been made between ESP-r simulation results and experimental data.

The following sections explain the implementation of this experimental validation. How the needed information for the RHB validation was measured or derived from the measured data is first covered in the sections describing the experimental house, the instrumentation and data acquisition system, and the analysis of the experimental data. Sections describing the simulation approach, the result discussion, and the conclusion follow.

6.1 Experimental House

It needs to be noted at first that the description of the experimental house in this section and the instrumentation and data acquisition in the next section is based on the information provided by Bruce A. Wilcox, who is the manager and experimental designer of the Cardinal Fort Wayne Project.

As mentioned above, the house identified for experimental validation of ResHB is in Ft. Wayne, Indiana. For the Cardinal Fort Wayne Project, there are four essentially identical houses built with different orientations. Each house has a number that is used for reference. Specifically, the four house numbers are 10905, 10803, 3219 and 3235. The experimental data used for the ResHB validation are those from house 3219, of which the front side faces the north. Figure 6-1(a) shows a front view and Figure 6-1(b) shows a back view of the house. The house has a total living area of 202 m² (2178 ft²), consisting of two stories. Figure 6-2 shows the floor plans of both stories. Table 6-1 lists the materials of the house constructions, including the roof, internal and external walls, and internal and external floors. Table 6-2 lists the windows installed in individual rooms, including the windows orientation and width and height. During the experimental period (09/21/2005) of which the data collected are used in this study, High Solar gain Low E glasses (referred to by Wilcox as HSLE) were used for the windows.

There are electric heaters located in the kitchen and the master bedroom, artificially producing internal heat gains. The target total internal heat gain is about 900W, split between the kitchen and the master bedroom. Also, there is an electric heater

located in the basement, controlling the basement air temperature to be about 20 °C (68 °F).



Figure 6-1(a). Front view of the house in Ft. Wayne, Indiana (Wilcox 2004)

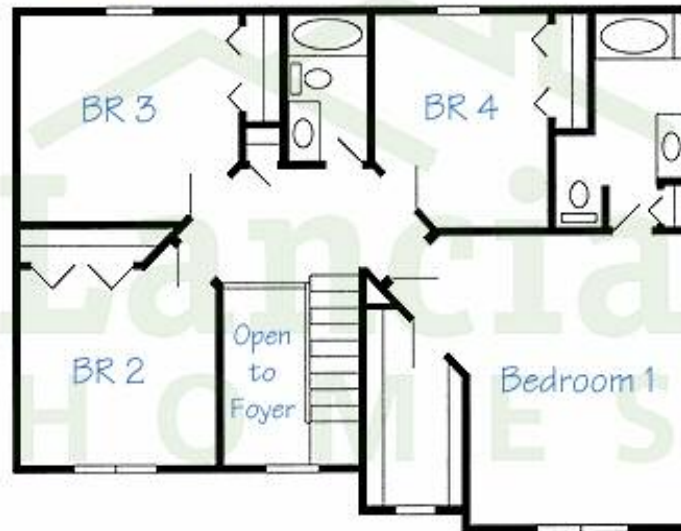


Figure 6-1(b). Back view of the house in Ft. Wayne, Indiana (Wilcox 2004)

First Floor



Second Floor



Total Living Area: 2,178 sq. ft.

Figure 6-2. Floor plans of the house in Ft. Wayne, Indiana (Wilcox 2004)

Table 6-1 Construction materials of the Fort Wayne house

Construction	Material	Note
Roof	asphalt shingles	outside
	building paper	
	1/2" OSB sheathing board	inside
Attic floor	2x10 16" OC rafter with R-38 cellulose insulation	up
	1/2" GWB with paint finish	down
External wall	vinyl lap siding	outside
	1/2" OSB sheathing board	
	2x4" 16" OC frame wood with 3/4" closed cell polyurethane spray foam and R-13 batt insulation	
	1/2" GWB with paint finish	inside
Internal wall	1/2" dry wall	
	2x4 16" OC stud	
	1/2" dry wall	
External floor	carpet	up
	1/2" plywood floor finish	
	3/4" T&G OSB floor sheathing	
	engineered floor joist with R-19 batt insulation	down
Internal floor	carpet	up
	1/2" plywood floor finish	
	3/4" T&G OSB floor sheathing	
	engineered floor joist	
	1/2" GWB with paint finish	down

Note: OC – On Center, OSB – Oriented Strand Board, GWB – Gypsum Wall Board

Table 6-2 Windows of the Fort Wayne house

Room	Unit description ¹	Orientation ²	Floor	Width (m)	Height (m)
Dining	CW15-3	Front	1st	2.169	1.521
Great	CW15-3	Back	1st	2.169	1.521
Master bedroom	CW14-3	Front	2nd	2.169	1.219
Bedroom 2	CW14-3	Front	2nd	2.169	1.219
Bedroom 3	CW14-3	Back	2nd	2.169	1.219
Bedroom 4	CW24	Back	2nd	1.435	1.219
Foyer	CW24	Front	2nd	1.435	1.219
Master bedroom closet	CW135	Front	2nd	0.721	1.037
Nook	PS8	Back	1st	2.438	2.092
Kitchen	CW23	Back	1st	1.435	0.913
Laundry	CW13	Left	1st	0.721	0.913
Master bathroom	CW13	Left	2nd	0.721	0.913

Note: ¹Unit description taken from windows order form, referring to a specific window unit from Andersen Windows.

²Assuming viewers facing the front side of the house, orientation defined in clockwise order as front, left, back, right.

The air conditioning system for the house is a 4-ton split system with air handler and sheet metal trunk ducts located in the basement. There are air supplies and returns in all major rooms. There is a very small area of return duct in the attic. The ducts have been sealed and tested and the duct leakage is very low (essentially 0). There is a constant outdoor ventilation air pumped by a ventilation fan from outside and sent through a duct directly (no heat recovery system is used) into the first floor at ceiling level at the entry/living room near the basement door.

During the experimental period (09/21/2005) of which the experimental data are used in this study, the air conditioning system control was based on a single master room temperature – the dining room air temperature, using the Campbell Datalogger and the room temperature sensors discussed below. This was intended to mimic a standard thermostatic temperature control.

6.2 Instrumentation and Data Acquisition

A Campbell Scientific CR10X data logger (Figure 6-3), which consists of a measurement and control module and a detachable wiring panel CR10XWP were used for the measurement and data collection. There was an aspirated temperature thermocouple (Figure 6-4) in each room, basement, attic, and garage, measuring the room temperatures. There was also an aspirated temperature thermocouple outside the house, measuring outdoor dry bulb temperature. The outdoor and indoor relative humidities were measured using Vaisala T&RH sensors. The indoor relative humidity was measured at one location in the living room. The outdoor wind speed was measured with Vaisala wind sensor. A class 2 pyranometer was used to measure incident solar radiation on

horizontal surface. There are 16 thermocouples used to measure system supply air temperatures near the air handler cooling coil. As will be discussed later, a flow-weighted run-time supply air temperature was derived from the temperatures measured by these 16 thermocouples and was used in the calculation of experimental cooling load. There is one thermocouple used to measure the system return air temperature at the return air duct. As will be discussed in the data analysis section, the measured system return air temperature was also used in the experimental cooling load calculation.



Figure 6-3. Campbell Scientific CR10X data logger: measurement and control module (left), wiring panel CR10XWP (right). (Picture from <http://www.campbellsci.com>)

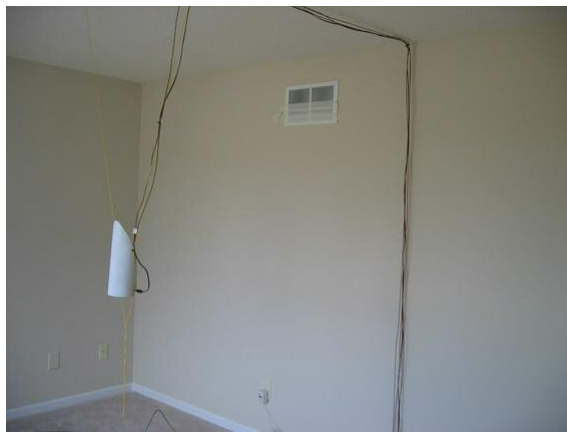


Figure 6-4. Aspirated temperature thermocouple (Wilcox 2004)

There were four electric power measurements (total house electric, air handler electric, air conditioning outdoor unit electric, and basement heater electric) made with

Wattnode power meters. These electric power measurements were used to calculate the internal heat gain of the house, by subtracting the electric power of the three HVAC devices from the house total.

The above measurements were made at minutely intervals during the experimental period. In addition to the above measurements, there were also one-time measurements for the system airflow rate to each room, the outdoor ventilation rate, and the airflow rate at the air handler. The system airflow rate to each room and the outdoor ventilation rate were measured with Alnor LowFlo Balometer, with an airflow accuracy of $\pm(3\%$ of reading + 2 CFM). The airflow rate at the air handler was measured with Duct Blaster, which is a calibrated airflow measurement system. The Duct Blaster fan was connected directly to the supply plenum and a DG-700 pressure and flow gauge was used to provide simultaneous readings of the supply plenum pressure and the Duct Blaster fan flow. The air handler flow rate was assumed to be the same as the Duct Blaster fan flow when the supply plenum pressure with the Duct Blaster fan matched the supply plenum pressure at air-conditioning mode. The airflow accuracy measured with Duct Blaster was $\pm 3\%$.

There were blower door measurements made over a week-long-period in the winter of 2004, using the Automated Performance Testing (APT) System from The Energy Conservatory (TEC). There were two test methods used in the measurement: the CGSB Standard (149.10-M86) method and the ACH50 method. The CGSB standard method consists of an 8 point Blower Door test conducted at building target pressures varying from 50 to 15 Pascals. The ACH50 method consists of a 5 point Blower Door

test conducted at building target pressures around 50 Pascals. There were three duplications of measurements made with each blower door test method. As will be discussed later, an effective leakage area derived from the blower door tests was used as a reference while defining the house leakage in the ESP-r airflow network, which affects the house infiltration used in the RHB simulation.

6.3 Data Analysis

Figure 6-5 shows how the needed information for the RHB validation was measured or derived from the measured data. This drawing is based on my understanding of the system from the information provided by Bruce Wilcox and his answers to my questions.

The minutely experimental data collected for the RHB validation purpose is available for the period from 09/14/2005 through 11/11/2005. As a clear sky model is assumed and single design day simulation is implemented in ResHB, experimental data for 09/21/2005 was selected for use in the ResHB simulation. It is the second day of a two-day sequence that appears to be the most continuously clear and sunny during the experimental period. For ESP-r simulation, experimental data from 09/14/2005 through 09/21/2005 was used, covering the day of the ResHB simulation and 7 prior days for simulation initialization.

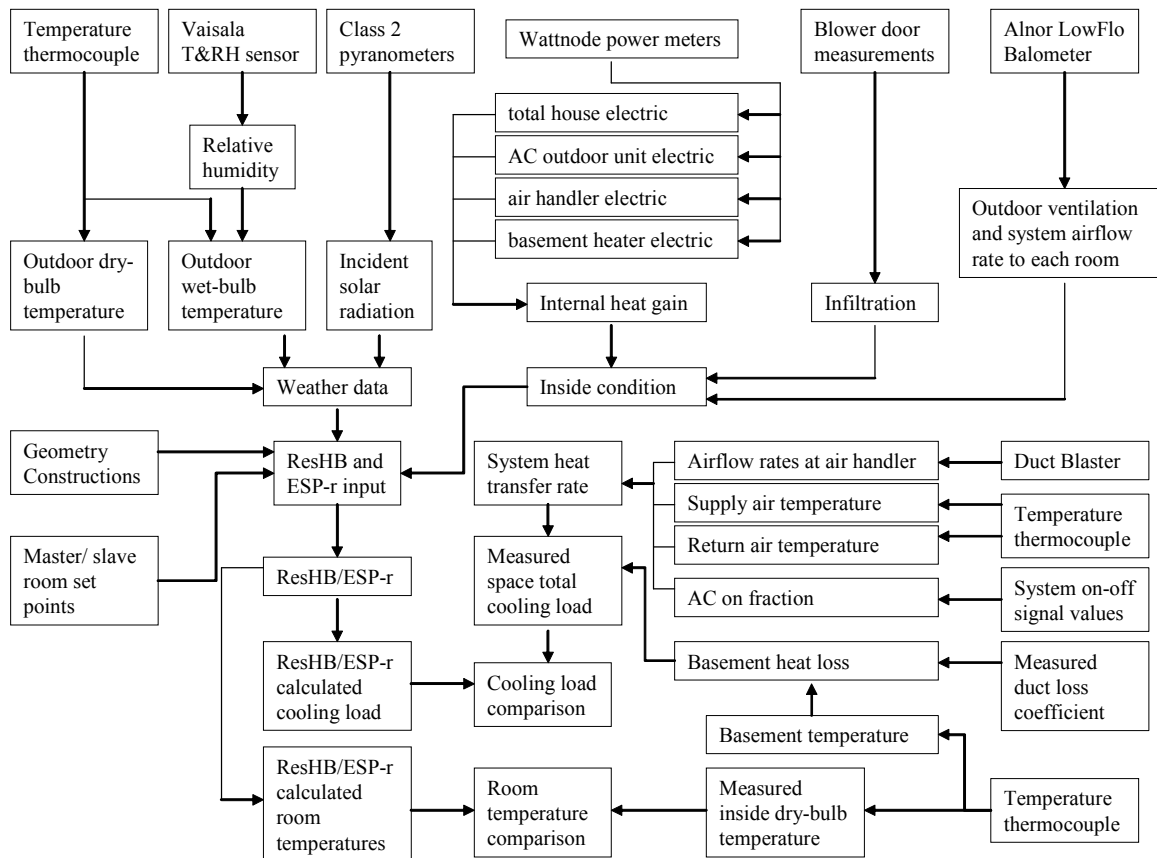


Figure 6-5. Conceptual flow chart of the experimental validation

As ResHB only permits hourly simulation, the minutely experimental data were processed into hourly format for ResHB input and comparison. The process involves an hourly average of the minutely data. The minutely data during the 60 minutes preceding an indicated hour were averaged and used for that specific hour in the hourly format. For example, the value used for hour 4:00 a.m. in the hourly format is the average of the minutely data between 3:00 a.m. and 4:00 a.m.

Specifically, outdoor dry-bulb temperature and relative humidity were hourly averaged. The ResHB-required hourly outside wet-bulb temperature was calculated from the hourly outside dry bulb temperature and relative humidity, using the psychrometrics

calculation routines taken from Brandemuehl (1993) and ASHRAE (1997: Chapter 6). The hourly outside dry-bulb and wet-bulb temperatures for 09/21/2005 are plotted in Figure 6-6. As the ResHB program requires the input of solar radiation in the form of beam and diffuse radiation, empirical correlations developed by Reindl et al. (1990) were used to split the minutely total incident solar radiation on a horizontal surface into the beam and diffuse parts. The resultant minutely beam and diffuse solar radiations were then hourly averaged for ResHB input. The hourly beam and diffuse solar radiation for 09/21/2005 are plotted in Figure 6-7.

As minutely simulation was used in ESP-r, the minutely outside dry-bulb temperature, relative humidity, wind speed, and beam and diffuse solar radiation were directly used as ESP-r input.

As mentioned earlier, the minutely measured electrical energies were used to calculate the internal heat gain of the house, by subtracting the electrical energy of the three HVAC devices (air handler, air conditioning outdoor unit, and basement heater) from the house total. The resultant minutely internal heat gain was then averaged hourly for both ResHB and ESP-r input. As shown in Figure 6-8, the hourly internal heat gain was almost a constant. Therefore, as a simplification, a daily averaged internal heat gain of 0.882 KW was actually used in the simulation input.

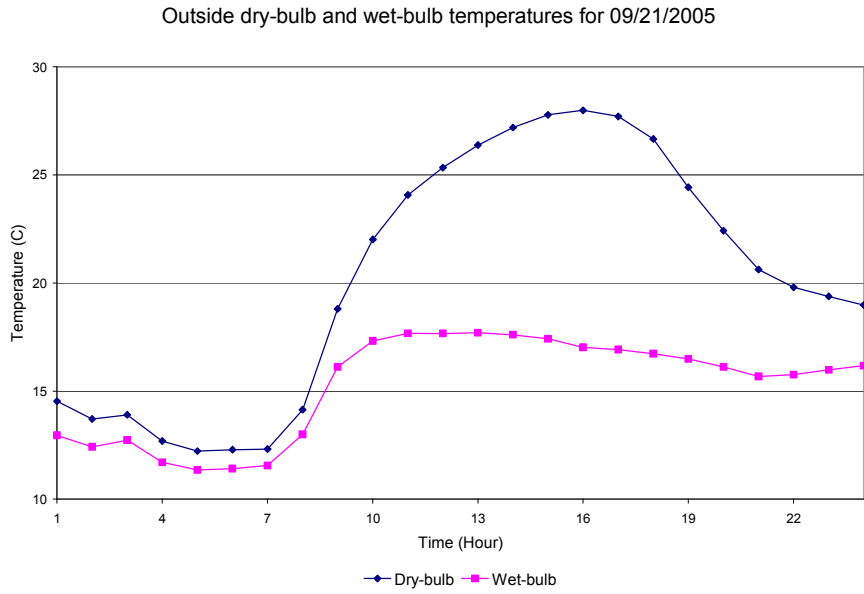


Figure 6-6. Hourly averaged outside dry-bulb and wet-bulb temperature for 09/21/2005

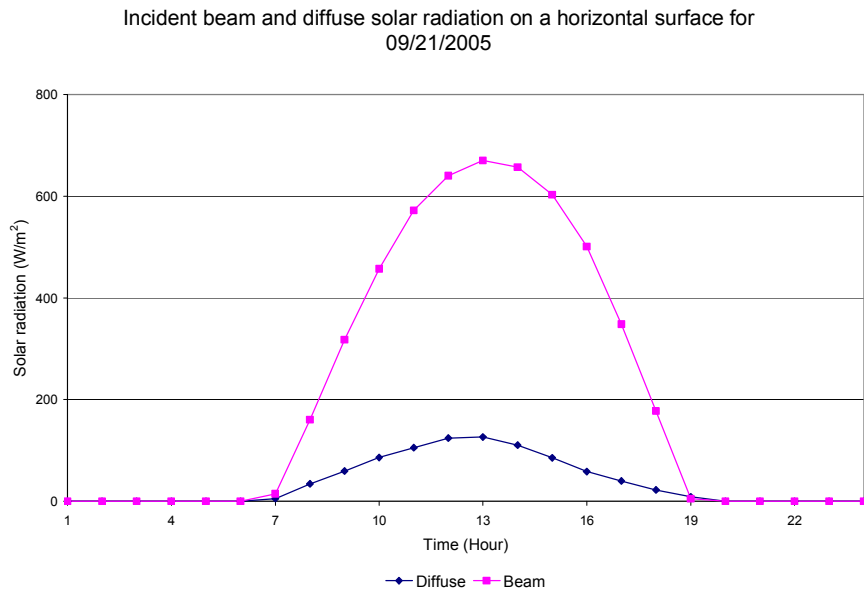


Figure 6-7. Hourly averaged beam and diffuse solar radiation for 09/21/2005

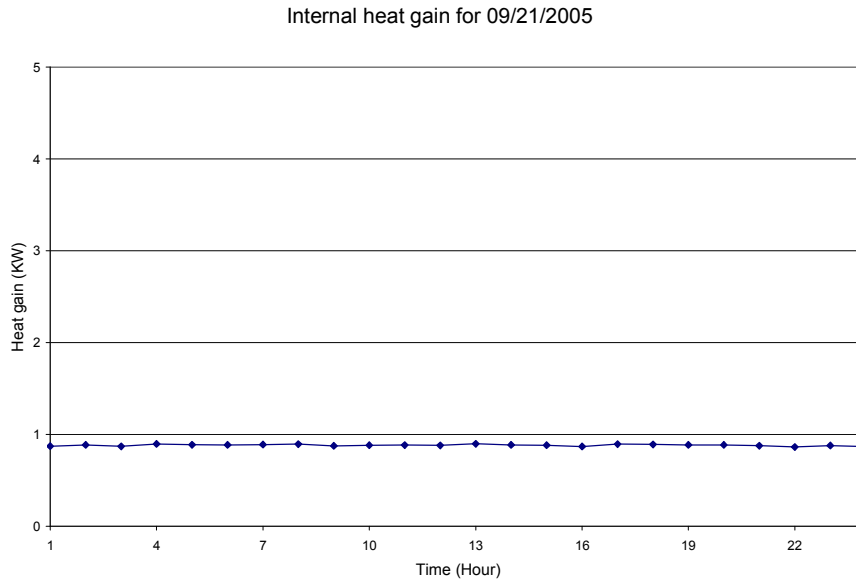


Figure 6-8. Hourly averaged internal heat gain for 09/21/2005

Regarding the blower door measurements, the measured pressure differences across the house envelope and the measured flow rates they induced were fit to an empirical equation of the form:

$$Q = c\Delta p^n \tag{6.1}$$

Where:

Q = volume flow rate of the fan, CFM

Δp = pressure difference across the house envelope, Pa

c, n = empirical constants from regression analysis

The resultant values of the constants c, n are listed in Table 6-3. With the constants c, n values, flow rates were estimated at a reference pressure difference of 4 Pa, which is typical of the weather-induced pressures that cause infiltration. The Effective

Leakage Area (ELA) of the house envelope is then calculated with the square-root flow model, which assumes the flow through the apertures in the building shell is similar to orifice flow, where the flow rate is proportional to the square root of the pressure difference (Grimsrud, et al. 1982):

$$Q = ELA \sqrt{\frac{2}{\rho} \Delta p} \quad (6.2)$$

Where:

$$\rho = \text{the air density, Kg/m}^3$$

The ELA values calculated at 4 Pa reference pressure are also listed in Table 6-3. The average ELA values derived from the blower door measurements with both the CGSB Standard method and the ACH50 method were used as references (but not directly as inputs) while defining the house leakage in the ESP-r airflow network, which in turn affects the house infiltration used in the ResHB simulation. More details on specifying house infiltration in both programs are covered in the simulation approach section.

Table 6-3 Constants c, n and ELA values derived from blower door measurements

Test Number	Tests using CGSB Standard method			Tests using ACH50 method		
	C	N	ELA (in ²)	C	N	ELA (in ²)
1	36.5	0.782	30.6	44.1	0.731	34.4
2	39.5	0.764	32.3	46.9	0.722	36.1
3	47.1	0.717	36.0	48.8	0.708	37.0
Average	41.0	0.754	33.0	46.6	0.720	35.8

The measured outdoor ventilation rate of 70 CFM was directly used in both the ResHB and ESP-r simulations.

As will be discussed later, it was desired to use the hourly averaged master room temperature while setting the room temperature control in the ESP-r simulation. Hourly averaged temperatures for all conditioned rooms were desired while specifying the room set points in the ResHB simulation. Therefore, minutely measured room temperatures were averaged hourly to be used as simulation input.

The above data analysis was done for the purpose of creating input files for the ResHB and ESP-r simulations. The following data analysis was done for the purpose of comparing simulation results with experimental data.

As will be discussed later, there are basically two types of comparisons made between the simulation results and experimental data. One is the comparison of simulated total house cooling load with measured house load; the other is the comparison of simulated room temperatures with measured room temperatures. For room temperature comparisons, the minutely measured room temperatures for all rooms (including conditioned rooms and unconditioned spaces) were hourly averaged.

For house cooling load comparisons, the hourly system sensible heat transfer rate was first estimated as the product of the total volume airflow rate at the air handler, the air density and specific heat (ρc_p), the hourly difference between the system supply and return air temperature (ΔT), and the hourly air conditioning “on” fraction. The measured volume airflow rate at the air handler of 1421 CFM was directly used. The air density used was 1.235 Kg/m^3 and the specific heat used was 1.004 KJ/kg.K , which correspond to the air density and specific heat at $13 \text{ }^\circ\text{C}$ (as the system supply air temperature was

approximately 13 °C). To get an hourly ΔT , the return air temperatures were hourly averaged. The run-time supply air temperatures (the supply air temperatures when the system was on) for each air register were hourly averaged first and then flow-weighted to get the hourly flow-weighted run-time supply air temperature. The weighting factors used were derived by dividing the airflow rate at each air register by the total airflow rate at all registers. The hourly ΔT was the difference between the hourly return air temperature and the hourly flow-weighted run-time supply air temperature, both of which are shown in Figure 6-9. The hourly air conditioning “on” fraction is the average of the minutely on-off signal values during a specific hour. The minutely on-off signals are values between 0 and 1, which in turn are the minutely average of the on-off signal values (0 or 1) at the data logger’s data acquisition intervals. The hourly air conditioning “on” fraction is plotted in Figure 6-10.

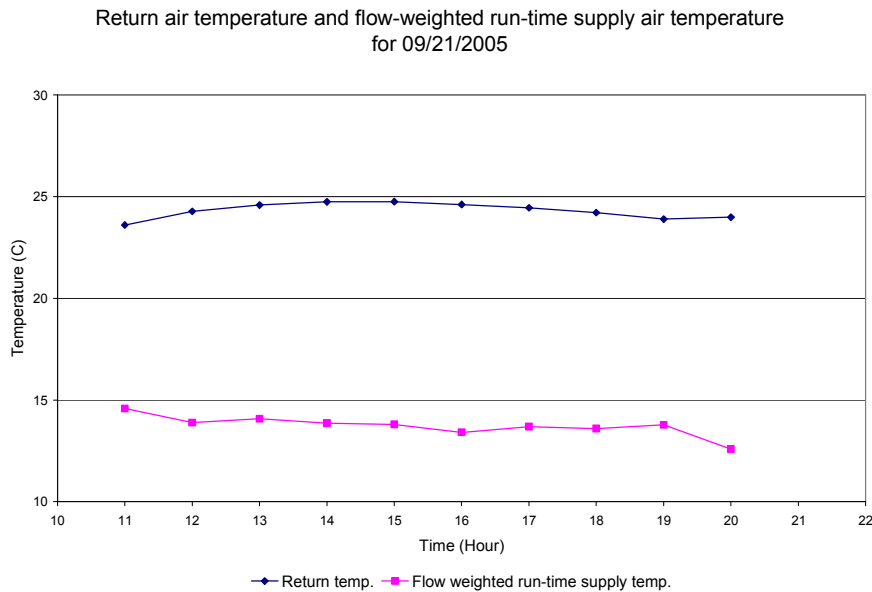


Figure 6-9. Hourly return air temperature and hourly flow-weighted run-time supply air temperature for 09/21/2005, values shown only for hours when the system was on

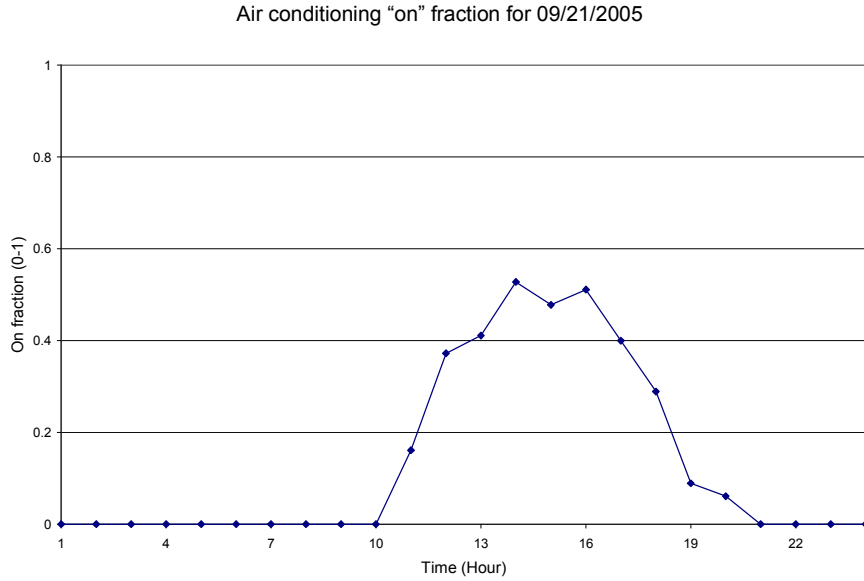


Figure 6-10. Hourly air conditioning "on" fraction for 09/21/2005

To account for the heat gain to the supply air before it reaches the supply air registers, the basement duct gain was subtracted from the hourly system sensible heat transfer rate to get the sensible cooling load of the house. The only noticeable heat gain to the supply air was observed to be in the supply air duct located in the basement. The basement duct gain was calculated as two parts: the run-time part (q_{on}) and the average ΔT part (q_{avg}), based on the measurements and derivations made by Wilcox (2004). The run-time part was the product of the hourly air conditioning "on" fraction (F_{on}), the difference between the hourly averaged basement air temperature (T_b) and the hourly flow-weighted run-time supply air temperature (T_s), and the run-time duct gain coefficient (C_{on}):

$$q_{on} = F_{on} (T_b - T_s) C_{on} \quad (6.3)$$

The average ΔT part was the product of the difference between the hourly averaged basement air temperature and the hourly flow-weighted run-time supply air temperature, and the average ΔT duct gain coefficient (C_{avg}):

$$q_{avg} = (T_b - T_s)C_{avg} \quad (6.4)$$

Both the run-time duct gain coefficient and the average ΔT duct gain coefficient used were derived by Wilcox (2004) from measurements done in 2004. The total basement duct gain was the sum of the run-time part and the average ΔT part of the duct gain, as shown in Figure 6-11. The calculated house total sensible cooling loads are plotted in Figure 6-12.

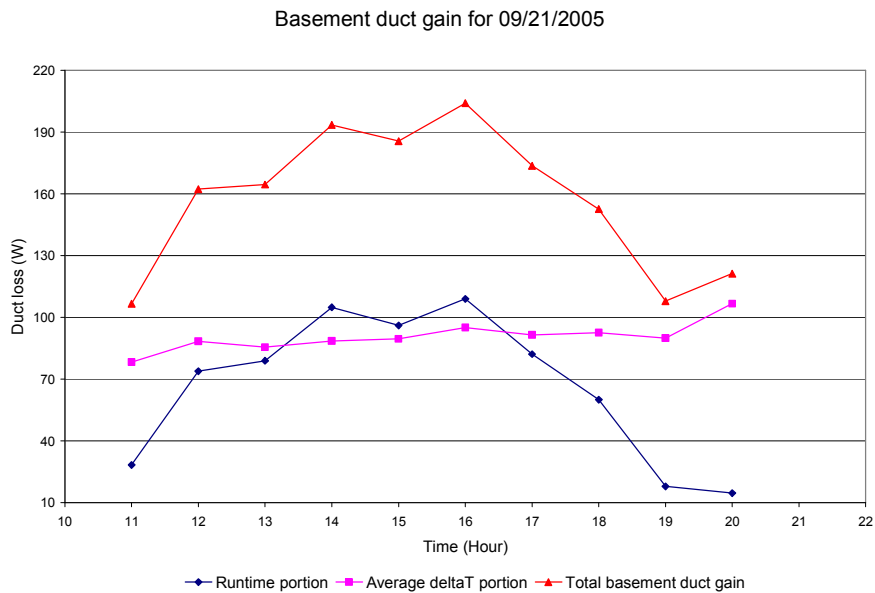


Figure 6-11. Hourly basement duct gain (including run-time part and average ΔT part) for 09/21/2005, values shown only for hours when the system was on

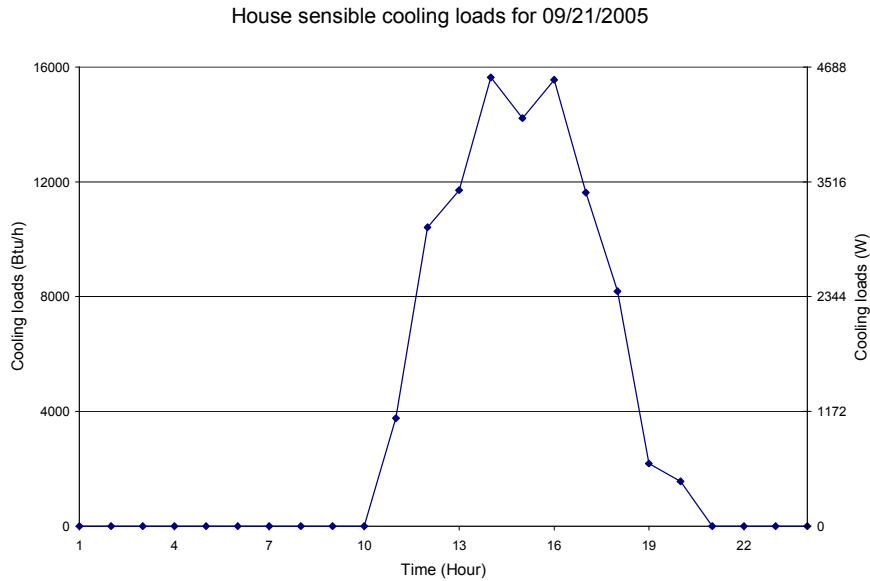


Figure 6-12. House total sensible cooling load for 09/21/2005

6.4 Simulation Approach

With the house information and experimental data collected, ResHB simulation has been done for the purpose of validating RHB. In addition to the ResHB simulation, ESP-r simulation has also been done to help troubleshoot differences between ResHB simulation results and experimental data, for the reasons discussed earlier in this chapter. This section explains how the house information and experimental data were used to create ResHB/ESP-r input files, what simulation component models were used, and what types of comparison have been made between the simulation results and experimental data.

6.4.1 Simulation Inputs

As mentioned earlier, the basic simulation inputs include the house geometry and constructions, weather data, infiltration and ventilation, internal heat gain, room

temperature set points and system controls, and airflow network if applicable. The specifications of these inputs in both ResHB and ESP-r are described below.

6.4.1.1 Geometry

House geometry was specified according to the floor plans and section figures provided by Wilcox (2004). The roof pitch of the house is 7 inch 12 and was used in calculating the attic geometries. External window shadings were specified if applicable. In ResHB, geometries are specified through surface areas, orientations, and tilt angles. The basement was not included in the ResHB input and the floor surfaces over the basement were set to be exposed to a constant basement air temperature of 20 °C. In ESP-r, geometries are specified through vertex coordinates. The basement was included in the ESP-r input for the purpose of creating airflow network in ESP-r, as discussed below. The basement was set to be controlled at a constant air temperature of 20 °C.

6.4.1.2 Constructions

Both ResHB and ESP-r require a layer-by-layer input of the thermal properties of the building envelope components. For opaque house constructions listed in Table 6-1, Table 6-4 lists the corresponding thermal properties input used in both ResHB and ESP-r. As mentioned in the literature review, ResHB includes an algorithm that derives fictitious material properties for a homogeneous layer that corresponds to a framed layer. This algorithm was used to calculate the thermal properties for framed layers shown in the table. Table 6-5 lists the short wave absorptances and long wave emissivities used for the inside and outside surfaces of the constructions in both ResHB and ESP-r. The values basically are the default values listed in Table 3 of the ASHRAE 1199-RP final report

(Barnaby et al. 2004), except that an outside short wave absorptance of 0.9 was used for the roof instead of the default 0.8 (as the roof of the experimental house has a dark color). For glazing surfaces, one of the built-in fenestration classes of ResHB (FCA-17c, low-e/high solar gain) was used. This fenestration class was selected as it was considered to be most close to the High Solar gain Low E (HSLE) glasses used in the house, based on the information provided by Wilcox (2004). The associated characteristics of the ResHB built-in fenestration classes are taken from Table 13 of Chapter 30 (Fenestration) in the *ASHRAE Handbook of Fundamentals* (2001). The fenestration class used has an ID of 17c in the table, composed of one layer of clear glass and one layer of low-e (low emissivity coating) glass. For readers' convenience, the corresponding characteristics of this fenestration class are listed in Table 6-6.

6.4.1.3 Weather Data

The hourly outside dry-bulb and wet-bulb temperatures plotted in Figure 6-6 and the hourly beam and diffuse solar radiation plotted in Figure 6-7 were specified through hourly schedules in ResHB to serve as the weather data. The minutely measured outside dry-bulb temperature, relative humidity and wind speed; and the minutely beam and diffuse solar radiation derived from the minutely measured total incident solar radiation on a horizontal surface were used to create a temporary definition file (.tdf file) in ESP-r to serve as the weather data. Wind direction required by ESP-r was specified as the design value at Fort Wayne, IN, listed in Table 1B of Chapter 27 in the *ASHRAE Handbook of Fundamentals* (2001).

Table 6-4 Construction thermal properties input in ResHB/ESP-r simulation

Construction		Material	Thickness (m)	Conductivity (W/mK)	Density (kg/m ³)	Specific heat (kJ/kgK)
Roof	outside	Asphalt shingles	0.006	0.120	1100	1.26
		building paper	0.002	0.151	45	1.38
	inside	OSB sheathing board	0.013	0.105	800	1.30
Attic floor	up	R-38 cellulose insulation	0.013	0.038	38	1.38
		2x10 16" OC rafter and R-38 cellulose insulation	0.241	0.045	81	1.51
	down	GWB with paint finish	0.013	0.160	800	1.09
External wall	outside	Vinyl lap siding	0.010	0.030	500	1.00
		OSB sheathing board	0.013	0.105	800	1.30
		closed cell polyurethane spray foam, 2x4" 16" OC FrameWood and R-13 batt insulation	0.089	0.035	66	1.43
	inside	GWB with paint finish	0.013	0.160	800	1.09
Internal wall		dry wall (GWB)	0.013	0.160	800	1.09
		2x4 16" OC stud and Empty	0.089	0.442	47	1.60
		dry wall (GWB)	0.013	0.160	800	1.09
External floor	up	carpet	0.006	0.060	300	1.40
		plywood floor finish	0.013	0.140	550	1.50
		T&G OSB floor sheathing	0.019	0.105	800	1.30
	down	Engineered floor joist and R-19 batt insulation	0.140	0.050	79	1.47
Internal floor	up	carpet	0.006	0.060	300	1.40
		plywood floor finish	0.013	0.140	550	1.50
		T&G OSB floor sheathing	0.019	0.105	800	1.30
		Engineered floor joist and Empty	0.305	1.221	63	1.60
	down	GWB with paint finish	0.013	0.160	800	1.09

Note: OC – On Center, OSB – Oriented Strand Board, GWB – Gypsum Wall Board

Table 6-5 Surface absorptances and emissivities input in ResHB/ESP-r simulation

Surface	Short wave absorptances		Long wave emissivities	
	Outside	Inside	Outside	Inside
Roof	.9	.45	.9	.9
Wall	.6	.45	.9	.9
Fenestration	per fenestration class	per fenestration class	.84	.84
Floor	0	.6	.9	.9

Table 6-6 Solar Heat Gain Coefficient (SHGC), Solar Transmittance (T) and Layer Absorptances (A) for ResHB fenestration class FCA-17c

Incidence angles	0	40	50	60	70	80	90	Hemis. Diffuse
SHGC	0.70	0.68	0.65	0.59	0.46	0.24	0.00	0.61
T	0.59	0.56	0.54	0.48	0.36	0.18	0.00	0.50
A ₁	0.11	0.12	0.13	0.13	0.14	0.15	0.00	0.12
A ₂	0.14	0.14	0.14	0.13	0.11	0.07	0.00	0.13

Note: A₁ for outside layer, A₂ for inside layer, Hemis. – Hemispherical

6.4.1.4 Internal Heat Gain

As mentioned before, a daily averaged internal heat gain of 0.882 KW was used in the simulation input. Although the electric heaters producing the internal heat gains were located in the kitchen on the first floor and in the master bedroom on the second floor, there is a question of how the internal heat gain should be distributed to individual rooms in the simulation input, as inter-zone air-mixing caused by inter-zone airflows was very obvious. There is some other evidence of the inter-zone airflow and mixing discussed later in the result section, here I discuss one proof that can be directly observed from the experimental data.

As shown in Figure 6-13, during the system-off hours (measured data during the system-on hours are not shown in the figure, as the measured data during the system-off hours are of the most interest here), measured air temperatures in adjacent rooms are very close to the measured air temperature in the room where the heater is located: In Figure 6-13(a), the air temperature in the living room is close to the kitchen room temperature; In Figure 6-13(b), the air temperature in the master bathroom is close to the master bedroom temperature. An interesting phenomenon in Figure 6-13 is the temperature spikes occurring during the system-off hours. Presumably these temperature spikes were

caused by the start and stop of the electric heaters, which became the main heat gain source of the rooms at night. Interestingly, air temperature spikes in both adjacent rooms follow the same trends as those in the heater-located rooms. Although not shown in the figure, air temperatures in other non-adjacent rooms had no or very little evening spikes and were much more different from the heater-located room temperatures. The close relationships between room air temperatures in adjacent rooms over short time periods when the cooling system is off are obvious indications of the inter-room air-mixing between these rooms.

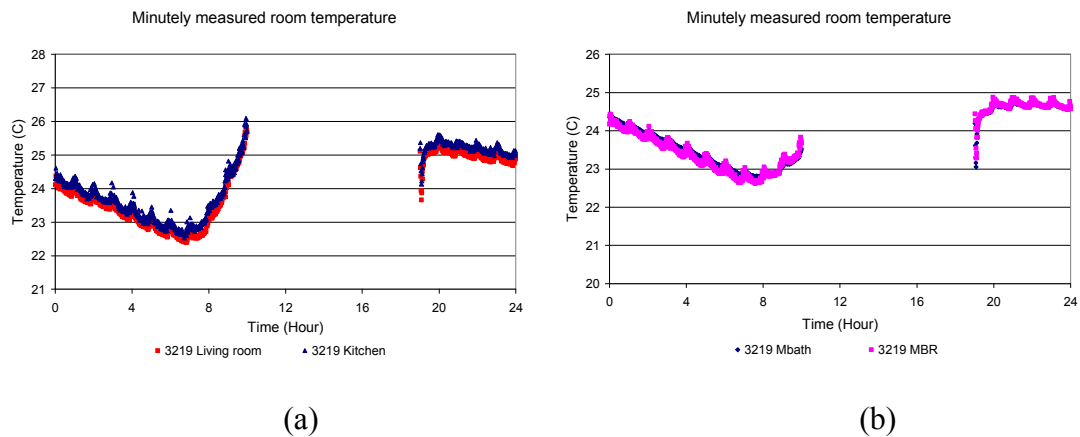


Figure 6-13. Minutely measured room air temperature during the system-off hours for 09/21/2005: (a) kitchen and living room (b) master bedroom and master bathroom

The treatment of the internal heat gain distribution depends on whether the simulation program has the ability to model inter-zone airflow. For ESP-r, inter-zone airflow was modeled by setting up an airflow network in the simulation. As the inter-zone airflow has already been accounted for via the airflow network, internal heat gains were not distributed but were directly specified to be in the rooms where the heaters were located. For ResHB, no inter-zone airflow can be modeled directly. As an approximate

way to account for the inter-zone airflow in the ResHB simulation, internal heat gains were distributed to adjacent rooms (including the heater-located rooms) through area-weighting. Specifically, half of the total internal heat gain (0.882 KW) was distributed among the master bedroom and rooms adjacent to the master bedroom; another half was distributed among the kitchen and rooms adjacent to the kitchen. Note that “adjacent” here means there is a direct opening (doorway or large opening) in between.

6.4.1.5 Infiltration and Ventilation

To account for the house infiltration in the ESP-r simulation, the average house Effective Leakage Area (ELA) derived from the blower door test data was used as a reference while defining the house leakage in the ESP-r airflow network. The total house leakage area defined in ESP-r was within 10% of the average house ELA values derived from the blower door measurements with both the CGSB Standard method and the ACH50 method. Infiltration was specified as a fixed ACH (Air Changes per Hour) value in ResHB, using the infiltration rates predicted in ESP-r as a reference. ResHB simulation results presented in the results section have an infiltration rate of 0.4 ACH, except the results of those simulations especially designed for infiltration sensitivity analysis.

As mentioned before, the measured outdoor ventilation rate of 70 CFM was directly used in both the ResHB and ESP-r simulations. As was done for the internal heat gain, an area-weighted ventilation distribution was made to account for inter-zone airflow when specifying the room ventilation rates in ResHB. For ESP-r, the ventilation was specified to be in the room where outdoor air was introduced.

6.4.1.6 Room Temperature Set Points and System Control

As mentioned before, the air conditioning system control used in the experiment was based on a single master room temperature – the dining room air temperature. The set point of the master room air temperature was 23.89 °C, with a dead band of 1.67 °C. The meaning of this dead band control can be better understood by looking at the minutely measured dining room air temperature. As shown in Figure 6-14, during each cycle that the system turns on and off (between 10 a.m. and 8 p.m.), the dining room temperature keeps increasing until it hits about 24.7 °C and then keeps decreasing until it hits about 23 °C, which implies that the system does not turn on until the dining room temperature hits an upper limit of 24.7 °C and then keeps running until the dining room temperature hits the lower limit of 23 °C. During the evening and early morning hours (from 8 p.m. to 10 a.m.), the system never turns on as the dining room temperature is always below 24.7 °C. As the system was off during these hours, room temperatures all through the house including the dining room temperature were free-floating. So the 1.67 °C dead band covers a range of the master room temperature swing during the cooling hours, with the 23.89 °C set point in the middle of the dead band.

To model this system control in ESP-r, an airflow network was created to function as the air-conditioning system. A mixing zone controlled at the average system supply air temperature was used as a substitute for the cooling coil. The measured system supply airflow rate to each room was represented by constant volumetric airflow from the mixing zone to each room. Return airflows were represented by airflows through return grills from all major rooms to the mixing zone. The constant volumetric airflow components and return grills were under on-off control based on the dining room air

temperature. As ESP-r does not have a dead band control for the airflow network components, an approximate system control was used so that it resembles the real system control. The dining room set point was set to have two schedules, so that the simulated hourly average temperature in the dining room has a good match with the experimental hourly average temperature. During the hours when the real system was running, the dining room set point was set to be 23.95 °C. During the hours when the real system was not running, the dining room set point was set to be 24.6 °C, so that the simulated system will not turn on for most of the time and the house room temperatures will be free-floating as in the experiment. Note that in the results section below, there are some intermediate ESP-r results discussed using controls different from the basic control strategy described above. In that case, the specific controls used will be explained accordingly.

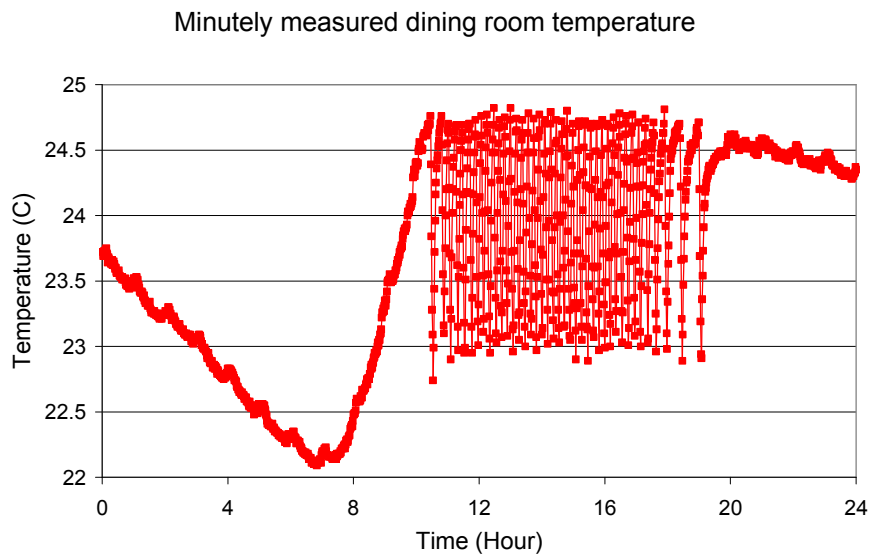


Figure 6-14. Minutely measured room air temperature for 09/21/2005: dining room

As neither system nor airflow can be modeled in ResHB, the system control was implemented by manipulating the hourly room temperature set points in the ResHB input. The room temperature set points in ResHB were also set to have two schedules. During the hours when the real system was running, the set points for each conditioned room were set to be equal to the corresponding experimental hourly average room temperature. During the hours when the real system was not running, the set points for each conditioned room were set to be values so that each room temperature will be free-floating as in the experiment during those hours (24.7 °C for the dining room, for example). The reason that separate set point schedules were used for individual rooms in ResHB is discussed later in the results section, where some intermediate simulation results with other control methods (such as master-slave control) are presented to show why the current control strategy was selected.

6.4.1.7 Airflow Network

As the airflow can not be modeled in ResHB, no airflow network was involved in the ResHB input. The airflow network created in ESP-r has been mentioned above. In summary, the airflow network was created for the purpose of modeling the air conditioning system control, infiltration and inter-zone airflow, using standard ESP-r airflow components. A schematic representation of the airflow network for the first and second floor is shown in Figure 6-15. For air conditioning system, a mixing zone (not shown in the figure) was defined to serve as a substitute for the cooling coil. The system supply airflows to individual rooms were represented by constant volumetric airflows through “fans” from the mixing zone to each room. The “fans” were defined as ESP-r constant volumetric airflow components (type 30). Return airflows were represented by

airflows through “return grills” from all major rooms to the mixing zone. The “return grills” were defined as ESP-r specific air flow opening components (type 110).

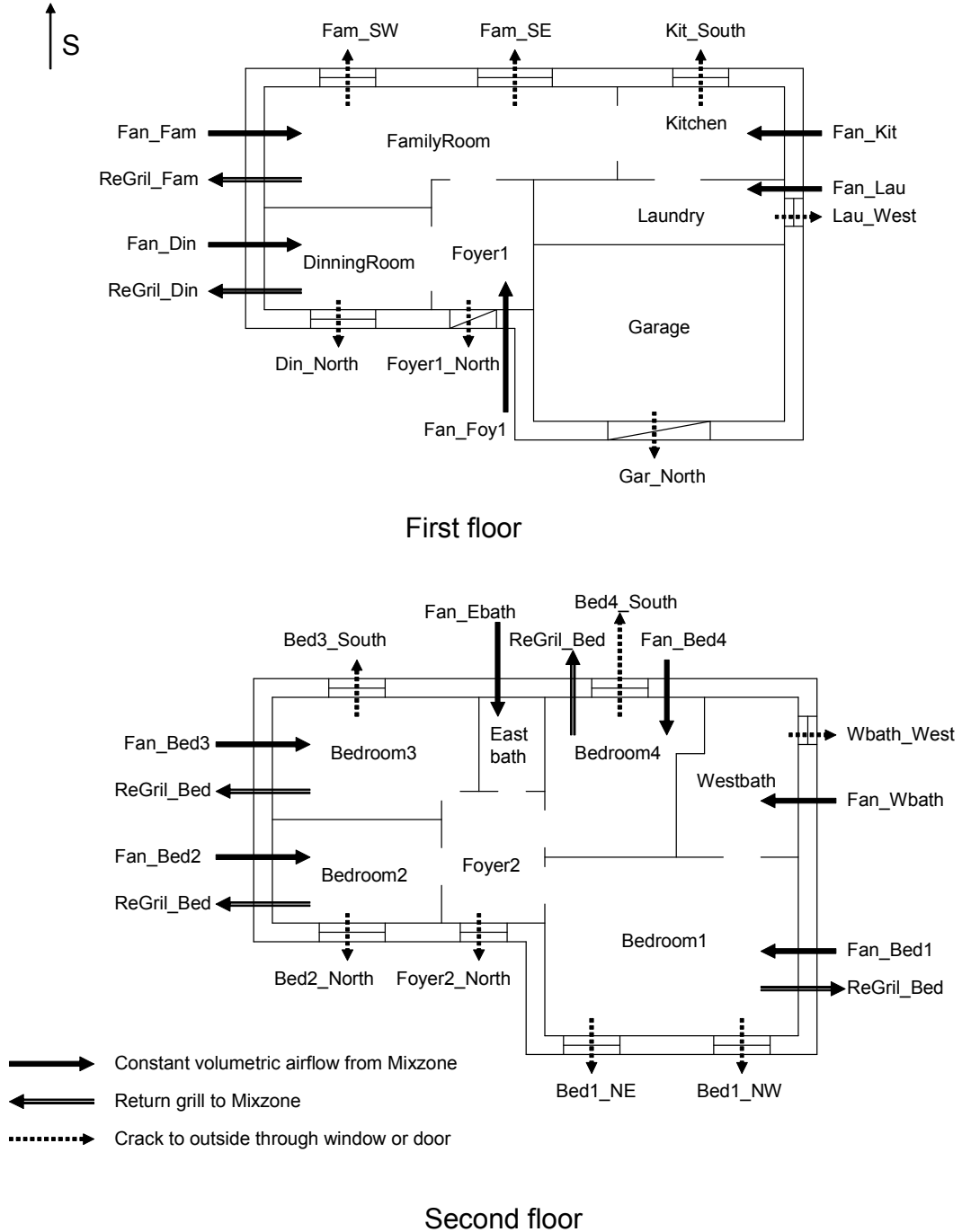


Figure 6-15. Schematic representation of the ESP-r airflow network for the first and second floor

For infiltration, specific air flow crack components (type 120) were defined to model the house leakage. As shown in the figure, cracks were distributed in the house envelope according to the presence of windows and doors. In addition to the cracks shown in the figure, there were also cracks defined for the basement windows. Attic infiltration was represented by defining specific air flow opening components (type 110).

Inter-zone airflows were modeled by defining specific air flow door components (type 130), representing the doorways between rooms. In addition to the doorways shown in the figure, there was a door defined between the basement and the living room. Two specific air flow opening components (type 110) were defined to represent the stairway between Foyer 1 and Foyer 2, considering the possibility of two-way flows. Also, there were cracks defined between each room on the second floor and the attic, accounting for the cracks introduced by the supply air ducts.

6.4.2 Simulation Component Models

In addition to the interpretation of the house information and experimental data to simulation inputs, there is another aspect of the simulation approach that needs to be considered: the selection of component models. The simulation component models used in the experimental validation are slightly different from those used for the design evaluation mode of the inter-model comparisons (Chapter 4). For readers' convenience, Table 6-7 summarizes the component models used for the simulation results discussed below. (Again, models that have not caused significant discrepancies between ResHB and ESP-r in the detailed studies of the inter-model comparisons were ignored in the table.)

Table 6-7 Component models used in ResHB and ESP-r for experimental validation

Models		ESP-r	RHB	
Solar irradiance	Clear sky solar	ASHRAE clear sky model with Machler/Iqbal revised A, B, and C coefficients (1985)	ASHRAE clear sky model with Machler/Iqbal revised A, B, and C coefficients (1985)	
	Sloped surface incident diffuse solar (i.e. short wave sky model)	Perez (1990, 1987)	Perez (1990, 1987)	
Internal solar distribution		Beam distribution calculated with detailed ESP-r model (by Module <i>ish</i>), diffuse distributed on an area/absorptance weighting basis	Beam on the floor with internal mass surfaces treated as “half floor”, diffuse distributed in proportion to surface area-absorptance product	
External long wave radiation	Clear sky temperature model	Martin and Berdahl (1984)	Martin and Berdahl (1984)	
	Outside ground surface temperature	ESP-r algorithm ¹	Equals outside air temperature	
	Surrounding buildings’ surface temperature	ESP-r algorithm ²	Equals outside air temperature	
	View factor for vertical surfaces	To the sky	0.45	0.35
		To the ground	0.45	0.5
To surrounding buildings		0.1	0.15	
Convection coefficients	Inside	Fixed-Ceiling: 1.25 W/m ² -K (0.22 Btu/hr-ft ² -F) Walls: 4.7 W/m ² -K (0.82 Btu/hr-ft ² -F) Floor: 4.4 W/m ² -K (0.77 Btu/hr-ft ² -F)	Fixed-Ceiling: 1.25 W/m ² -K (0.22 Btu/hr-ft ² -F) Walls: 4.7 W/m ² -K (0.82 Btu/hr-ft ² -F) Floor: 4.4 W/m ² -K (0.77 Btu/hr-ft ² -F)	
	Outside	Fixed-12.5 W/m ² -K (2.2 Btu/hr-ft ² -F)	Fixed-12.5 W/m ² -K (2.2 Btu/hr-ft ² -F)	
	Elevation adjustment	No	No	
Conduction	Conduction methods	Finite volume method	Conduction Transfer Function method (CTF method)	
	Inter-zone conduction	Modeled in detail, inter-zone partition modeled as is	Not modeled, inter-zone partition modeled in half thickness with adiabatic outside condition	
Simulation time step		Minutely	Hourly	

^{1,2} Algorithms as described in Table 4-5, Chapter 4.

6.4.3 Comparisons Made

There are basically two types of comparison made between ResHB/ESP-r simulation results and measured data. Firstly, the ResHB/ESP-r simulated hourly total house cooling load was compared to the measured hourly total house cooling load. The ResHB simulated hourly total house cooling load was obtained by summing up the hourly cooling load for each room, which was directly reported by the ResHB simulation result. To get the simulated hourly total house cooling load by ESP-r, the minutely system sensible cooling output for each room was first estimated as the product of the volume airflow rate from the mixing zone to each room (representing the system airflow rate to each room), the air density ($\rho=1.235 \text{ Kg/m}^3$) and specific heat ($c_p=1.004 \text{ KJ/kg.K}$), and the temperature difference between the mixing zone and each room (representing the difference between the system supply and return air temperature, ΔT). The minutely mixing zone temperature, room temperature, and volume airflow rate from the mixing zone to each room were directly reported by the ESP-r simulation result. The minutely system sensible cooling output for each room was then summed and hourly averaged to obtain the hourly total house cooling load in ESP-r.

Secondly, the ResHB/ESP-r calculated hourly room temperatures were compared to the measured hourly room temperatures. There were three types of room temperatures compared: the master room temperature, the slave room temperatures, and the temperatures in the unconditioned space (attic). Details of the comparison result are discussed in the results section below.

6.5 Results

This section discusses the comparisons between ResHB/ESP-r simulation results and experimental data. As in any validation study, there was actually a diagnostic process involved in the comparisons. Intermediate results produced during this diagnostic process helped to draw the final conclusions. Therefore, the discussion below was organized to gradually show this diagnostic process, presenting both the intermediate and final results. Finally, some sensitivity analysis results were included for the purpose of uncertainty analysis.

6.5.1 Inter-zone Airflow

As mentioned earlier, the inter-zone air mixing caused by the inter-zone airflow was very obvious in the experimental house. Evidence observed directly from the measured room temperatures has been discussed in the simulation approach section. Further evidence from simulation results is shown below in Figure 6-16. There are four simulated total house cooling loads compared to the measured loads in this figure: ESP-r simulated loads with and without inter-zone airflow and ResHB simulated loads with and without internal heat gain and ventilation distribution. For these simulation results, ideal control was used both in ResHB and ESP-r, with a 23.89 °C cooling set point in every conditioned room. As described earlier, inter-zone airflow was considered in the airflow network setup in the ESP-r simulation. (Note that the airflow network used for the ESP-r result with inter-zone airflow shown in this figure was a simplified version of the one described in the simulation input section, with the corresponding parts representing the air conditioning system eliminated, as an ideal load calculation was done for this case.) In

ResHB, inter-zone airflow was approximately accounted for by the area-weighted distribution of internal heat gain and ventilation.

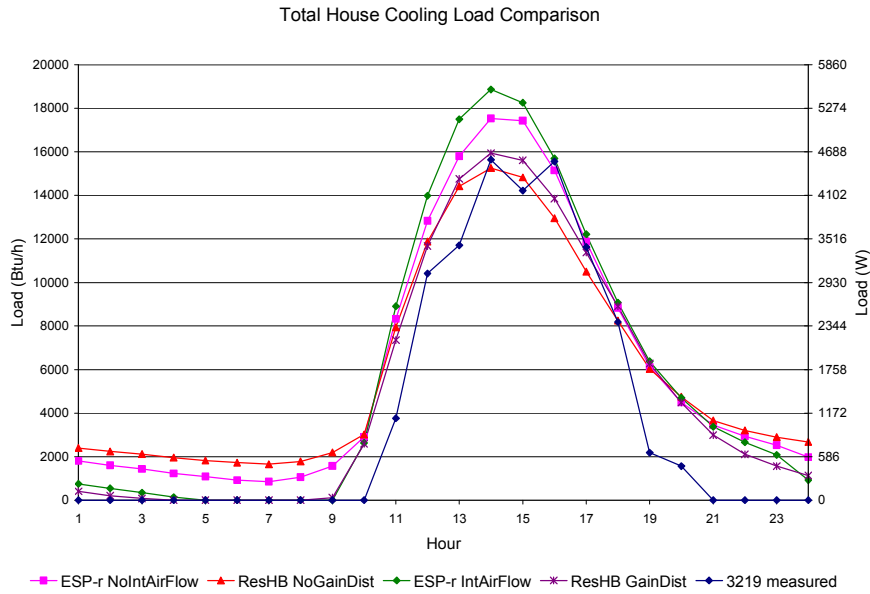


Figure 6-16. Simulated and experimental total house cooling load comparison: ESP-r with/without inter-zone airflow, ResHB with/without internal heat gain and ventilation distribution

As can be seen in the figure, without accounting for inter-zone airflow in the simulations, both ESP-r and ResHB predicted loads never fall to zero during the hours when there is no measured load. While there may be several reasons involved here, not considering inter-zone airflow in the simulation at least contributes partly to the continuing loads predicted by both programs in the early morning hours. During these hours, internal heat gain becomes the primary load source of the house. A look into the individual room load predictions in the simulation shows that most of the early morning loads predicted are from the kitchen and the master bedroom, where the electric heaters producing internal heat gains were located. In the real house, air mixing caused by inter-

zone airflows transferred the loads in these rooms to adjacent rooms, where the room temperatures may be well below the set point. Relatively speaking, the adjacent rooms can act as a heat sink of the internal heat gains from the heated rooms, so that no cooling loads are expected for the whole house. If inter-zone airflow was considered in the simulation, the ResHB/ESP-r predicted loads should literally come to zero at least for a few hours. As shown in Figure 6-16, with inter-zone airflow accounted for in the simulations, both ESP-r and ResHB predicted loads drop to zero (or very small values) during the early morning hours, which is in agreement with the measurements and the analysis made above. (Again, in ResHB, the inter-zone airflow is accounted for by distributing the internal heat gains to adjacent rooms.)

Note that both the ResHB and ESP-r predicted peak loads increase after the inter-zone airflow was considered in the simulation, with the difference between predicted and measured peak load changing from -2.5% to 1.9% for ResHB, and from 12.1% to 20.6% for ESP-r. The ESP-r predicted peak load gets worse when accounting for inter-zone airflow, but better results will be presented after additional refinements are made to the simulation. As will be discussed in section 6.5.4, a better match between ESP-r predicted and measured peak load can be obtained with the system control properly approximated in the ESP-r simulation.

Based on the improvement in the predicted loads during the early morning hours due to including the inter-zone airflow in the simulations, inter-zone airflow was accounted for in the subsequent simulations presented below.

6.5.2 Master-slave Control

As mentioned before, the air conditioning system control in the experiment was based on a single master room temperature – the dining room air temperature. This control strategy was selected for the purpose of testing the master-slave control modeling implemented in RHB. As explained in the literature review, RHB handles the master-slave control by its temperature swing algorithm. By definition, a slave room has the same air supply flow rate profile as its master. In a ResHB simulation with master-slave control specified, the peak slave room supply air volume flow rate is set such that the maximum room temperature does not exceed the set point (plus allowed swing if any). Then the slave room flow rates for all hours are set by applying the master room profile.

To test this algorithm, ResHB simulations using master-slave control were firstly done with the master room selected as the dining room, which was also the master room set in the experiment. A few temperature swings (0.0, 0.2, 0.4, 0.6, 0.8 °C) in combination of a 23.89 °C master room set point were tried in the simulation, considering the upper limit of the experimental dead band control was 24.7 °C (0.8 °C above set point 23.89 °C). Figure 6-17 compares the simulated total house cooling loads to the measured load. We see that overall there is a big over-prediction of total house cooling load by the simulation, although permitting some temperature swing in the simulation results in a significant reduction in cooling load prediction (as demonstrated in the ASHRAE 1199RP final report (Barnaby et al. 2004)). The difference between the predicted peak load and measured peak load ranges from 28.3% (the case with 0.8 °C temperature swing) to 70.2% (the case with zero temperature swing).

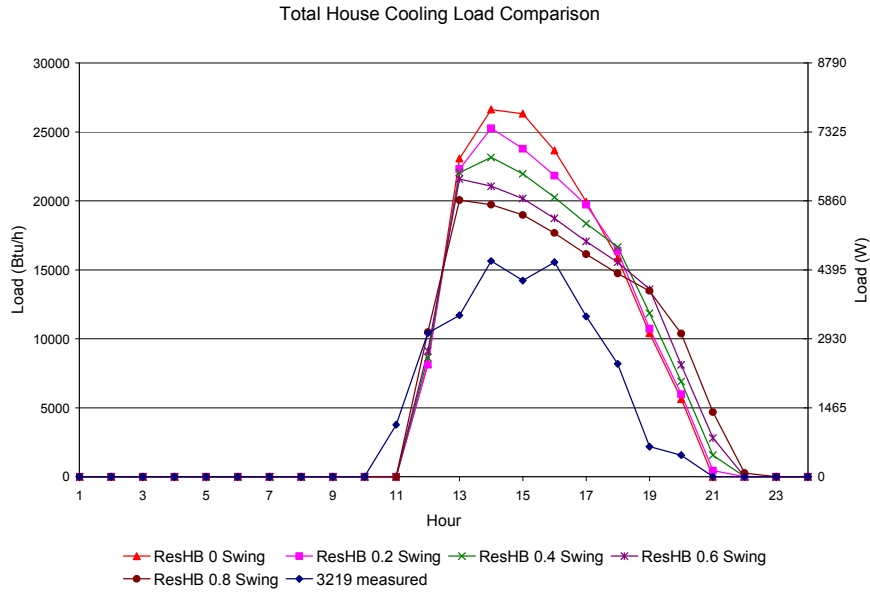


Figure 6-17. Simulated and experimental total house cooling load comparison: ResHB with dining room specified as master room, fixed set point of 23.89 °C with 0.0, 0.2, 0.4, 0.6, 0.8 °C temperature swing, with internal heat gain and ventilation distribution

Figure 6-18 compares the simulated room temperatures in the dining room (master room) and living room (a representative slave room) to the corresponding measured room temperatures. We see that the simulated temperature response in the master room (Figure 6-18(a)) is acceptable both from the point of view of matching the experimental data and according to the controls set for the master room in the simulation. During the cooling hours, the simulated dining room temperature has a maximum drift above the set point as the specified temperature swing, with the maximum difference from measured temperature ranging from 0.45 °C (for the zero swing case) to 0.86 °C (for the 0.8 °C swing case). At other hours when there is no cooling load, it floats below the set point, with a maximum difference from measured values within 1.10 °C.

The simulated temperatures in the slave room (Figure 6-18(b)), however, are significantly different from the measured temperatures, although they are consistent with the RHB master-slave control algorithm. The simulated living room temperatures are below the measured temperatures all the time except at 11:00 a.m., with the maximum difference ranging from 8.65 °C (for the 0.8 °C swing case) to 9.86 °C (for the zero swing case). The living room is uncomfortably sub-cooled especially during the cooling hours, which is understandable as the living room (facing south) has significantly different load profile from the dining room (facing north) and the simulation applies the dining room supply air flow rate profile to the living room.

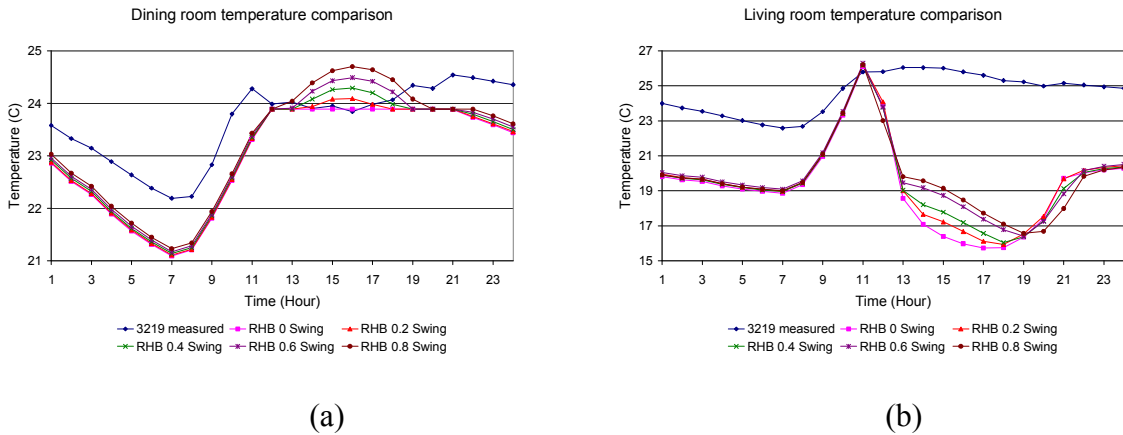


Figure 6-18. Simulated and experimental room temperature comparison, ResHB with dining room specified as master room, fixed set point of 23.89 °C with 0.0, 0.2, 0.4, 0.6, 0.8 °C temperature swing, with internal heat gain and ventilation distribution: (a) Dining room (b) Living room

As there is a significant over-sizing in the load prediction and a significant discrepancy between the predicted and measured slave room temperatures in the above simulation, there is a question of whether the RHB master-slave control algorithm is appropriate for design load calculation. Considering the fact that neither inter-zone

conduction nor inter-zone airflow are modeled in RHB and the way that the master-slave control is handled by RHB, it is probably not appropriate to use the RHB master-slave control option for design load calculation purposes. Imagine that if a room with very insignificant loads (literally zero loads) or a room with more diverse load profile was used as the master room in the RHB simulation, the predicted load difference and room temperature discrepancy may become even worse. On the other hand, if a room with a load profile close to the total house load profile was selected as the master room in the simulation, the predicted load difference and room temperature discrepancy may become better, as shown in the simulations discussed below.

There were a series of ResHB simulations done with the master-slave control option. For each case, a different conditioned room was specified as the master room. The master room set point was scheduled with the method described for ResHB in the simulation input section: it equals the corresponding experimental hourly average room air temperature during the cooling hours and free floats during other hours. As the master room set point was fitted to be the corresponding experimental room temperature, zero temperature swing was used in the simulation.

For representative cases in this series (with the master room specified as the dining room, living room, foyer 1 and bedroom 2), Figure 6-19 compares the corresponding simulated total house cooling loads to the measured load. We see that for the case with dining room as master room, the predicted total house cooling load is significantly higher than measured load, with 84.8% peak load difference. Compared to a similar case discussed in Figure 6-17 (with fixed 23.89 °C set point and zero temperature

swing in the dining room), this case has higher total house cooling load prediction as a result of the change in the master room set point. For the case with foyer 1 as master room, the cooling load over-prediction becomes even worse: the peak load difference reaches 114.9% (the worst over-prediction case). Also in this case, the predicted load shape is far different from the measured load shape: the measured load starts at 11:00 a.m. and ends at 8:00 p.m. while the predicted load starts at 4:00 p.m. and ends at 6:00 p.m. Besides the over-predicting cases, there are cases that under-predict cooling load. The case with bedroom 2 as master room is an extreme example of the under-predicting cases: the predicted total house cooling loads are always zero (which is incorrect), as there is no cooling load predicted for bedroom 2 in ResHB.

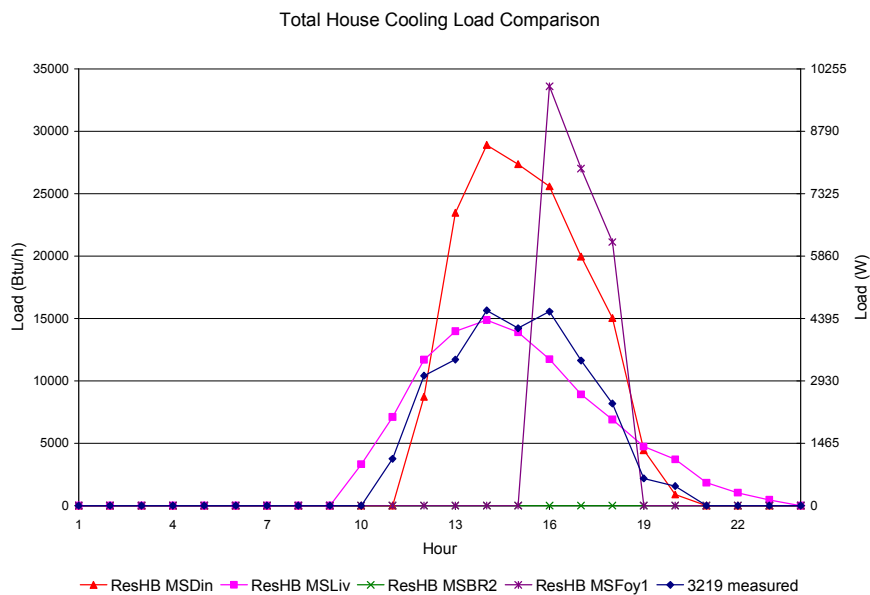
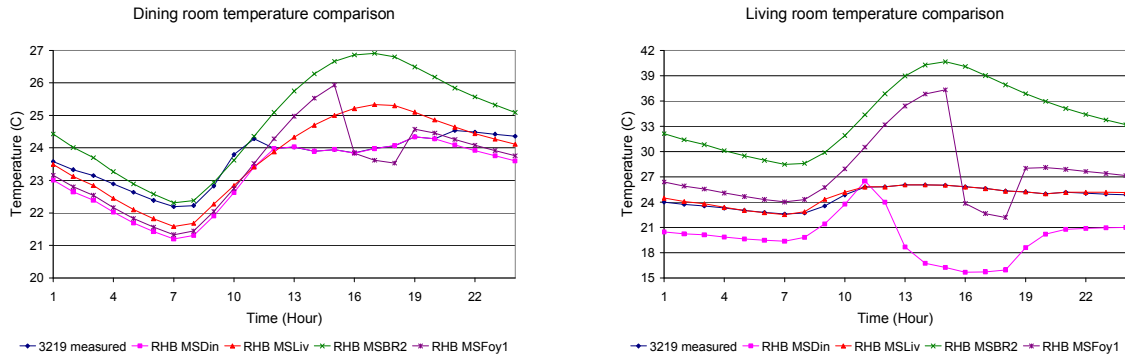


Figure 6-19. Simulated and experimental total house cooling load comparison: ResHB with master room specified as dining room, living room, Foyer 1 and bedroom 2, master room uses experimental hourly average room air temperature as set point without temperature swing, with internal heat gain and ventilation distribution

On the other hand, the case with living room as master room predicts cooling load that is much closer to measured load: the peak load difference is only -4.9% and the maximum hourly load difference is -24.4% of the measured peak load. Compared to the case using foyer 1 or bedroom 2 as master room, the predicted load shape for this case has a better match with the measured load shape. Obviously, the case with living room as master room has a better load prediction. Presumably, this is because the living room produces a big part of the total house cooling load (with two big windows on its south facade) and hence has a load profile closer to the total house load profile than other rooms.

For the same simulation cases discussed above (with cooling loads compared in Figure 6-19), Figure 6-20 compares the corresponding simulated room temperatures for two representative rooms (the dining room and living room) to the measured room temperatures. Compared to the master room temperatures discussed in Figure 6-18, the simulated master room temperatures in this figure (dining room temperature when dining room was master room in Figure 6-20(a) and living room temperature when living room was master room in Figure 6-20(b)) have some improvement during the cooling hours. At these hours, the simulated master room temperature exactly matches the experimental value, as specified by the master room set point schedule. At other hours when there is no cooling load, it floats below or above the measured room temperature, with a maximum difference from measured values of 0.99 °C for the dining room and of 0.81 °C for the living room. This is again considered to be acceptable both from the point of view of matching the experimental data and according to the controls set for the master room in the simulation.



(a)

(b)

Figure 6-20. Simulated and experimental room temperature comparison, ResHB with master room specified as dining room, living room, Foyer 1 and bedroom 2, master room uses experimental hourly average room air temperature as set point without temperature swing, with internal heat gain and ventilation distribution: (a) Dining room (b) Living room

The simulated temperature in the slave rooms (dining room temperature when dining room was not master room in Figure 6-20(a) and living room temperature when living room was not master room in Figure 6-20(b)) is actually more complicated and more interesting. When dining room was the master room, the simulated temperature response in the slave room is similar to that of a case discussed in Figure 6-18 (with fixed 23.89 °C set point and zero temperature swing in the dining room): the simulated living room temperature is below measured temperature all the time except at 11:00 a.m., with a maximum difference of 10.14 °C. The living room is uncomfortably sub-cooled especially during the cooling hours, due to the significant difference between the dining room and living room load profiles.

When foyer 1 was the master room, the simulated slave room temperature is higher than the experimental value when predicted cooling load is zero but measured load

is not (the living room is uncomfortably over-heated during these hours). It is lower than the experimental value when both predicted and measured load is non-zero. When both predicted and measured loads are zero, the dining room temperature is lower and the living room temperature is higher than the experimental value. The maximum difference between the predicted and measured room temperature is 1.98 °C for the dining room and 11.32 °C for the living room.

When bedroom 2 was the master room, the simulated slave room temperature is basically higher than the experimental value, with a maximum difference of 3.02 °C for the dining room and 14.63 °C for the living room. The simulated slave room temperature is higher because no cooling load is predicted for this case (but in reality there is cooling load) and the room temperatures are free floating in the simulation. In this case, the discrepancy between the predicted and measured slave room temperatures is the worst and the living room is uncomfortably over-heated especially during the cooling hours.

Note that for all three cases discussed above, there is significant discrepancy between the predicted and measured slave room temperatures, especially the living room is either uncomfortably sub-cooled or over-heated. On the other hand, when the living room was used as the master room, the simulated slave room (dining room) temperature is much closer to the measured temperature. Compared to the cases with foyer 1 or bedroom 2 as master room, the discrepancy between the predicted and measured slave room temperatures in this case is the smallest, with a maximum difference of 1.37 °C.

Both the total house cooling load comparisons shown in Figure 6-19 and the room temperature comparisons shown in Figure 6-20 indicate that using the RHB master-slave control modeling for design load calculation may lead to significant error in cooling loads. The more different the master room load profile is from the rest of the house, the higher the error. Due to the fact that neither inter-zone conduction nor inter-zone airflow is modeled in RHB and in view of the way that the master-slave control is handled by RHB, it does not seem appropriate to directly use the RHB master-slave control option for design load calculation purposes.

From the study results, it might be inferred that reasonable cooling load predictions are possible with the master-slave control if the room with thermostat has a load profile that is very close to the rest of the house. However, in a design load calculation there is no experimental data or other model results to compare against, so it is impossible to confirm that the room with the thermostat has a sufficiently close load profile. Barnaby et al. (2005) suggested that simulation with the RHB master-slave control may allow the identification of zoning problems. While this seems likely, it has not been investigated in this work and further investigation would be needed to prove (or disprove) its usefulness in this regard. In the ResHB results discussed below, ideal control was used instead of master-slave control.

6.5.3 Ideal Control

The ResHB ideal control option, which can be used directly for design cooling load calculation, permits the user to specify a fixed set point with or without temperature swing. When using this ideal control option in the ResHB simulation, a fixed set point of

23.89 °C was specified for every conditioned room, with 0.8 °C temperature swing specified to account for the dead band control involved in the experiment. This set point and temperature swing was selected as the best match to the temperature control used in the experiment, which has a 23.89°C set point in the middle of a 1.67°C dead band, as explained in Section 6.4.1.6. However, as will be explained later, the ideal control strategy is not an exact representation of the experimental control strategy.

Figure 6-21 compares the simulated total house cooling loads to the measured load. In addition, the ResHB-predicted cooling loads with 0°C swing are also plotted. Overall, both sets of ResHB loads match the actual cooling load reasonably well, but the 0.8°C swing loads under-predict the actual peak loads by 11%, while the 0°C swing loads over-predict the actual peak loads by 2%. As will be explained later, this is primarily due to the fact that the ideal control strategy is not an exact representation of the experimental control strategy. ResHB with 0.8°C swing over-predicts the total daily cooling load by 26.9%. With 0°C swing, it over-predicts by 28.0%. Note that the difference between the simulated and measured load during the off-peak load hours can be significantly affected by the infiltration rate, as will be discussed in the sensitivity analysis section. Also note that the most important factor considered in a design cooling load calculation is the peak load, not the off-peak loads.

There is one obvious difference regarding when the load begins and stops. The experimental load begins at 11:00 a.m. and ends at 8:00 p.m. The ResHB predicted loads begin at 9:00 a.m. and end at 3:00 a.m., although the loads are relatively small during the hours when the experimental load is zero. Again, as will be demonstrated later, the

difference in start/stop times is related to the difference between the ideal control strategy and the actual control strategy.

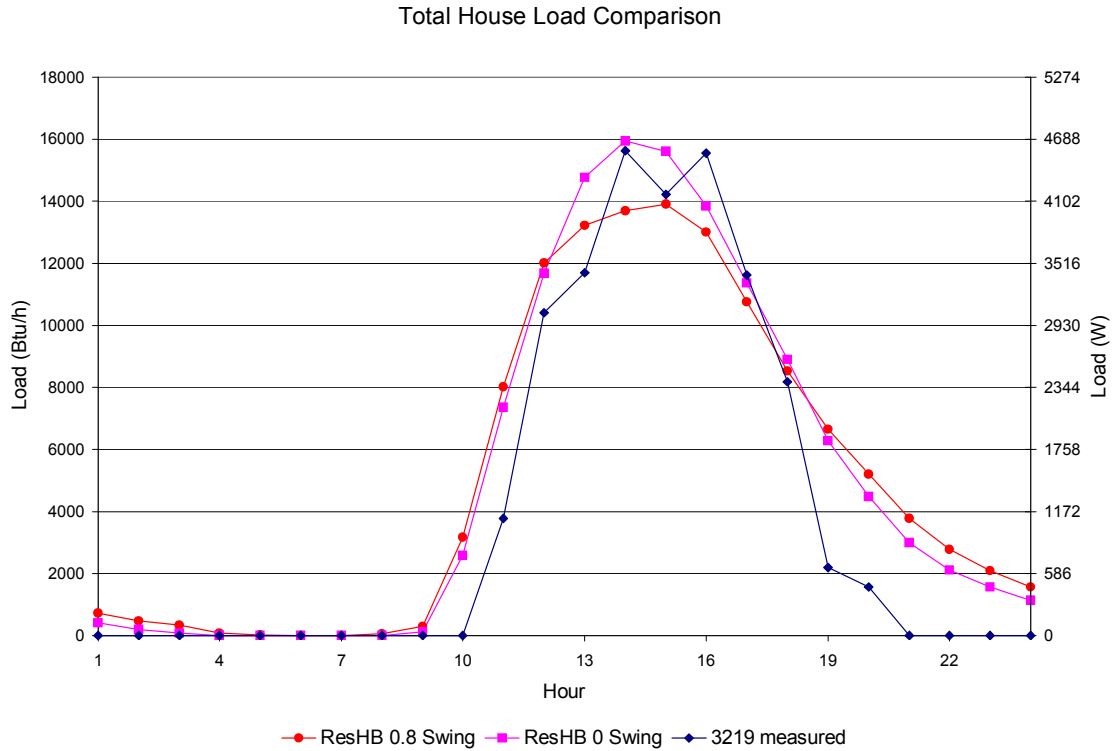


Figure 6-21. Simulated and experimental total house cooling load comparison: ResHB uses ideal control, every room uses fixed set point of 23.89 °C with 0.8 °C or 0.0 °C temperature swing, with internal heat gain and ventilation distribution

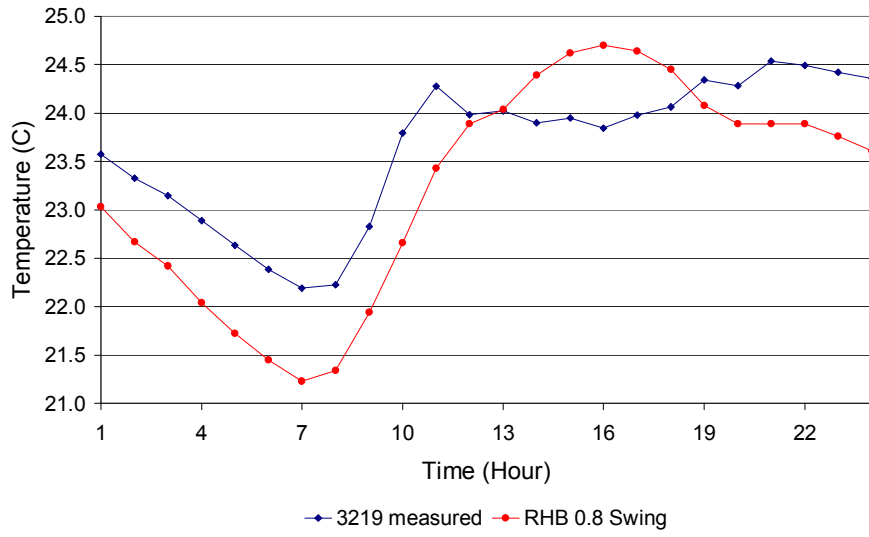
Figure 6-22 compares the simulated room temperatures to the measured room temperatures for three representative rooms (the dining room, the kitchen and bedroom 3). As can be seen in Figure 6-22a, the net effect of the experimental house control strategy is that the master room is, on average, controlled to near 23.89°C during the peak cooling load hours, but the temperature is allowed to float up to 24.69°C (23.89 °C + 0.8°C) during the off-peak hours. Contrarily, in ResHB, the ideal control strategy tends

to keep the temperature near to 23.89 °C (or lower) during the off-peak hours, but allows it to swing up during the on-peak hours. For the slave rooms (Figure 6-22b and 6-22c) there are a number of evening hours where the ResHB ideal control strategy holds the room temperature right at 23.89°C, while in the experiment, the room temperatures drift to higher levels. The difference in the two control strategies results in a lower peak load and higher off-peak loads for ResHB. Another way of looking at it is that lower off-peak room temperatures of the ResHB ideal control strategy effectively results in “cool storage” within the rooms and has the effect of damping the cooling load in the hours from 2 p.m. to 6 p.m.

Accordingly, as shown in Figure 6-21, the actual cooling load is bracketed by the ResHB with 0.8 °C swing and ResHB with 0 °C swing. However, the 0 °C swing case overpredicts, because it allows no swing, while the actual control strategy allows swing during the off-peak hours. In fact, the actual swing cannot be replicated by the ResHB ideal control strategy exactly, regardless of the setpoint and swing settings.

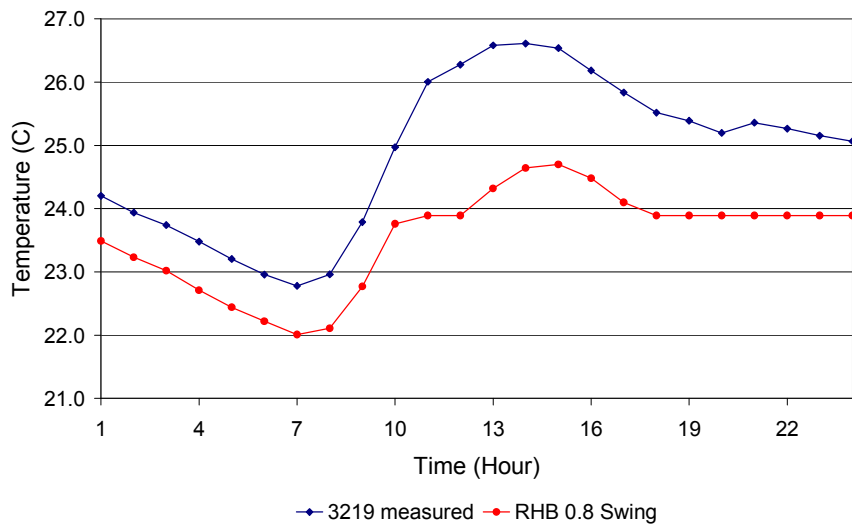
This can be better demonstrated by customizing the ideal control strategy in such a way as to more closely match the actual control strategy. This will be done by using time-varying set points for each room, which exactly match the experimental hourly average room temperatures during hours when the system is on. When the system was off, the temperatures were allowed to float freely. Although this cannot be done in practice for cooling load calculations, it does demonstrate that much of the under-prediction (with the 0.8°C swing) or over-prediction (with the 0°C swing) is caused by the mismatch between the ResHB control strategy and the actual control strategy.

Dining room temperature comparison

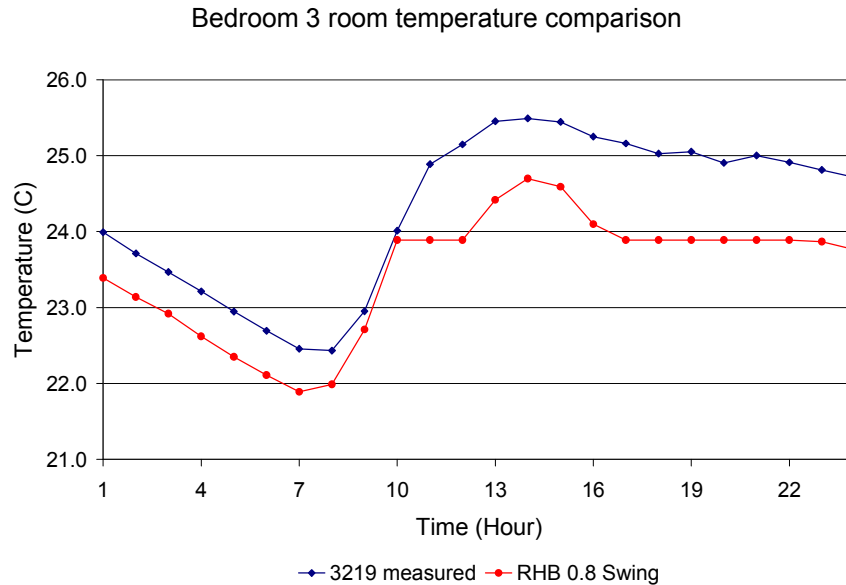


(a)

Kitchen room temperature comparison



(b)



(c)

Figure 6-22. Simulated and experimental room temperature comparison, ResHB uses ideal control, every room uses fixed set point of 23.89 °C with 0.8 °C temperature swing, with internal heat gain and ventilation distribution: (a) Dining room (b) Kitchen (c) Bedroom 3

Figure 6-23 compares the ResHB predicted total house cooling loads with 0.8 °C swing, 0 °C swing and hourly-varying setpoints (“fitted setpoint”) to the measured loads. The improvement in cooling load prediction is quite significant – with fitted setpoints, ResHB overpredicts by 0.3%; the total cooling load is overpredicted by 11.8% and the start/stop times are matched correctly.

Correspondingly, Figure 6-24 compares the ResHB predicted room temperatures with 0.8 °C swing and hourly-varying setpoints (“fitted setpoint”) to the measured room temperatures for the three representative rooms (the dining room, kitchen and bedroom 3) shown in Figure 6-22. We see that when the fitted setpoints are used, the ResHB temperatures match the experimental room temperatures more closely. When the system

is on (Hours 11:00 a.m. to 8:00 p.m.), the simulated room temperatures exactly match the measured room temperatures, as defined. At other hours, the simulated room temperatures are generally much closer to the measured room temperatures than those with the ideal control option.

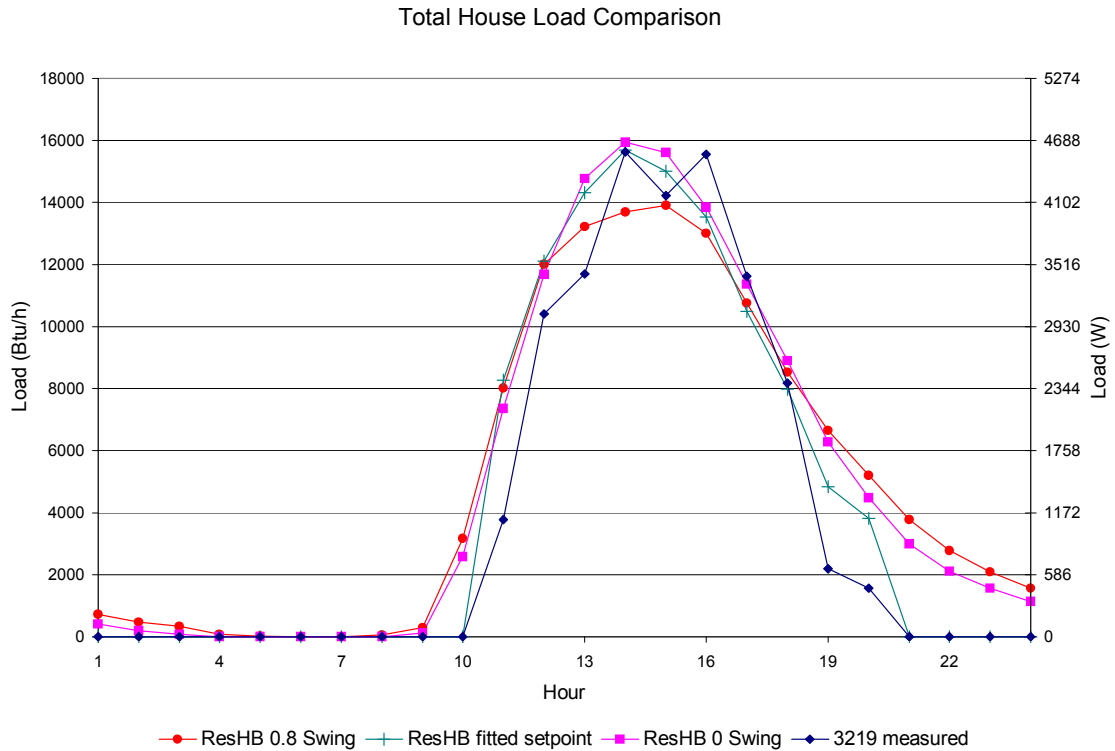
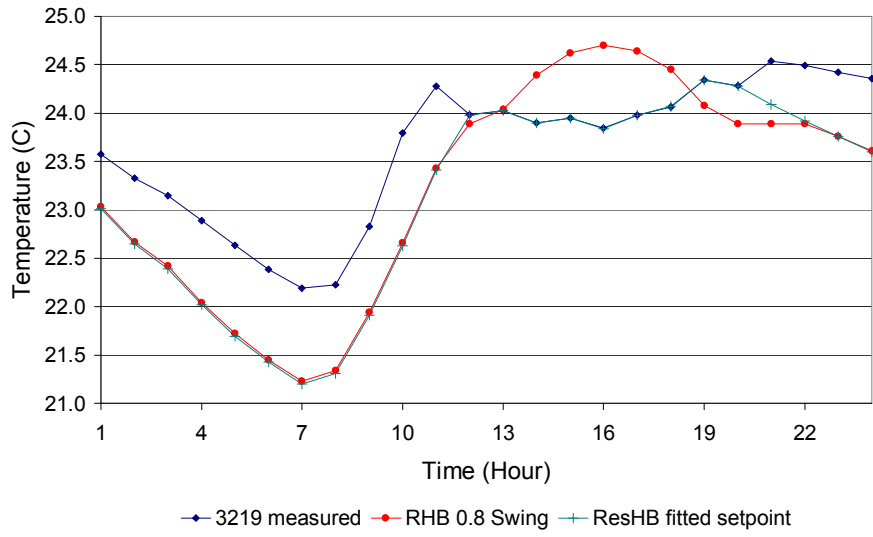


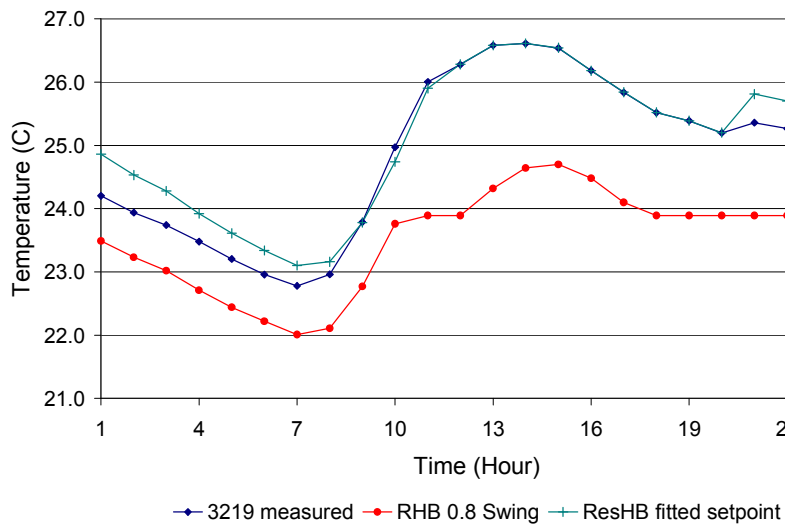
Figure 6-23. Simulated and experimental total house cooling load comparison: ResHB uses ideal control, every room uses fixed set point of 23.89 °C with 0.8 °C or 0.0 °C temperature swing or every room uses experimental hourly average room air temperature as set point without temperature swing, with internal heat gain and ventilation distribution

Dining room temperature comparison

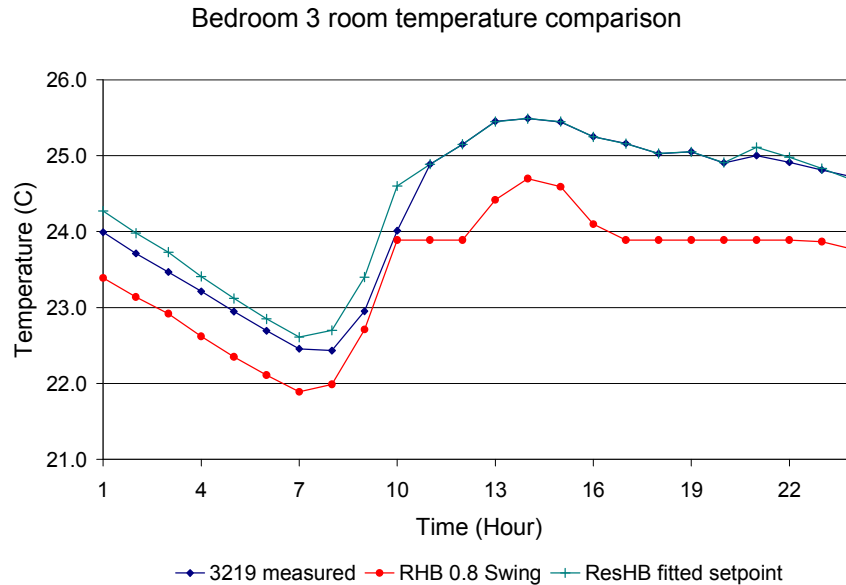


(a)

Kitchen room temperature comparison



(b)



(c)

Figure 6-24. Simulated and experimental room temperature comparison, ResHB uses ideal control, every room uses fixed set point of 23.89 °C with 0.8 °C temperature swing or every room uses experimental hourly average room air temperature as set point without temperature swing, with internal heat gain and ventilation distribution: (a) Dining room (b) Kitchen (c) Bedroom 3

Both the cooling load comparison in Figure 6-23 and the room temperature comparison in Figure 6-24 indicate that significant improvement can be achieved with fitted setpoints. While this option is not applicable to general design cooling load calculations, it does help to confirm that the ideal control strategy is the limiting factor in matching the experimental cooling loads, and that the overall performance of the heat transfer models is satisfactory. Furthermore, this demonstrates the significant sensitivity of the design cooling load to the temperature swing. The fact that the actual cooling load was bracketed by the two ideal control options suggests that further refinement of the ideal control strategy in ResHB would be a fruitful topic for further research.

6.5.4 ResHB and ESP-r Result Comparison

The above two sections have been focused on discussing the ResHB simulation results using the RHB master-slave control and ideal control options. No ESP-r results have been discussed in the above two sections, as there was no issue with selecting master-slave or ideal control on the ESP-r side. The system control was modeled in a different way in ESP-r: using the airflow network under master-slave on-off control, as described in the simulation input section. The airflow network option is adopted in ESP-r as it could model (approximately) the experimental master-slave control and it gave reasonable results from the start. (The ideal control option was adopted in the ResHB simulation after the RHB master-slave control option had been tried and was considered inappropriate for direct use in design cooling load calculations.) In this section, both the ResHB simulation results using the ideal control option and the ESP-r simulation results using the airflow network under master-slave on-off control are compared to the experimental data.

Figure 6-25 compares the ResHB and ESP-r simulated total house cooling loads to the measured loads. ESP-r gives a much closer match to the overall load profile, though it over-predicts the peak cooling load by 7.6%. This can be attributed to the fact that ESP-r can more closely match the actual hourly average room temperatures, simply by choosing the setpoint for the master room to mimic the actual control – a setpoint of 23.95°C during the hours when the system was on and 24.6°C when the system was off. These setpoints were chosen as an approximation to the actual system control results rather than the actual system control setpoints. Other than choosing the master room setpoints, the system operation and all other temperatures were determined by the

simulation. This was only possible because of the capability for modeling interzone airflow and interzone conduction heat transfer.

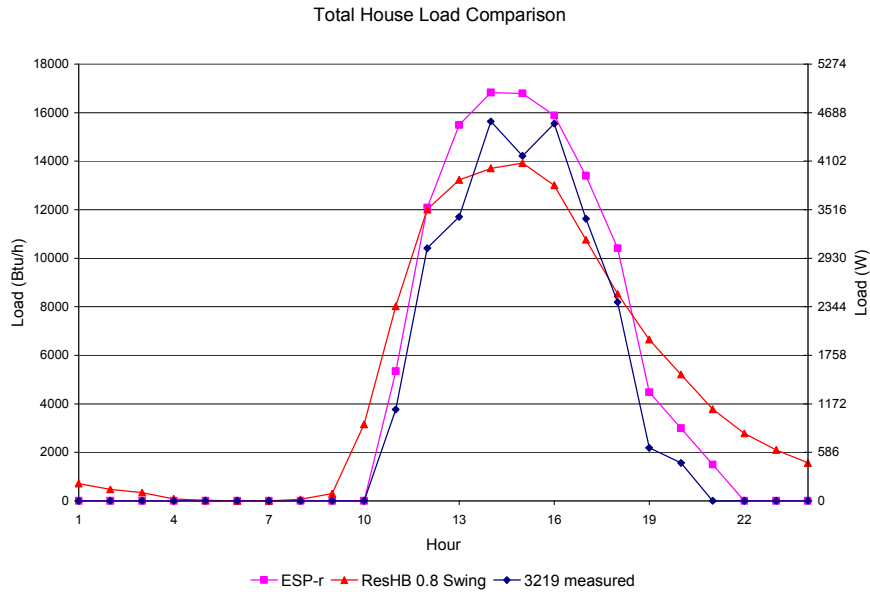


Figure 6-25. Simulated and experimental total house cooling load comparison: ResHB uses ideal control, every room uses fixed set point of 23.89 °C with 0.8 °C temperature swing, with internal heat gain and ventilation distribution; ESP-r models system control with airflow network under master-slave on-off control

Figure 6-26 shows the minutely experimental and ESP-r simulated dining room (master room) temperatures. As can be seen, the overall temperature trend is quite close, but the actual system temperatures vary more than the ESP-r system temperatures. Presumably, this could be improved by adjusting the ESP-r time step and/or adding a deadband control to ESP-r, but this was not investigated further. Figure 6-27 shows a comparison of the hourly average room temperatures for three rooms. For both the master room (the dining room) and a typical slave room (the kitchen) ESP-r shows better temperature agreement. The third room is the attic, and both models give reasonably

good matches, with ESP-r giving better results at night and ResHB giving better results in the morning hours. However, as the attic is isolated from the rest of the house by a thick layer of insulation, the differences in attic temperatures has little impact on the cooling loads calculated.

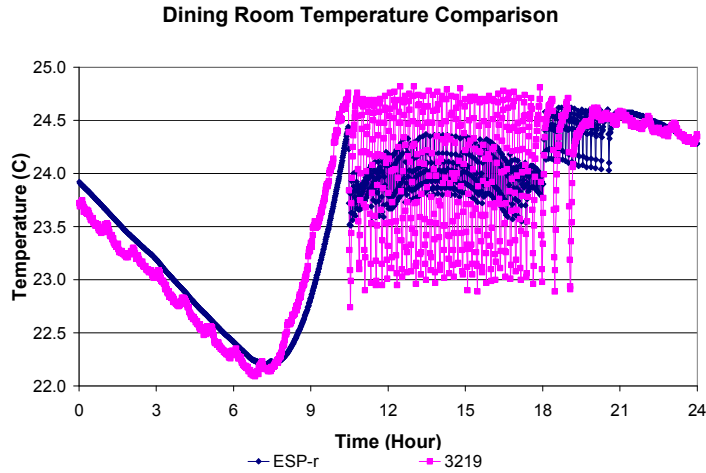
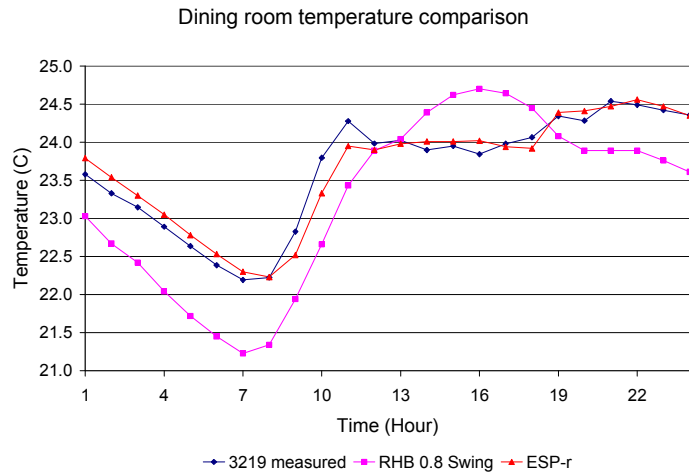
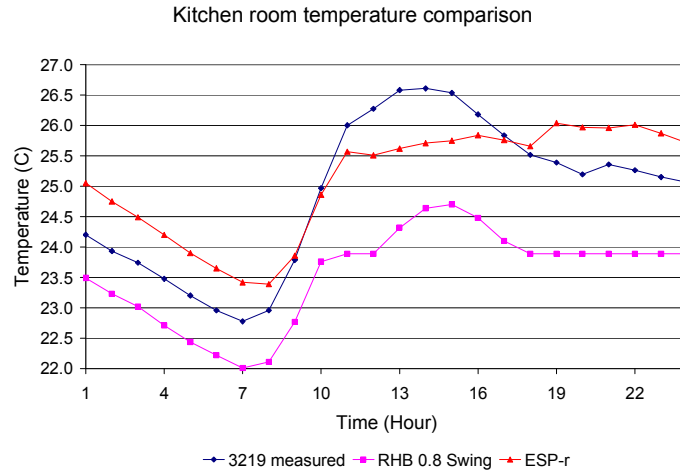


Figure 6-26. Minutely ESP-r simulated and experimental dining room (master) temperature comparison:

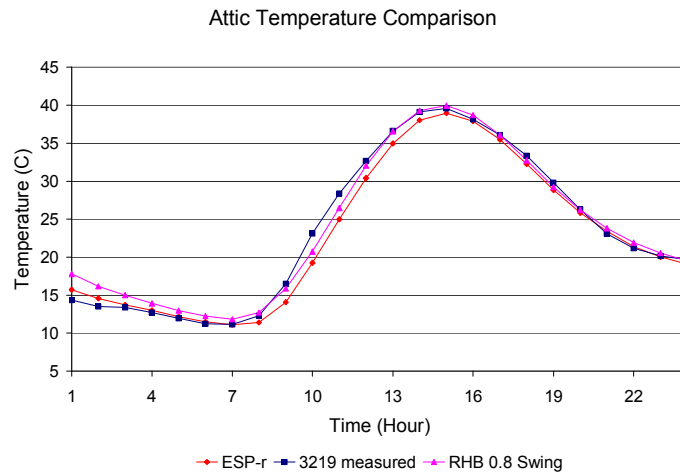
ESP-r models system control with airflow network under master-slave on-off control



(a)



(b)



(c)

Figure 6-27. Simulated and experimental room temperature comparison: ResHB uses ideal control, every room uses fixed set point of 23.89 °C with 0.8 °C temperature swing, with internal heat gain and ventilation distribution; ESP-r models system control with airflow network under master-slave on-off control: (a) Dining room (b) Kitchen (c) Attic

6.5.5 Uncertainty Analysis

The uncertainty of the results discussed above comes from two aspects: one is the uncertainty in the simulation inputs and the other is the uncertainty in the experimental

measurement. Both the simulated and measured cooling loads are functions of many factors. Each factor may include some uncertainty that contributes to the final uncertainty. The uncertainty analysis discussed here does not intend to cover every possible factor, but to give an idea of how much uncertainty could result from some input uncertainties. The uncertainties considered for simulation inputs are the overall U-factors of the building fabric (roof, external wall and floor), the SHGC (Solar Heat Gain Coefficient) of the fenestration, the outside solar absorptance of the external wall, and the infiltration rate. The uncertainties considered for experimental measurements are the total volume airflow rate at the air handler and the difference between the system supply and return air temperatures (ΔT). A significant uncertainty not covered here is the system control modeling described in the last two sections; this is more important than any of the individual uncertainties described in this section. Table 6-8 summarizes the uncertainties resulted from these factors. The comparison of simulated results is based on the ResHB simulation results using fitted setpoints, as presented in section 6.5.3. The error percentage in the peak cooling load is based on the measured peak cooling load.

Table 6-8 Uncertainties resulting from representative simulation inputs and experimental measurements

Uncertainty category	Uncertainty source	Uncertainty	Resulting uncertainty in peak cooling load
Simulation inputs	Overall U-factors of the building fabric	$\pm 5\%$	$\pm 0.3\%$
	SHGC of the fenestration	$\pm 5\%$	$\pm 5.0\%$
	Outside solar absorptance of the external wall	± 0.2	$\pm 2.8\%$
	Infiltration rate	$\pm 0.2\text{ACH}$	$\pm 2.7\%$
Experimental measurements	Volume airflow rate at the air handler	$\pm 3\%$	$\pm 3.0\%$
	Difference between the system supply and return air temperatures	$\pm 0.2^\circ\text{C}$	$\pm 1.8\%$

Note that the sensitivity of the peak cooling load to infiltration rate in this study seems relatively small ($\pm 2.7\%$ in response to ± 0.2 ACH), as the outside air temperature is relatively low (the maximum outside dry bulb temperature is 27.98 °C) during the experiment (09/21/2006). The peak cooling load may show more sensitivity to the infiltration rate under typical summer design conditions, when the outside air temperature is higher (the 1% design maximum outside dry bulb temperature is 30.9 °C at Fort Wayne, Indiana).

Also note that the sensitivity of the hourly load prediction to infiltration rate varies hourly. Figure 6-28 compares the ResHB simulated hourly loads under various infiltration rate (0.2, 0.4, 0.6 and 0.8 ACH) to the measured hourly loads. Generally the simulated hourly load decreases as the infiltration rate increases. The sensitivity of the hourly load to the infiltration rate is greater in the morning hours than in the afternoon hours. The greatest sensitivity is at 11:00 a.m., when the maximum difference between the ResHB simulated and measured hourly load occurs. At this hour, varying infiltration rate by 0.2 ACH has caused 9-11% (based on measured peak load) difference on the predicted load for this hour.

As a fixed infiltration rate was used in the ResHB simulation, the infiltration rate has been assumed to be a constant all through the day, while the real infiltration rate of the house may be changing during the day. The fixed infiltration rate used in the ResHB simulation provides one possible explanation to the relatively large difference between the ResHB predicted and measured cooling load during the off-peak hours, in addition to the system control.

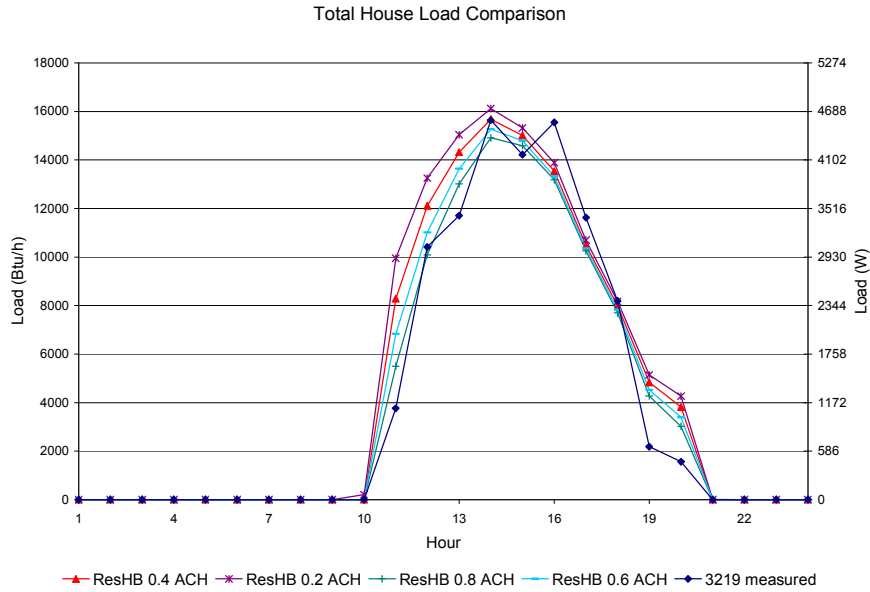


Figure 6-28. Simulated and experimental total house cooling load comparison: ResHB uses ideal control, every room uses experimental hourly average room air temperature as set point without temperature swing, with internal heat gain and ventilation distribution, cases with infiltration rate of 0.2, 0.4, 0.6 and 0.8ACH

The infiltration rate has a significant effect on the room temperatures during the system-off hours, when the room temperatures are free-floating. Figure 6-29 plots the sensitivity of ResHB simulated room temperatures to various infiltration rates (0.2, 0.4, 0.6 and 0.8 ACH) for two rooms: the dining room and the master bedroom. We see that the corresponding simulated room temperatures during the system-off hours change significantly when the infiltration rate varies. Both the simulated dining room temperature and master bedroom temperature decreases as the infiltration rate increases. However, the simulated dining room temperature is closest to the measured temperature when the infiltration rate is the lowest; the simulated master bedroom temperature is closest to the measured temperature when the infiltration rate is the highest. Although not

plotted here, other room temperatures have been found to better match the measured temperatures at either the highest, lowest or other middle infiltration rates.

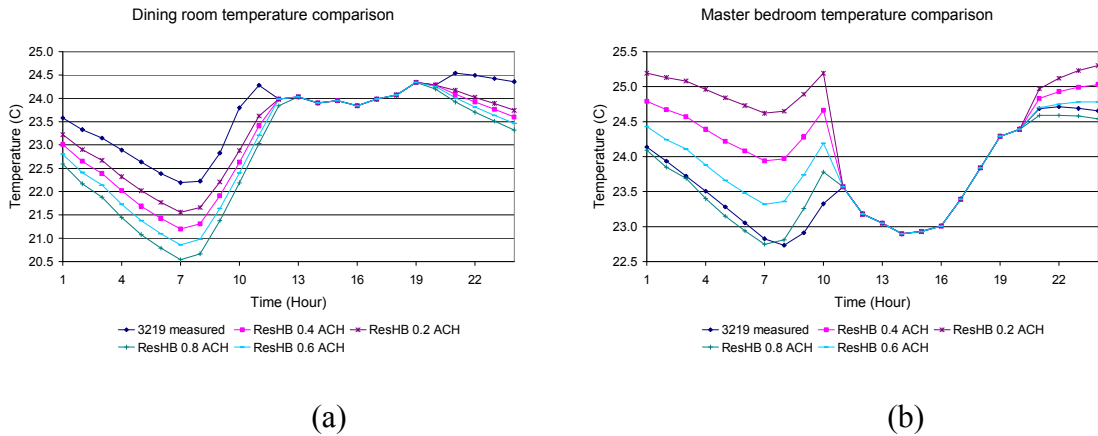


Figure 6-29. Simulated and experimental room temperature comparison: ResHB uses ideal control, every room uses experimental hourly average room air temperature as set point without temperature swing, with internal heat gain and ventilation distribution, cases with infiltration rate of 0.2, 0.4, 0.6 and 0.8ACH: (a) Dining room (b) Master bedroom

Again, as a fixed infiltration rate was used all through the house in the ResHB simulation, the leakage distribution through the house has been assumed to be even, while in the real house it might have been different. It is possible that one room may have higher infiltration rate than another. The even leakage distribution used in the ResHB simulation may also contribute to errors in room temperatures and cooling load.

Finally, it should be noted that, in practice, infiltration rates will not be well known. The resulting uncertainty in the cooling load will likely be larger than any uncertainties in the method.

6.6 Conclusions

An experimental validation has been done for the Residential Heat Balance (RHB) cooling load calculation procedure, using experimental data collected from a Cardinal Project house located in Fort Wayne, Indiana. During the diagnostic process of the experimental validation of RHB, comparisons have also been made between the ESP-r simulation results and experimental data. The main conclusions from this experimental validation include the following:

1. The effects of interzone heat transfer via interzone airflow and/or interzone conduction are important. Presumably, interzone airflow is more important, but this has not been proven as part of this work. This has been demonstrated directly from experimental measurements. It has also been demonstrated that it is required for use in calculating cooling loads with master-slave zone control. A simple heuristic approximation of distributing heat gains that occurred in one room to the adjacent rooms was used with ResHB. This improves the cooling load calculation, but it suggests that further research might be useful to either improve the approximation and/or to implement a simple interzone airflow and/or interzone conduction algorithm within ResHB. Such an algorithm would necessarily have to be suitable for use in design load calculations, which suggests that it would have to rely on a fairly simple input scheme.

2. The ideal control scheme utilized in ResHB doesn't quite match the actual thermostatic control used in the experiment. This has an effect on the cooling load prediction, resulting in an 11% underprediction of the peak cooling load with 0.8°C temperature swing and a 5% overprediction of the peak cooling load with 0.0°C swing.

Arguably, the actual control falls somewhere in between the two variations of the ideal control strategy. In addition, the experiment didn't operate in the way that the developers of ResHB envisioned – it was intended to size equipment just large enough so that it could just barely maintain the inside design temperature plus swing. However, in this experiment, the equipment had a nominal cooling capacity of three times the experimental peak cooling load for the September day that was used. This suggests further investigation of system performance for systems designed with temperature swing. To some degree, this has been done with intermodel comparisons in Chapter 4, but further experimental research is warranted.

3. ESP-r demonstrated the advantages of master-slave zone control when interzone airflow and interzone conduction heat transfer are modeled. ESP-r has an extremely rich feature set and is extremely flexible. This made it invaluable for diagnosing the need for interzone airflow and the unsuitability of using master-slave zone control for cooling load calculations in ResHB. However, the rich feature set and flexibility make it overly complicated for most practitioners to use as a design tool.

4. Using the RHB master-slave control modeling for design load calculation may lead to significant error in cooling loads. The more different the master room load profile is from the rest of the house, the higher the error. In view of the fact that neither interzone conduction nor inter-zone airflow is modeled in RHB and the way that the master-slave control is handled by RHB, it does not seem appropriate to directly use the RHB master-slave control option for design load calculation purposes. From the study results, it might be inferred that reasonable cooling load predictions are possible with the master-

slave control if the room with thermostat has a load profile that is very close to the rest of the house. However, in a design load calculation there is no experimental data or other model results to compare against, so it is impossible to confirm that the room with the thermostat has a sufficiently close load profile. Barnaby et al. (2005) suggested that simulation with the RHB master-slave control may allow the identification of zoning problems. While this seems likely, it has not been investigated in this work and further investigation would be needed to prove (or disprove) its usefulness in this regard.

5. Regarding the suitability of ResHB for design cooling load calculations, it would be difficult to reach a conclusion on the basis of a single house on a single day in September. Again, further experimental research is warranted.

7. CONCLUSIONS

A systematic validation and evaluation of the new ASHRAE heat balance based residential cooling load calculation procedure (RHB) has been performed with the three most commonly used validation methods of building energy simulation programs: inter-model comparison, analytical verification and experimental validation. An analytical verification test suite for building fabric models of whole building energy simulation programs has been developed and used to perform analytical verification of ResHB. (Note that ResHB is the computer program developed as the reference implementation of the RHB procedure.) For each part of the validation conducted, conclusions have been included at the end of the corresponding chapter. The main conclusions and recommendations from this series of validation study are summarized as follows.

1. Inter-model validation of the RHB procedure was performed using ESP-r as the reference model. The testing process was automated through parametric generation and simulation of large sets of test cases for both RHB and ESP-r. The house prototypes used in the parametric testing include both a simple shoebox prototype and a real 4-bedroom house prototype.

In the load comparison mode, the load differences are considered reasonable, with ResHB predicted peak cooling loads ranging within $\pm 15\%$ of ESP-r. Excluding input discrepancies, load comparison results have been found to be largely dependent on the

sub-models used in both programs. Parametrically, the main sources of difference have been shown to be the different external long wave radiation models, internal solar distribution models and inter-zone conduction models used in each program. Different conduction methods also contribute to the load difference. For a worst case with no windows, internal heat gains, and infiltration, a 10% difference in peak cooling load was found. For real residential buildings with windows, internal heat gains, and infiltration, a 10% error in conduction heat gain would result in a much smaller error in cooling load. Never the less, it should be possible to eliminate this error. A cross-check using an analytical verification with sinusoidal boundary conditions could only show a 1.6% error in the ResHB conduction model. However, the actual boundary conditions are not sinusoidal; they include absorbed solar irradiation. It is possible that this creates additional error that is not present in the sinusoidal test. Further research, possibly involving development of an analytical model for combined conduction and radiation absorption, may be useful in resolving this issue. The load difference caused by different internal long wave radiation models has been shown to be small and negligible for design load calculation purposes.

In the system design evaluation mode, ESP-r simulations have been run with capacities gradually reduced from the RHB designed system capacity. Integrated PPD values and average room and whole house DH values have been used as the figures of merit in the evaluation. The quality of the system designs made with the RHB procedure has been shown to be reasonable and the RHB temperature swing option has been found useful to reduce the chance of system over-sizing if temperature swing is permitted in the residential designs.

2. An analytical verification test suite for building fabric models of whole building energy simulation programs has been developed. The test suite consists of a series of sixteen tests covering convection, conduction, solar irradiation, longwave radiation and infiltration phenomena, as well as ground-coupled floors.

Using the test suite, a total of twelve analytical tests have been done with the ResHB program. The analytical verification has been shown to be useful in the development and maintenance of the ResHB program. The analytical tests show the validity of ResHB in modeling several basic heat transfer phenomena, including steady state convection and conduction, transient conduction, solar radiation and internal solar distribution, and internal and external long wave radiation. Based on what was covered by the analytical tests in this study, no significant problem has been found regarding its underlying mechanisms for modeling the basic heat transfer phenomena in building fabric.

One problem was diagnosed with earlier versions of ResHB in the solar shading test. The problem has been fixed in later versions of ResHB after the diagnosis was reported. Another problem was diagnosed in the window reveal shading test. The problem has been reported to and confirmed by the ResHB developer.

3. The experimental validation for the RHB procedure has been conducted using experimental data collected from a well-instrumented house in Ft. Wayne, Indiana, which is one of the four houses used by Cardinal Glass Industries to conduct thermal performance tests in distinct U.S. regions (known as the Cardinal Project). During the diagnostic process of the experimental validation of RHB, comparisons have also been

made between ESP-r simulation results and experimental data. The main conclusions from the experimental validation include:

a. The effects of interzone heat transfer via interzone airflow and/or interzone conduction are important. Presumably, interzone airflow is more important, but this has not been proven as part of this work. This has been demonstrated directly from experimental measurements. It has also been demonstrated that it is required for use in calculating cooling loads with master-slave zone control. A simple heuristic approximation of distributing heat gains that occurred in one room to the adjacent rooms was used with ResHB. This improves the cooling load calculation, but it suggests that further research might be useful to either improve the approximation and/or to implement a simple interzone airflow and/or interzone conduction algorithm within ResHB. Such an algorithm would necessarily have to be suitable for use in design load calculations, which suggests that it would have to rely on a fairly simple input scheme.

b. The ideal control scheme utilized in ResHB doesn't quite match the actual thermostatic control used in the experiment. This has an effect on the cooling load prediction, resulting in an 11% underprediction of the peak cooling load with 0.8°C temperature swing and a 5% overprediction of the peak cooling load with 0.0°C swing. Arguably, the actual control falls somewhere in between the two variations of the ideal control strategy. In addition, the experiment didn't operate in the way that the developers of ResHB envisioned – it was intended to size equipment just large enough so that it could just barely maintain the inside design temperature plus swing. However, in this experiment, the equipment had a nominal cooling capacity of three times the

experimental peak cooling load for the September day that was used. This suggests further investigation of system performance for systems designed with temperature swing. To some degree, this has been done with intermodel comparisons in Chapter 4, but further experimental research is warranted.

c. ESP-r demonstrated the advantages of master-slave zone control when interzone airflow and interzone conduction heat transfer are modeled. ESP-r has an extremely rich feature set and is extremely flexible. This made it invaluable for diagnosing the need for interzone airflow and the unsuitability of using master-slave zone control for cooling load calculations in ResHB. However, the rich feature set and flexibility make it overly complicated for most practitioners to use as a design tool.

d. Using the RHB master-slave control modeling for design load calculation may lead to significant error in cooling loads. The more different the master room load profile is from the rest of the house, the higher the error. In view of the fact that neither interzone conduction nor inter-zone airflow is modeled in RHB and the way that the master-slave control is handled by RHB, it does not seem appropriate to directly use the RHB master-slave control option for design load calculation purposes. From the study results, it might be inferred that reasonable cooling load predictions are possible with the master-slave control if the room with thermostat has a load profile that is very close to the rest of the house. However, in a design load calculation there is no experimental data or other model results to compare against, so it is impossible to confirm that the room with the thermostat has a sufficiently close load profile. Barnaby et al. (2005) suggested that simulation with the RHB master-slave control may allow the identification of zoning

problems. While this seems likely, it has not been investigated in this work and further investigation would be needed to prove (or disprove) its usefulness in this regard.

e. Regarding the suitability of ResHB for design cooling load calculations, it would be difficult to reach a conclusion on the basis of a single house on a single day in September. Again, further experimental research is warranted.

4. Overall, it is concluded that RHB is acceptable as a design tool on a typical North American house, looking from the analytical verification, inter-model comparison and experimental validation points of view:

First, based on what was covered by the analytical tests in this study, no significant problem has been found regarding its underlying mechanisms for modeling the basic heat transfer phenomena in building fabric.

Second, based on the results of the inter-model comparison, which covered both a simple shoebox prototype and a real 4-bedroom house prototype, RHB compares favorably. Most of the difference founds in the prediction of loads can be traced to differences in the sub-models used by RHB and ESP-r, particularly the external long wave radiation models, internal solar distribution models and inter-zone conduction models. If desired, new sub-models could always be added into the RHB procedure. In the system design evaluation mode, the quality of the system designs made with the RHB procedure has been shown to be reasonable and the RHB temperature swing option has been found helpful in reducing system over-sizing.

Third, based on the comparisons made between the ResHB simulation results and measured data from a real house, RHB gives acceptable results. It has been shown that the key limitation is the deviation of the actual room temperatures resulting from the ideal control model. The performance of the heat transfer models was shown to be quite good when the room temperatures were matched to the measured temperatures. Therefore, systems designed with the method will have adequate size to meet the room temperatures specified in the design, whether or not swing is utilized. However, actual system operation may cause deviations in the room temperatures, particularly in the slave rooms. For better prediction of these deviations, simulation or a better approximation for interzone airflows and heat transfers would be needed. With the limited amount of testing done, the RHB procedure may be said to give cooling loads that are as accurate as the inputs. In practice, uncertainties about inputs such as infiltration will result in significantly larger errors than that caused by the method. Therefore, it is concluded that RHB provides an acceptable approximation to real-world performance.

5. In addition to the recommendations included with the conclusions, future research is recommended on the following topics:

- a. The peak load calculations have been shown to be sensitive to external long wave radiation and internal solar distribution models in the inter-model comparison between RHB and ESP-r. This suggests a likely topic for further research and refinement of the external long wave radiation and internal solar distribution models.

b. Window models, which are another possible source of the load differences between RHB and ESP-r, have not been thoroughly investigated in the inter-model comparison. As the solar heat gain through windows is a main source of the residential cooling load, it is suggested future research be conducted on this topic.

c. RHB ideal control is very sensitive to the amount of temperature swing but does not match thermostatic control well. The key limitation has been shown to be the deviation of the actual room temperatures from those simulated with the ideal control model. Therefore, it is recommended that a better control model that more closely matches thermostatic control be investigated.

d. The experimental validation conducted in this study was limited to a single day in a single house in a single location. Further more, the installed system was significantly over-sized for the day that was investigated. It would be useful to extend the experimental validation to other houses, days, locations and system sizes.

REFERENCES

- Ahmad, Q.T. 1997. Validation of Building Thermal and Energy Models. *Building Services Engineering Research & Technology* 19(2): 61-66.
- Alamdari, F. and G.P. Hammond. 1983. Improved data correlation for buoyancy-driven convection in rooms. *Rep. SME/J/83/01* (Cranfield: Applied Energy Group: Cranfield Institute of Technology)
- Alexander D.K. 1997. HTB2 (A Model for the Thermal Environment of Buildings in Operation) User Manual 2.0b. UWIST, Cardiff.
- Alexander D.K. 2001. Personal communication.
- Alexander, D.K., K.A.K. Hassan, P.J. Jones 1997. Simulation of solar gains through external shading devices. *Proceedings of the IBPSA Building Simulation '97 conference*, Prague, Czech Republic.
- Alexander D.K. and P.T. Lewis 1986. HTB2 (A Model for the Thermal Environment of Buildings in Operation) Technical Reference Manual. UWIST, Cardiff.
- Allen, E., D. Bloomfield, N. Bowman, K. Lomas, J. Allen, J. Whittle, A. Irving. 1985. Analytical and empirical validation of dynamic thermal building models. *Proceedings of Building Energy Simulation Conference*. Seattle, WA.
- Anderson, J. L. 1986. A Network Language for Definition and Solution of Simulation Problems. Lawrence Berkeley Laboratory.
- ASHRAE. 2004. ANSI/ASHRAE 152-2004, Method of Test for Determining the Design and Seasonal Efficiencies of Residential Thermal Distribution Systems.
- ASHRAE 2000. Updating the ASHRAE/ACCA residential heating and cooling load calculation procedures and data (1199-TRP). *ASHRAE Work Statement from TC4.1: Load Calculation Data and Procedures*.
- ASHRAE. 1998. ASHRAE Standard 140P: Standard method of test for the evaluation of building energy analysis computer programs. Working Draft 98/2. Atlanta: American Society of Heating, Refrigerating and Air-Conditioning engineers.

- ASHRAE. 1994. Air Leakage Performance of Detached Single-Family Residential Buildings. ANSI/ASHRAE Standard 119-1988 (RA 94).
- ASHRAE 1997. *Handbook of Fundamentals*. ASHRAE, Atlanta, GA.
- ASHRAE 2001. *Handbook of Fundamentals*. ASHRAE, Atlanta, GA.
- Asmundsson, Jakob. 2000. A Study of Solution Techniques and Process Models for Heat Balance Based Thermal Load Calculations. M.S. Thesis, Department of Mechanical and Industrial Engineering, University of Illinois, Urbana, IL.
- Austin, M. and R.J. Cole 1974. A thermal design model based on energy exchange: Part 2 The prediction of the atmospheric radiation incident at the external surface of buildings. SERC ref B/RG/2472.
- Bahnfleth, D. R., T.D. Moseley, W.S. Harris 1957. Measurement of infiltration in two residences, Part 1: Technique and measured infiltration. *ASHRAE Transactions* 63: 439-452.
- Barnaby, C. S., J. D. Spitler, and D. Xiao. 2004. Updating the ASHRAE/ACCA Residential Heating and Cooling Load Calculation Procedures and Data. 1199-RP Final Report. ASHRAE, Atlanta, GA.
- Beausoleil-Morrison, I. 2000. The adaptive coupling of heat and air flow modeling within Dynamic whole-building simulation. Ph.D. Thesis, University of Strathclyde.
- Berdahl, P. and M. Martin. 1984. Emissivities of Clear Skies. *Solar Energy* 23(5): 663-664.
- Björnsell, N., A. Bring, L. Eriksson, P. Grozman, M. Lindgren, P. Sahlin, A. Shapovalov, M. Vuolle 1999. IDA Indoor Climate and Energy. *Proceedings of the IBPSA Building Simulation '99 conference*, Kyoto, Japan.
- Bland, B.H., 1992. Conduction in dynamic thermal models: Analytical tests for validation. *Building Services Engineering Research and Technology* 13(4): 197-208.
- BLAST. 1995. *BLAST Users' Manual*. United States Army Construction Engineering Research Laboratory, Champaign, IL.
- Bloomfield, D., R. Brewer, B. Stringer, I. Cooper, and S. Lera. 1988. IEA Task 8, the UK Experience: Improving the design of low energy passive solar houses. *Building Research & Practice, the Journal of CIB*, no. 6.

- Bloomfield, D.P. 1999. An Overview of Validation Methods for Energy and Environmental Software. *ASHRAE Transactions* 105(2): 685-693.
- Bloomfield, D.P. 1989. Evaluation Procedures for Building Thermal Simulation Programs. *Proceedings of Building Simulation '89*, Vancouver, British Columbia, Canada.
- Blottner, F.G., 1990. Accurate Navier-Stokes Results for the Hypersonic Flow over a Spherical Nostip, *AIAA Journal of Spacecraft and Rockets*, Vol. 27, No. 2, March-April 1990, pp. 113-122.
- Boehm, B.W., 1981. *Software Engineering Economics*, Prentice-Hall, 1981.
- Brandemuehl, M. J. 1993. *HVAC 2 Toolkit: A Toolkit for Secondary HVAC System Energy Calculations*. Joint Center for Energy Management, University of Colorado.
- Brandemuehl, M.J., S. Gabel and I. Andresen, 1993. A Toolkit for Secondary HVAC for System Energy Calculations (629-RP). Atlanta, GA: ASHRAE.
- BRE. 1988. Final Report of BRE/SERC Collaboration, An investigation into analytical and empirical validation techniques for dynamic thermal models of buildings. Building Research Establishment, U.K.
- Bring A., P. Sahlin and M. Vuolle 1999. Models for Building Indoor Climate and Energy simulation: A Report of IEA SHC Task 22 Building Energy Analysis tools Subtask B. Version 1.02.
- Brown, G. 1990. The BRIS simulation program for thermal design of buildings and their services. *Energy and Buildings* 14: 385-400.
- Brown, G. and E. Isfält 1974. *Solinstrålning och solavskärmning (Solar Irradiation and Sun Shading Devices)*. Nat. Swedish Inst. For Building Res., Report 19:1974 (in Swedish w an English summary), Stockholm.
- Brunger A., Dubrous F. and Harrison S. 1999. Measurement of the solar heat gain coefficient and U value of windows with insect screens. *ASHRAE Transactions* 105(2): 1038-1044.
- Building America. 2003. Building America Research Benchmark Definition, Version 3.1. http://www.eere.energy.gov/buildings/building_america/pdfs/benchmark_def_ver_3.pdf

- Building Systems Laboratory, University of Illinois at Urbana-Champaign 2001. *A Toolkit for Building Load Calculations Manual*.
- Building Research Establishment/Science and Engineering Research Council 1988. An investigation into analytical and empirical validation techniques for dynamic thermal models of buildings. Vols 1-6, BRE.
- CGSB 1986. *Determination of the Airtightness of Building Envelopes by the Fan Depressurization Method*. CAN/CGSB 149.10-M86.
- CSA 1990. *Determining the Required Capacity of Residential Space Heating and Cooling Appliances*. CAN/CSA-F280-M90. Canadian Standards Association, Rexdale (Toronto), ON, Canada.
- Carroll, J.A. 1981. A comparison of radiant interchange algorithms. ASME/SSEA Conf., April 1981.
- CEN 1997. Thermal Performance of Buildings: Room Sensible Cooling Loads Calculation – General Criteria and Validation Procedures: Appendix A, CEN/TC/89/WG6 N. 225, pp. 52.
- Chantrasrisalai, C., D.E. Fisher, I.S. Iu, and D. Eldridge. 2003. Experimental validation of design cooling load procedures: The heat balance method. *ASHRAE Transactions* 109(2): 160-173.
- Clarke, J.A. 1985. *Energy Simulation in Building Design*. Adam Hilger Ltd., Bristol & Boston.
- Clarke, J.A. 1977. Environmental Systems Performance. Ph. D. Thesis, University of Strathclyde, Glasgow UK.
- Coblentz, C.W., P.R. Achenbach 1963. Field measurements of air infiltration in ten electrically-heated houses. *ASHRAE Journal*, 5(7): 69-74.
- Crawley, Drury B, Linda K Lawrie, Curtis O Pedersen, Richard J Liesen, Daniel E Fisher, Richard K Strand, Russell D Taylor, Frederick C Winkelmann, W F Buhl, A Ender Erdem, and Y Joe Huang. 1999. EnergyPlus, A New-Generation Building Energy Simulation Program. *Proceedings of Building Simulation '99*, Volume I: 81-88, Kyoto, Japan, September 1999. IBPSA.
- Davies M.G. 1993. Heat Loss from a Solid Floor: A New Formula. *Building Services Engineering Research & Technology*, 14(2): 71-75.

- Delsante A.E., A.N. Stokes, P.J. Walsh, 1983. Application of Fourier Transforms to Periodic Heat Flow into the Ground under a Building. *International Journal of Heat Mass Transfer*, 26(1): 121-132.
- Duffie J.A., W.A. Beckman 1991. *Solar Engineering of thermal Processes*. New York: Wiley.
- EnergyPlus 2004. <http://www.eere.energy.gov/buildings/energyplus/>
- ESRU 2000. The ESP-r System for Building Energy Simulation: User Guide Version 9 Series. ESRU Manual U00/1, University of Strathclyde, Glasgow UK.
- Grimsrud, D.T., M.P. Modera, M.H. Sherman 1982. A predictive air infiltration model - long term field test validation. *ASHRAE Transactions* 88(1): 1351-1372.
- Gu, L., J.E. Cummings, M.V. Swami, P.W. Fairey 1998. Comparison of duct computer models that could provide input to the proposed thermal distribution standard method of test. *ASHRAE Transactions* 104(1B): 1349-1359.
- Guyon, G., S. Moinard, N. Ramdani 1999. Empirical validation of building energy analysis tools by using tests carried out in small cells. *Proceedings of the IBPSA Building Simulation '99 conference*, Kyoto, Japan.
- Hoellwarth, G.W. 1980. Certification of Energy Analysis Computer Program in California. *ASHRAE Transactions* 86(1): 781-792.
- Holmes, M.J. and A. Wilson, 1996. Revised Sections A5, A8, A9 of the CIBSE Guide : Second Draft. London: Ove Arup and Partners, p. 148.
- Howell R. H., Harry J. Sauer Jr., Coad W.J. 1998. *Principles of Heating, Ventilating and Air Conditioning*. ASHRAE, Atlanta, GA.
- IEA 1981. Comparison of Load Determination Methodologies for Building Energy Analysis Problems. IEA Confidential Memo, IEA Energy Conservation, Buildings and Community Systems, Annex 1.
- Incropera, F.P. and DeWitt, D.P., 1990. *Introduction to Heat Transfer*. 2nd Ed. New York: John Wiley.
- Iu, I.S., D.E. Fisher, C. Chantrasrisalai, and D. Eldridge. 2003. Experimental validation of design cooling load procedures: The radiant time series method. *ASHRAE Transactions* 109(2): 139-150.

- James, P.W., J. Cummings and J.K. Sonne. 1997. The effect of residential equipment capacity on energy use, demand, and run-time. *ASHRAE Transactions* 103(2): 297-303.
- Jones, P.J., D.K. Alexander, A.M. Rahman 1993. Evaluation of the thermal performance of low-cost tropical housing. *Proceedings of the IBPSA Building Simulation '93 conference*, Adelaide, Australia.
- Judkoff, R., J. Neymark. 1995. *Building Energy Simulation Test (BESTEST) and Diagnostic Method*. NREL/TP-472-6231. Golden, CO: National Renewable Energy Laboratory.
- Judkoff, R. 1988. Validation of building energy analysis simulation programs at the Solar Energy Research Institute. *Energy and Buildings* 10(3): 221-239.
- Judkoff, R., D. Wortman, B. O'Doherty, J. Burch. 1983. *A Methodology for Validating Building Energy Analysis Simulations*. SERI/TR-254-1508. Golden, CO: Solar Energy Research Institute (now NREL).
- Judkoff, R.D. et al. 1980. A Comparative Study of Four Building Energy Simulations. *SERI/TP-721-837*, Golden, CO: Solar Energy Research Institute.
- Judkoff, R.D., R.J. O'Doherty and D.N. Wortman 1981. A Comparative Study of Four Building Energy Simulations: Phase II. *SERI/TP-721-1326*, Golden, CO: Solar Energy Research Institute.
- Khattar, M.K., M.V. Swami, and N. Ramanan. 1987. Another aspect of duty cycling: effects on indoor humidity. *FSEC-PF-118-87*. Cocoa: Florida Solar Energy Center.
- Kimura, K 1977. *Scientific Basis of Air Conditioning*. Applied Science Publishers Ltd., London.
- Kusuda, T. 1967. *NBSLD, the computer program for heating and cooling loads in building*. National Bureau of Standards, BSS 69. Washington, D.C.: National Bureau of Standards (now NIST).
- Kusuda, T., and P.R. Achenbach. 1965. Earth temperature and thermal diffusivities at selected stations in the United States. *ASHRAE Transactions* 71(1): 61-75.
- LBL 1984. *DOE-2 Reference Manual*. Lawrence Berkeley Laboratory.

- LBL and Ayres Sowell Associates 1997. *SPARK User's Manual*. Lawrence Berkeley National Laboratory and Ayres Sowell Associates, Inc.
- Liesen, R.J. and C.O.Pedersen. 1997. An Evaluation of Inside Surface Heat Balance Models for Cooling Load Calculations, *ASHRAE Transactions* 103(2): 485-502.
- Lomas, K.J. et al. 1994. Empirical validation of thermal simulation programs using test room data. International Energy Agency (IEA), Building energy analysis and design tools for solar applications (task 12).
- Lomas, K.J. 1992. Applicability Study I: Executive Summary, *ETSU Report S1213*.
- Lomas, K.J., D.P. Bloomfield, A. Cole, F. Parand, A.A. Pinney 1991. Dynamic thermal models: reliability for domestic building design. *Building Serv. Res. Technol.* 12(4): 115-128.
- Machler, M. A. and Iqbal, M. 1985. A Modification of the ASHRAE Clear Sky Irradiation Model. *ASHRAE Transactions* 91(1A): 106-115.
- McClellan, T.M., C. Pedersen, 1997. Investigation of outside heat balance models for use in a heat balance cooling load calculation procedure. *ASHRAE Transactions* 103(2): 469-484.
- McQuiston, F.C. and J.D. Spitler 1992. *Cooling and Heating Load Calculation Manual*, 2nd edition. ASHRAE, Atlanta, GA.
- McQuiston F.C., Thomas T.E., Harris S.M., Lankford L.H. and Ali A. 1984. A Study and Review of Existing Data to Develop a Standard Methodology for Residential Heating and Cooling Load Calculations. RP-342. ASHRAE, Atlanta, GA.
- McQuiston F.C. 1984. A study and review of existing data to develop a standard methodology for residential heating and cooling load calculations. *ASHRAE Transactions* 90(2): 102-136.
- Nataf, J. M. and F. C. Winkelmann 1992. *Automatic Code Generation in SPARK: Applications of Computer Algebra and Compiler-compilers*. Berkeley, CA, Simulation Research Group, Lawrence Berkeley Laboratory.
- Neal, L., and D. O'Neal. 1994. The impact of residential air-conditioner charging and sizing on peak demand. *ACEEE Summer Study on Energy Efficiency in Buildings* 2: 189-200.

- Neymark, J., R. Judkoff 2002. *International Energy Agency Building Energy Simulation Test and Diagnostic Method for HVAC Equipment Models (HVAC BESTEST)*. Golden, CO: National Renewable Energy Laboratory. NREL/TP-550-30152. January 2002.
- Palmiter, L. and T. Bond. 1991. Interaction of Mechanical Systems and Natural Infiltration. Proceedings of the 12th AIVC Conference on Air Movement and Ventilation Control Within Buildings, Air Infiltration and Ventilation Centre, Coventry, Great Britain.
- Palmiter, L. and P. Francisco. 1997. Development of a Practical Method of Estimating the Thermal Efficiency of Residential Forced-Air Distribution Systems. *Electric Power Research Institute report TR-107744*. Palo Alto, CA.
- Perez, R., P. Ineichen, R. Seals, J. Michalsky and R. Stewart. 1990. Modeling daylight availability and irradiance components from direct and global irradiance. *Solar Energy* 44(5): 271-289.
- Perez, R., R. Seals, P. Ineichen, R. Stewart and D. Menicucci. 1987. A new simplified version of the Perez diffuse irradiance model for tilted surfaces. *Solar Energy* 39: 221-231.
- Park, C., D. Clark, G. Kelly 1986. HVACSIM+ building systems and equipment simulation program: building loads calculation. National Bureau of Standards, NBSIR 86-3331.
- Pedersen, C. O., R. J. Liesen, R. K. Strand, D. E. Fisher, L. Dong, and P. G. Ellis. 2001. A Toolkit for Building Load Calculations. ASHRAE, Atlanta, GA.
- Pedersen, C.O., D.E. Fisher, R.J. Liesen. 1997. A heat balance based cooling load calculation procedure. *ASHRAE Transactions* 103(2): 459-468.
- Pedersen, C. O., D. E. Fisher, J. D. Spitler, and R. J. Liesen.. 1998. *Cooling and heating load calculation principles*. ASHRAE, Atlanta, GA.
- Pipes, L.A. 1957. Matrix analysis of heat transfer problems. *Journal of the Franklin Institute* 263(3): 195-206.
- Proctor, J., Katsnelson Z., Wilson B. 1995. Bigger is not better: Sizing air conditioners properly. *Home Energy* 12(3): 19-26.
- Proctor, J. 1998. Monitored in-situ performance of residential air conditioning systems. *ASHRAE Transactions* 104(1B): 1833-1840.

- Reddy, T.A. and D.E. Claridge. 1993. Effect of air-conditioner oversizing and control on electric-peak loads in a residence. *Energy* 18(11): 1139-1152.
- Rees, S.J., D. Xiao, J.D. Spitler. 2002. An analytical verification test suite for building fabric models in whole building energy simulation programs, *ASHRAE Transactions* 108(1): 30-41.
- Rees, S.J., J.D. Spitler, M.G. Davies, P. Haves 2000. Qualitative Comparison of North American and U.K. Cooling Load Calculation Methods. *International Journal of Heating, Ventilating, Air-Conditioning and Refrigerating Research* 6(1): 75-99.
- Rees, S.J., J.D. Spitler, P. Haves. 1998. Quantitative comparison of North America and U.K. cooling load calculation procedures – Results. *ASHRAE Transactions* 104(2): 47-57.
- Rees, S.J., J.D. Spitler 1999. Proposals for a Building Loads Diagnostic Test Procedure. *ASHRAE Transactions* 105(2): 514-526.
- Reindl, D.T., W.A. Beckman, J.A. Duffie 1990. Diffuse Fraction Correlations. *Solar Energy* 45(1): 1-7.
- Rodriguez E. A., S. Alvarez 1991. Solar Shading Analytical Tests (I). IEA21RN136.
- Romine, T.B. 1992. Cooling Load Calculation: Art or Science? *ASHRAE Journal*. 34(1): 36-46.
- Rutkowski, H. 1986. *Load calculation for residential winter and summer air conditioning – Manual J, 7th Edition*. Air Conditioning Contractors of America, Washington, DC.
- Rutkowski, H. 2002. *Residential load calculation – Manual J, 8th Edition*. Air Conditioning Contractors of America, Washington, DC.
- Sherman, M.H. 1992. Superposition in infiltration modeling. *Indoor Air* 2:101-14.
- Sowell, E. F. and W. F. Buhl 1988. Dynamic Extension of the Simulation Problem Analysis Kernel (SPANK). *Proceedings of the USER-1 Building Simulation Conference*. Ostend, Belgium, Soc. for Computer Simulation International.
- Spitler, J.D., S.J. Rees, D. Xiao. 2001. *Development of an analytical verification test suite for whole building energy simulation programs – building fabric (1052-RP): Final Report*, ASHRAE, Atlanta GA.

- Spitler, J.D. 2000. Updating the ASHRAE/ACCA residential heating and cooling load calculation procedures and data. *ASHRAE 1199-TRP Research Proposal*.
- Spitler, J.D. and D.E. Fisher 1999. On the relationship between the radiant time series and transfer function methods for design cooling load calculations. *International Journal of Heating, Ventilating, Air-Conditioning and Refrigerating Research* 5(2): 125-138.
- Spitler, J.D., S.J. Rees. 1998. Quantitative comparison of North American and U.K. cooling load calculation procedures -- Methodology. *ASHRAE Transactions* 104(2): 36-46.
- Spitler, J.D., D.E. Fisher, and C.O. Pedersen 1997. The radiant time series cooling load calculation procedure. *ASHRAE Transactions* 103(2): 503-515.
- Spitler, J.D. 1990. An Experimental Investigation of Air Flow and Convective Heat Transfer in Enclosures Having Large Ventilative Flow Rates. Ph.D. Thesis. University of Illinois, Urbana-Champaign, IL.
- Stefanizzi, P., A. Wilson and A. Pinney, 1988. The internal longwave radiation exchange in thermal models. *BRE/SERC Report An Investigation into Analytical and Empirical Validation Techniques for Dynamic Thermal Models of Buildings*. Vol. 2.
- Strachan, P. 2000. ESP-r: Summary of Validation Studies. ESRU Technical Report, University of Strathclyde, Glasgow UK.
- Strachan, P. 1993. Model Validation Using the PASSYS Test Cells. *Building and Environment* 28(2): 153-165.
- Strand, R., F. Winkelmann, F. Buhl, J. Huang, R. Liesen, C. Pederson, D. Fisher, R. Taylor, D. Crawley, and L. Lawrie 1999. Enhancing and extending the capabilities of the building heat balance simulation technique for use in EnergyPlus. *Proceedings of Building Simulation '99*, Volume II: 653-660, Kyoto, Japan, September 1999. IBPSA.
- USNO 2001. U.S. Naval Observatory: Astronomical Applications Department, Sun or Moon Altitude/Azimuth Table for One Day, <http://aa.usno.navy.mil/data/docs/AltAz.html>
- Walker, I. S. and D. J. Wilson. 1998. Field validation of equations for stand and wind driven air infiltration calculations. *International Journal of HVAC&R Research* 4(2).

- Walker, I. S. and D. J. Wilson. 1990. The Alberta Air Infiltration Model. The University of Alberta, Department of Mechanical Engineering, Technical Report 71.
- Walton, G.N. 1993. *Computer programs for simulation of lighting/HVAC interactions*. NISTIR 5322. National Institute of Standards and Technology, Gaithersburg, MD.
- Walton, G.N. 1983. *Thermal analysis research program reference manual*. NBSIR 83-2655. Washington, D.C.: U.S. Department of Commerce, National Bureau of Standards, National Engineering Laboratory, Building Physics Division.
- Walton, G. N. 1981. *Passive solar extension of the building loads analysis and system thermodynamics (BLAST) program*. Technical Report, United States Army Construction Engineering Research Laboratory, Champaign, IL.
- Walton, G.N. 1980. A new algorithm for radiant interchange in room loads calculations. *ASHRAE Transactions* 86(2): 190-208.
- Wilcox, B. 2004. Personal communication.
- Willmott, C.J. 1982. Some comments on the evaluation of model performance. *Bulletin of the American Meteorological Society* 63:1309-1313.
- Witte, M.J., R.H. Henninger, and D.B. Crawley. 2004. Experience Testing EnergyPlus with the ASHRAE 1052-RP Building Fabric Analytical Tests. *Proceedings of the SimBuild 2004*: 4-6 August 2004, Boulder, Colorado. IBPSA-USA.
- Xiao, D., S.J. Rees, J.D. Spitler, R. Dougherty. 2005. Transient Conduction Analytical Solutions for Testing of Building Energy Simulation Programs. *Building Services Engineering Research & Technology*, approved for publication.
- Xiao, D., J.D. Spitler, and S.J. Rees. 2002. An Analytical Verification Test Suite for Multi-zone Building Fabric and Control Models in Whole Building Energy Simulation Programs, *Proceedings of eSim 2002*, Montreal, Canada. September 11-13, 2002. pp. 260-267.
- Xiao, D., J.D. Spitler. 2002. Documentation of the Analytical Verification Tests for Multi-zone Control Models in Whole Building Energy Simulation Programs, *BETSRG Report 2002-1*, Building & Environmental Thermal System Research Group, Oklahoma State University, Stillwater.

Yazdanian, M. and J.H. Klems. 1994. Measurement of the exterior convective film coefficient for windows in low-rise buildings. *ASHRAE Transactions* 100(1): 1087-1096.

APPENDIX A. ANALYTICAL VERIFICATION OF ESP-R

This appendix describes the analytical verification tests of the selected inter-model comparison tool – ESP-r, using an extension of the test suite developed by Spitler et al. (ASHRAE 1052-RP, 2001). These analytical tests, together with previous validation work done during the evolution of ESP-r and reported in the literature (as those summarized in Table 4-4), gave me much confidence in choosing ESP-r as the inter-model comparison tool of RHB. It also helped in diagnosing any modeling problem that might arise when using ESP-r to evaluate RHB in detailed simulation.

While the test cases designed in the ASHRAE 1052-RP test suite are good for testing single zone applications, inter-zone heat transfer, inter-zone air flow and master-slave zone controls are also important features in residential load calculations. Therefore, a set of inter-zone heat transfer, inter-zone airflow, and master-slave zone control tests were developed on the basis of the ASHRAE 1052-RP test suite and are used in checking the inter-zone features of ESP-r (Xiao, et al. 2002). Table A-1 summarizes the analytical verification tests that have been done with ESP-r. The test results are documented in detail in a separate file (Xiao and Spitler 2002) and are briefly discussed below.

Table A-1: Analytical Verification Tests of ESP-r

Test group	Test title	Abbreviation	Analytical solution	ESP-r test	
Single zone tests	Convection and conduction	Steady State Convection	SSConv	As from 1052RP	√
		Steady State Conduction	SSCond	As from 1052RP	√
		Transient Conduction – Adiabatic Wall	TC1	As from 1052RP	√
		Transient Conduction – Step Response	TC2	As from 1052RP	√
	Solar gains and shading	Exterior Solar Radiation – Opaque Surfaces	ExtSolRad	As from 1052RP	√
		Solar Radiation – Glazed Surfaces	SolRadGlazing	As from 1052RP	√
		Solar Radiation – Window Shading	SolRadShade	As from 1052RP	*
		Solar Radiation – Window Reveal Shading	WinReveal	As from 1052RP	*
	Long wave radiation	Solar Radiation – Internal Solar Distribution	IntSolarDist	As from 1052RP	*
		Interior Long Wave Radiation	IntRad	As from 1052RP	*
		External Long Wave Radiation	ExtLWRad	As from 1052RP	√
	Infiltration	Infiltration – Fixed Infiltration Rate	Infiltration 1	As from 1052RP	*
		Infiltration – Stack Effect	Infiltration 2	As from 1052RP	√
Internal heat gains	Internal Heat Gains – Convective and Radiant	IntHeatGain	As from 1052RP	√	
Multi-zone tests	Inter-zone conductive heat transfer	Steady State Convection	IZSSConv	As from 1052RP but applied to an inter-zone wall	√
		Steady State Conduction	IZSSCond	As from 1052RP but applied to an inter-zone wall	√
		Transient Conduction – Step Change Air Temperature vs. Free Floating Air Temperature	IZTC1	As from 1052RP but applied to an inter-zone wall	√
		Transient Conduction – Step Change Air Temperature vs. Fixed Air Temperature	IZTC2	As from 1052RP but applied to an inter-zone wall	√
	Inter-zone air flow	Inter-zone Air Flow – Fixed Airflow Rate	IZAirFlow-1	As from 1052RP but applied to an inter-zone test	√
		Inter-zone Air Flow – Stack Effect	IZAirFlow-2	As from 1052RP but applied to an inter-zone test	√
	Master-slave zone control	Master-slave Zone Control – Ideal control	MSIdealCon	Developed	*
		Master-slave Zone Control – VAV Control	MSVAVCon	Developed	√
		Master-slave Zone Control – On-off Control	MSONOffCon	Developed	√

Note: √ Test has been done and comparison is satisfactory

* Test has been done but comparison is unsatisfactory, the problem causing the discrepancy is not important for the project

A.1 Single Zone Tests

1. For the convection and conduction test group: ESP-r test results are in good agreement with the analytical results.
2. For the solar gains and shading test group:

There are two deviations between the ESP-r results and analytical results: First, ESP-r under-predicts zone loads from east-facing windows and over-predicts zone loads from west-facing windows due to the ESP-r weather data interpolation algorithm. For simulation time steps less than one hour, ESP-r linearly interpolates between the hourly values in the weather file. (They are taken to be instantaneous rates, rather than hourly averages. The weather file generator created to write ESP-r format weather file generates average hourly values rather than instantaneous values – following the TMY-2 convention.) In order to overcome this problem, weather data will be generated with the hourly values being instantaneous rather than average.

Figure A-1a shows the initial comparison between the ESP-r test result and the analytical solution for an east, west, and south facing window. ESP-r under-predicts zone loads from the east-facing window and over-predicts zone loads from the west-facing window. The maximum differences between ESP-r predicted and analytical loads reaches 10.3% and 7.4% of the analytical peak load for the east and west facing window, and 1.3% of the analytical peak load for the south facing window.

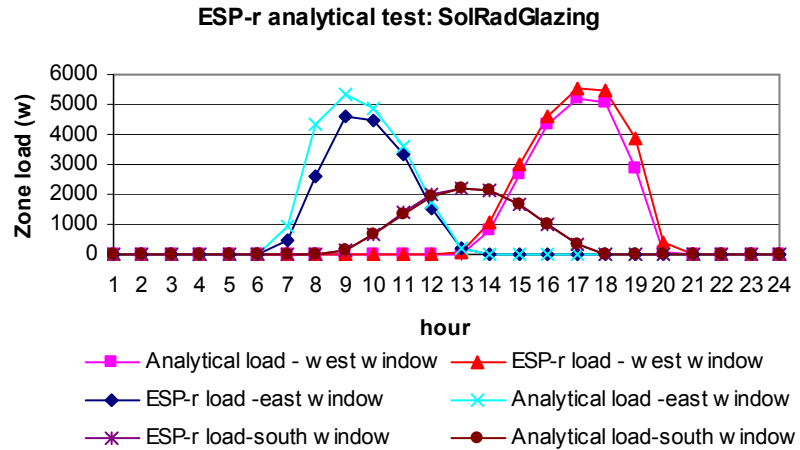


Figure A-1a Analytically calculated zone loads and those calculated by ESP-r for Solar Radiation –
Glazed Surfaces test: East, west and south facing window

Figure A-1b shows the same tests but with the weather file generated to be consistent with the ESP-r expectations. There is a significant improvement, but some small discrepancies remain. Figure A-1c shows a comparison of the direct normal irradiance used in the analytical model to that used by ESP-r with the original (hourly average) weather file and the revised model (instantaneous). The linear interpolation causes some minor discrepancies in the irradiance, particularly early and late in the day when the values change abruptly from hour to hour. If absolutely necessary, it is possible to specify weather data to ESP-r at the sub-hourly time step used in the program.

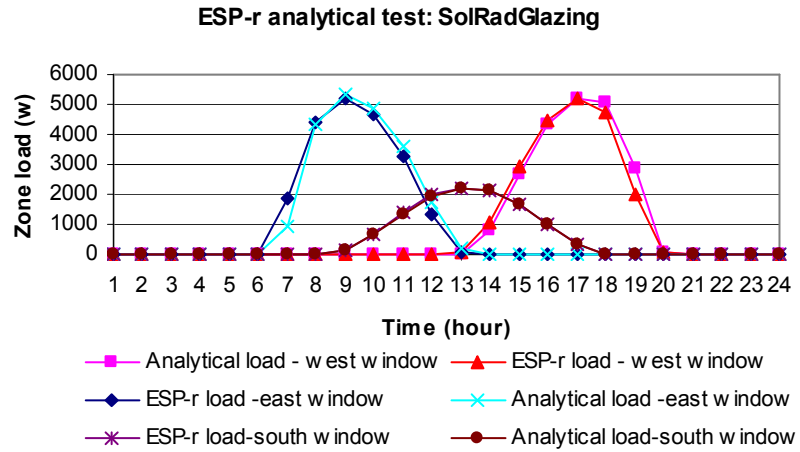


Figure A-1b Analytically calculated zone loads and those calculated by ESP-r for Solar Radiation – Glazed Surfaces test: East, west and south facing window (with hourly instantaneous weather data)

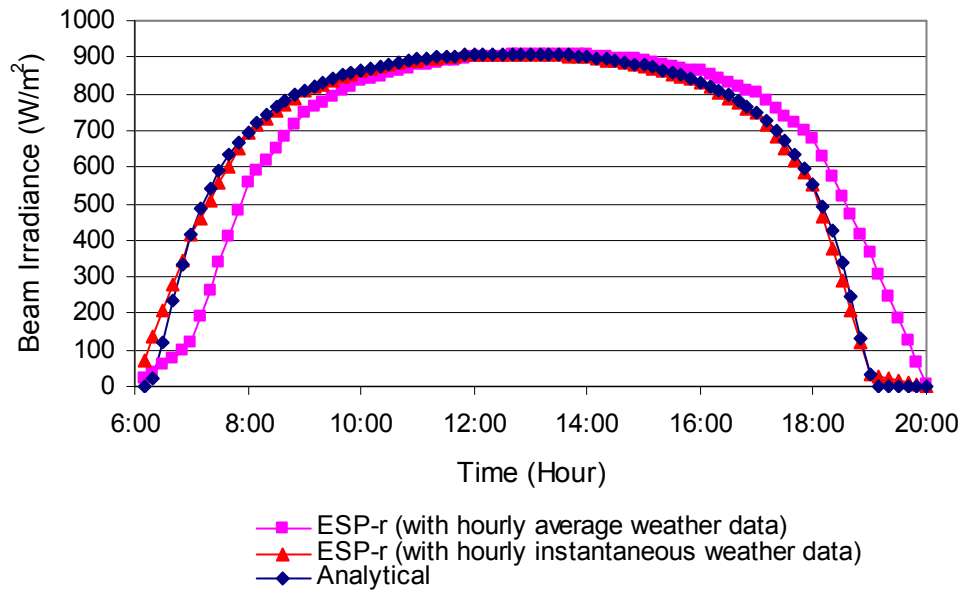


Figure A-1c Comparison of solar beam irradiance used by ESP-r and Analytical solution

Second, ESP-r shows higher shading effects than the analytical solution in the solar shading tests. This is due to the approximation made in using solar shading factors computed for a single “average” day within a month. (As explained by

ESRU (2001), this is done to keep the shading data file of reasonable size.) Figure A-2 shows the comparison between the ESP-r test result and the analytical solution for a south facing window with a left-side vertical fin. ESP-r shows more shading effect in the afternoon. The maximum zone load difference (410.4 W) reaches 18.7% of the analytical peak load. However, writing our own shading factor file can mitigate this problem. This was done, and as can be seen in Figure A-2, this (“ESP-r load with analytical shading factor”) now gives a very good match to the analytical solution. The plan is either to write our own file or to modify ESP-r to create a file specific to the design day rather than the average for the month.

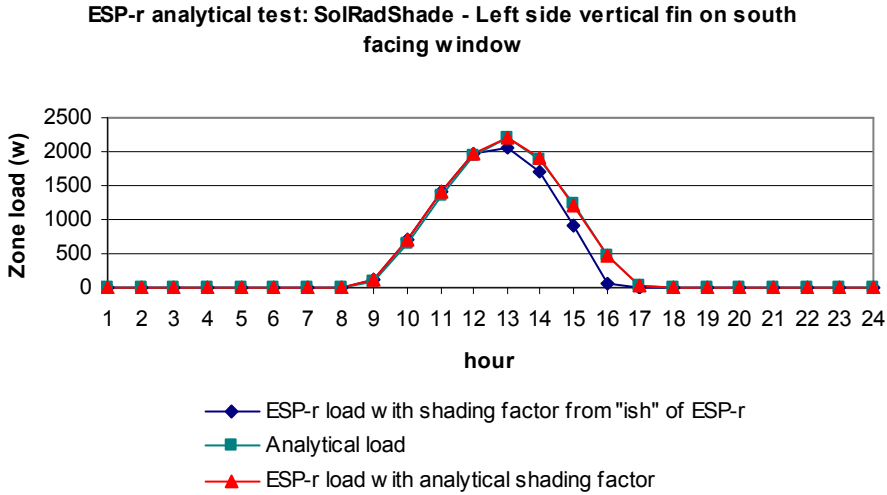


Figure A-2 Analytically calculated zone loads and those calculated by ESP-r for Solar Radiation – Window
 Shading test: south facing window with left side vertical fin

3. For long wave radiation group:

The ESP-r results match the analytical results for the external long wave radiation test.

ESP-r results for internal long wave radiation are partially unsatisfactory because it considers the ray paths of diffuse reflections involving only three surfaces at a time. This simplification becomes inaccurate in the case of very low emissivity surfaces (Clarke 2001). This should not be a big problem for residential buildings, where low emissivity surfaces are rarely used.

Figure A-3 and A-4 show the comparison between ESP-r and analytical results for two test cases. In test case 1, ESP-r results diverge from analytical results since in this test, the emissivities of all internal surfaces are set at 0.1 (except for the only one external surface set at 0.9). In test case 2, in which the emissivities of all surfaces are 0.9, ESP-r load matches analytical load.

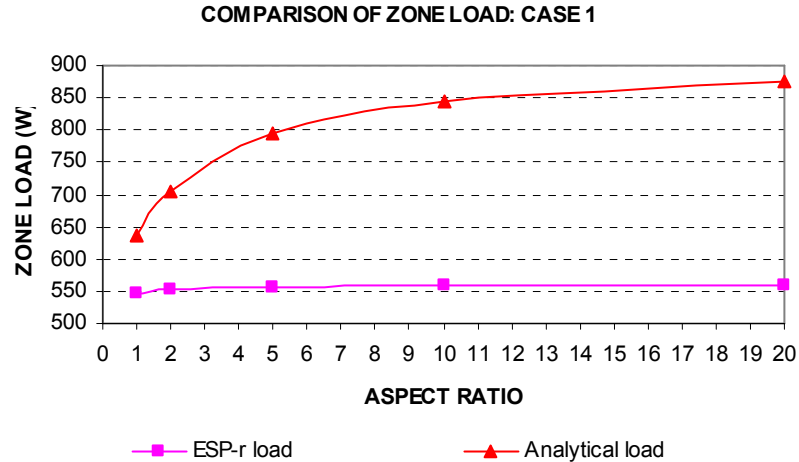


Figure A-3 Analytically calculated zone loads and those calculated by ESP-r for the Internal Long Wave Radiation test: emissivity of the external surface = 0.9, emissivity of other surfaces = 0.1

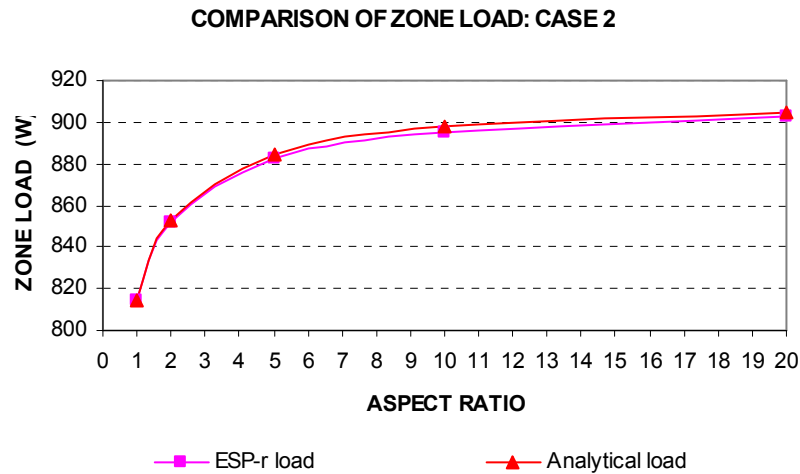


Figure A-4 Analytically calculated zone loads and those calculated by ESP-r for the Internal Long Wave

Radiation test: emissivity of all surfaces = 0.9

4. For infiltration group:

The ESP-r result of infiltration test under fixed infiltration rate deviates from analytical result by 5.8% due to the different air density it uses in calculating the infiltration load in this simple test case. However, the problem shown in the fixed infiltration rate test should not be a problem for the intended research, as an airflow network is going to be used, which is not subject to this problem.

The ESP-r infiltration test result with stack effect matches well with the analytical result.

5. For the internal heat gain test:

Comparisons between ESP-r and the analytical solutions are satisfactory.

A.2 Multi-zone Tests

1. For the inter-zone heat transfer group:

ESP-r results for this test group are in good agreement with analytical results.

2. For the inter-zone airflow group:

ESP-r results for this test group are in good agreement with analytical results.

3. For the master-slave zone control tests group:

ESP-r results for this test group are in good agreement with analytical results except for the ideal control test.

Test results for the VAV and On-Off control tests under convective heat input profiles scheduled as in Fig. A-5 are given in Fig. A-6 and Fig. A-7. Both the analytical and numerical results were obtained using a simulation time step of six seconds. (In this case, the “analytical” test still requires a numerical solution.) For both cases, ESP-r gives a reasonable approximation to the analytical solution.

The ESP-r ideal control test was done using the heating/cooling control functions in the zone models. The ESP-r simulation results showed that the master zone air temperature is controlled as expected, but the slave zone air temperature is not controlled. Instead, it appears to float as if there is no system heat input. However, there are other ways to model the master-slave zone control in ESP-r, so I did not investigate further.

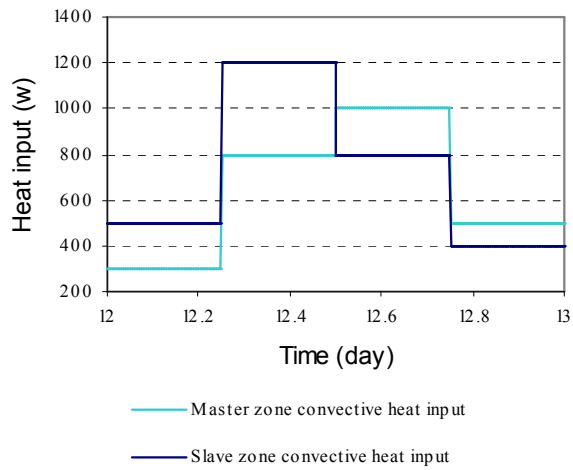


Figure A-5 The convective heat input profiles of the test zones used in the VAV and On-Off control tests with ESP-r program

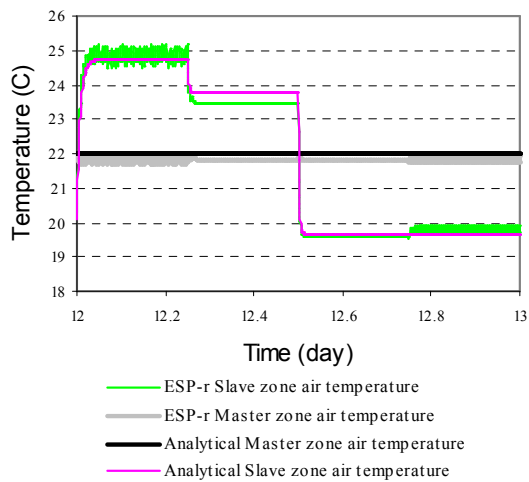


Figure A-6 Zone air temperatures predicted by ESP-r program and analytical solution for the VAV control test

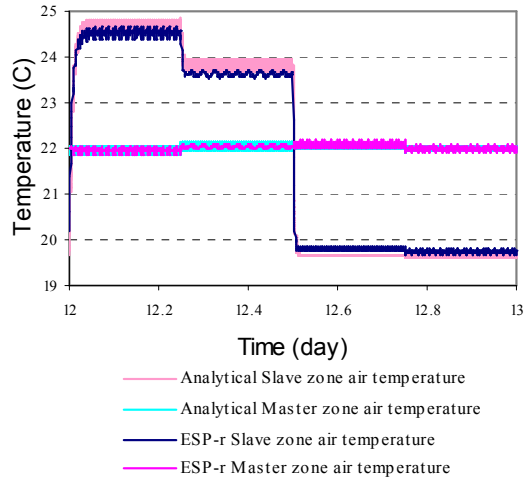


Figure A-7 Zone air temperatures predicted by ESP-r program and analytical solution for the On-Off control test

APPENDIX B. PARAMETRIC CODE USED FOR THE INTER-MODEL COMPARISON

This appendix describes the parametric code used for the inter-model comparison. Table B-1 lists the parametric code with a brief description and variant range. Table B-2 through Table B-9 give more detailed information for the constructions and/or configurations of the roofs, ceilings, walls, fenestrations, floors, partitions, and internal thermal mass. All information is extracted from the documentation of RHBGen (Barnaby, et al. 2004). The tables may include some abbreviations that originated from the ResHB and RHBGen documentation. For their specific meanings, the ASHRAE 1199RP final report (Barnaby, et al. 2004) should be consulted.

Table B-1: Parametric Code

Code	Description	Value Range	
Rr	Revision	r	Code revision. Current = 2
Hm	House model	m	House prototype
Lstcc	Location	st	State abbreviations
		cc	City code
Oxxx	Orientation	xxx	000 - 360: orientation of building front
Qgitsx	Gains, infiltration, and controls	g	internal gain: 0: 0, l: .5 std, m: 1 std, h: 2 std; A-l: parametric variation of intgain components
		i	Infiltration code: 0: 0, l: .1 ACH, m: .4 ACH, h: 1 ACH; A-J: AIM2 model w/ specified leakage class
		t	cooling setpoint. l: 21 C, m: 24 C, h: 27 C
		s	Room temp swing. 0: 0 C, l: 0.83 C, m: 1.67 C, h: 2.5 C
		x	control options: 0: sp as specified, 1: sp reduced by .5 swing, 2: sp reduced by swing
Awifl	Interior surface absorptivity	w	Wall / partition / ceiling SW absorp: 0lmhdb1 (see note)
		i	Internal mass SW absorp: 0lmhdb1 (see note)
		f	Floor SW absorp: 0lmhdb1 (see note)
		l	LW absorp (all surfaces): 0: 0, l: .2, m: .9 (fen .84), h: .95, 1: 1
Ccifra	Exterior ceiling / roof	c	Ceiling construction: 0: massless; w: wood frame, c: solid concrete
		i	Ceiling insulation (l, m, h)
		f	Configuration: x: ceiling only (no roof), f: flat; h: hip
		r	Roof construction: a: asphalt, t: tile
		a	Exterior surface SW abs: 0lmhdb1 (see note)
Wcia	Exterior wall	c	Construction. 0: massless, w: wood frame, c: solid concrete
		i	Insulation (l, m, h)
		a	Exterior surface SW abs: 0lmhdb1 (see note)
Gtietfbl	Fenestration	t	Base fenestration type: 1, 2, e, x, 3
		i	IAC: 0: 0, l: .4, m: .6, h: .8, 1: 1
		e	EAC: 0: 0, l: .4, m: .6, h: .8, 1: 1
		tfibr	Fen area multiplier (adjusts prototype fen area) 0: 0, l: .5, m: 1, h: 2; A-C: area * 2, IAC = l, m, h
Pwf	Interior partition	w	Partition construction: w: wood frame
		f	Interior floor/ceiling construction: w: wood frame
Mcr	Interior mass	c	Construction type: w: wood
		r	Surface area ratio (fraction of room cfa) 0: 0, l: .5, m: 1, h: 2
Fcifx	Exterior floor	c	Construction. 0: massless, w: woodframe, c: concrete, s: slab
		i	Insulation (l, m, h)
		f	Boundary conditions: 0: adiabatic, a: ambient, c: crawlspace
		x	Crawlspace wall insulation (l,m, h)

Notes:

- SW absorptance codes: 0: 0, l: .3, m: .6, h: .8, d: .85, b: .95, 1: 1
- All codes case sensitive, however upper and lower case variants are not used in same code position because this would result in non-unique generated file names (file name are not case sensitive)
- Floor exterior SW abs set to same value as wall (required only for exposed floor)

Table B-2: Roof constructions

Config code 'f'	Attic	Roof cons code 'r'	Type	Constructions
h	hip attic, 4/12 roof	a	Asphalt	ROOF-ASPH
		t	Tile	ROOF-TILE
all others	(no roof)			

Table B-3: Ceiling constructions

Config code 'f'	Boundary conditions	Cons code 'c'	Type	Insul codes 'i'	Constructions
x	AMB	0	Massless	l, m, h	MASSLESS-L, -M, -H
		w	Wood frame	l, m, h	CEIL-WL, -WM, -WH
		c	Concrete	l, m, h	CONC-L, -M, -H
f	AMB	0	Massless	l, m, h	MASSLESS-L, -M, -H
		w	Wood frame	l, m, h	CLRF-WL, -WM, -WH
		c	Concrete	l, m, h	CONC-L, -M, -H
h	Attic	0	Massless	l, m, h	MASSLESS-L, -M, -H
		w	Wood frame	l, m, h	CEIL-WL, -WM, -WH
		c	Concrete	l, m, h	CONC-L, -M, -H

Note: MASSLESS resistances match corresponding CONC

Table B-4: Wall constructions

Cons code 'c'	Type	Insul codes 'i'	Constructions
0	Massless	l, m, h	MASSLESS-L, -M, -H
w	Wood frame	l, m, h	WALL-WL, -WM, -WH
c	Concrete	l, m, h	CONC-L, -M, -H

Note: MASSLESS resistances match corresponding CONC

Table B-5: Fenestration

Type code 't'	Glazing	Frame	ASHRAE ID ¹	NFRC ² U-factor W/m ² -K	SHGC
1	Single clear	none	1a	5.91	.86
2	Double clear	none	5a	2.73	.76
e	Double low-e high solar	none	17c	1.99	.70
x	Double low-e low solar	none	25a	1.70	.41
3	Triple clear	none	29a	1.76	.68

¹from Table 13, Chapter 30 of *ASHRAE Handbook of fundamentals* (2001).

²NFRC: National Fenestration Rating Council

Table B-6: Partition wall constructions

Cons code 'w'	Type	Insul codes	Construction
w	Wood frame	--	IWALL-W (1/2 thickness, adiabatic)

Table B-7: Partition floor/ceiling constructions

Cons code 'f'	Type	Insul codes	Construction
w	Wood frame	--	ICEIL-W, IFLOR-W (1/2 thickness, adiabatic)

Table B-8: Interior mass constructions

Cons code 'c'	Type	Insul codes 'i'	Constructions
w	Wood	--	IMASS-W

Table B-9: Exterior floor constructions

Cons code	Type	Insul codes 'i'	Constructions
0	Massless	l, m, h	MASSLESS-L, -M, -H
w	Wood frame	l, m, h	FLOR-WL, -WM, -WH
c	Concrete	l, m, h	CONC-L, -M, -H
s	Slab	--	FLOR-S (adiabatic exterior)

Note: MASSLESS resistances match corresponding CONC

APPENDIX C. SAMPLE PERL AND SHELL SCRIPTS USED FOR THE INTER-MODEL COMPARISON

This appendix gives some sample Perl and shell scripts used for the inter-model comparison. Section C.1 gives a part of the Perl script having the main flow of the parametric run management on the ESP-r side, along with a few subroutines it calls. Section C.2 gives four sample shell scripts: 1. *Climate* for changing the climate information. 2. *Rotate* for rotating the shoebox prototype. 3. *Simulate* for running the ESP-r simulation in on-off control mode for system evaluation. 4. *Analyse* for analyzing and outputting the results on system evaluation mode.

C.1 Sample Perl Scripts

```
#!/usr/bin/perl -w

# File type: PERL scripts
# Purpose: manage parametric run for 1199RP
# Author: Dongyi Xiao -- December, 2003
# Modified:

use Shell;
use ParRun;

# define parameters

# define variables
%CodeID = (
    Revision => "",
    House    => "",
    Location => "",
    Orientation => "",
    GainInfCtl => "",
    IntSurfAbs => "",
    ExtRoofCeil => "",
    ExtWall   => "",
    Fenestration => "",
    IntParFlrCeil => "",
    IntMass   => "",
    ExtFloor  => "",
); # Code ID
```

```

%Code = (
    Revison => "",
        House => "",
        Location => "",
        Orientation => "",

        IntGain => "",
        Infiltration => "",
    ControlSetPt => "",
        TempSwing => "",
        LowerSetPt => "",

        IntWallSW => "",
        IntMassSW => "",
    IntFloorSW => "",
        IntSurfLW => "",

        ExtCeilCon => "",
        ExtCeilInsul => "",
        ExtRoofConf => "",
        ExtRoofCon => "",
        ExtRfCeilSW => "",

        ExtWallCon => "",
        ExtWallInsul => "",
        ExtWallSW => "",

        WinType => "",
    WinIntSh => "",
    WinExtSh => "",
        FFront => "",
        FLeft => "",
        FBack => "",
        FRight => "",
        FTop => "",

        IntParCon => "",
        IntFlrCeilCon => "",

        MassCon => "",
    MassArea => "",

        ExtFlrCon => "",
        ExtFlrInsul => "",
        ExtFlrConf => "",
        ExtFlrCrawl => "",
); # Code

%HouseType = (
    k => "Karns",
        c => "Cardinal",
        f => "FSEC",
        d => "DOE",
        s => "Shoebox",
); # House types

%Latitude = (
    AKNE => "64.55",
        AZPH => "33.43",
        CABD => "34.85",
        CAPR => "35.67",
    CARB => "40.15",
        CASA => "38.70",
        CASD => "32.73",
        FLKW => "24.55",
        HIKA => "21.45",
    MISC => "45.92",
        NVEL => "40.83",
        ORME => "45.52",

```



```

        TNKN => "35.82",
    TNME => "35.05",
        TXLA => "27.55",
        WYBP => "42.57",
        DCWJ => "38.85",
        COAL => "37.45",
        MNMI => "44.88",
        GAAT => "33.65",
        TXDA => "32.90",
    ); # Latitude of a location

%LongDiff= (
    AKNE => "-14.08",
        AZPH => "-7.02",
        CABD => "3.22",
        CAPR => "-0.63",
    CARB => "-2.25",
        CASA => "-1.58",
        CASD => "2.83",
        FLKW => "-6.75",
        HIKA => "-7.77",
    MISC => "-10.92",
        NVEL => "4.22",
        ORME => "1.60",
        TNKN => "-8.98",
    TNME => "0.00",
        TXLA => "-9.47",
        WYBP => "-5.10",
        DCWJ => "-2.03",
        COAL => "-0.87",
        MNMI => "-3.22",
        GAAT => "-9.42",
        TXDA => "-7.03",
    ); # LongDiff of a location

$DirTestProc1 = "."; # the test procedure directory relative to the perl scripts directory
$DirParCode   = "$DirTestProc1/parcode"; # the parametric run codes directory
$DirGrdTemp   = "$DirTestProc1/climate/grdtemp"; # the ground teperature file directory
$DirConstruct = "$DirTestProc1/construction"; # the construction file directory
$DirPrototype = "$DirTestProc1/prototype"; # the prototype directory

$DirTestProc2 = "../.."; # the test procedure directory relative to the working directory of a test case
$DirScript    = "$DirTestProc2/scripts"; # the scripts file directory
$DirSysInput  = "$DirTestProc2/sysinput"; # the system input file directory
$DirResult    = "$DirTestProc2/result"; # the system input file directory
$DirClimate   = "$DirTestProc2/climate/cooling"; # the climate file directory

$DirBasecase = ""; # the basecase directory
$WorkDir     = ""; # working directory
$NewCaseDir  = ""; # directory for the new case

$ParCodeFile = "ParCode"; # the file holding the parametric run code
$GrdTempOutFile = "GrdTempOut.csv"; # the file holding the ground temperatures at 1.2m depth
$GrdTempInFile = "GrdTempInJuly.csv"; # the file holding the ground temperatures for slab-on-grade floors

$ConstructionIndexFile = "ConIndexName"; # the file holding the construction indexes and names
$SysInputFile = ""; # the system input file
$ConfigFile   = ""; # the ESP-r configuration file name
$ClimateFile  = ""; # the ESP-r climate file name
$IdealConfigFile = ""; # the ESP-r configuration file name for ideal control case
$IdealControlFile = ""; # the ESP-r control file name for ideal control case
$IdealNetFile = ""; # the ESP-r network airflow file name for ideal control case

$SimPeriodFlag = 1; # this flag determines the simulation period in ESP-r,
    # it will be set to different values according to the construction code
$IdealControlFlag = 1; # this flag is set to be true when ideal control case needs to be run
$HouseChangeFlag = 0; # the flag indicating the house type change from the previous case
$PreHouseCode = ""; # the house code for the previous case
$NumCase      = 0; # the number of cases to run

```

```
@ConIndex = (); # the array holding the construction indexes
@ConOutName = (); # the array holding the constructoin names
```

```
# declare subroutines
sub ConfigIdealCase;
sub ModIdealInfiltration;
sub ReadConIndexName;
sub MapConIndexName;
sub MapConNameCode;
sub ReadCode;
sub HouseModel;
sub CreatNewCase;
sub LocationClimate;
sub RotateBuilding;
sub ModConstruction;
sub ModWinAreaTyIsh;
sub ModWinEsh;
sub ModIntGain;
sub ModInfiltration;
sub ModThermalMass;
sub ModViewFactor;
sub ModShInsolation;
sub ModShade;
sub ModHcConvIdeal;
sub ModHcConvOnOff;
sub ConfigFloor;
sub GetSetPoint;
sub ModSetPoint;
sub ModIdealSetPoint;
sub GetWinIndex;
sub DelLibrary;
sub ReadGrdTemp;
sub ModGrdTempIn;
sub ModGrdTempOut;
```

```
#
```

```
# main flow:
```

```
# read in the ground temperatures
ReadGrdTemp;
```

```
# read in the construction indexes and names
ReadConIndexName;
```

```
# open the file holding the parametric run code for read
open (FILEHANDLE, "<$DirParCode/$ParCodeFile") or die ("Cannot open $ParCodeFile");
```

```
# read in head line for number of codes
$Step = <FILEHANDLE>;
# read in the number of codes
$Step = <FILEHANDLE>;
$NumCase = $Step;
```

```
close (FILEHANDLE);
```

```
for ($i = 1; $i <= $NumCase; $i++)
```

```
{
  # Read in the parametric run "code"
  ReadCode;
```

```
    # Get the control set point
    GetSetPoint;
```

```
    # map the construction codes to the construction indexes
    MapConNameCode;
```

```
# Determine house model
```

```

HouseModel;

# create a new case
CreatNewCase;

# change to the new case working directory
chdir $WorkDir;
#print pwd(); # for debug use only

# Determine location and change climate information
LocationClimate;

    # Modify the user defined ground temperature profile for
# external long wave radiation calculation (1.2m depth earth temperature)
    ModGrdTempOut;

    # Modify the user defined ground temperature profile for
# slab-on-grade floors (0.1m depth earth temperature)
    #ModGrdTempIn;

    # config boundary condition for the external floor
    ConfigFloor;

# Modify construction information
ModConstruction;

    # modify thermal mass construction and surface area ratio
    ModThermalMass;

# Modify window area, type, and internal shading
ModWinAreaTyIsh;

    # modify window external shading
    ModWinEsh;

    # modify internal gain level
#ModIntGain;

    # modify infiltration level
#ModInfiltration;

# Rotate the building to the orientation code
RotateBuilding;

    # update view factors
ModViewFactor;

    # update shading/insolation files
    #ModShInsolation;
    ModShade;

    # update convection coefficient files for on-off control
    ModHcConvOnOff;

    # modify the set point in the master-slave control file
    ModSetPoint;

    # determine if the house code has been changed
    if ($PreHouseCode ne $Code{House})
    {
        $HouseChangeFlag = 1;
    }
    else
    {
        $HouseChangeFlag = 0;
    }

# Run the simulation and analyze result for master-slave control case
#SimRes($ConfigFile, $DirSysInput, $SysInputFile, $Code{House}, $DirResult, $HouseChangeFlag, $SimPeriodFlag);

```

```

# Run the simulation and analyze result for ideal control case
# if the ideal control flag is true
if ($IdealControlFlag)
{
# create the configuration file for the ideal control case
ConfigIdealCase;

# need to modify the infiltration level for the ideal case
# since the airflow network has been cleared up
ModIdealInfiltration;

# modify the set point in the ideal control file
ModIdealSetPoint;

# update convection coefficient files for on-off control
ModHcConvIdeal;

# simulate and analyze result for the ideal control case
SimResIdeal($IdealConfigFile, $DirResult, $HouseChangeFlag, $ParCaseCode, $Code{House},
$DirSysInput, $SysInputFile, $SimPeriodFlag);
}

# save the house code for next case comparison
$PreHouseCode = $Code{House};

# delete the result libraries for this case
DelLibrary;

# change to the script directory
chdir $DirScript;
}

#

```

```

sub HouseModel
{
# Purpose: determine the house model and base case directory
# Author: Dongyi Xiao -- December, 2003
# Modified:

if (defined($HouseType{$Code{House}}))
{
$ConfigFile = "$HouseType{$Code{House}}.cfg";
$IdealConfigFile = "$HouseType{$Code{House}}_Ideal.cfg";
$IdealControlFile = "$HouseType{$Code{House}}_Ideal.ctl";
$IdealNetFile = "$HouseType{$Code{House}}_Ideal.afn";
$DirBasecase = "$DirPrototype/$HouseType{$Code{House}}";
# print "House model: $ConfigFile\n"; # for debug use only
# print "Base case dir: $DirBasecase\n"; # for debug use only
}
else
{
die "No house model $Code{House} defined! Please specify another house model and try again.\n";
}
}

#

```

```

sub LocationClimate
{
# Purpose: determine the location and change climate information by calling shell script "Climate".
# Author: Dongyi Xiao -- December, 2003
# Modified:

$ClimateFile = "$DirClimate/$Code{Location}.clm";

```

```

# print "Climate file: $ClimateFile\n"; # for debug use only

if (defined($Latitude{$Code{Location}}) && defined($LongitudeDiff{$Code{Location}}))
{
# call the shell script "Climate" to change climate information
@a = ("./Climate", "$ConfigFile", "$ClimateFile", "$Latitude{$Code{Location}}", "$LongitudeDiff{$Code{Location}}");
system(@a);
# print "Latitude: $Latitude{$Code{Location}}\n"; # for debug use only
# print "Longitude difference: $LongitudeDiff{$Code{Location}}\n"; # for debug use only

}
else
{
die "No latitude or longitude difference defined for $Code{Location}! Please check and try again.\n";
}
}
#

```

```

sub RotateBuilding
{
# Purpose: rotate the building by calling shell script "Rotate".
# Author: Dongyi Xiao -- December, 2003
# Modified:

# call the shell script "Rotate" to rotate the building
if ($Code{Orientation} ne "000")
{
@a = ("./Rotate", "$ConfigFile", "-$Code{Orientation}", "$Code{WinExtSh}");
system(@a);
}
}
#

```

C.2 Sample Shell Scripts

Shell script 1: Climate

```

#!/bin/sh

# File type: shell scripts
# Purpose: Change climate information (climate file name, site latitude and longitude difference)
# Author: Dongyi Xiao -- September, 2003
# Modified:

ConfigFile=$1
ClimateFile=$2
Latitude=$3
LongitudeDiff=$4

prj -file $ConfigFile -mode text<<XXX
- # exit to entry level for database maintenance
b # select database maintenance
a # select climate
b # climate database options: select from list

```

```

< # user defined climate db
$ClimateFile
n # do not browse or edit climate data
- # exit database maintenance menu
d # select existing model
y # continue with the current model
c # model context
c # site latitude
$Latitude
d # longitude difference
$LongDiff
- # exit this menu
Y # update any existing shading databases to reflect these site changes
! # save model

- # exit this menu
- # exit project Manager
y # make sure to quit
XXX

```

Shell script 2: Rotate

```

#!/bin/sh

# File type: shell scripts
# Purpose: Rotate the Shoebox prototype
# Author: Dongyi Xiao -- September, 2003
# Modified:

CONFIG=$1
RotateDegree=$2
ExtShCode=$3

case "$ExtShCode" in
0)
$ExtSh="0"
;;
-)
$ExtSh="0"
;;
s)
$ExtSh="1"
;;
*)
esac

if [ $ExtSh -ne 0 ] ; then
prj -file $CONFIG -mode text<<XXX
e # select composition
a # browse/creat model using project manager
* # select global tasks
b # select rotate
$RotateDegree # rotation degree +=anticlockwise
a # rotate around site origin
* # rotate all items
- # exit current menu
- # exit this menu
! # update model description

- # exit model definition
- # exit project manager
y # be sure to quit
XXX
else
prj -file $CONFIG -mode text<<XXX
e # select composition

```

```

a # browse/creat model using project manager
* # select global tasks
b # select rotate
$RotateDegree # rotation degree +=anticlockwise
a # rotate around site origin
* # rotate all items
- # exit current menu
y # rotate obstructions in GreatRoom
y # rotate obstructions in LivingRoom
- # exit this menu
! # update model description

- # exit model definition
- # exit project manager
y # be sure to quit
XXX
Fi

```

Shell script 3: Simulate

```

#!/bin/sh

# File type: shell scripts
# Purpose: do the simulation for the on-off control case
# Author: Dongyi Xiao -- February, 2004
# Modified:

CONFIG=$1
TimeSteps=$2
StartDay=$3
StartMon=$4
EndDay=$5
EndMon=$6

bps -file $CONFIG -mode text<<XXX

y # use indicative simulation startup period

c # initiate simulation

libf
$StartDay $StartMon # simulation start day/month
$EndDay $EndMon # simulation end day/month
60 # time steps/hour
n # no hourly results integration
t # invoke time step controller
3 # user specified time step value

$TimeSteps
- # exit time step controller
g # simulation toggles
101
t # convection methods (external)
b # MoWiTT low rise hc
- # exit simulation toggles menu
s # invoke simulation
y # yes change save level to 4
y # use current control model & result-set description

y # yes continue the simulation
y # save simulation results
- # exit to main menu
- # quit the ESP-r integrated simulator
y # be sure to quit
XXX

```

Shell script 4: Analyse

```
#!/bin/sh

# File type: shell scripts
# Purpose: Analyse result -- two files will be output,
#         one temperature profile, one summary file
# Author: Dongyi Xiao -- December, 2003
# Modified:

RESFILE="libb"

MinTempFile=$1
HourTempFile=$2
SummaryFile=$3
MinPPDFile=$4
HourPPDFile=$5
StartDayMonTime=$6
EndDayMonTime=$7

res -file $RESFILE -mode text<<XXX

3 # define output period
$StartDayMonTime # start day-of-month, month & time
$EndDayMonTime # end day-of-month, month & time
1 # output time-step increment
c # time step reports
> # output to file
$MinTempFile
# use current title for 3rd party graph
^ # choose delimiter to use between columns of data
e # choose comma
g # choose performance metrics to output
b # choose temperatures
a # select zone db T
! # list data
> # closing output file
> # output to file
$MinPPDFile
# use current title for 3rd party graph
c # choose comfort metrics
c # PPD: Percentage dissatisfied
0.5
a # activity level units: MET units
1.34
0.24
a # occupancy: always occupied
! # list data
- # exit performance metrics menu
- # exit tabular output menu
d # enquire about
> # closing output file
> # output to file
$SummaryFile
# use current title for 3rd party graph
a # Summary statistics
b # choose temperatures
a # select zone db T
c # comfort metrics
c # PPD: Percentage dissatisfied
y # yes, use existing comfort parameters
3 # Display period
$StartDayMonTime # start day-of-month, month & time
$EndDayMonTime # end day-of-month, month & time
60 # output time-step increment
y # yes, average results over each output interbal
b # choose temperatures
a # select zone db T
```



```
c # comfort metrics
c # PPD: Percentage dissatisfied
y # yes, use existing comfort parameters
- # exit Summary statistics
- # exit equire about
c # time step reports
g # choose performance metrics to output
> # closing output file
> # output to file
$HourPPDFile
  # use current title for 3rd party graph
c # choose comfort metrics
c # PPD: Percentage dissatisfied
y # yes, use existing comfort parameters
! # list data
> # closing output file
> # output to file
$HourTempFile
  # use current title for 3rd party graph
b # choose temperatures
a # select zone db T
! # list data
- # exit performance metrics menu
- # exit tabular output menu
- # quit result analysis
y # be sure to quit
XXX
```

VITA

Dongyi Xiao

Candidate for the Degree of

Doctor of Philosophy

Thesis: INTER-MODEL, ANALYTICAL, AND EXPERIMENTAL
VALIDATION OF A HEAT BALANCE BASED RESIDENTIAL
COOLING LOAD CALCULATION PROCEDURE

Major Field: Mechanical Engineering

Biographical:

Personal Data: Born in Yizhang, Hunan, P. R. China on December 26, 1973, the daughter of Cuiying Liu and Huijun Xiao.

Education: Received the Bachelor of Science degree in Thermal Engineering from Shenyang Architectural and Civil Engineering Institute, Shenyang, P. R. China in July 1995. Received the Master of Science degree in Thermal Engineering from Tongji University at Shanghai, P. R. China in April 1998. Completed the requirements for the Doctor of Philosophy degree with a major in Mechanical Engineering at Oklahoma State University, Stillwater, Oklahoma in December 2006.

Experience: Employed as lecturer at the School of Mechanical Engineering, Shanghai University of Engineering Science, Shanghai, P.R.China from April 1998 to July 1999. Employed as research assistant at the School of Mechanical & Aerospace Engineering, Oklahoma State University, Stillwater, Oklahoma from August 1999 to May 2006.

Professional Membership: American Society of Heating, Refrigerating and Air Conditioning Engineers (ASHRAE), International Building Performance Simulation Association, Affiliate in the United States (IBPSA-USA), American Society of Mechanical Engineers (ASME).

Name: Dongyi Xiao

Date of Degree: December, 2006

Institution: Oklahoma State University

Location: Stillwater, Oklahoma

Title of Study: INTER-MODEL, ANALYTICAL, AND EXPERIMENTAL
VALIDATION OF A HEAT BALANCE BASED RESIDENTIAL
COOLING LOAD CALCULATION PROCEDURE

Pages in Study: 304

Candidate for the Degree of Doctor of Philosophy

Major Field: Mechanical Engineering

Scope and Method of Study: A systematic validation of the ASHRAE heat balance based residential cooling load calculation procedure (RHB) has been performed with inter-model comparison, analytical verification and experimental validation. The inter-model validation was performed using ESP-r as the reference model. The testing process was automated through parametric generation and simulation of large sets of test cases for both RHB and ESP-r. The house prototypes covered include a simple Shoebox prototype and a real 4-bedroom house prototype. An analytical verification test suite for building fabric models of whole building energy simulation programs has been developed. The test suite consists of a series of sixteen tests covering convection, conduction, solar irradiation, long-wave radiation, infiltration and ground-coupled floors. Using the test suite, a total of twelve analytical tests have been done with the RHB procedure. The experimental validation has been conducted using experimental data collected from a Cardinal Project house located in Fort Wayne, Indiana. During the diagnostic process of the experimental validation, comparisons have also been made between ESP-r simulation results and experimental data.

Findings and Conclusions: It is concluded RHB is acceptable as a design tool on a typical North American house. Analytical tests confirmed the underlying mechanisms for modeling basic heat transfer phenomena in building fabric. The inter-model comparison showed that the differences found between RHB and ESP-r can be traced to the differences in sub-models used by RHB and ESP-r. It also showed that the RHB-designed systems can meet the design criteria and that the RHB temperature swing option is helpful in reducing system over-sizing. The experimental validation demonstrated that the systems designed with the method will have adequate size to meet the room temperatures specified in the design, whether or not swing is utilized. However, actual system operation may cause deviations in the room temperatures, particularly in the slave rooms. For better prediction of these deviations, simulation or a better approximation for interzone airflows and heat transfers would be needed. The RHB procedure may be said to give cooling loads that are as accurate as the inputs and real-life uncertainties inputs will be more significant than errors that caused by the method.

ADVISER'S APPROVAL: Dr. Jeffrey D. Spitler
